

**UNESCO-IHE**  
**Transient Groundwater Flow, Analytical  
Solutions**

Prof. T. N. Olsthoorn, PhD, MSc

December 2019

# Contents

<b>1</b>	<b>Introduction</b>	<b>9</b>
1.1	Objectives of the course . . . . .	9
1.2	Note with respect to the exercises . . . . .	10
<b>2</b>	<b>Introduction to transient phenomena in groundwater</b>	<b>12</b>
<b>3</b>	<b>Irreversible transient phenomena</b>	<b>14</b>
3.1	Consolidation . . . . .	14
3.2	Liquefaction . . . . .	15
3.3	Intrusion of salt water . . . . .	17
3.4	Questions . . . . .	19
<b>4</b>	<b>Reversible groundwater storage</b>	<b>20</b>
4.1	Phreatic storage (water table storage, specific yield, $S_y$ ) . . . . .	20
4.1.1	Phreatic responses . . . . .	26
4.1.2	Questions . . . . .	27
4.2	Elastic Storage . . . . .	30
4.2.1	Introduction . . . . .	30
4.2.2	Loading efficiency . . . . .	30
4.2.3	Barometer efficiency . . . . .	31
4.2.4	How much are the loading efficiency and the barometer efficiency when expressed in the properties of the water and the porous medium ? . . . . .	34
4.2.5	Specific (elastic) storage coefficient . . . . .	36
4.2.6	Application (not for exam) . . . . .	38
4.2.7	Questions . . . . .	39
4.3	Earth tides (not for exam) . . . . .	41
<b>5</b>	<b>One-dimensional transient groundwater flow</b>	<b>43</b>
5.1	Scope . . . . .	43
5.2	Governing equations . . . . .	43
5.3	Sinusoidal fluctuations of the groundwater head and flows . . . . .	45
5.3.1	Groundwater fluctuations due to sinusoidal tides . . . . .	45
5.3.2	Fluctuations of temperature in the subsurface . . . . .	50
5.3.3	Concluding remarks . . . . .	51
5.3.4	Questions . . . . .	52
5.4	Non-fluctuating interaction with surface water . . . . .	54
5.4.1	Basins of half-infinite lateral extent . . . . .	54

5.4.2	Questions . . . . .	59
5.4.3	Higher-order solutions (not for exam) . . . . .	60
5.4.4	Questions . . . . .	62
5.4.5	Superposition in time, half-infinite aquifer . . . . .	62
5.5	Groundwater basins as land strips of limited width between straight head boundaries . . . . .	67
5.5.1	Introduction . . . . .	67
5.5.2	Water level at the left hand side suddenly rises by a height $a$ , the level at the right-hand side remains at zero . . . . .	68
5.5.3	Shifting the zero point of the $x$ -axis . . . . .	71
5.5.4	Arbitrary non-symmetrical case . . . . .	71
5.5.5	Symmetrical case, $A = B$ . . . . .	74
5.5.6	Questions . . . . .	77
5.6	Symmetrical drainage from a land strip bounded by straight head boundaries (characteristic time of flow basins) . . . . .	78
5.6.1	Analytical solution . . . . .	78
5.6.2	Long-term drainage behavior, characteristic drainage time . . . . .	80
5.6.3	Questions . . . . .	85
<b>6</b>	<b>Transient flow to wells</b>	<b>86</b>
6.1	Introduction . . . . .	86
6.2	Wells and well functions overview . . . . .	86
6.3	Theis: transient well in an infinite aquifer with constant transmissivity and storativity . . . . .	91
6.3.1	Implementation of the Theis well function . . . . .	94
6.3.1.1	In Python . . . . .	94
6.3.1.2	Implementation in Excel . . . . .	95
6.3.2	Type-curve for the Theis well function . . . . .	96
6.3.3	Theis classic pumping-test analysis . . . . .	98
6.3.4	Standard behavior obtained from simplified Theis well function . . . . .	102
6.3.5	Derived behavior using the logarithmic approximation of $W(u)$ . . . . .	105
6.3.6	Drawdown at a fixed time at different $r$ . . . . .	108
6.3.7	Radius of influence . . . . .	110
6.3.8	Relation with the solution for the steady-state situation . . . . .	111
6.3.9	Exercises . . . . .	112
6.3.10	Flow at distance $r$ from the well . . . . .	115
6.3.11	Superposition in time . . . . .	119
6.3.12	Superposition in space . . . . .	120
6.3.13	Questions . . . . .	122
6.4	Partial penetration of well screens . . . . .	125
6.4.1	Huisman's method . . . . .	125
6.4.2	Hantush's solution for partial penetrating screens . . . . .	127
6.4.3	Example . . . . .	129
6.4.3.1	Python implementation of partial penetration . . . . .	131

6.4.4	Questions . . . . .	132
6.5	Hantush: transient flow due to a well in a semi-confined (leaky) aquifer . . . . .	133
6.5.1	Hantush's partial differential equation and solution . . . . .	133
6.5.2	Implementing Hantush's well function . . . . .	135
6.5.3	Hantush type curves and comparison with Theis . . . . .	137
6.5.4	Questions . . . . .	140
6.5.5	Pumping test Dalem (Kruseman & De Ridder, 1994) . . . . .	142
6.6	Delayed yield (delayed water-table response) . . . . .	142
6.6.1	Introduction . . . . .	142
6.6.2	Water-table aquifer . . . . .	144
6.6.3	Generalization to semi-confined aquifers . . . . .	145
6.6.4	The two Theis bounding curves . . . . .	149
6.6.5	Influence of partial penetration of the well screen . . . . .	149
6.6.6	Questions . . . . .	152
6.7	Large-diameter wells (not for the exam) . . . . .	152
<b>7</b>	<b>Convolution</b>	<b>158</b>
7.1	What convolution is and how it works . . . . .	158
7.2	Examples . . . . .	162
7.2.1	Arbitrarily fluctuating river stage . . . . .	162
7.2.2	Impulse response, block response, and step response comparison . . . . .	167
7.2.3	Arbitrarily fluctuating extraction of multiple Theis wells . . . . .	169
7.2.4	Convolution using recharge as input time series to simulate varying groundwater levels . . . . .	171
7.3	Questions . . . . .	174
<b>8</b>	<b>Laplace solutions (illustration, not for exam)</b>	<b>177</b>
8.1	Sudden head rise at the boundary of a one-dimensional semi-infinite aquifer	177
8.2	Laplace solution for the Theis well function . . . . .	178

# Nomenclature

## General

$x, y, z$  [L] Coordinates.  $z$  is upward positive relative to top of model, sea level, ground surface, top of aquifer or any other suitable fixed datum elevation.

$r$  [L] Distance from the well or center of model in the case of axial symmetric flow. Also used for the radius of a capillary.

$R$  [L] Radius of influence, outer radius of circular aquifer or island.

$t, \Delta t$  [T] Time.

$A$  [L<sup>2</sup>] Surface area

$V$  [L<sup>3</sup>] Volume.

## Hydraulic and mechanical properties

$\mu$  [FT/L<sup>2</sup>] Water viscosity, e.g. [Ns/m<sup>2</sup>] = [Pa s]

$\kappa$  [L<sup>2</sup>],  $k$  [L/T] Permeability (independent of fluid) and hydraulic conductivity.  $k = \rho_w g \frac{\kappa}{\mu}$ . Note that  $\kappa$  and  $k$  are vectors, i.e. they are direction dependent.

$c$  [T] Vertical hydraulic resistance of aquitards or a low-conductive layer,  $c = d/k_v$  with  $d$  [L] the thickness of this layer and  $k_v$  [L/T] its vertical hydraulic conductivity.

$S$  [-] Elastic storage coefficient [L<sup>3</sup>/L<sup>2</sup>/L]

$S_s$  [L<sup>-1</sup>] Specific elastic storage coefficient [L<sup>3</sup>/L<sup>3</sup>/L]

$S_y$  [-] Specific yield [L<sup>3</sup>/L<sup>2</sup>/L]. Specific yield is storage from draining pores.

$\alpha, \beta$  [L<sup>2</sup>/F] compressibility of water and bulk porous matrix respectively.  $\beta = 1/E$  where  $E$  is the compression modulus.

$E_w, E_m$  [F/L<sup>2</sup>] Compression modulus of water and porous medium respectively.  $E = 1/\beta$ , where  $\beta$  is the compressibility.

$\rho_w, \rho_s, \rho_b, \rho$  [M/L<sup>3</sup>] Density of water, solids, bulk porous medium respectively

## Heat properties and flow

$c, c_w, c_s$  [E/M/K] Bulk heat capacity, heat capacity of water and solids.  $c = \epsilon c_w + (1 - \epsilon) c_s$

$\lambda, \lambda_w, \lambda_s$  [E/T/L/K] Bulk, water and solids heat conductance,  $\lambda = \epsilon \lambda_w + (1 - \epsilon) \lambda_s$

$\epsilon$  [-] Porosity of the porous medium

$\mathbb{D}$  [L<sup>2</sup>/T] For heat flow  $\mathbb{D} = \frac{\lambda}{\rho c}$ , i.e. heat conductivity over bulk volumetric heat capacity of water plus medium,  $\lambda = \epsilon \lambda_w + (1 - \epsilon) \lambda_s$  and  $\rho c = \epsilon \rho_w c_w + (1 - \epsilon) \rho_s c_s$ . For diffusivity in the context of groundwater flow see under **Aquifer system**.

$\mathbb{R}$  [-] Retardation, i.e. the factor by which transport of mass or heat is delayed relative to that of the pore water. It is the amount of mass or heat in the water over the total amount of mass or heat in the water plus sorbed to/in the grains. Hence for heat  $\mathbb{R} = \rho_w c_w \epsilon / (\rho_w c_w \epsilon + \rho_s c_s (1 - \epsilon))$  with indices  $w$  and  $s$  referring to water and grains respectively.

## Aquifer system

$q, q_x, q_y, q_z$  [L/T] Specific discharge, which generally is direction-specific (a vector)

$Q$  [L<sup>3</sup>/T], [L<sup>2</sup>/T] Discharge. It can mean the total discharge over the thickness of the aquifer in a cross section [L<sup>2</sup>/T] or the extraction or injection of a well, in which case its dimension is L<sup>3</sup>/T.

$N, \bar{N}$  [L/T] Net recharge and the time or space average net recharge respectively

$h$  [L] Phreatic head, in the case of a water table aquifer, the head relative to the bottom of this aquifer, i.e. the wetted aquifer thickness

$\phi$  [L] Head in semi-confined and confined aquifers, relative to some predefined datum, i.e. sea level.

$s$  [L] Drawdown, or head relative to initial situation (lower case  $s$ )

$p, \sigma_w, \sigma_s, \sigma_e$  [F/L<sup>2</sup>] Pressure, water pressure, total or soil pressure and effective pressure.  $\sigma_t$  also used for total pressure.

$H$  [L] Thickness of aquifer. Often used only for water table aquifer, sometimes for any aquifer.

$D$  [L] Total thickness of aquifer

$kD$  [L<sup>2</sup>/T] Transmissivity of an aquifer.  $kH$  may be used in an water-table aquifer.

$T$  [T] Characteristic time of a dynamic groundwater system.

$\mathbb{D} [\text{L}^2/\text{T}]$  Diffusivity. For flow  $\mathbb{D} = \frac{kD}{S}$  for thermal flow  $\mathbb{D} = \frac{\lambda}{\rho c}$ , see under Heat

$\lambda [\text{L}]$  Characteristic length or spreading length of a semi-confined aquifer system, i.e.  $\lambda = \sqrt{kDc}$  with  $kD [\text{L}^2/\text{T}]$  the aquifer's transmissivity and  $c [\text{T}]$  the aquitard's vertical resistance.

$R, R_0 [\text{L}]$  Fixed radial distance to the center of axial symmetric flow system at which the head is fixed or zero.

$LE [-]$  Loading efficiency,  $LE = \frac{\beta_m}{\epsilon\beta_w + \beta_m}$ . Note that  $LE + BE = 1$

$BE [-]$  Barometric efficiency.  $BE = \frac{\epsilon\beta_w}{\epsilon\beta_w + \beta_m}$ . Note that  $LE + BE = 1$

## Groundwater waves

$A [\text{L}], B \text{ L}$  Wave amplitude.

$L [\text{L}]$  Width of the groundwater system.

$a$  Damping factor of groundwater head wave moving through the aquifer, caused by a kind of tide.  $a = \sqrt{\frac{\omega}{2\mathbb{D}}}$

$\omega [\text{T}^{-1}]$  or rather radians per time. The angle velocity of the wave. Full wave time  $T = 2\pi/\omega$

$T [\text{T}]$  Cycle time, time of a full wave.  $T = 2\pi/\omega$

## Physics, math and mechanics

$g [\text{F/M}], [\text{L/T}^2]$  Gravity, acceleration in the Earth's gravity field or the force with which the earth's gravity field pulls at a unit mass at ground surface in the direction of the earth's center.

$\gamma [\text{F/L}]$  Surface tension, cohesion in capillary systems.

$IR(\tau), BR(\tau, \Delta\tau), SR(\tau)$  Respectively: Impulse response, Block response, Step response of a system.  $\Delta\tau$  step size,  $\tau$  lapsed time since event started. See chapter on convolution.

$\text{erfc}(u)$  Complementary Error function, i.e.  $\text{erfc}(u) = \frac{2}{\sqrt{\pi}} \int_u^\infty e^{-\zeta^2} d\zeta$ , and, therefore,  $\frac{d\text{erfc}(u)}{du} = -\frac{2}{\sqrt{\pi}} e^{-u^2}$

$\mathbf{W}(u)$  Theis' well function, for transient flow to a well in a confined aquifer, i.e.  $\mathbf{W}(u) = \text{iexp}(u) = \int_u^\infty \frac{e^{-\zeta}}{\zeta} d\zeta$ , iexp is the exponential integral.

$W(u, \frac{r}{\lambda})$  Hantush's well function for semi-confined transient flow to a well,  $W(u, \frac{r}{\lambda}) = \int_u^\infty \frac{1}{\zeta} \exp\left(-\zeta - \frac{1}{4\zeta} \left(\frac{r}{\lambda}\right)^2\right) d\zeta$

$u [-]$  In 1D (cross sections as argument of the erfc-function),  $u = \sqrt{\frac{x^2 S}{4kDt}}$ . In axial symmetric situations, as argument of the Theis and Hantush solutions,  $u = \frac{r^2 S}{4kDt}$

$I_o(z)$ ,  $I_1(z)$ ,  $K_o(z)$ ,  $K_1(z)$  dimensionless modified Bessel function using in axial-symmetric semi-confined steady-state solutions. They depend on the scaled distance  $z = r/\lambda$ , with  $\lambda = \sqrt{kDc}$

# 1 Introduction

This syllabus has been prepared as part of the IHE masters program in Hydrology and Water Resources, at IHE Delft. The part given by the author, i.e. transient analytical solutions, consists of a total of 20-24 lecture hours divided over five days, half of which are oral lectures and half are practical exercises in which the students learn to solve their own problems by implementing the given groundwater solutions in Python.

The material for this course will be stored on [Github](#). Search for Olsthoorn combined with groundwater. The material includes Jupyter notebooks used to generate most of the figures in this syllabus.

## 1.1 Objectives of the course

- The students will become familiar with the basic 1D and axially symmetric transient groundwater solutions that can readily be applied in practical situations when a computer models is not readily available, where a fast idea of the effect of groundwater impacts is required, where a model is to be verified and so on.
- Students will learn how to deal with and apply superposition, which is perhaps the most important tool to handle more complex systems with analytically.
- Students will obtain insight in the transient behavior of groundwater systems, with their characteristics such as halftime and the relations between parameters and the way parameters workout in the effect on the system.
- Students will learn to simplify analytical solution to extract behavior characteristics that are easy to understand and apply for under specified conditions.
- Closed analytical solution for transient groundwater flow are only available for linear systems, i.e. systems with a constant transmissivity and storativity. Students will learn how to deal in an approximate way with situations where transmissivity varies due to extractions or injection.
- Students will gain insight in the behavior of real-world groundwater systems and learn how to read their reaction.
- Students will also learn what physics cause a given behavior of groundwater systems. Storage characteristics and barometric and tidal reactions will be dealt with.
- Students will learn and exercise how to implement transient analytical solutions in Python and visualize their results.

- Students will learn how to analyze basic pumping tests to obtain parameter values for a groundwater system.
- Depending on the group, students will learn how to handle complicated time varying systems by means of convolution.
- Students will carry out an assignment in which the various aspects learned are applied.

## 1.2 Note with respect to the exercises

Today there are two skills that students should acquire: Python and QGIS.

With Python, there is no limit to what you as student of professional may compute (and visualize) on your laptop, neither is there any practical limit to the amount of data you can handle and process, or the complexity you can handle. And, perhaps the best, it is free.

With QGIS there is no limit to spatial data you can handle and analyze and process. And it is also free.

With these two tools you are equipped for the future as an engineer and scientist. Both are free, which is a unique feature of our time. Never before was so much computing power in your hands. And nobody can ever take it from you, just because it is free, sitting on your own laptop. Therefore, it is only up to you to acquire the skills. There is an immense amount of resources and information on the internet about both, so you should never be without an answer to your questions. There are also numerous tutorials, both written and on video on the internet, and, of course, there is a large pile of books. Python and QGIS, which have been around for only a little over 1.5 decades, have already changed the world for scientists and are doing this more every day. So if you don't want to be left behind, pick it up. My advice to you, dear students, is to start using both for all your projects from now on.

The exercises for this course will be done in IPython notebooks (now called Jupyter notebooks), which are a terrific means to communicate your work with others, including your teachers. These notebooks, which were originally developed for Python only, have since a few years been extended to over 47 other computer languages, like *R* and *Julia*. That is why the name was changed to Jupyter notebooks. These notebooks allow you to combine, text, formulas and code, neatly formatted, while computations are done and visualized within the notebook itself. Therefore, if your notebook is correct, then your work is correct. And because the text, with formulas, code and graphical results can be nicely formatted within the notebook, the notebook is also great for sharing your results as a living document or, if you like, you can save it also as a pdf document, and send that to your teacher is doesn't have Python.

- To convince yourselves read what Nature (world's most famous scientific journal) said about Ipython notebooks in 2014:

<https://www.nature.com/news/interactive-notebooks-sharing-the-code-1.16261>

- If you want some examples and tutorials see:

<https://github.com/Carreau/iPython-wiki/blob/master/A-gallery-of-interesting-IPython-Notebooks.md>

<https://github.com/iPython/iPython/wiki/A-gallery-of-interesting-IPython-Notebooks>

- Just do a few of the examples. You'll see that you can reach out over the entire internet, and could even embed a live webcam from home (or from your data loggers, of course) in your own notebook.

- For exploratory computing, which is what you'll be doing most of the time, see:

[http://nbviewer.jupyter.org/github/mbakker7/exploratory\\_computing\\_with\\_Python/blob/master/notebooks](http://nbviewer.jupyter.org/github/mbakker7/exploratory_computing_with_Python/blob/master/notebooks)

- Jupyter notebook implies: 1) Rich web client. 2) Text and Math 3) Code 4) Results  
5) Share and reproduce

See [https://www.dataone.org/sites/default/files/sites/all/documents/perez2017webinar\\_sm.pdf](https://www.dataone.org/sites/default/files/sites/all/documents/perez2017webinar_sm.pdf)

[https://www.dataone.org/sites/default/files/sites/all/documents/perez2017webinar\\_sm.pdf](https://www.dataone.org/sites/default/files/sites/all/documents/perez2017webinar_sm.pdf)

Theo Olsthoorn, Dec. 2017

## 2 Introduction to transient phenomena in groundwater

Transient phenomena can only occur if there is some form of storage for water under pressure. Without storage, at least theoretically, all changes of water pressures would spread out with infinite speed across the entire medium. The studied system would then always be in steady state. Clearly, this is never the case in physical reality. Every groundwater system has ways to store and release water under changes of pressure. The specific change of water volume in the porous medium per unit change of pressure (or head) determines the transient behavior of the groundwater system.

Under confined groundwater-flow conditions, part of the storage comes from compressibility of the porous medium and part from the compressibility of the water. Under conditions of a free water table, i.e. under unconfined flow conditions, meaning when a free water table is present, also called phreatic groundwater, most storage comes from filling and emptying pores above the water table and only a minor part from elastic storage. The elastic storage is about two orders of magnitude smaller than the phreatic storage. Because of this, elastic storage is mostly neglected for aquifer systems with a free water table.

Groundwater systems can be very slow and very fast. Whether a groundwater system is slow or fast depends on factors that we will study later in section [5.6.2 on page 80](#). An example of a very slow groundwater system, one that takes tens of thousands of years to reach equilibrium, is presented in figure [2.1 on the next page](#), which shows the ongoing decay of the groundwater mound in the Kalahari Desert since the last wet episode, which happened some 12500 years ago (De Vries, 2000). The line along which the cross section was made is shown in figure [2.2 on the following page](#) together with the elevation profile.

Dynamics of groundwater may also be divided into **reversible** and **irreversible** behavior. In this syllabus, we will deal with reversible systems only. Forms of irreversible storage may nevertheless be important under specific circumstances, or may even be quite common. Therefore, we will start with an illustration of some forms of irreversible transient behavior of water-filled porous media.

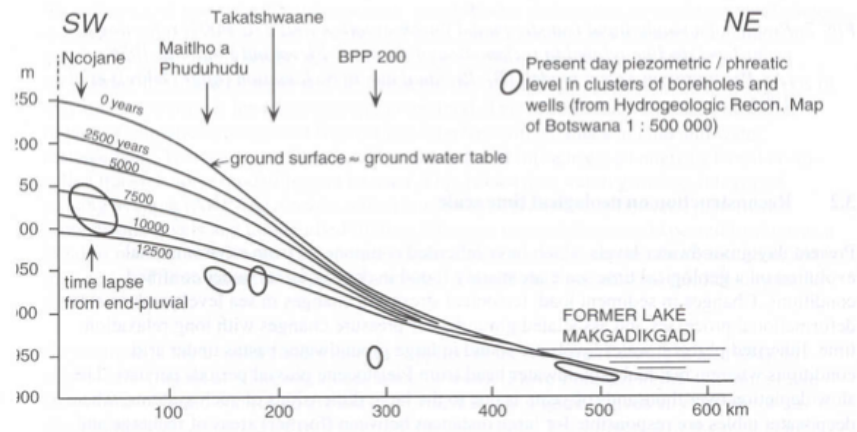


Figure 2.1: Gradual decay of the water table in the Kalahari Desert (De Vries, 1984)

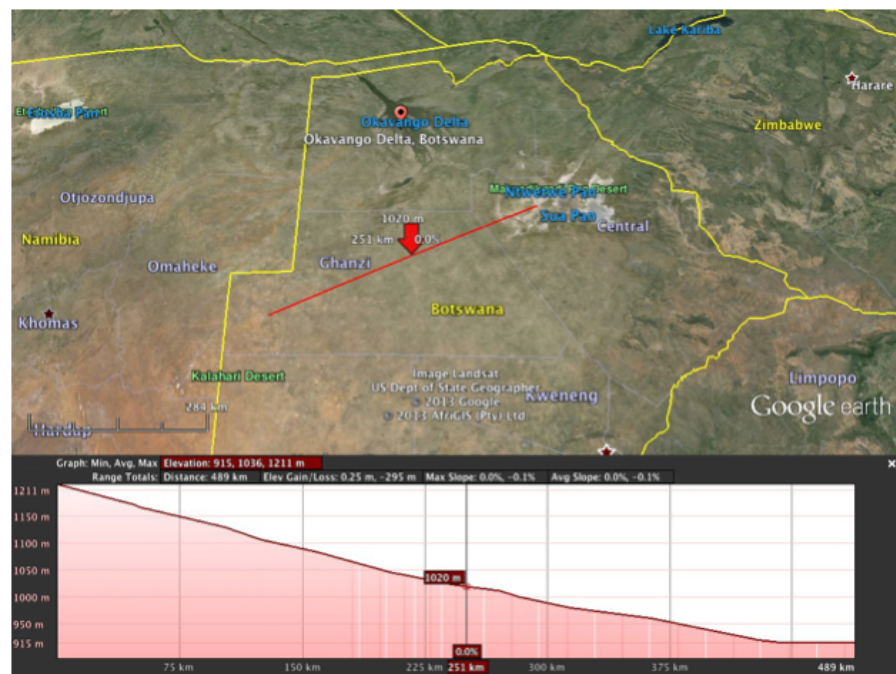


Figure 2.2: Approximately 500 km long cross section studied by De Vries (1984), the water table of which is shown in figure 2.1

# 3 Irreversible transient phenomena

## 3.1 Consolidation

One possible form of volume change is due to reordering of ground particles, which may happen due to an increase of the effective pressure (= grain pressure), and is characterized by the squeezing out water which leads to an irreversible decline of pore space. This phenomenon is called consolidation and leads to land subsidence. The effective stress,  $\sigma_e$ , is the pressure transmitted between the grains. Consolidation is especially well known for clay. In clay, under increased effective stress, micrometer-scale clay plates get reordered and the pore space thus becomes irreversibly smaller.

As long as grain stresses on vertical planes are horizontal, as is the case in undisturbed horizontal sediments, the total vertical stress,  $\sigma_z$ , (in following chapters we will often use the symbol  $p$  instead of  $\sigma_e$ , but they are the same), working on a horizontal plane in the subsoil always equals the total weight above this plane. This weight includes possible loads on ground surface. The total vertical stress  $\sigma_z$  itself is the sum of the water pressure,  $\sigma_w$ , and the effective vertical stress  $\sigma_e$

$$\sigma_z = \sigma_w + \sigma_e$$

If we increase the vertical stress, for instance by loading the surface with a layer of sand, or by filling a surface reservoir, or due to rainwater infiltrating during the winter season, both stresses will change

$$\Delta\sigma_z = \Delta\sigma_w + \Delta\sigma_e$$

If the water pressure changes, while the total weight remains constant, as is the case when we lower the head in a confined aquifer (reflect on why this must be so?), then the water pressure and the effective stress are directly related

$$\begin{aligned} 0 &= \Delta\sigma_w + \Delta\sigma_e \\ \Delta\sigma_w &= -\Delta\sigma_e \end{aligned}$$

Therefore, if we lower the head, i.e. the water pressure, the effective stress increases and the water pressure decreases. This works the other way around in case the head were increased instead of lowered.

It follows that the lowering of the water pressure puts the grains of the porous medium under higher stress, which may, therefore, lead to (irreversible) subsidence in vulnerable soils.

An increased effective stress causes a reduction of the volume of the porous medium and, therefore, also of its pore space. To compensate for this reduced space, water will be squeezed out. The speed at which this happens depends on the conductivity of the compressed layer as well as its thickness, as with thicker layers it takes more time for the compressed water to reach the top or bottom of the layer, from which the water could escape.

Large-scale groundwater extractions have, therefore, led to large subsidences affecting large areas in, among others, Mexico, USA and the UK (figure 3.1 on the next page).

Subsidence can be relatively fast (happening within weeks) or slow (taking place over centuries) on local to regional scales.

Subsidence also occurs as a result of drainage of wetlands and peat areas. Peat means organic soil, which can decay. This lowering of the shallow water table also increases the effective stress as we saw above. This subsidence is especially evident in a low country like the Netherlands, where drainage of wetlands by ditches has taken place for about thousand years.

With regard to organic soils, called peat, it is not only the increase of the effective stress caused by drainage that causes the subsidence. It is also the entry of oxygen that can enter peaty soils when they are drained. This oxygen causes oxidation (“burning”) of the peat, giving an extra boost to the subsidence. Subsidence caused by oxidation may continue until it all peat has disappeared!

The peaty areas in the west and north of the Netherlands have thus subsided several meters (figure 3.2 on page 17). This is why about half the Netherlands lies nowadays below sea level.

In case the original soil layers consisted of alternations of peat and clay, as they often do, the shallow subsoil will consist more and more of pure clay at the top where all peat was burnt away by oxidation, with the original mixture still present below the water table. This clay layer at the top is the collection of all the clay that was present in the original profile, which may have been several meters thick.

## 3.2 Liquefaction

Another irreversible phenomenon involving reordering of grains, is known as liquefaction, which can happen very fast and spectacularly. Liquefaction is associated with pressure waves, or shocks. Fine sand may have been at rest for thousands of years, even with its pore space being greater than according to the most dense packing of the grains. In the case of a shock, for instance due to an earthquake, the sudden change of water pressure may be so great as to cause the effective stress to be zero for a fraction of a second, during which the grains lose their mutual friction. The ground then loses its internal friction and momentarily turns into a quicksand. In fact, it suddenly becomes a dense liquid in which grains float as freely moving particles. The matrix will resettle within minutes at a smaller overall volume. During this resettling, the pore water no longer fits between the grains in their denser packing. As soon as the surplus water has escaped the



Figure 3.1: Over 3 m subsidence in the UK

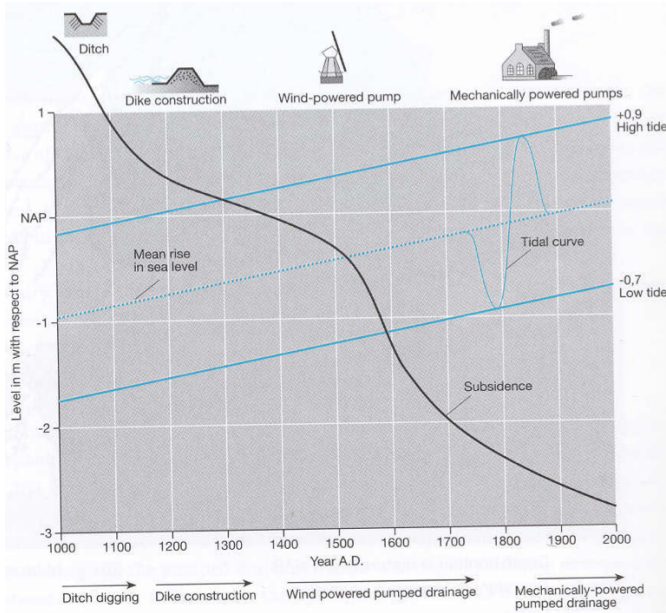


Figure 3.2: Rising sea level since the year 1000 with tide fluctuation curve and subsidence (descending curve) all relative to mean sea level (about NAP). Also shown are water management technologies available over time (From Dufour (1998))

soil resettles and everything sunk into the heavy liquid is stuck forever (see figure 3.3 on the next page <http://www.ce.washington.edu/~liquefaction>)

### 3.3 Intrusion of salt water

In many regions, especially deltaic regions, fresh groundwater floats on saline water, which is heavier (denser) than fresh water. (The difference in density between fresh and ocean water is about 2.5%). The fresh groundwater in the Netherlands is largely floating on salt water as is shown in the cross section in Figure 6. It will generally take several hundred years to a thousand years for a freshwater lens to build up from natural precipitation. The equilibrium may easily be disturbed by extraction of fresh water, but also by construction of harbors, canals and polders. This will cause upconing of salt water from below and lateral intrusion of salt water into aquifers along the coast. Given the time it takes to restore such systems under natural conditions, mining of these systems may be considered irreversible under many practical situations as there are no real means (or sufficient fresh water) to restore the systems within the time horizon of a generation. Good groundwater management is, therefore, essential, but hard to realize in situations of water scarcity.



Figure 3.3: Liquefaction in the USA (<http://www.ce.washington.edu/~liquefaction>)

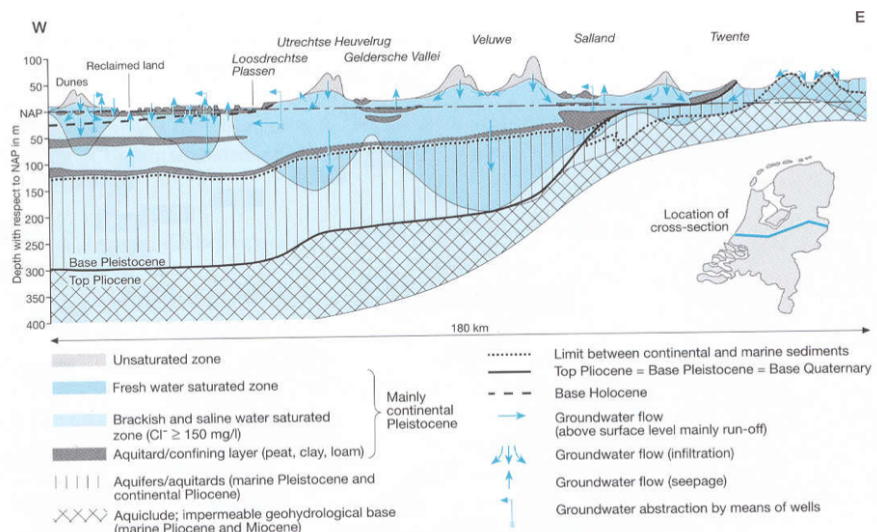


Figure 3.4: Dynamically floating fresh water on salt water in the cross section through the Netherlands. The interface may take hundreds of years to reach its equilibrium. It will continuously adapt to changing circumstances such as climate and sea level rise, as well as to artificial changes in the water cycle (from Dufour (1998), Dufour (2000))

### **3.4 Questions**

1. Mention some processes due to which the subsurface may lose water irreversibly.
2. Explain how these processes work, i.e. what the mechanisms behind them are and under which preconditions they occur.
3. Why would one call extraction of fresh water from a freshwater body floating on salt water irreversible?

# 4 Reversible groundwater storage

In the remainder of this syllabus, we will restrict ourselves to reversible groundwater storage phenomena, i.e. phenomena in which the porous medium is not changed.

In groundwater flow systems, three separate forms of storage may be distinguished:

1. Phreatic storage, which occurs in unconfined aquifers, i.e. aquifers with a free water table. It is due to filling and emptying of pores at the top of the saturated zone.
2. Elastic storage, which is due to combined compressibility of the water, the grains and the porous matrix (soil skeleton). This storage releases or stores water wherever the pressure changes.
3. Sometimes, the interface between fresh water and another fluid (be it saline water, oil or gas) can provide a third type of storage. This works by displacement of the interface, generally between the fresh water and the saline water. When displacing an interface, the total volume of water in the subsurface remains essentially the same, however, the amount of usable fresh water may increase (or decrease) at the cost of saline water, and therefore, one may consider this storage of fresh water.

## 4.1 Phreatic storage (water table storage, specific yield, $S_y$ )

Phreatic storage is due to the filling and emptying of pores above the saturated zone, i.e. above the water table. Because it is related to changes of the water table, it is limited to phreatic (unconfined) aquifers.

The storage coefficient for an unconfined aquifer is called specific yield and is denoted by the symbol  $S_y$ . It is dimensionless, as follows from its definition

$$S_y = \frac{\partial V_w}{\partial h} \quad (4.1)$$

where  $\partial V_w$  is the change of volume of water from a column of aquifer per unit of surface area and  $\partial h$  is the change of the water table elevation.

$S_y$ , therefore, is the amount of water released from storage per square meter of aquifer per m drawdown of the water table.

Hydrogeologists, and groundwater engineers alike, often treat specific yield as a constant. In reality, the draining and filling of pores is more complex and this should be kept in mind in order to judge differences of  $S_y$  values under different circumstances even with the same aquifer material. This will be explained further down.

There is no such thing as a sharp boundary between the saturated and the unsaturated porous medium above and below the water table. In fact, the water content is continuous across the water table.

***The water table is, by definition, the elevation where the pressure equals atmospheric pressure.***

Because we relate all pressures relative to atmospheric, we may say the water table is the elevation where the water pressure is zero (relative to the pressure of the atmosphere).

The simplest conceptual model for the zone above the water table is a vertical straw or radius  $r$  standing with its open end in water. Due to adhesion between the water and the straw, the water level will be sucked upward in the straw against gravity, thereby reaching an equilibrium height  $h$  as shown in figure 4.1.

The soil itself may be considered to consist of a dense network of connected tortuous pores of small but widely varying diameter that may be fully or partially filled with water. Due to adhesive forces, pores may even be fully filled above the water table.

*In pores above the water table the pressure is negative (i.e. below atmospheric).*

If grains can be wetted (attract water), as is generally the case with water, water will be sucked against gravity, into the pores above the water table over a certain height. This height mainly depends on the diameter of the pores.

One can immediately compute the equilibrium of the water in the pore. We have gravity pulling down the water column reaching above the water table, and we have the cohesion force. Hence,

$$\rho gh\pi r^2 = 2\pi r\gamma \cos(\alpha)$$

where  $\rho$  [kg/m<sup>3</sup>] is the density of water,  $g$  [N/kg] is gravity,  $\gamma$  [N/m<sup>2</sup>] is the cohesion stress, and  $\alpha$  the angle between the cohesion stress and the vertical. Hence,

$$h = \frac{2\gamma}{\rho gr} \cos(\alpha)$$

which shows that the suction height  $h$  is proportional to  $1/r$ , the inverse radius of the straw.

In practical situations,  $\alpha$  is small so that  $\gamma \cos \alpha \approx \gamma$ . As  $\gamma$  points is in the direction of the surface tension  $\tau$  (see figure 4.1) where the water surface meets the wall of the straw, we also have

$$\tau \approx \gamma$$

with  $\tau$  the surface tension of the water surface, which equals  $\tau = 75 \times 10^{-3}$  N/m, see any physical handbook or look it up on Wikipedia. Therefore, we can compute the suction head  $h$  immediately given a pore radius.

$$h \approx \frac{2\tau}{\rho gr}$$

Numerically,

$$\begin{aligned} h &\approx \frac{150 \times 10^{-3}}{10^4} \frac{1}{r} \\ &\approx \frac{1.5 \times 10^{-5}}{r} [\text{m}] \end{aligned}$$

If we express  $h$  and  $r$  in mm, (using  $h^*$  and  $r^*$  to indicate mm), we get

$$h^* = \frac{15}{r^*}$$

This implies that water in a pore of 1 mm radius may be sucked up over about 15 mm, and water in a pore with a radius of 0.1 mm over 15 cm and water in a pore with a radius of 0.01 mm radius over 1.5 m. In reality, the suction may be 50% smaller because of the angle  $\alpha$  that was ignored here.

A porous medium has pores of varying diameter, which may conceptually be imagined as in figure 4.2 on the following page. This implies that the line of filled pores will not be sharp. Therefore, the saturation above the water table will gradually decline as shown in the right-hand figure.

The diameter of the widest pores will determine the height fully saturated above the water table, i.e. the thickness of the so-called capillary fringe. In gravel, the capillary fringe will be almost zero, but it may be several decimeters or even meters thick in fine-grained materials such as fine sand, loess, loam and clay. In sands, the capillary zone is usually 15-30 cm thick, depending on the grain size. The thickness of the capillary zone is sometimes visible as a wet zone in the banks of surface water. Note that all water above the water table is under negative pressure.

When the water table is lowered, for instance in a column of sand, and we measure the amount of water drained over time, we see that drainage is not immediate (Figure 4.3). After a couple of days, the drainage rate becomes negligibly small. We may thus call the amount drained during a couple of days the specific yield. It is immediately obvious that specific yield is not a unique physical parameter. The more time we take, the higher the specific yield becomes. It implies that the duration of the test determines the value to some extent. It also implies that a specific yield, when determined from a pumping test of a couple of days duration, is likely to be smaller than that determined from the seasonal fluctuation of the water table.

While the amount of water drained from the subsurface due to lowering of the water table is called *specific yield*, the amount retained in the soil is called the *specific retention*. Together they add up to the soil's porosity (figure 4.4). *Specific retention* is essentially the same as the so-called *field capacity*, i.e. the amount of water the soil can hold against gravity. It is defined as the amount of water retained in an originally saturated soil sample after a few days of free drainage at a suction head of about 200 cm.

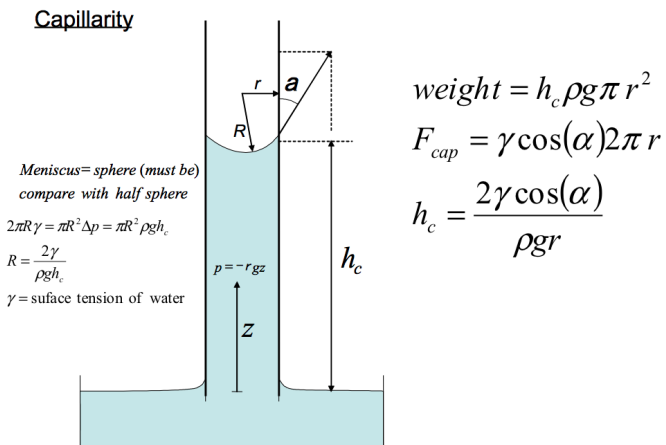


Figure 4.1: Straw of radius  $r$  representing a pore connected to the water table

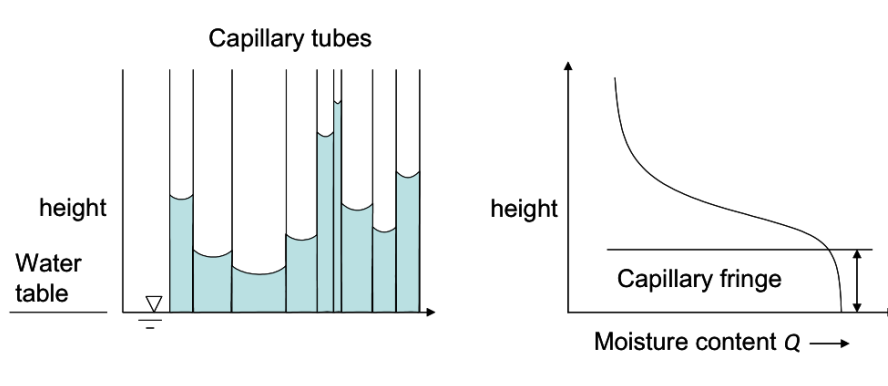


Figure 4.2: A porous medium imagined as a large set of pores of varying diameter

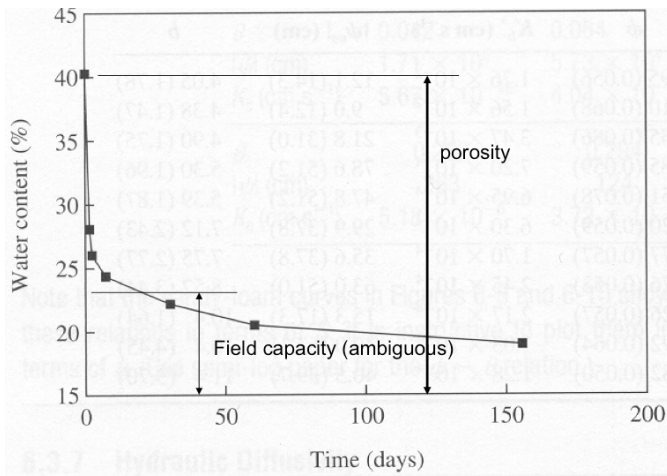


Figure 4.3: Drainage of water from column after lowering the water table

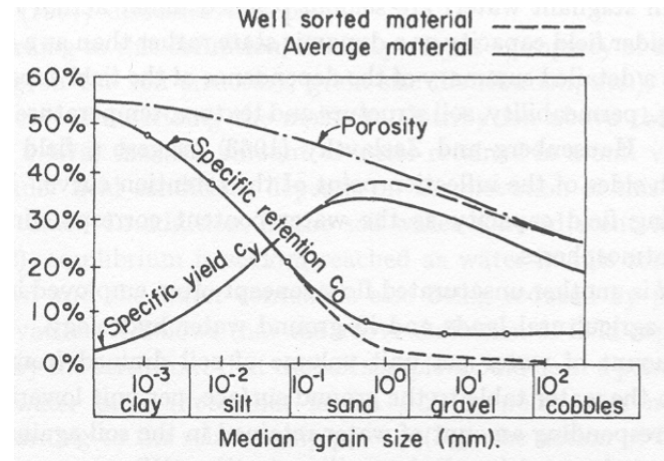


Figure 4.4: Relation between grain size, porosity, specific yield and specific retention (Bear, 1972)

The porosity of porous materials varies, but that of sands is often about 35%. Fine sands tend to have somewhat higher values, while coarse sands tend to have somewhat lower porosities (see figure 4.4). This is related to the ease of compaction at the original time of sedimentation. Smaller grains have a higher surface area and are, therefore, more difficult to compact. In natural gravels, the pore space is often filled by finer grains. This reduces the porosity further. Figure 4.4 shows that for very fine sands, the specific yield declines despite the higher porosity. This is mainly due to the higher specific retention (field capacity) of the finer-grained materials (figure 4.5) as well as to the lower hydraulic conductivity of such fine materials, and, therefore, further reduces their specific yield.

The behavior of water in the unsaturated zone is determined largely by the soil's moisture retention curve of which a number is sketched in figure 4.5 (For the moisture retention curves of the Dutch soils see Wösten et al. (1994)).

These curves relate the moisture content to suction head, i.e. the negative head in the pores. Figure 4.5 gives the general shape of these curves for typical soil materials. Therefore, in the case of perfect equilibrium between suction and gravity, the moisture characteristic curves represent the moisture content in the soil above the water table. The moisture content at 200 cm suction is generally taken as the field capacity. For sandy soils, the moisture content at this suction head is a good measure of the amount of water the soil can hold against gravity under free drainage conditions.

This implies that the moisture content depends on the distance to the water table (i.e. the suction). Hence, the ground surface above a shallow water table tends to be wetter than above a deep water table under otherwise the same circumstances. This must influence the specific yield as illustrated in figure 4.6.

When the water table is lowered, the entire moisture retention curve is lowered as is shown in figure 4.6-a. The specific yield times the difference of the two water tables

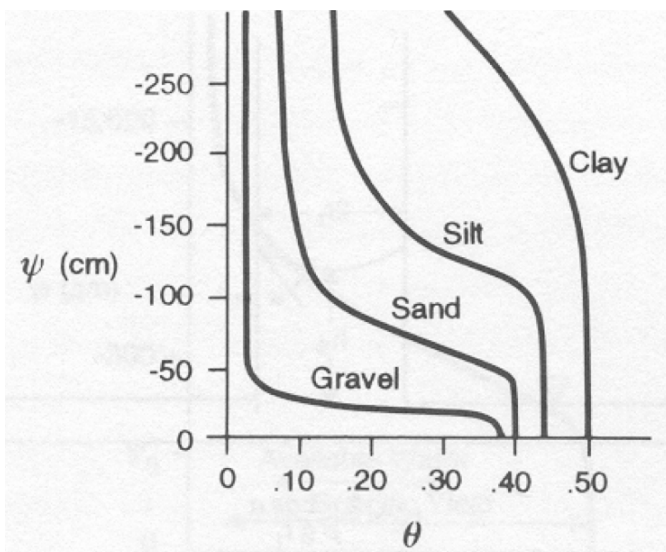


Figure 4.5: Moisture content versus pressure head  $\Psi$ , moisture retention curves (Bear, 1972).

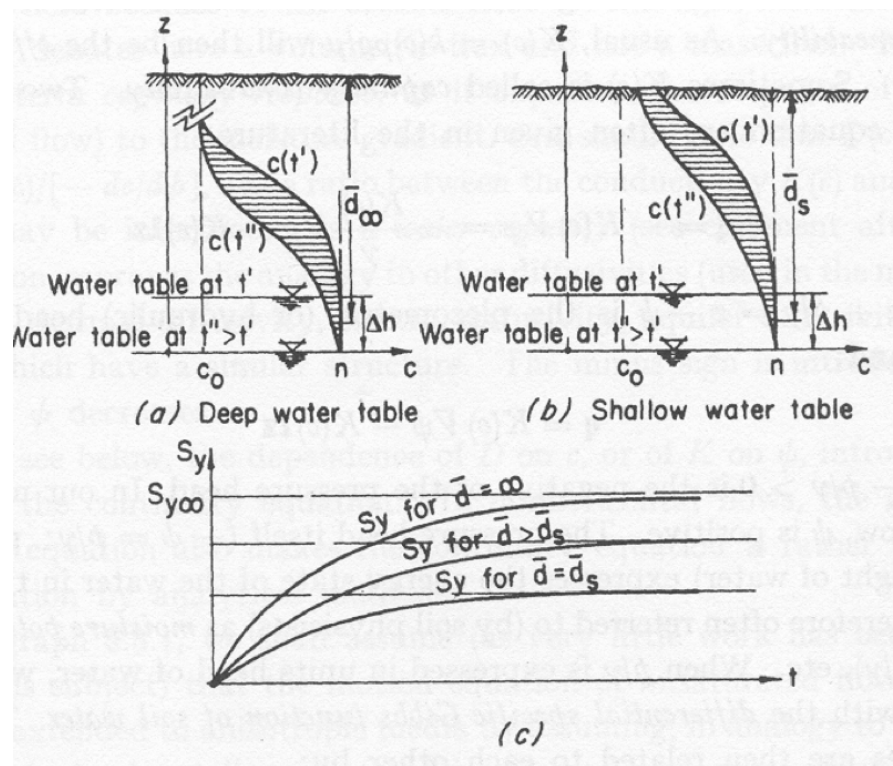


Figure 4.6: Influence of depth and time on specific yield (Bear, 1972)

equals the water from the hatched area times. It demonstrates that the entire unsaturated profile is involved in the specific yield. As already mentioned and shown in figure 4.6-c, specific yield increases with available drainage time.

If the water table is shallow (and the soil material is fine), a major part of the *moisture retention curve* will be cut off at ground surface as is shown in figure 4.6-b. Lowering of the water table will thus miss a portion of the hatched area of 4.6-a. Therefore, the specific yield is smaller the shallower the water table is. This is also shown in figure 4.6-c.

We should thus not be surprised to find that the same fine dune sand may have a specific yield of 22% inside a large dune area, where the water table is usually several meters below ground surface, and only 8% in an adjacent flower bulb field with the same sand, but with a water table of only 60 cm below ground surface.

Soil characteristics may vary between wide limits. Generally, the coarser the soil, the thinner the capillary fringe (see Figure 11). A complication is that the moisture characteristic curves differ during wetting and drying. This phenomenon is called hysteresis, but this is beyond this course.

Groundwater hydrologists dealing with saturated groundwater usually just use a single constant value for the specific yield in their formulas and models. The specific yield can be estimated from the soil in question, from moisture characteristic curves, in the laboratory, from field measurements, from pumping tests or groundwater-model calibration.

Even though this approach may seem doubtful or just wrong in the eyes of some, using a constant but appropriately chosen specific yield works remarkably well in practice. It is more a matter of realizing oneself when a constant specific yield of a certain value is not applicable. The above outline is meant as a help in deciding on this and to consciousness about what is behind this “simple” hydrologic parameter that we denote by the symbol  $S_y$ .

Some groundwater models, like MODFLOW, have an option to vary specific yield automatically with water-table depth.

#### 4.1.1 Phreatic responses

By sensitive continuous measurements of the phreatic head, daily variations in evapotranspiration can be often determined. While in the past the groundwater head could be gauged continuously on paper only, modern head loggers may register the head at short regular intervals and store large amounts of data internally for later use. With such instruments, accurate data become widely available and allow more detailed views on phenomena to be studied and analyzed. Such measurements are already known from Todd (1959) also printed in Todd and Mays (2005). Figure 4.7 shows the daily fluctuation of the water table due to daily evapotranspiration measured more than sixty years ago. However, we find such fluctuations in all frequent registrations of shallow water tables under summer circumstances.

If the specific yield is known, evapotranspiration rates can sometimes be determined from such water-table registration. This can be demonstrated on the hand of these old

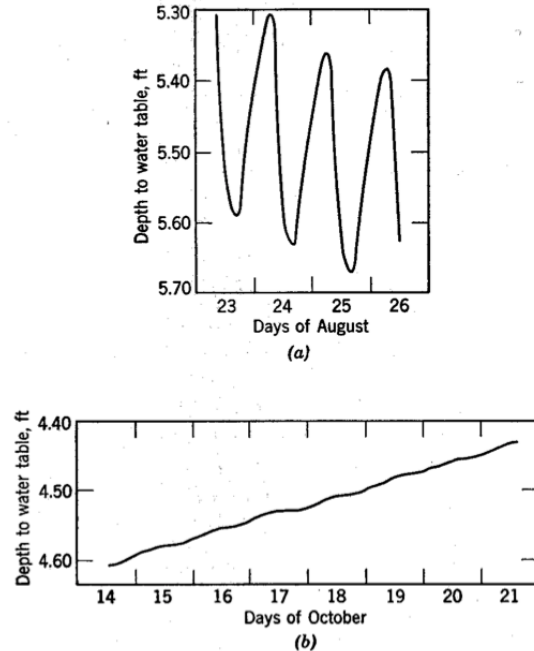


Figure 4.7: Measured water-table fluctuations due to evapotranspiration variations Todd and Mays (2005)

measurements (figure 4.7 and figure 4.8). The groundwater balance at this point may be expressed as

$$\bar{N} + N(t) = S_y \frac{\partial \phi}{\partial t}$$

where  $\bar{N}$  is the long-term trend of the net water-table recharge (positive or negative, i.e. precipitation minus evapotranspiration from the water table).  $N(t)$  is the short-term variation (during the day). So if one plots the derivative of the water table in a point versus time, it may be split into a more or less constant (long-term) trend and a the remainder due to short-term (daily) variation. If this short-term variation can be attributed to evapotranspiration from the water table, as it obviously is the case in the figure, one may determine it by taking the surface area between the measured head curve and its long-term trend, multiplied by the specific yield (hatched surface in figure 4.8).

#### 4.1.2 Questions

1. What is the dimension of specific yield? What is the dimension of the elastic storage coefficient. What is the dimension of the specific storage coefficient?
2. How do specific retention, specific yield and porosity relate to each other?
3. How does porosity relate to grain size in general, and what is the reason?

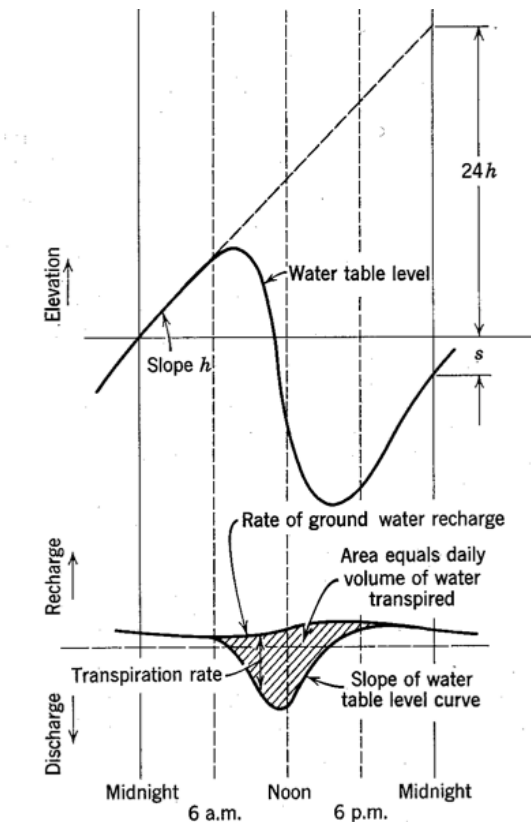


Figure 4.8: Determining the evapotranspiration from water-table variations and a given specific yield Todd and Mays (2005).

4. Given another term for specific retention, one that is generally used in agriculture.
5. How does specific retention relate to grain size?
6. If the water table is lowered, which water is released around or above the water table?
7. What is the definition of the unsaturated zone?
8. Is it likely that the water from a rain shower easily infiltrates through worm and rabbit holes? If so explain why. If not also explain why?
9. What is a probable value for specific yield in a sand with porosity of 35%? And why?
10. How does capillary zone relate to air-entry pressure?
11. What is actually measured with the air-entry pressure?
12. How does the specific yield relate to the depth of the water table?
13. Using the model of a straw, how does capillary rise relate to the straw radius and the water surface tension?
14. Given a grain diameter of 0.2 mm, a radius that is 1/7th of this radius, and a water surface tension  $\gamma = 75 \times 10^{-3} \text{ N/m}$ , what would be the capillarity rise if the angle of the water surface and the straw is assumed to be zero?

## 4.2 Elastic Storage

### 4.2.1 Introduction

Till now, we only considered storage at the water table and gave very simple, but practical examples largely ignoring spatial dimensions. Spatial dimensions will be dealt with later. In this section, we handle the physics of elastic storage and will give some interesting everyday examples that are sometimes easily overlooked.

Elastic storage is the only storage occurring in confined and semi-confined aquifers, i.e. in aquifers without a water table, meaning aquifers that are completely filled with water from floor to ceiling. In such aquifers, we have no lowering of the water table whatsoever, unless the head is lowered to beneath the ceiling of the aquifer, a case further ignored here.

Therefore, in confined aquifer storage can only result from compression of the water and depression of the aquifer. The compressibility of the water and the grains themselves is quite obvious, but often the less obvious storage is the most important part. This is the deformation of the soil skeleton, the bulk matrix or the (bulk) porous medium as it is called.

### 4.2.2 Loading efficiency

To analyze the physics of elastic storage, we start with noting that the total load at any depth is carried by the total (vertical pressure)  $\sigma_z$  or  $p \text{ N/m}^2$ . This total pressure must equal the sum of the vertical grain pressure (the so-called effective stress,  $\sigma_e$ ) and the water pressure  $\sigma_w$

$$p = \sigma_e + \sigma_w$$

This is indicated in figure 4.9. The brown horizontal beams and the springs in this figure are imaginary; they replace the volume  $V_0$  (1 m<sup>3</sup> say) that has been cut out of the aquifer. The two imaginary springs have the same properties as the water and the porous medium respectively. Let us see what happens when the pressure is increased by  $\Delta p$ .

In that case, the volume (or height)  $V_0$  is reduced by  $\Delta V$  and the springs pressures are increased by  $\Delta\sigma_w$  and  $\Delta\sigma_e$  respectively. The springs have a different stiffness, so  $\Delta\sigma_w \neq \Delta\sigma_e$ . However, each string will always carry a fixed proportion of the total stress. Therefore, we may write

$$\Delta\sigma_w = LE \Delta p$$

where  $LE$  is this fixed proportion and is called the *loading efficiency*. The  $LE$  must obviously lie between 0 and 1 and is fixed for any particular porous medium. So if we put a weight, like a layer of sand, on ground surface,  $p$  in figure 4.9 will increase by  $\Delta p$ , a change that is equal to the weight of the layer of sand per m<sup>2</sup> placed on ground surface. We may then say  $\Delta\sigma_w = LE \Delta p$ , where the loading efficiency  $LE$  is a fixed number between 0 and 1, specific to a aquifer in question. If we have a piezometer in the

aquifer, we'll notice that the water level (hence, the head) has risen by placing the sand on ground surface. The head rise is given by

$$\Delta\phi = \frac{LE}{\rho g} \Delta p$$

Now assume that  $\Delta p$  is not due to a layer of sand placed on ground surface, but due to a change of the barometer pressure as in figure 4.11. Then the same reasoning applies, because the subsoil cannot know the difference between a pressure change due to a layer of sand placed on ground surface or due to an equivalent rise of the barometer pressure.

A nice and famous early example of loading efficiency is the impact of a train stopping at a station and leaving again some time later (figure 4.10). The weight of the locomotive compresses the aquifer a bit, thus reducing its pore space. This in turn compresses the groundwater, which cannot readily escape. Hence, its pressure rises and it starts to flow sideways, so that the pressure gradually decreases towards its original trend. When the train leaves, the opposite occurs. The removal of the load reduces the effective stress, which causes the aquifer to bounce back, providing more pore space to the water, which depressurizes and increases somewhat in volume. This reduced water pressure causes surrounding groundwater to flow inward to fill up the gap due to which the pressure gradually normalizes.

*Q: Think of another way for the water to escape from a semi-confined aquifer.*

#### 4.2.3 Barometer efficiency

Figure 4.11 left shows the situation where the pressure increase is caused by a load (of sand) on ground surface; the right-hand picture shows how the same pressure increase is caused by an increase of the barometer pressure. The question is, how does the change of the barometer pressure alter the head (water level) in the piezometer?

As said above, for the pressure in the aquifer there is no difference between the two pictures. However, there is a difference between the head (i.e. the water level) in the piezometer in the left picture and in that of the right picture. When placing a layer of sand on ground surface, the pressure on the water surface in the piezometer does not change. However, when the barometer pressure changes, the pressure on the water surface in the piezometer does change. That change is, of course, exactly equal to the change of the barometer pressure. To see how the head changes due to a change of the barometer pressure let us just write out the water pressure at the bottom of the piezometer. It is clear that this pressure changes due to the change at ground surface such that  $\Delta a = \Delta p$ , with  $\Delta a$  the change of the barometer pressure.

Now assume that the head (i.e. the water level) in the piezometer changes by an amount  $\Delta\phi$ . The change of the water pressure at the bottom of the piezometer then is

$$\Delta\sigma_w = \rho g \Delta\phi + \Delta a$$

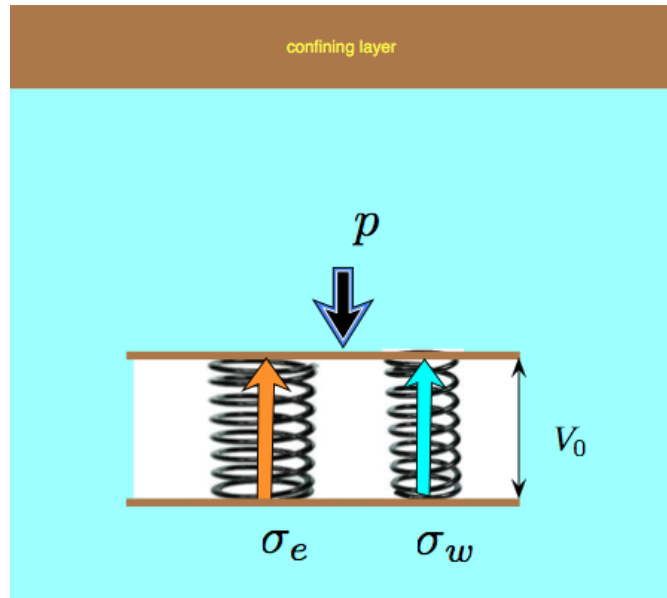


Figure 4.9: The weight of the ground plus water is supported by two pressures, the water pressure  $\sigma_w$  and the effective pressure  $\sigma_e$

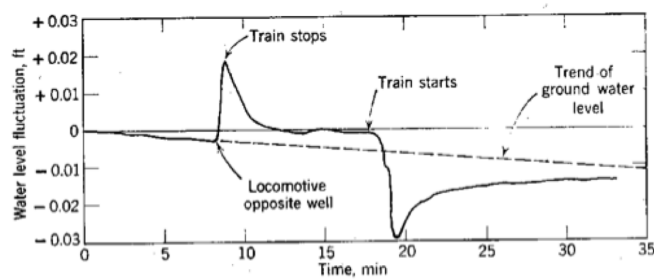


Figure 4.10: Water level fluctuation in a confined aquifer produced by a train stopping near an observation well [Todd (1959), Todd and Mays (2005)]

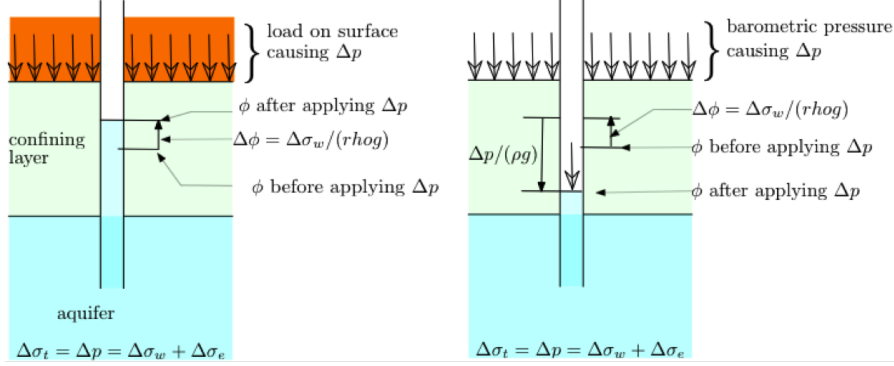


Figure 4.11: Effect on head in confined aquifer by a load  $\Delta p$  on surface versus an increase of the barometric pressure.

But we already know the change of the water pressure

$$\Delta\sigma_w = LE \Delta a$$

Hence,

$$\rho g \Delta\phi + \Delta a = LE \Delta a$$

and so

$$\begin{aligned} \rho g \Delta\phi &= -(1 - LE) \Delta a \\ &= -BE \Delta a \end{aligned}$$

where  $1 - LE$  is called the *barometer efficiency*,  $BE$ . Just like the loading efficiency, the barometer efficiency varies between 0 and 1.

The minus sign indicates that the head in the piezometer declines when the barometer goes up. This should be obvious as the the water pressure increases by  $LE \Delta a$  which is a fraction of the barometer pressure, which would cause the water level in the piezometer to rise, but at the same time the full barometer pressure pushes on the water table in the piezometer, which causes the water level to decline accordingly. Together, the net effect is a decline of the head in the piezometer by  $BE \Delta a$ , a fraction of the barometer pressure change.

From the equivalence of the previous equation couple, it follows that

$$BE + LE = 1$$

A famous example of the barometer efficiency was given by [Todd (1959), Todd and Mays (2005)], figure 4.12. This example is used here because it is famous as one of the first-ever published. However, barometer effects are always seen in piezometers in confined aquifers. The barometer efficiency generally varies between 20% and 80%.

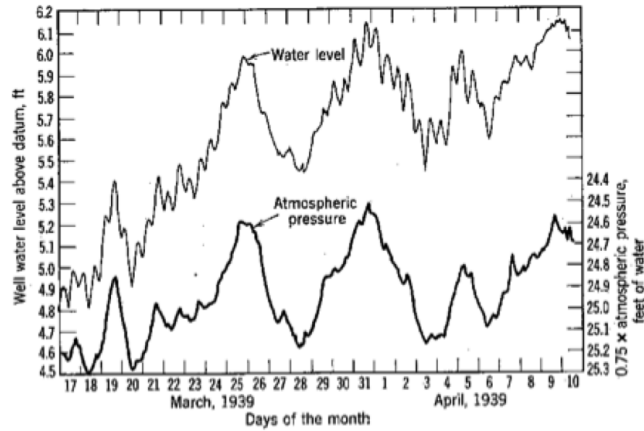


Figure 4.12: Example of a high degree (75%) of barometric efficiency [Todd (1959), Todd and Mays (2005)]. It shows the response of the head in a well penetrating a confined aquifer together with the barometric pressure. Note that the axes on the right is reversed to show the similarity of the two curves (head down when barometer pressure goes up and vice versa).

The barometer influence causes a normally observed noisy behavior of the head time series from confined and semi-confined aquifers. This noisy behavior occurs also when groundwater is in perfect rest. Barometer pressure fluctuations do affect both the head measured in piezometers as the pressure measured in pressure gauges. Only if heads are measured at short time intervals of hours rather than weeks, would the noisy behavior of the head in confined aquifers actually show its clear one-to-one relation with the course of the barometer pressure. Therefore, such a noisy time series behavior actually shows that a piezometer is in a (semi-)confined aquifer. Unless we have very thick unsaturated zones with substantial resistance against air flow, we will not see much if any barometer fluctuation in water-table aquifers ([Rasmussen and Crawford (1997)]).

#### 4.2.4 How much are the loading efficiency and the barometer efficiency when expressed in the properties of the water and the porous medium ?

If the total pressure  $p$  is increased by  $\Delta p$ , the porous medium is compressed together with the water that it contains. Clearly, the increase of the water pressure will also compress the individual grains. However, sand grains are about 50 times less compressible than water. Therefore, the effect of the grains being compressed themselves can be safely neglected.

On the other hand, the porous medium (the skeleton of grains) itself is far less stiff than the grains themselves. The porous medium is essentially compressed due to some deformation of the grains at the expense of the porosity of the medium. In fact, as it turns out, the compressibility of the porous medium is of the same order of magnitude

as that of the water, so they must both be taken into account.

Hence, the volume  $V_0$  is compressed by  $\Delta V$  when the pressure  $p$  is increased by  $\Delta p$ .

Assume the aquifer to be of infinite lateral extent, so that the only possible compression is downward. This implies that  $\Delta V = \Delta H$ , which is the change of the thickness of the considered part of the layer that we replaced by the springs in figure 4.9. Hence, both springs underlie the same compression  $\Delta H$ .

Let the water have a compressibility  $\alpha$  meaning that a  $m^3$  of water would be compressed by the fraction  $\alpha$  for each increase of the water pressure by  $1\text{ N/m}^2$ . Similarly, let the porous medium have a compressibility of  $\beta$ , meaning that one  $m^3$  of the porous medium would be compressed by the factor  $\beta$  for each  $N/m^2$  increase of effective stress,  $\sigma_e$ . These compressibilities, therefore, have dimension  $m^3/m^3/(N/m^2) = m^2/N$ .

Now consider that the soil was put under an extra total pressure of  $\Delta p$  causing it to be compressed by the fraction  $\Delta H/H_0 = \Delta V/V_0$ . Then the effective pressure increases due to this compression  $\Delta H$  by

$$\Delta\sigma_e = -\frac{\Delta V/V_0}{\beta}$$

Because the grains are considered incompressible, it follows that the change of pore volume equals the change of the total volume. Therefore, for the water we have a relative volume change (= compression) of  $\Delta V$  per  $\epsilon V_0$ . Therefore, the water pressure increase is

$$\begin{aligned}\Delta\sigma_w &= \frac{\Delta V/(\epsilon V_0)}{\alpha} \\ &= \frac{\Delta V/V_0}{\epsilon\alpha}\end{aligned}$$

Because we have now related both  $\Delta\sigma_w$  and  $\Delta\sigma_e$  to the relative volume change  $\Delta V/V_0$ , we also know the ratio between the change of the effective pressure and the water pressure

$$\frac{\Delta\sigma_e}{\Delta\sigma_w} = \frac{\epsilon\alpha}{\beta}$$

and so

$$\Delta\sigma_e = \frac{\epsilon\alpha}{\beta} \Delta\sigma_w$$

With this, we can eliminate  $\Delta\sigma_e$  from the pressure equation:

$$\Delta p = \Delta\sigma_w + \Delta\sigma_e$$

to obtain

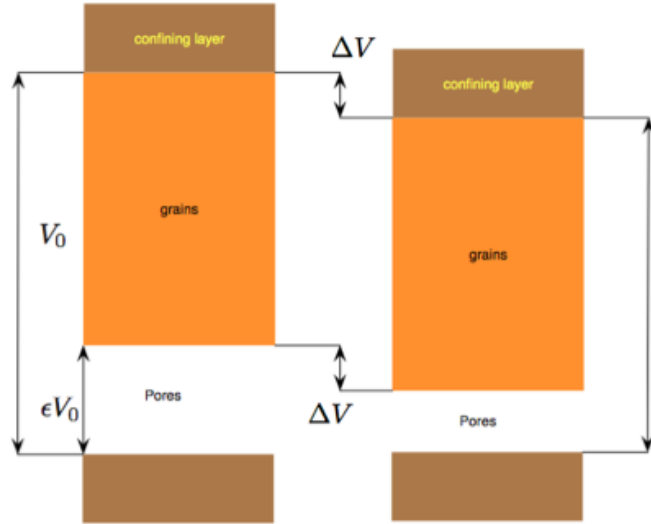


Figure 4.13: Compression of the porous medium, while the volume of the grains remains unchanged because their compressibility is negligible compared to that of both the water and the porous medium.

$$\Delta p = \left(1 + \frac{\epsilon\alpha}{\beta}\right) \Delta\sigma_w$$

And because  $\Delta\sigma_w/\Delta p = LE$  we have

$$LE = \frac{\beta}{\beta + \epsilon\alpha}$$

And because  $BE = 1 - LE$  we also have

$$BE = \frac{\epsilon\alpha}{\beta + \epsilon\alpha}$$

#### 4.2.5 Specific (elastic) storage coefficient

The specific storage coefficient is

$$S_s = -\frac{\partial V/V_0}{\partial \phi} \quad (4.2)$$

it is the volume of water released from the porous medium per m of lowering of the head  $\phi$  (a negative  $\Delta\phi$  yields a positive amount of water). It is also immediately clear that the dimension of  $S_s$  is  $(m^3/m^3)/m = m^{-1}$ , the volume of water released per  $m^3$  of the porous medium per m of head decline.

Now consider the situation in which we lower the water pressure, for instance by extracting water from the aquifer. Lowering of the water pressure in no way changes the total pressure. Therefore,  $\Delta p = 0$ , which yields

$$0 = \Delta\sigma_w + \Delta\sigma_e \quad (4.3)$$

However, the amount of water squeezed out of the porous medium changes. A lowering of head causes an increase of the effective pressure (grain pressure), and, hence, is associated with a compression of the porous medium. Therefore, an increase of the effective pressure ( $\Delta\sigma_e > 0$ ), reduces the pore volume by  $\Delta V$  due to which the same volume of water is squeezed from the porous medium

$$\Delta V_{pm} = +V_0\beta\Delta\sigma_e$$

where *pm* means "porous medium".

An increase of the water, would cause a compression of the water within the pores  $\epsilon V_0$ , by

$$\Delta V_w = -\alpha(\epsilon V_0) \Delta\sigma_w$$

The total amount of water released equals the volume squeezed out due to the reduction of the pore space plus the volume that is generated by expansion of the water due to the reduction of the water pressure:

$$\Delta V = -\alpha(\epsilon V_0) \Delta\sigma_w + V_0\beta\Delta\sigma_e$$

and because  $\Delta\sigma_e = -\Delta\sigma_w$  in this case (see equation 4.3) we have

$$\frac{\Delta V}{V_0} = -(\alpha\epsilon + \beta)\Delta\sigma_w$$

and so

$$\frac{\Delta V/V_0}{\Delta\sigma_w} = -(\epsilon\alpha + \beta)$$

using  $\Delta\sigma_w = \rho g \Delta\phi$  yields

$$S_s = -\frac{\Delta V/V_0}{\Delta\phi} \quad (4.4)$$

$$= \rho g (\epsilon\alpha + \beta) \quad (4.5)$$

which, considering that we reduce the  $\Delta$  to the infinitesimally small  $\partial$ , completes the proof (see equation 4.2).

#### 4.2.6 Application (not for exam)

The compressibility of water is

$$\alpha = -\frac{1}{V_{w,0}} \frac{\partial V_w}{\partial \sigma_w} [L^2/F]^2$$

where  $\alpha \approx 4.4 \times 10^{10} \text{ m}^2/\text{N}$ . Clearly,  $\partial V_w/V_{w,0}$  is the relative change of the water volume. There is some dependency on dissolved components, water containing dissolved gas, may be up to three times more compressible than water without dissolved gas under normal pore pressure (Lyons, William C. (2010): Working Guide to Reservoir Engineering; Elsevier).

The compressibility of the porous medium is

$$\beta = -\frac{1}{V_{T,0}} \frac{\partial V_T}{\partial \sigma_e}$$

where  $\partial V_T/V_{T,0}$  is the relative change of the volume of the porous medium.  $V_T$  is, the total volume of the considered soil (including its pores).  $\sigma_e$  is the effective stress (=pressure), i.e. that part of the total stress,  $p$ , that is not carried by the water pressure  $\sigma_w$ . The total pressure equals the weight of the overburden, i.e. that of the overlying formations including the water that it contains. Hence  $\sigma_e = p - \sigma_w$ .

The soil compressibility  $\beta$  is the gradient of a stress-strain curve (relative volume change as a function of effective stress) of a dry soil sample put under increased stress in the laboratory, such that side-ward movement is prevented, exactly as it is the case in the actual aquifer under uniform vertical stress. Unlike water, the compressibility of soil is not necessarily a constant. If the soil is put under higher stress than it ever supported, then it consolidates, meaning that the change of volume is largely irreversible. But under lower than historic stresses, a compressibility can be determined, and truly elastic behavior can be assumed. It is clear that this compressibility depends on porosity.

[Van der Gun (1980)] presented the following relation between the compressibility of aquifers and depth based on laboratory measurements carried out by Van der Knaap (1959)

$$\beta = \epsilon (3 \times 10^{-11} + 6.6 \times 10^{-11} z^{-0.7}) \quad (4.6)$$

where  $z$  is the depth below ground surface and  $\epsilon$  is porosity. Then applying 4.4

$$S_s = \rho g (\epsilon \alpha + \beta)$$

With the relation of [Van der Gun (1980)], we obtain the graphs shown in 4.14. As can be concluded from the graph, values in the order of  $10^{-5} \text{ Pa}^{-1}$  are often found in practice, where we generally have porosities of around 35% in fluvial and eolian sandy aquifers.

*Question:* Is it feasible that compressibility of the porous medium is proportional to porosity?

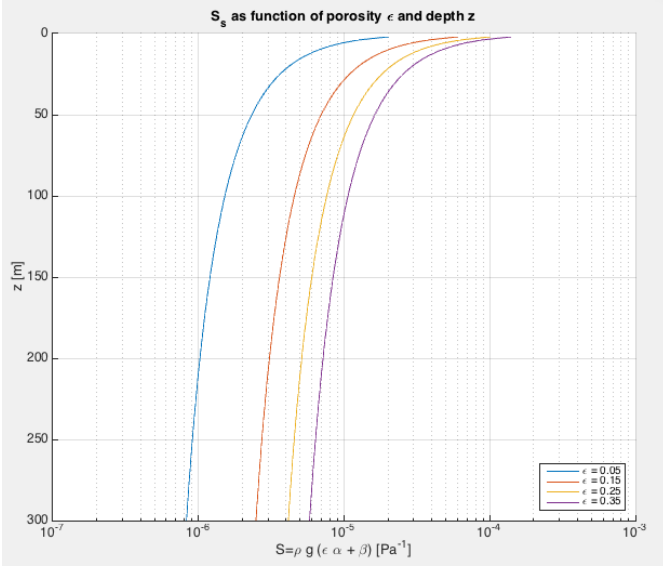


Figure 4.14: Computed specific storage coefficient  $Ss = \rho g (\epsilon\alpha + \beta) [\text{m}^{-1}]$  as a function of depth below ground surface using the relation by [Van der Gun (1980)])

#### 4.2.7 Questions

1. Explain what loading efficiency is.
2. What factors contribute to the elastic storage coefficient and what factor may be neglected?
3. If a load  $\Delta p$  is placed on top of a confined aquifer and the water pressure in the aquifer is increased to  $\Delta\sigma_w = LE \Delta p$ , then how much does the head change in a piezometer in that aquifer?
4. The same question for the situation where  $\Delta p$  is caused by an increase of the barometer pressure.
5. Assume we have a pressure gauge (often also called pressure transducer or pressure sensor) in a piezometer in the confined aquifer that measures the absolute pressure (i.e. the atmospheric pressure + the water pressure). On day 1, the barometer rises by  $\Delta p$  and is constant thereafter. Later, a load  $\Delta p$  is placed on ground surface. What is the difference, if any, in the registration done by the pressure gauge in the piezometer, and what is the difference with the hand-measured head in the piezometer?
6. The measurements by pressure gauges in confined and semi-confined aquifers are corrected for barometer pressure changes by subtracting the barometer pressure from the measured pressure. Does this mean that the fluctuations of the barometer pressure are eliminated by this correction? If so, explain why. If not, also explain why.

7. What is actually the result of this correction of the registered pressures? What actually do we get by this correction?
8. How can we compute the specific elastic storage coefficient  $S_s$  from the measured barometric efficiency? Note:

$$BE = 1 - \frac{\beta}{\epsilon\alpha + \beta}$$

$$Sy = \rho g(\epsilon\alpha + \beta)$$

Think of what we can easily estimate and what we know, respectively what we don't know? Assume that porosity  $\epsilon$  can be reasonably well estimated.

9. Consider a confined aquifer and the following two situations. First there is a loading at ground surface with value  $\Delta p$ . The head is measured both in a piezometer and in a pressure gauge (which measures the absolute water pressure in the aquifer). What is the difference between the two measurements?
10. In the same location, consider an increase of the barometer pressure that is of the same magnitude as the surface loading  $\Delta p$  before, so  $\Delta a = \Delta p$ . What is the difference in the head measured with a piezometer and that measured with a pressure gauge?
11. What is the difference between the heads measured with the piezometer in the two cases?
12. What is the difference between the pressures measured with the pressure gauges in the two cases?
13. How much is the barometer effect in an unconfined aquifer?
14. How will the head or pressure in a piezometer in a semi-confined aquifer after a uniform surface load was put on the ground surface? Think of compression and leakage through the overlying aquitard.
15. What aquifer parameter might we derive from this behavior? Think of the leakage.
16. With two pressure transducers, one measuring the barometer pressure and the other the water pressure in some piezometer in a confined aquifer, how can we compute the barometer efficiency? What parameter do we still miss to obtain true numerical values?
17. How does the head in a water-table aquifer react to barometer fluctuations?
18. How large may the variation of the head due to barometer fluctuations become given a range of atmospheric pressure from variation between 970 to 1040 mbar (=cm head)?

19. What values do you expect for total elastic storage coefficients of aquifers in practice?
20. How could we measure the elastic storage coefficient in a confined aquifer below the sea bottom?
21. Does the value of the specific yield that we may derive from barometer efficiency, water storativity and porosity refer to the value of the measuring point or to the thickness of the entire aquifer?
22. How useful is it to measure local porosity at the screen position of the piezometer to compute the storage coefficient of the aquifer?

### 4.3 Earth tides (not for exam)

Even far from the ocean and even after correcting for varying barometer pressures, the groundwater head in confined aquifers may show a response that closely resembles tides. This fluctuation matches the passage of the sun and the moon due to a rotating earth , exactly like it is the case with sea tides, ([[Todd \(1959\)](#), [Todd and Mays \(2005\)](#), [Bloemen et al. \(1989\)](#)]), Figure 4.15.

Like normal tides, earth tides are an indirect consequence such gravity variations. It can be shown that they are caused as an indirect effect of the deformation of the earth's mantle on which the stiff crust floats. A bulge is formed by the mantle by the attraction of the sun and the moon. The earth crust itself is so thin compared to the earth mantle that it behaves like a thin hard sheet floating on the mantle and is stretched by the mantle as it bulges out under tidal attraction. During stretching, porosity increases and the head lowers. When the stretching is released, the opposite occurs as is shown in equation 4.15.

This variation may be estimated with up to 50% accuracy from solid earth-tide theory [?]. The dilatation (stretching) is more or less fixed due to the relation with the mantle, but different, for any point on earth. According to [[Bredehoeft \(1967\)](#)] it is about

$$\Delta\phi \approx \frac{10^{-8}}{S_s}$$

at moderate latitudes. Using this number, one may relate the expected magnitude of the water-level fluctuations directly to the specific storage coefficient. With  $S_s$  in the order of  $10^{-6}/m$  for sandstones and  $10^{-7}/m$  for granites, a fluctuation amplitude of 1 to 10 cm may be expected.

A thorough analysis of earth tides is beyond the scope of this course. There is a wealth of literature on the subject; a good quantitative paper is [[Kamp and Gale \(1983\)](#)].

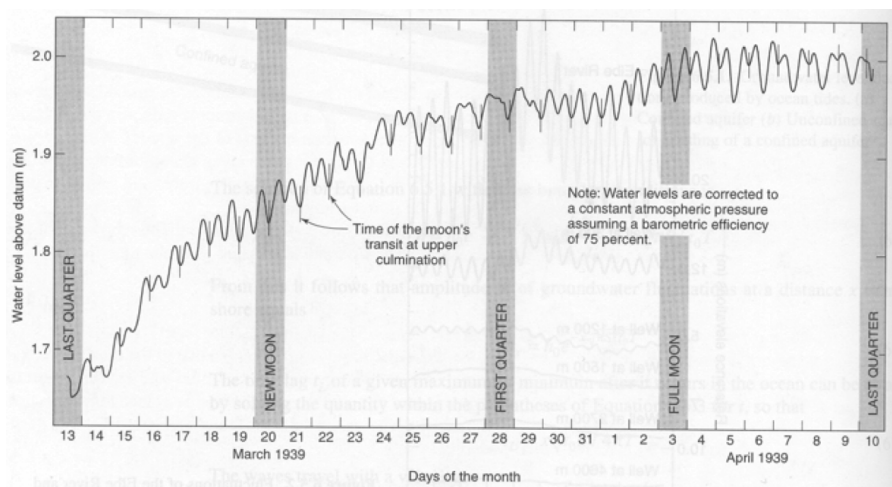


Figure 4.15: Water level fluctuations in a confined aquifer produced by earth tides (from [Todd (1959), Todd and Mays (2005)])

# 5 One-dimensional transient groundwater flow

## 5.1 Scope

In this course, we will deal with transient groundwater flow in one-dimensional and radial situations (wells) for which analytic solutions are available. Analytic solutions are important because they allow insight in the behavior of the groundwater system, whereas numerical solutions do not; they only produce numbers. Analytic solutions are also important because they allow checking numerical models and checking numerical models is always necessary, not just because of possible errors in the model, but also because of possible errors in the input of the model. Analytical solutions also allow analysis of numerical models, which helps to understand their outcome. Finally, analytical solutions are powerful because they allow a rapid result with minimal input. They become even more powerful if combined with superposition and convolution.

## 5.2 Governing equations

We will always start our discussion with the governing differential equation at hand. Once we have it, we need to solve it. To be able to do that we need boundary conditions specifying fixed heads or fixed discharges along certain parts of the model boundaries. In the case of transient solutions, we also need initial conditions that specify the head everywhere in the considered domain at time zero. Initial and boundary conditions are as important as the differential equation itself.

One-dimensional flow means a cross section with no-flow components perpendicular to it.

We will treat analytical solutions for one layer only. Analytical solutions for more than one layer exist and have been extended to arbitrary numbers of layers in the 1980s by Kick Hemker and Kees Maas, see for instance Maas (1986) and Hemker and Maas (1987). These solutions require matrix computations, which were cumbersome at the time, but which may nowadays be readily computed in programs like Python. Nevertheless, we limit ourselves in this course to single-layer cases.

Let us first derive the partial differential equation, starting with continuity. Considering a small portion of length  $\Delta x$  the cross section, the water balance over a short time  $\Delta t$  may, can be expressed as follows:

$$\left[ Q_x - \left( Q_x + \frac{\partial Q_x}{\partial x} \Delta x \right) \right] \Delta t + N \Delta x \Delta t = S \Delta x (\phi_{t+\Delta t} - \phi_t)$$

with  $Q$  [ $L^2/T$ ] the discharge in the aquifer integrated over its full height,  $N$  [ $L/T$ ] recharge and  $S$  [–] the storage coefficient. Taking the limit for  $\Delta x \rightarrow dx$  and  $\Delta t \rightarrow dt$  yields the continuity equation

$$-\frac{\partial Q}{\partial x} + N = S \frac{\partial \phi}{\partial t} \quad (5.1)$$

Inserting Darcy's law, with  $Q = -kD \frac{\partial \phi}{\partial x}$  yields the governing partial differential equation

$$-\frac{\partial}{\partial x} \left( -kD \frac{\partial \phi}{\partial x} \right) + N = S \frac{\partial \phi}{\partial t} \quad (5.2)$$

and with  $kD$  being considered a constant, we obtain

$$\frac{\partial^2 \phi}{\partial x^2} + \frac{N}{kD} = \frac{S}{kD} \frac{\partial \phi}{\partial t} \quad (5.3)$$

We will predominantly ignore the recharge, so  $N = 0$  in the previous equation. Ignoring the recharge is seldom a issue because we can solve most of our groundwater problems using superposition and deal with recharge separately if needed. Further notice that we may write  $s(x, t) = \phi(x, t) - \phi_0$  where  $s(x, t)$  is the head change relative to the initial situation  $\phi_0$ , which may even depend on  $x$ .

This means that for 1D groundwater dynamics, we will mostly work with solutions of the following partial differential equation where  $s = s(x, t)$  is called the head change or often also the drawdown, especially when dealing with groundwater extraction and wells

$$\frac{\partial s}{\partial t} = \frac{kD}{S} \frac{\partial^2 s}{\partial x^2} \quad (5.4)$$

Equation 5.4 is known as the diffusion equation. It appears in many scientific fields like like diffusion, dispersion, heat conduction, sorption, consolidation, etc. Many researchers have derived solutions for this partial differential equation for specific boundary and initial conditions. The coefficient  $S/kD$  is called the diffusivity, often written as a thick D, like  $\mathbb{D}$ , which always has dimension [ $L^2/T$ ] whatever the scientific application is. The diffusivity is the ratio of the ease of the flow (transmissivity) and the storage:

$$\mathbb{D} = \frac{kD}{S}$$

In the case of a phreatic (unconfined, water-table) aquifer, the aquifer thickness is no longer constant. Unfortunately, there are no transient solutions that take a time-varying aquifer thickness into account. Linearization is then unavoidable, meaning that one has to choose a proper average aquifer thickness (or transmissivity) and remain vigilant that the head change should remain small with respect to the saturated thickness of the aquifer.

## 5.3 Sinusoidal fluctuations of the groundwater head and flows

This section deals exclusively with sinusoidal fluctuations of groundwater heads and flows caused by a head of flow that fluctuates like a sine at  $x = 0$ . We deal with tidal fluctuations in groundwater first and then show temperature as a second application of the same basic partial differential equation.

### 5.3.1 Groundwater fluctuations due to sinusoidal tides

A number of transient problems can be analyzed by assuming sinusoidal water-level or flow fluctuations at a boundary, at  $x = 0$  say. Generally, the resulting heads and flows within the aquifer will then also behave like a sine which will have the same frequency. If we have the analytic solution for head or flow in the aquifer due to harmonic fluctuating at the boundary, we may solve many related and more complex problems by superposition, that is by combining solutions of arbitrary frequencies, amplitudes and phase shifts. This way, hourly, daily, weekly and seasonal fluctuations may be readily combined. Examples of applications are tides in groundwater en the depth penetration of temperature fluctuations at ground surface.

Figure 5.1 shows a cross section through a confined aquifer (yellow) that extends to infinity at the right. At  $x = 0$  this aquifer is in direct connection with a surface-water body with a fluctuating water level, which causes fluctuations of head and flow in the adjacent aquifer, which are delayed and damped relative to the forced fluctuation at  $x = 0$ .

The partial differential equation for this system has already been derived (see equation 5.4). It may be solved for a sinusoidal fluctuation of the water level at  $x = 0$ . We just assume the solution of the head  $s$  in the aquifer relative to the mean value without fluctuation, to be also sinusoidal with the same frequency (same angular velocity  $\omega$

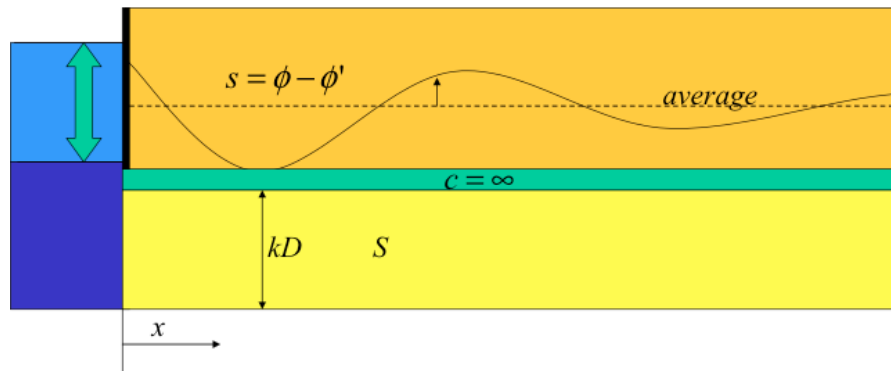


Figure 5.1: Sinusoidal water level fluctuation in surface water causing tide in the groundwater system

[radians/T]), but add a phase shift ( $-bx$ ) and assume an amplitude which is reduced by the factor  $e^{-ax}$  relative to the amplitude  $A$  of the tide at  $x = 0$ :

$$s(x, t) = A e^{-ax} \sin(\omega t - bx) \quad (5.5)$$

The full tide time  $T$  relates to the angular velocity  $\omega$  as

$$\omega T = 2\pi \quad (5.6)$$

Notice that we can always change the phase of the tide by adding an arbitrary angle  $\nu$  to the argument of the sine. For an aquifer with constant  $kD$  and storage coefficient  $S$  this solution is indeed valid for

$$a = b, \quad a = \sqrt{\frac{\omega}{2D}} = \sqrt{\frac{\omega S}{2 kD}} \quad (5.7)$$

The proof is given in the box below. The proof fills the presumed solution into the partial differential equation and sees under which conditions the solution is true. It turns out to be as given in equation 5.7. The relations may also be derived for the situation in which the aquifer is semi-confined. Of course, this is more complicated and beyond this course. However, the solution is given in the box below for possible future reference.

#### **Semi-confined case (not for exam)**

Notice that in the semi-confined case, where linear tide-induced leakage occurs between the aquifer and the overlying layer with constant head,  $a <> b$ . In that was worked out in the PhD Thesis of Bosch (1951). The results are

$$\begin{aligned} a &= \frac{1}{\lambda} \sqrt{\frac{1}{2} + \frac{1}{2} \sqrt{1 - (\omega Sc)^2}} \\ b &= \frac{1}{\lambda} \sqrt{-\frac{1}{2} + \frac{1}{2} \sqrt{1 + (\omega Sc)^2}} \\ \lambda &= \sqrt{kDc} \end{aligned}$$

Below the proof is given for the solution

**Proof that the solution in equation 5.8 is correct.** We have to proof that equation 5.5 fulfills equation 5.4. The constant is dropped, as it does not affect the proof. Taking the needed derivatives

$$\begin{aligned}\frac{1}{A} \frac{\partial s}{\partial x} &= -a e^{-ax} \sin(\omega t - bx) - b e^{-ax} \cos(\omega t - bx) \\ \frac{1}{A} \frac{\partial^2 s}{\partial x^2} &= a^2 e^{-ax} \sin(\omega t - bx) + ab e^{-ax} \cos(\omega t - bx) + \\ &\quad + ab e^{-ax} \cos(\omega t - bx) - b^2 e^{-ax} \sin(\omega t - bx) \\ \frac{1}{A} \frac{\partial s}{\partial t} &= \omega e^{-ax} \cos(\omega t - bx)\end{aligned}$$

by collecting the sines and the cosines separately, we get

$$a^2 - b^2 = 0 \rightarrow a = b$$

and so,

$$\frac{kD}{S} ab = \omega \rightarrow a = \sqrt{\frac{\omega}{2} \frac{S}{kD}}$$

Which completes the proof.

As can be seen, an the arbitrary constant  $\beta_0$  does not affect the proof of correctness. This constant is merely a phase shift at  $t = 0$ . Therefore, the solution can also be given including this extra phase shift at  $t = 0$ , which may be useful when superimposing many fluctuations that differ in amplitude was well as in phase:

$$s(x, t) = A e^{-ax} \sin(\omega t - ax + \beta_0) \quad (5.8)$$

To see that  $\beta_0$  is a phase shift, just fill in  $x = 0$  and  $t = 0$ .

The discharge is obtained by using Darcy

$$\begin{aligned}Q(x, t) &= -kD \frac{\partial s}{\partial x} \\ &= a kD A [e^{-ax} \sin(\omega t - ax + \beta_0) + e^{-ax} \cos(\omega t - ax + \beta_0)] \quad (5.9)\end{aligned}$$

$$= a kD A \sqrt{2} e^{-ax} \sin\left(\omega t - ax + \beta_0 + \frac{\pi}{4}\right) \quad (5.10)$$

Hence, phase the flow is shifted by  $\pi/4$  relative to the head.

As an example, figure 5.2 upper image shows the head as a function of  $x$  for different times and the lower image shows the head as a function of  $t$  at different distances from the boundary. The upper figure also shows the upper and lower envelopes, although a bit difficult to see. The third picture is the discharge as a function of time at different  $x$ -values. The head in the second picture reaches its top when the discharge at the considered point is already declining.

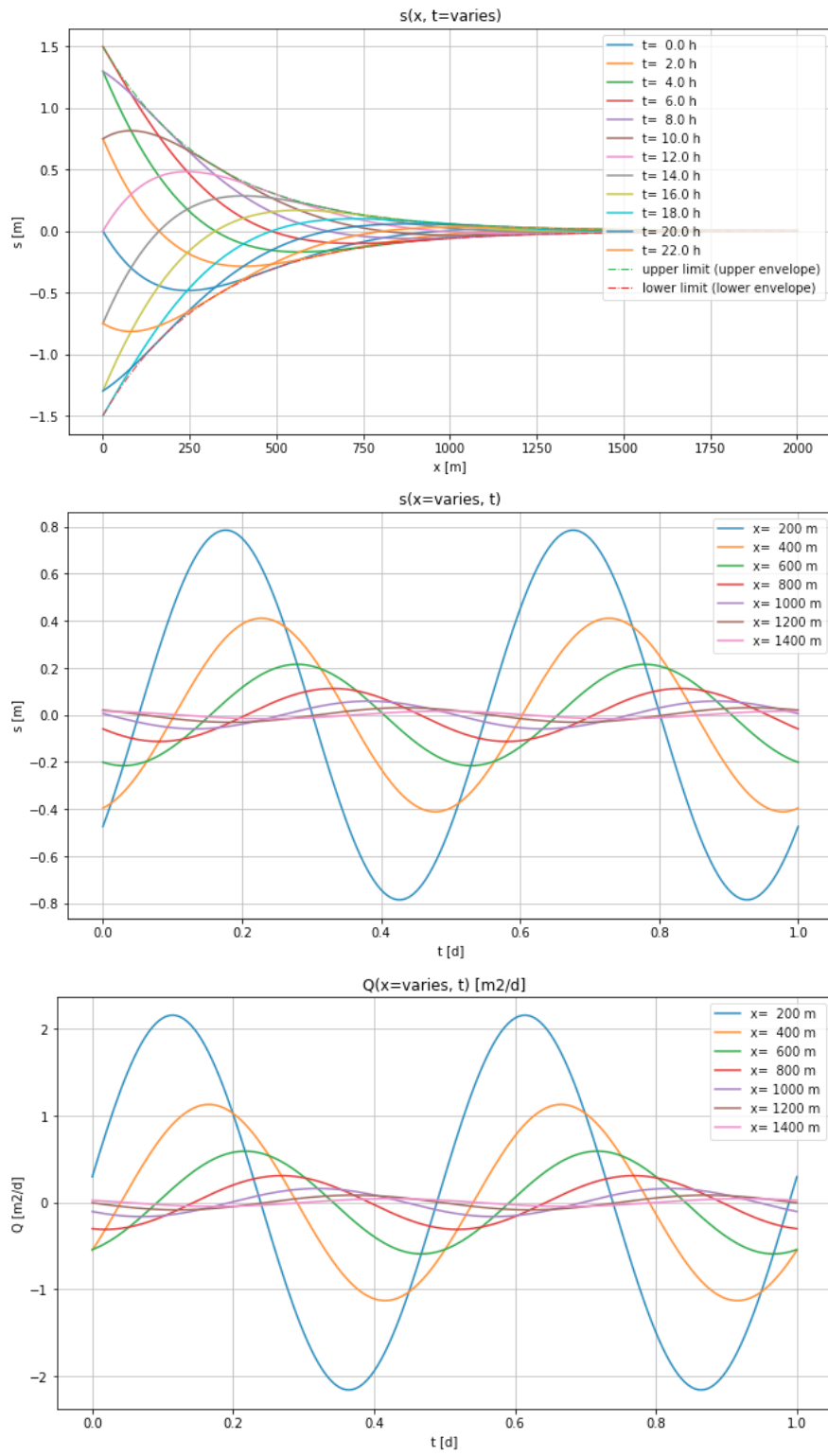


Figure 5.2: First picture: head a function of  $x$  at different times, also shows the upper and lower envelopes. Second picture: head as function of  $t$  at different distances.  $A = 1.5 \text{ m}$ ,  $kD = 600 \text{ m}^2/\text{d}$ ,  $S = 0.001$ ,  $\omega = 4\pi$  (i.e. two full tide cycles in 1 d). Third picture, discharge  $Q$  [ $\text{m}^2/\text{d}$ ] (to the right positive) as a function of time for different  $x$ -values.

**What is the velocity of the wave, or what is the delay of the wave at any distance  $x$  from the sea or river?** To find the answer, we move along with the wave such that the phase is constant, e.a. equal to  $c$ . Hence

$$\omega t - ax + \beta_0 = c$$

Then determine the velocity by computing  $dx/dt$ . So

$$\omega - a \frac{dx}{dt} + 0 = 0$$

This leads to

$$v = \frac{dx}{dt} = \frac{\omega}{a} \quad (5.11)$$

The delay of the wave at any  $x$  relative to the wave at  $x = 0$  is then

$$t = \frac{x}{v}$$

The wave velocity can be measured in figure 5.2 as the velocity of the top of the sines in the third figure.

Alternatively, one may say, that when the argument must be constant, it doesn't matter which constant, but only constant, then we can just well say that

$$\omega t - ax = 0$$

so that immediately we have  $x/t = \omega/a$ , which is the same answer.

**How much is the wavelength in the ground?** A direct approach is taking the argument of the sinus and demanding that the argument of the sine at  $t + T$  at  $x$  (where  $T$  is the cycle time) is the same as the argument of the sine at  $t$  but at location  $x + \Delta x$

$$[\omega(t + T) - ax + \beta_0] = [\omega t - a(x + \Delta x) + \beta_0]$$

hence

$$\omega T = a\Delta x = 0$$

$$\Delta x = \frac{\omega}{a} T$$

noting that the cycle time equals  $T = \frac{2\pi}{\omega}$ , we get

$$\Delta x_{full\ wave} = \frac{2\pi}{a}$$

with  $a = \sqrt{\frac{\omega S}{2kD}}$ , we also have

$$\Delta x_{full\ wave} = 2\pi \sqrt{\frac{2kD}{\omega S}}$$

So, the larger  $kD$  the longer the wave length, the larger the  $S$  the shorter and the larger the  $\omega$ , the shorter the wavelength will be, which all makes sense.

We have now seen that the head is indeed a damped sine. The damping is stronger for higher frequencies, larger storage coefficients and lower conductivities. It's difficult to measure the wave length from the upper figure in figure 5.2 because the damping is so strong that essentially full damping takes place within a single wavelength.

### 5.3.2 Fluctuations of temperature in the subsurface

For heat conduction in the subsurface, the same partial differential equation (also called “diffusion equation”) applies if we replace head change by temperature change. The only thing that changes is the so-called diffusivity  $kD/S$ . The ease of flow, i.e.  $kD$  with groundwater flow, is now replaced by the heat conduction  $\lambda$  [W/m] =  $[(E/T)/L^2] / (K/L) = [E/(TKL)]$  and the storage is replaced by the heat capacity  $\rho c$  [E/L<sup>3</sup>/K]. The dimension is again [L<sup>2</sup>/T] :

$$\mathbb{D} = \frac{\lambda}{\rho c} \left[ \frac{E/(TKL)}{E/(KL^3)} \right] = \left[ \frac{L^2}{T} \right]$$

Notice that in the dimension  $E$  = energy,  $T$  = time,  $L$  = length,  $K$  = temperature (from Kelvin). Because both the heat conduction and the heat capacity consist of a contribution from both the water and the grains (solids) of the aquifer, we can compute them as a porosity-weighted combination of these contributions. With  $\epsilon$  for porosity we then have

$$\begin{aligned}\lambda &= \epsilon \lambda_w + (1 - \epsilon) \lambda_s \\ \rho c &= \epsilon \rho_w c_w + (1 - \epsilon) \rho_s c_s\end{aligned}$$

$\rho$  [M/L<sup>3</sup>] is density and  $c$  [E/(MK)], i.e. heat per kg solids per degree kelvin (= degree Celsius).

The heat capacity of saturated sandy soils is about  $\lambda = 3\text{ W/m/K} = 3\text{ J/s/m/K}$ . The specific heat capacity of water is  $c_w = 4018\text{ J/kg/K}$  and that of sand grains  $c_s \approx 800\text{ J/kg/K}$ . With  $\rho_s \approx 2650\text{ kg/m}^3$  and  $\epsilon \approx 35\%$  we get  $\rho c = 2.85 \times 10^6\text{ J/m}^3/\text{K}$ .

The diffusivity then becomes

$$\mathbb{D} = \frac{\lambda}{\rho c} = \frac{3}{2.85 \times 10^6} = 1.06 \times 10^{-3}\text{ m}^2/\text{s} = 0.091\text{ m}^2/\text{d}$$

From which we have

$$a = \sqrt{\frac{\omega}{2\mathbb{D}}} = \sqrt{\frac{\pi}{T\mathbb{D}}}$$

With these values, one can compute between what values the temperature varies at any given depth as a function of the cycle time. For instance, the temperature fluctuation due to daily, weekly, monthly or yearly temperature fluctuations at ground surface. These envelopes are defined by

$$T_{mean} - A \exp(-az) \leq temp \leq T_{mean} + A \exp(-az)$$

with  $A$  [K] the temperature fluctuation amplitude at ground surface.

The monthly temperature in the Netherlands varies between  $3.1^{\circ}\text{C}$  in January and  $17.9^{\circ}\text{C}$  in July. The yearly amplitude is thus  $7.4^{\circ}\text{C}$ ; the year mean temperature being  $10.5^{\circ}\text{C}$ . Using this, we can compute the temperature envelopes, that is, the lowest and highest temperatures between which the actual temperature will vary. Figure 5.3 shows the results, as computed for the same mean temperature and the same amplitude but for different cycle times as indicated in the legend. With these data, the yearly temperature variation will barely reach 20 m below ground surface. Ten-year temperature fluctuations will penetrate down to about 50 m and 30 year temperature variation would be recordable down to about 100 m. This implies that climate change may be measured using the change of the temperature at for instance 50 m below ground surface if measurements in the past are available, as is actually the case in the Netherlands.

### 5.3.3 Concluding remarks

The derived partial differential equation applies to both groundwater flow and heat conduction. The only change is that head change is replaced by temperature change, transmissivity by heat conductance and the storage coefficient is replaced by heat capacity. Both heat conductance and heat capacity can be computed as a porosity weighted average of the contribution of the water and of the grains.

Sinusoidal analysis is useful to study the impact of ongoing fluctuations of the input on the groundwater. It is straightforward to compute the head and temperature envelopes defining the limits of a given sine input at a given distance or depth. Often, this is enough to understand the physics and estimate potential impact. Most importantly it is enough to understand the relation between the different parameters that play in this setting.

More complicated inputs can be constructed as a sum of a number of sin (or cosine) fluctuations, each with its own amplitude, frequency and phase shift. In fact, any input can be so constructed, although this may require the summation of many waves. On the other hand a given i.e. measured input may be split into individual waves using Fourier Analysis. Python has modules for that. This helps to find the dominant ones, and allows limiting the following analysis on only a few dominant waves. This simply means that this sinusoidal solution of the partial differential equations offers many ways to analyze groundwater systems of the type we considered. By superposition, these analysis can also be combined with other features such as wells.

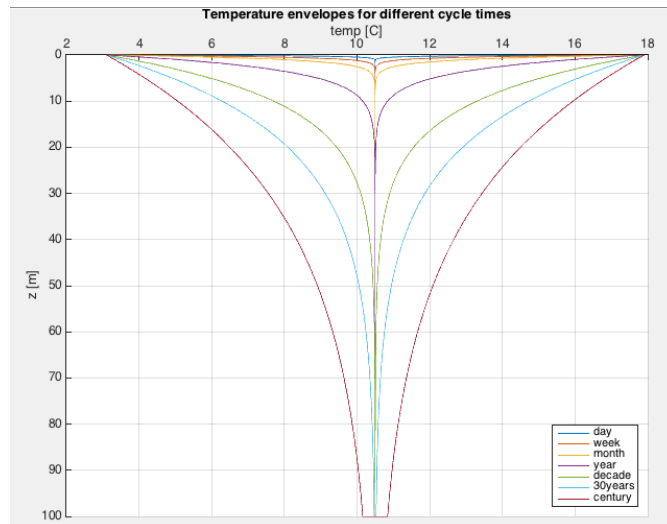


Figure 5.3: Temperature envelopes in the subsurface due to temperature fluctuations at ground surface with mean  $10^{\circ}\text{C}$  and amplitude  $7.4^{\circ}\text{C}$ . Envelopes depend on cycle time of the fluctuation (see legend).

#### 5.3.4 Questions

1. Prove the correctness of the given solution yourself. As an extra exercise you could prove that equation 5.9 is correct by filling it into the partial differential equation for continuity  $\frac{\partial Q}{\partial x} = -\frac{S}{kD} \frac{\partial s}{\partial t}$ .
2. If the transmissivity if doubled, what is the effect on the drawdown?
3. When the  $\omega$  is doubled, what is the effect on the drawdown?
4. Explain how the distance to where the fluctuation of the sea or lake reaches in the aquifer depends on the frequency of the wave.
5. How far in-land reaches the effect of waves on the beach with one cycle per second, tides with one cycle per 12 hours, moon-tides with one cycle per two weeks in an aquifer with transmissivity is  $kD = 500 \text{ m}^2/\text{d}$  and a storage coefficient of  $S = 0.001$  and  $S = 0.1$  respectively?
6. Let the solution to the diffusion equation for the confined aquifer be  $s(x, t) = A \exp(-ax) \sin(\theta_0 + \omega t - ax)$  and let  $kD = 1000 \text{ m}^2/\text{d}$ ,  $S = 10^{-3}$ , and the amplitude  $A = 2 \text{ m}$ , and let  $\theta_0$  be an arbitrary constant. Take time in days and show the head change  $s(x, t)$  in Python or in Excel. With this, answer the following 5 sub-questions:
7. Include the discharge  $Q(x, t)$
8. Compute and also show the envelope of the wave as a function of  $x$ .

9. How far inland can we still measure the tide if our device allows us to see a variation of 1 cm?
10. What is the velocity of the wave?
11. What is the delay at 1000 m from the shore (or show the delay graphically as function of  $x$ )?
12. Add the case for a storage coefficient,  $S_y = 0.2$ . And show the relation between the case with  $S = 0.001$  and  $S_y = 0.2$ .
13. Create a complex input using of 4 sines, each with a different initial angle  $\theta_0$ , amplitude  $A$  and angular velocity  $\omega$  and show the result.

Copy your code and alter the copy to answer the following questions:

1. The head in a lake above a clay bottom varies daily 30 cm. How deep does this fluctuation penetrate the underlying clay layer with conductivity of  $10^{-4}$  m/d and a specific storage coefficient of  $S_s = 0.0001$  /m? Assume that you could still measure variations down to 3 mm.
2. What if the variation is weekly, monthly and seasonally only?
3. If the sea is shallow and the clay layer is below the sea bottom, what will be the amplitude in the confined aquifer for the water compressibility  $\beta_w = 5 \times 10^{-5}$  and porous matrix compressibility  $\beta_s = 2 \times 10^{-5} \text{ m}^2/\text{N}$ ?
4. If the clay layer would be semi-pervious, what would this mean for the amplitude in the confined aquifer? Would it be greater, smaller compared with the case with a completely impervious layer?

### **Heat flow**

1. What is the penetration depth of a diurnal (twice-a-day), seasonal and centennial temperature fluctuation at ground surface given  $\lambda = 3 \text{ W/m/K}$ ,  $\rho_s c_s = 0.800 \text{ MJ/m}^3/\text{K}$  and  $\rho_w c_w = 4.2 \text{ MJ/m}^3/\text{K}$  and porosity of  $\epsilon = 0.35$ ?
2. Heat flow and groundwater flow show the same partial differential equation except that head change is replaced by temperature change. They both have one coefficient called diffusivity. What is the dimension of this diffusivity in both situations?
3. Diffusivity consists of a part that expresses the ease of flow,  $\lambda$ , and a part that expresses the storage,  $\rho c$ . What are the equivalent factors in the groundwater case?
4. Groundwater flow was ignored when we discussed heat flow. Describe how temperature envelopes would change due to upward groundwater seepage, would they shrink or stretch?

5. How would these envelopes change due to downward seepage? How much would you estimate the effect on the yearly temperature envelopes if the recharge is 333 mm per year and porosity is 33%? First estimate how deep the recharge penetrates in one year.

## 5.4 Non-fluctuating interaction with surface water

In the previous section we discussed the effect of sinusoidally variation of the level of a surface water that is in direct contact with a confined or unconfined aquifer. In this chapter, we'll discuss the same hydrological setting, but in which the surface water level changes suddenly by a fixed amount.

### 5.4.1 Basins of half-infinite lateral extent

Again, we consider a confined aquifer in direct contact with surface water as was done in the previous section. The situation is depicted in figure 5.4. The aquifer thickness, transmissivity and storage coefficient are everywhere the same. The aquifer is half-infinite, which means that its right end extends to infinity. We consider the aquifer as confined, because we will assume that its thickness is the same everywhere and stays so. This is required only to allow a closed analytical solution for the time-dependent groundwater flow. There are no time-dependent closed analytical solutions for water-table aquifers in which the transmissivity varies along with the head and, therefore, with time. We further assume the aquifer being in direct contact with the surface water. This implies that there is no hydraulic resistance of any kind between the surface water and the aquifer. This assumption keeps the analysis simple. However, solutions that take hydraulic resistance between the surface water and the aquifer do exist ([Bruggeman (1999)]) but are beyond this course. You may look them up when you need them.

We present here a basic analytical solution, which describes the change of head (and flow) caused by a sudden change of the surface-water level by an amount  $a$  [m].

In the confined case we use the elastic storage coefficient,  $S = DS_s$  and in the unconfined case we use the specific yield,  $S_y$ . In cases where we consider unconfined aquifers, the effective thickness of the aquifer changes with the water table, and hence with the head. However, as long as the change of head is small compared to the thickness of the aquifer we may still apply the solution in practical cases and accept the small error that will cause the assumption of constant thickness in those cases.

Initially, the head is  $\phi'$  in figure 5.4 and the head  $\phi(x, t)$  varies in space and time due to a sudden change of head of the bounding surface water by  $a$  at  $t = 0$ . The surface-water head remains at  $\phi' + a$  thereafter.

Because superposition applies (due to linear governing partial differential equation), we may just superimpose the change of head change  $s(x, t) = \phi(x, t) - \phi'$ , irrespective of the actual situation. The only thing that matters to us is the **change of head**  $s$  that is caused by the sudden change of the water level in the bounding surface water by the value  $A$ .

The case considered here is a base case. There exists a whole series of analytical solutions for different boundary conditions, which that are presented in the next section 5.4.3 for reference only, but they are not for the exam.

Consider a one-dimensional aquifer of infinity lateral extent as shown in figure 5.4 that is in direct contact with a fully penetrating water body at  $x = 0$ . Ignoring leakage and recharge, and assuming a constant transmissivity  $kD$  and storage coefficient  $S$ , the partial differential equation is the diffusion equation:

$$kD \frac{\partial^2 s}{\partial x^2} = S \frac{\partial s}{\partial t} \quad (5.12)$$

One well-known solution is for the case in which the head at  $x = 0$  is suddenly raised by a value,  $A$ , and maintained from that time on, while the initial head is zero throughout (Figure 23).

The solution is

$$s(x, t) = \phi(x, t) - \phi_0 = A \operatorname{erfc}(u), \quad u = \sqrt{\frac{x^2 S}{4 k D t}}$$

Where  $s(x, t)$  is the head change,  $\phi(x, t)$  the head and  $\phi_0(x)$  the initial head that may be a function of  $x$ , because that does not interfere with the principle of superposition.

By definition

$$\operatorname{erfc}(z) = \frac{2}{\sqrt{\pi}} \int_z^\infty e^{-y^2} dy \quad (5.13)$$

and so its derivative is

$$\frac{d \operatorname{erfc}(z)}{dz} = -\frac{2}{\sqrt{\pi}} e^{-z^2}$$

Therefore, the discharge is

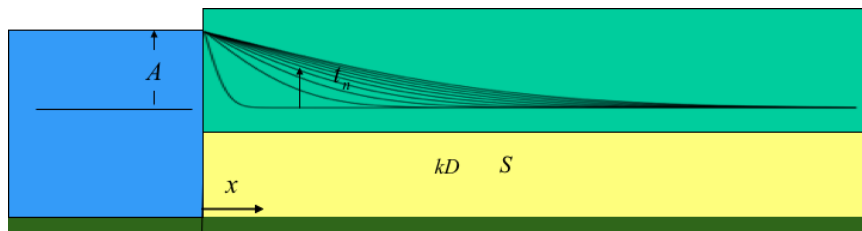


Figure 5.4: One-dimensional groundwater aquifer which extends to infinity to the right, and has constant transmissivity  $kD$  and storage coefficient  $S$ , while it is in direct contact with surface water at  $x = 0$  in which the water level is suddenly changed by  $a$  at  $t = 0$

$$Q = -kD \frac{\partial s}{\partial x} = A \sqrt{\frac{kDS}{\pi t}} \exp\left(-\frac{x^2 S}{4kDt}\right)$$

and, for  $x = 0$

$$Q_0 = A \sqrt{\frac{kDS}{\pi t}}$$

The function  $\text{erfc}(-)$  is the so-called complementary error function. Abramowitz & Stegun (1964) provide tables and expressions to compute this function in several ways. The  $\text{erfc}$  function is also one of the functions present in Excel. Its graph is shown in figure 5.5

Hence, the solution of head change versus distance to the shore always has the shape of this curve, be it that the horizontal axis will be squeezed or stretched depending on the values of the parameters in  $u$ . The shorter the time, the larger  $u$ , the more compressed is the horizontal axis. A small  $kD$  or large  $S$  also has the effect of compressing the horizontal axis.

For the understanding it is convenient to express  $u = x/L$  so that  $L = \sqrt{4kDt/S}$ , which is a constant for any fixed  $t$ . For this fixed  $t$ ,  $L$  may be considered a characteristic distance, as it scales  $x$ . For instance, half of the initial head change has been reached when  $u \approx 0.5$  that is at a distance  $x = 0.5L$ . Also, the head change is about 10% of  $A$  at  $u = 1$ , that is at  $x = L$ , with  $L$  fixed for the time of observation. No head rise has yet occurred for about  $u = 2.5$ , hence, for  $x > 2.5L$ . This is all practical information when judging an actual situation, without the need for a computer.

It is also possible to plot  $\text{erfc } u$  and its derivative versus  $1/u^2$ . To make the graph meaningful, we have to use a logarithmic scale for  $1/u^2$  as is shown in figure 5.6. The time scale is then proportional to  $t$ . We can write  $u^2 = t/T$  with  $T = 4kD/x^2S$ , where  $T$  can be considered a characteristic time for fixed distance  $x$ . We see that for  $t/T \approx 2$ , about half the final (maximum) head change has been reached. It is useful and practical to consider this graph from the perspective of  $t/T$  instead of just  $t$ . Taking this perspective, one only needs a single graph to cover all possible cases; the only thing that changes when choosing another observation point is the value of the characteristic time  $T$ . Then  $T$  can be considered time characteristic for the situation at a chosen distance  $x$ . The graph in figure 5.6 also shows that some time elapses before the influence of the river reaches the observation point. This value of  $1/u$  for this time is about 0.4 as can be read from figure 5.6. Hence,  $t/T = 0.16$ . This result is also universal. 90% of the final head is reach at about  $1/u^2 = 100$ , that is, so that  $t = 100T$ . And so forth.

For the discharge, we need the derivative, which is also shown in both figures.

**Exercise:** Proof that equation 5.13 fulfills the partial differential equation 5.12.

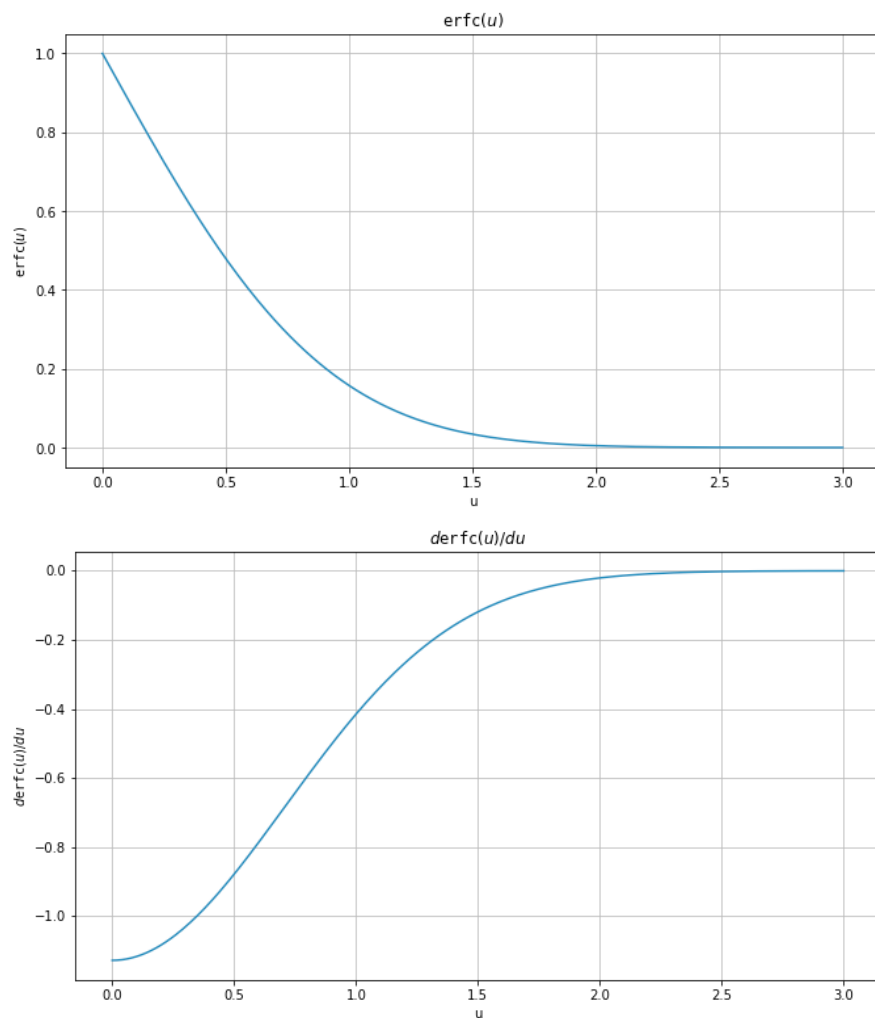


Figure 5.5:  $\text{erfc}(u)$  and its derivative  $-(2/\sqrt{\pi}) \exp(-u^2)$

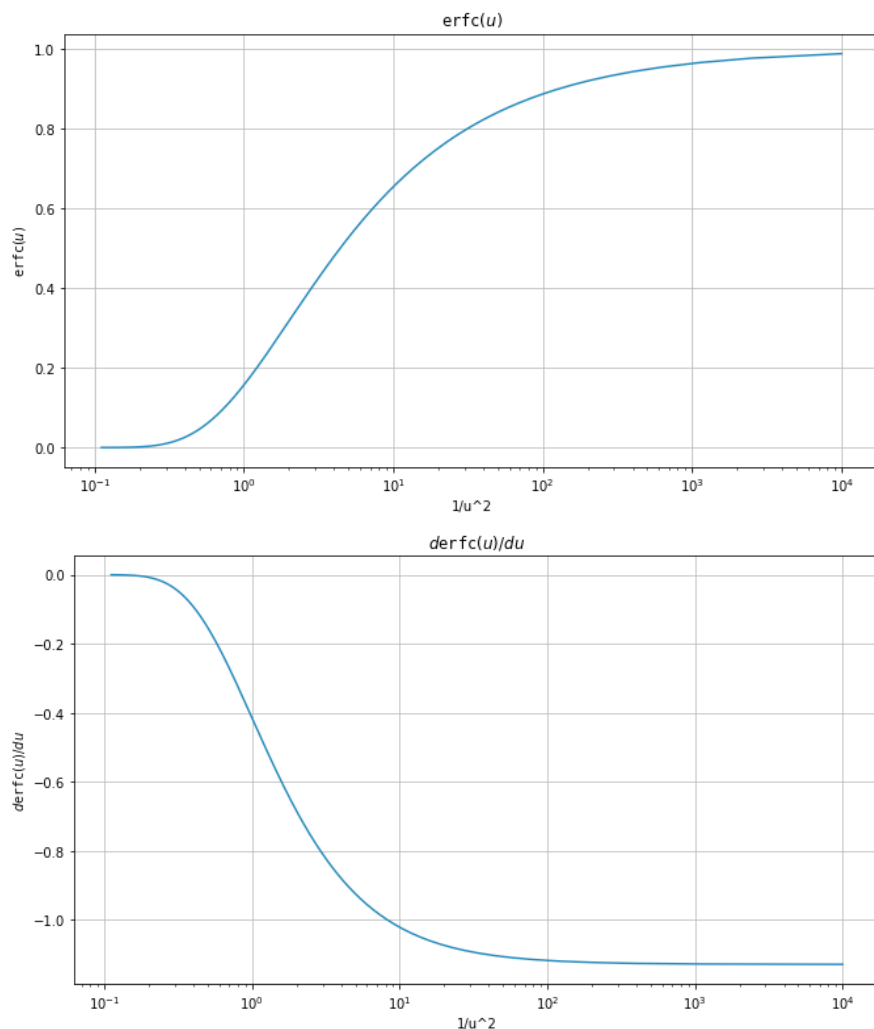


Figure 5.6:  $\text{erfc}(u)$  and its derivative as a function of  $1/u^2$  instead of vs.  $u$ . This makes the horizontal axis proportional to time, as  $1/u^2 = \frac{4kD}{x^2S}t$ .

### 5.4.2 Questions

1. All drawdowns due to a sudden change of river stage are expressed in a simple erfc-function. Can you express the argument  $u$  using a ratio of the distance  $x$  from the river and some characteristic distance  $X$  that is valid for a fixed time?
2. What is the ratio  $x/X$  for  $s(x) = 0.5s_0$ , i.e.  $s$  is half the head change at  $x = 0$  ?
3. Alternatively, how could you express the head change as a ratio of time  $t$  and a characteristic time  $T$  for a fixed distance?
4. What is then the ratio  $t/T$  for  $s = 0.5s_0$ ?
5. At what time, expressed at  $t/T$ , would you expect the head in the aquifer to start changing at some given fixed distance  $x$  after a sudden change of river stage at  $x = 0$ ?
6. Given the mathematical expression for the head change, derive the expression for the discharge  $Q(x, t)$ .
7. What is the discharge at  $x = 0$  mathematically?
8. An aquifer with properties  $kD = 400 \text{ m}^2/\text{d}$ ,  $S = 0.1$  is in good contact with a river. The water level in the river rises by 2 m in a very short time. What is the effect of this change for points  $x$  at 10, 100 and 1000 m?
9. How long does it take for the head change in the three points to reach 10 cm?
10. Using Python, show the head over time in these points.
11. Using Python, show the discharge over time in these points.
12. How long will it take until the head in the center of a 10 m thick aquitard with resistance  $c = 5000 \text{ d}$  and a specific storage coefficient  $S_s = 10^{-5} \text{ m}^{-1}$  has reached half the head change that was suddenly applied at both its top and bottom at  $t = 0$ ?

A canal in a dune area is used to provide storage for drinking water in the case of an emergency. The aquifer properties are  $kD = 100 \text{ m}^2/\text{d}$ ,  $S = 0.2$ . During such an emergency, the water level in the 50 m wide canal is suddenly lowered by 5 m.

1. How much water will flow into the storage canal from two sides in 1 day, 1 week, 6 weeks?
2. Compare these amounts with the amount of water stored in the canal?
3. What will be the drawdown over time at 10, 100, 300, 1000m?
4. Compute the flow to the canal in 6 weeks if there is a fixed-head boundary at 70 m distance. You must use superposition to compute this.

### 5.4.3 Higher-order solutions (not for exam)

The previous well-known basic solution is the first of an infinite series of solutions of the same partial differential equation but for different boundary conditions, namely  $s(0, t) = a t^{n/2}$  with  $a$  a constant and  $n \geq 0$ . The solution given above is for  $n = 0$ .

The entire series of solutions is given as

$$s(x, t) = A t^{n/2} \frac{i^n \operatorname{erfc} u}{i^n \operatorname{erfc} 0}, \quad u = \sqrt{\frac{x^2 S}{4 k D t}}$$

The function  $i^n \operatorname{erfc} u$  is the  $n^{th}$  repeated integral of the complementary error function (see Abramowitz & Stegun, 1964, section 7.2). A number of these functions is shown in figure 5.7. These higher order repeated integrals are not in Abramowitz and Stegun (1964) but can be easily computed using a recursive expression given below.

By definition

$$i^n \operatorname{erfc} z = \int_z^\infty i^{n-1} \operatorname{erfc}(\zeta) d\zeta$$

with

$$i^0 \operatorname{erfc} z = \operatorname{erfc} z$$

and

$$i^{-1} \operatorname{erfc} z = \frac{2}{\sqrt{\pi}} e^{-z^2}$$

Higher order functions may be computed by the following recursive relation

$$i^n \operatorname{erfc} z = \frac{-z}{n} i^{n-1} \operatorname{erfc} z + \frac{1}{2n} i^{n-1} \operatorname{erfc} z$$

By applying Darcy's law, we find the discharge

$$Q(x, t) = \frac{\sqrt{k D S}}{2 \sqrt{t}} A t^{n/2} \frac{i^{n-1} \operatorname{erfc} u}{i^n \operatorname{erfc} 0}$$

Instead of expressing  $s(0, t) = A t^{n/2}$  we could write  $Q(0, t) = B t^{n/2}$ ,  $n \geq 0$ , which is more convenient in some cases. Hence, This yields we write  $\frac{\sqrt{k D S}}{2 \sqrt{t}} A = B$ , which yields

$$Q(x, t) = B t^{n/2} \frac{i^{n-1} \operatorname{erfc} u}{i^n \operatorname{erfc} 0}$$

and

$$s(x, t) = \frac{2 \sqrt{t}}{\sqrt{k D S}} B t^{n/2} \frac{i^n \operatorname{erfc} u}{i^n \operatorname{erfc} 0}$$

A basic solution is immediately obtained for  $n = 0$ , so that  $Q(0, t) = B$  is constant. In that case the head at  $x = 0$  declines according to the  $\sqrt{t}$ . When the discharge increases linearly, the head at  $x = 0$  declines according to  $t\sqrt{t}$ . On the other hand, when the drawdown is constant at  $x = 0$ , the discharge is inversely proportional to  $\sqrt{t}$  and when the head at  $x = 0$  rises linearly with time, the discharge increases according to  $\sqrt{t}$ .

These functions may be used to compute the head and flow due to either a constant or changing head at  $x = 0$  or due to a constant or changing flow at  $x = 0$ . Computations are easily done in Python or even in Excel after the functions have been implemented.

**Example:** For instance, the water level in Lake Nasser in Egypt has risen by 60 m between 1971, when the dam at Aswan was closed, and 1991, when the new lake was full. This boils down to rise of the lake level of 3 m/year. Assume further that the bordering aquifer is 200 m thick and that it has a conductivity  $k = 1 \text{ m/d}$  and a specific yield  $S_y = 0.1$ . One could then ask the question, how far does the effect of the filling of the lake in the bordering aquifer reach, and hence how much lake water would have been stored in that same period.

We have

$$s(x, t) = A t^{n/2} \frac{i^n \operatorname{erfc} u}{i^n \operatorname{erfc} 0}, \quad u = \sqrt{\frac{x^2 S}{4kDt}}, \quad A = 3 \text{ m/y}, \quad n = 2$$

so that the rise is linear. With  $n = 2$

$$s(x, t) = A t \frac{i^2 \operatorname{erfc} u}{i^2 \operatorname{erfc} 0}, \quad Q(x, t) = \sqrt{\frac{kDS}{4t}} A \frac{i^1 \operatorname{erfc} u}{i^2 \operatorname{erfc} 0}$$

With proper values of  $kD$  and  $S$ , a graph can be made for  $s$  and  $Q$  as a function of  $x$  for given times. Alternatively, one can make graphs of the head as a function of time for given values of  $x$ . The results are shown in figure 5.8. The top figure shows the head in the aquifer as a function of  $x$  for different times. The middle figure shows the infiltration at  $x = 0$  as a function of time. The bottom figure shows the development of the head over time at different distances from the shore. Note that the lake level remains constant after  $t = 20$  years. The head at  $x = 0$ , therefore, remains equal to the lake level of 60 m thereafter. The infiltration then shows a sharp decline as soon as the head does not rise further. This is implemented by superposition, i.e. by superimposing the solution for a lake with a water level that declines with the same speed (i.e.  $A = -3 \text{ m/y}$ ). It's a good exercise to implement this yourself.

Of course, the same case can be simulated using the function for a sudden rise of the lake level. But then the actual gradual rise must be split in many small steps, and the effect of each step has to be superimposed on the overall solution. This is shown in figure 5.9, especially the rise of the head at  $x = 0$  in the lower image. The results are essentially

Figure 5.7:  $i^n \operatorname{erfc}$  functions

the same, however the infiltration at  $x = 0$  fluctuates quite heavily under the discrete yearly sudden head increments of 3 m each. However, at larger distances, these steps damp out. Of course, the smaller the steps, the smoother the result will be. On the other hand it is much more convenient and less work in this case to directly apply the solution for the linear rise of the head at  $x = 0$ .

#### 5.4.4 Questions

1. What is the mathematical expression for the head  $s(x, t)$  and the discharge  $Q(x, t)$  for the case in which the river stage increases linearly with time?
2. What is the mathematical expression for the case in which the discharge increases linearly with time.
3. Let a lake (like Lake Nasser) have a water level that rose linearly by 60 m between 1971 and 1991. Compute the change of head in the aquifer at 1 km from to the lake. Assume the  $kD = 1000 \text{ m}^2/\text{d}$  and  $S = 0.1$ .
4. Compute the total amount of water that infiltrated over this period.
5. Assume the aquifer has a constant thickness and its porosity is 35%. With this information compute how far the lake water penetrated the aquifer during this period.
6. When, after 1991, the water level has been more or less constant, then how much is the infiltration  $Q(0, t)$  at the lake shore in 2021? By how much has it declined since 1991?

#### 5.4.5 Superposition in time, half-infinite aquifer

Consider a half-infinite aquifer in direct connection with surface water at  $x = 0$ . The analytical solution of the change of the groundwater head  $s(x, t)$  caused by a sudden change of the surface water level by an amount  $A$  at  $t = 0$  was given earlier in this chapter:

$$s(x, t) = A \operatorname{erfc} \sqrt{\frac{x^2 S}{4kDt}}, \quad t \geq 0, \quad s(x, t) = 0 \quad t < 0$$

The head change  $s(x, t)$  due to an arbitrary sudden changes of the surface water level  $A_i$  happening at  $t_i$  can be obtained by superposition as usual. Using  $i$  as event index, we then get

$$s(x, t) = \sum_{i=1}^N \left\{ A_i \operatorname{erfc} \sqrt{\frac{x^2 S}{4kD(t - t_i)}} \right\}, \quad t \geq t_i$$

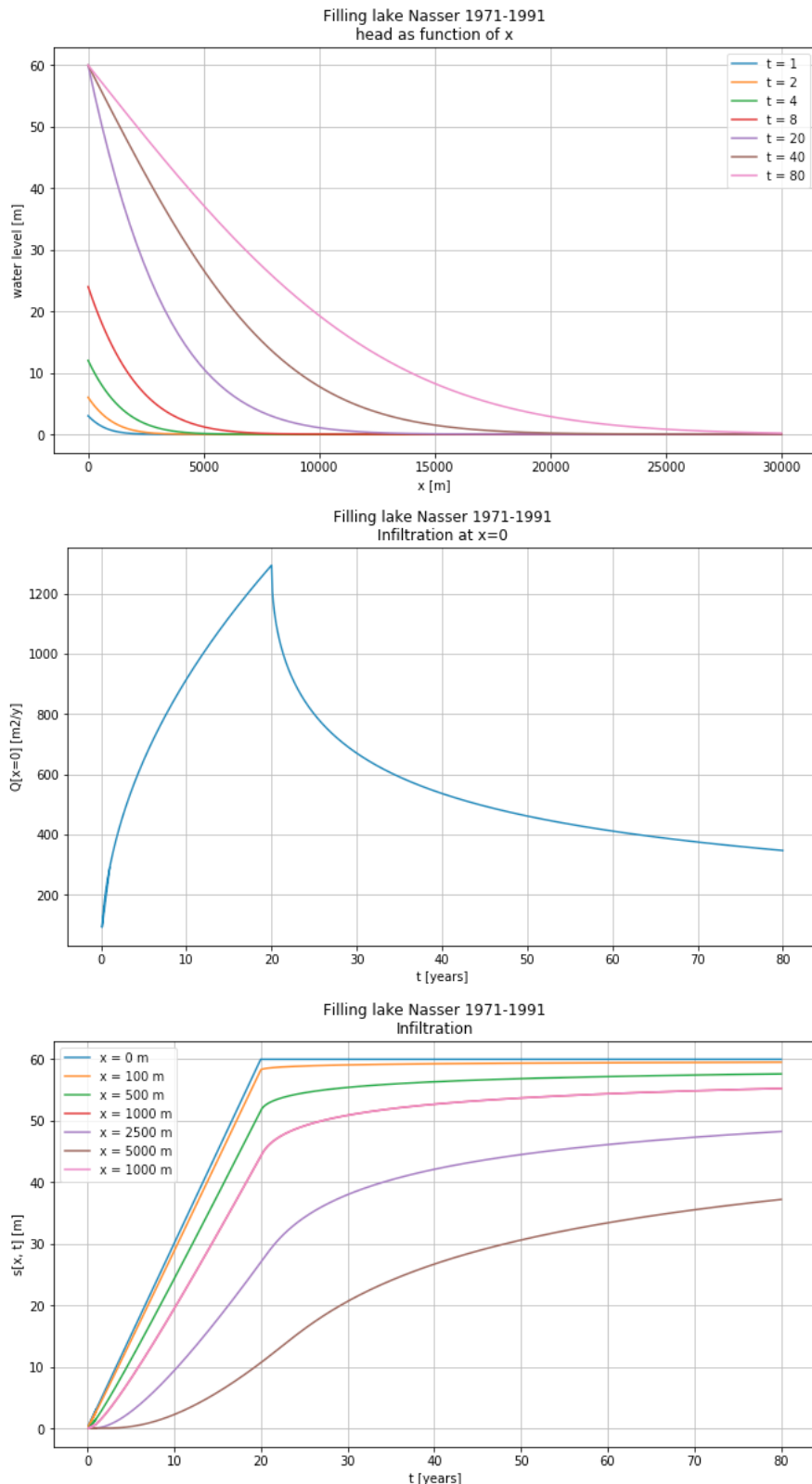


Figure 5.8: Lake Nasser example. Top: the head in the adjacent aquifer as a function of  $x$ , the distance to the shore, at different times. Middle: The infiltration into the aquifer at  $x = 0$  as a function of time. Bottom: The head development over time at different values of  $x$

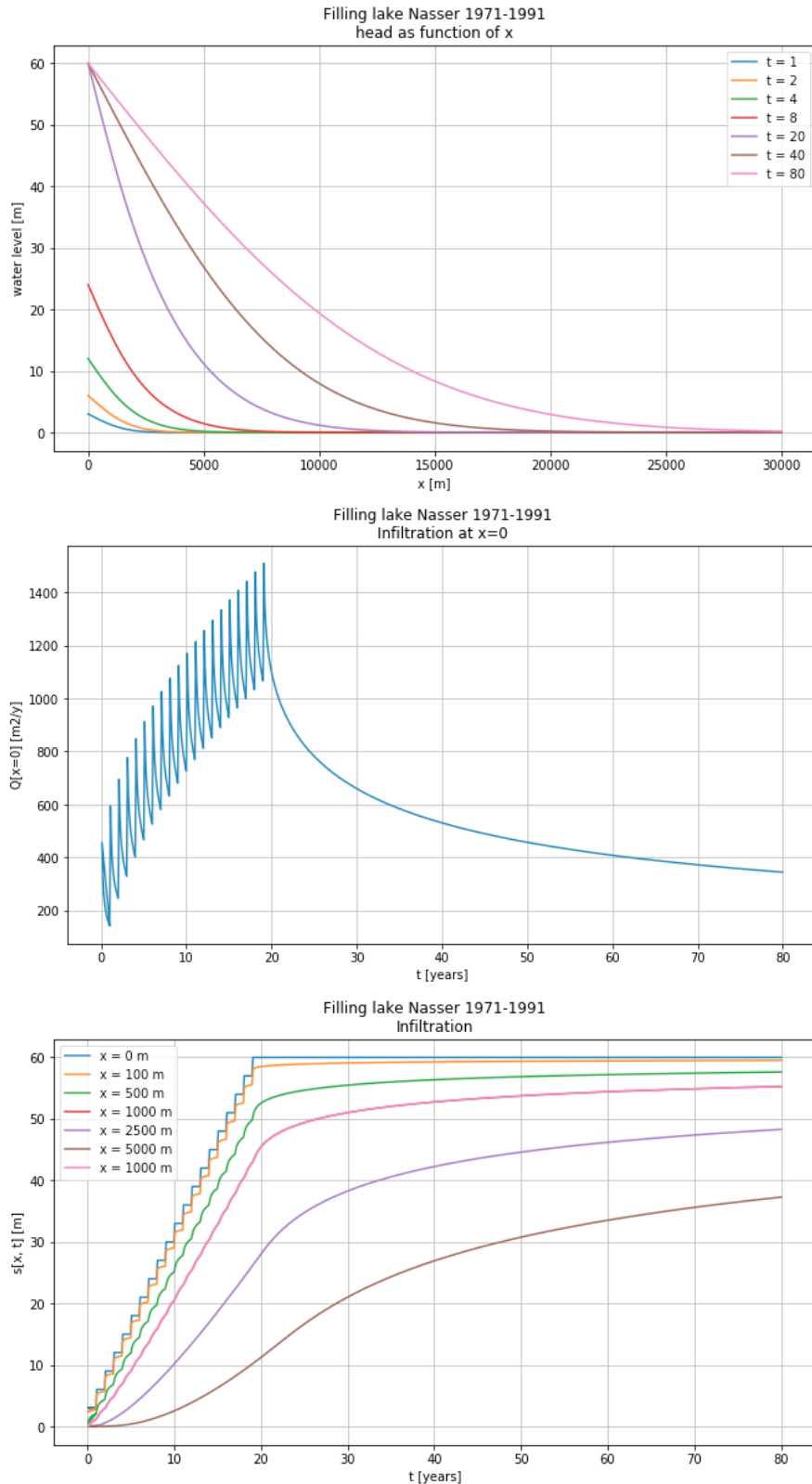


Figure 5.9: Lake Nasser example, simulated using the solution for a sudden change and dividing the linear rise over 20 years in 20 sudden changes of equal size. Top: the head in the adjacent aquifer as a function of  $x$ , the distance to the shore, at different times. Middle: The infiltration into the aquifer at  $x = 0$  as a function of time. Bottom: The head development over time at different values of  $x$

Each term is nonexistent, hence zero, for  $t < t_i$ . The surface-water level at any time is  $s(0, t) = \sum_1^N A_i$ ,  $t > t_i$ , because each sudden change of water level is supposed to last forever after it happened at  $t_i$ . This way, one can compute the head change and, of course, the flow in an aquifer due to an arbitrary variation of the surface water level at  $x = 0$ . Of course, if the the surface water would vary regularly, like a sin, one would rather use the solution for a sine boundary head to simplify the computations. Even a combination is possible, because superposition applies.

The problem to be solved in practice, would be find the impact of a irregular surface-water level fluctuation pattern. This may require a large number of erfc functions to carry along, which may become cumbersome. To simulate the results of detailed, say daily, river water level changes over a long period, one would rather look for convolution as the most efficient method, which is explained also in this syllabus.

While in this section, we look at superposition in time for a given value of  $x$ , in the following sections we will focus on superposition in space for a given value of  $t$ . But it should be clear from the beginning that superposition in space can readily be combined with superposition time to deal with both to more complex boundary conditions.

When computing the head change at a given  $x$  for a varying river level, we deal with time  $t$ , which is a detailed array of times, say daily values, representing the times at which we want the head-change value to be computed. Next to this, we will have an array or list of times, which we may call change times,  $t_{ch}$  at which the head in the river suddenly changes. The  $t_{ch}$  values are independent of the  $t$  values, and the number of  $t_{ch}$  values is usually much less than the number of  $t$  values. We will simply compute the head due to the change  $dA_i$  happening at  $t_{ch_i}$  for all  $t > t_{ch_i}$  and add this to the head changes already computed for changes that happened earlier.

**Example** Consider a situation with  $kD = 400 \text{ m}^2/\text{d}$  and  $S_y = 0.1$ . The river-water level  $A = [1.0, -0.5, +0.5, -0.25]$  at  $t_{ch} = [0.5, 0.8, 1.0, 2.0]$ . Show the groundwater level as a function of time for  $x = 50 \text{ m}$  for  $0 \leq t \leq 5 \text{ d}$ . In this case it is convenient to take  $t$  in hours to get sufficient detail.

Figure 5.10 gives the results for  $x = 100 \text{ m}$  as a function of time, both the change of head and the resulting flow both as a thick black line. Next to the values for  $x = 100$ , also the values for  $x = 0$  are shown, i.e. the fluctuation of the river level and the exchange of flow between river and aquifer, both as a thick-red line. The effect of the individual river-level changes are also shown as thinner lines in different colors, see legend. Each sudden change of river level corresponds to a change time  $t_{ch}$ , while the resulting head is computed for values of time  $t$ , i.e, in this example one point per hour, enough points to get a detailed picture of what happens in the aquifer.

The implementation of the examples in this chapter can be found in the accompanying Jupyter Notebook ‘Chap5\_4\_1d\_river\_level\_changes.ipnb’.

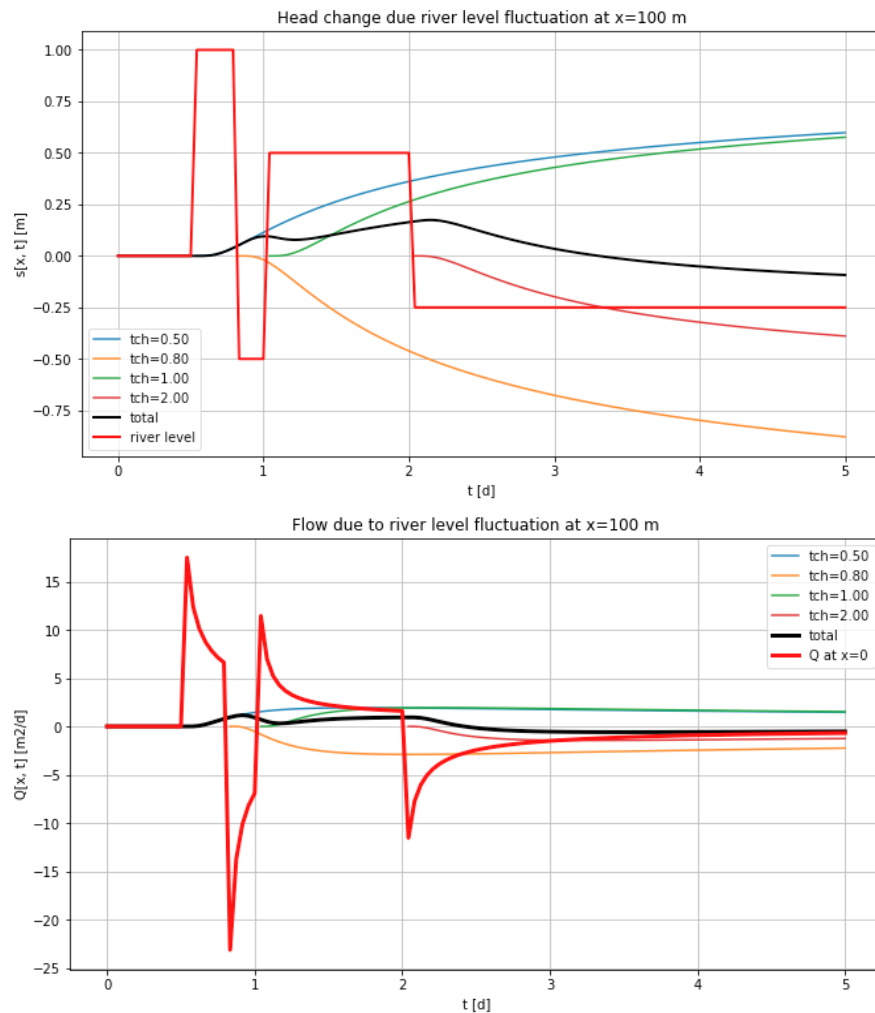


Figure 5.10: Superposition in time example

## 5.5 Groundwater basins as land strips of limited width between straight head boundaries

### 5.5.1 Introduction

In many practical situations, groundwater basins will have a limited width instead of  $x$  extending to infinity. Examples are groundwater basins that are bounded by a fixed-head boundary on either side. This includes basins that are closed on one side, because such a line of no flow is just the water divide, which is equivalent to a symmetrical basin of double width having the same head boundary on either side.

Often, watersheds can be regarded as a set of sub-basins bounded by river branches on either side of the water divide between them (see figure 5.11). The basins considered here can be regarded as a simplification of the groundwater system between two river branches, but also as a parcel of arable land bounded by two ditches. It's just a matter of scale. The basins considered here may, therefore, be as narrow as a parcel of arable land or meadows between ditches as one can find anywhere in the Netherlands of perhaps 100 m wide; but they can just as well be a strip of land between brooks or tributaries that are several km apart, between river branches tens of km apart or a deserts for which the boundaries that are several hundred of km out of each other.

Of course, the surface waters bounding most basins are not straight lines. Nevertheless, we limit ourselves to in this course to basins that are bounded by two parallel straight head boundaries. This makes the flow essentially one-dimensional when we ignore resistance due to vertical flow components within the aquifer. The latter is very often justified as the scale of the vertical flow components is minor compared to that of the horizontal ones.

Hence, in the cases considered in this chapter, we assume the head to depend only on  $x$  and  $t$ . If this is not warranted near shallow surface water due to convergence of flow lines locally, we may always at that phenomenon separately by superposition.

We learn to compute the variation of head and flow in one-dimensional basins as they are affected by the changes of their head boundary at one or both sides.

We first consider the case where the left-bounding head suddenly rises by a fixed amount, while the right-hand boundary head is kept the constant (see figure 5.12). We will see that maintaining the right head boundary at zero, requires superposition of the effect of an infinite number of "mirror" strips of land.. Then we'll consider a given change of head on either side of the strip, which also yields a solution by superposition of an infinite number of equal land strips. The case with sudden head change that is the same on either side of the land strip, is just a special case. We'll compare this solution by superposition with a different general solution for the same situation. We'll analyze the latter one to deduce the characteristic time of groundwater basins in general, for which our strip of land is a simplified version for which we possess an analytical solution. This results in both simple and practical insight into the dynamic behavior of such basins.

The mentioned superposition of an infinite number of strips leads to superposition patterns that are shown below the respective figures. These patterns allow immediate

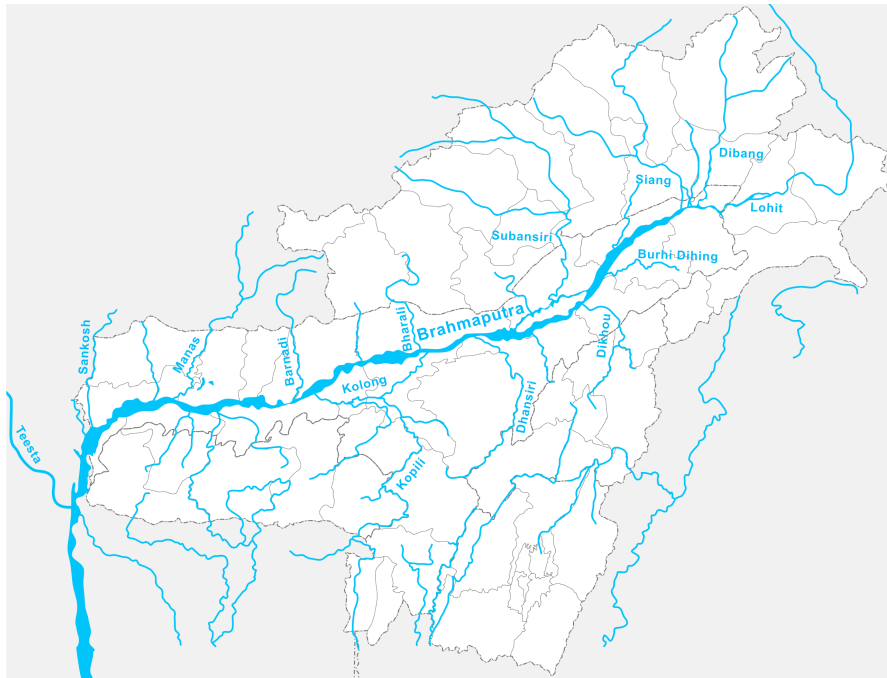


Figure 5.11: Map of the Brahmaputra basin (Wikipedia)

recognition of the boundaries that pertain to the strip between points A and B, which we want to analyze.

### 5.5.2 Water level at the left hand side suddenly rises by a height $a$ , the level at the right-hand side remains at zero

Figure 5.12 shows a groundwater basin with constant transmissivity  $kD$  and storage coefficient  $S$ . It has a width  $L$  and is bounded on either side by surface water in direct contact with the confined aquifer. The water level at the left changes suddenly by height  $A$ . How can we solve this, given the solution for the half space that we already have?

The answer is: by using mirror “ditches”.

We have shown the analytical solution for the infinite half space, where the surface water level at  $x = 0$  was suddenly raised by  $A$  m at  $t = 0$ . The solution gives the resulting head change and flow for  $x \geq 0$ . However, according to the analytical solution, after some time, the head at point  $B$ , the right-hand side of the strip will start rising. This is not what happens in reality, where the head at the right-hand side remains fixed at zero. How to deal with this mathematically?

When we forget the surface water at  $x = B$ , but instead assume a ditch at a distance  $L$  to the right, in which the water level was suddenly lowered at  $t = 0$  by an amount  $A$  (i.e. changed by an amount  $-A$ ), then the rising in point  $B$  due to the ditch at  $A$  would be exactly the decline in point  $B$  due to the ditch at a distance  $L$  to the right of  $B$ . As

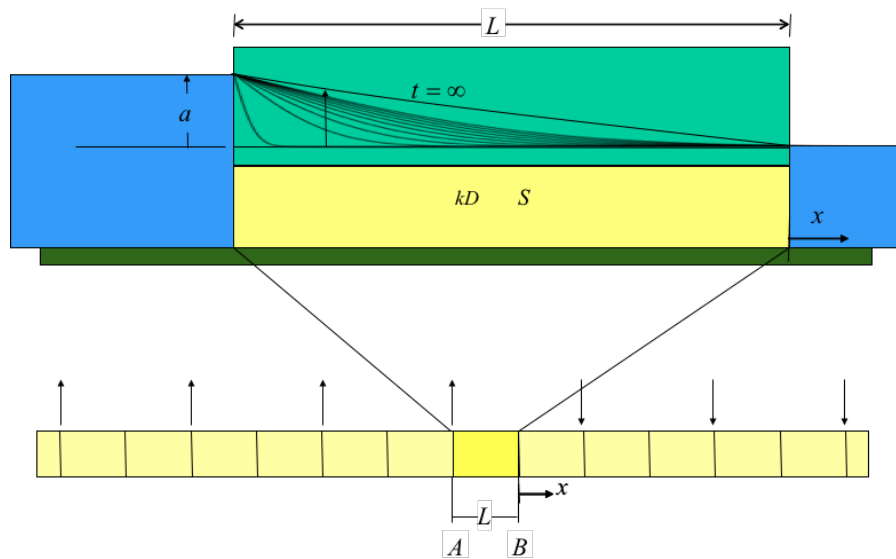


Figure 5.12: Confined groundwater basin to the left and right bounded by surface water in direct contact with the aquifer. Here the water level at the left boundary is suddenly raised by  $A$  at  $t = 0$  and that at the right side the surface-water level remains unchanged at zero. The lower picture shows the superposition scheme in which the strip of length  $L$  between points  $A$  and  $B$  is the one to be analyzed. The arrows in the lower picture show where the water level is suddenly raised or lowered in the mirror scheme.

a consequence of both, the head at point B remains zero, which is exactly the desired effect. In this case we have one mirror ditch with opposite change at distance  $L$  to the right of point B.

But this does not solve the whole problem, because after some more time, this right ditch will cause the head at point A to start declining, and so the head at point A does not remain fixed at the value  $A$  m. To compensate for that, we need another mirror ditch at distance  $2L$  to the left of point A with opposite change compared to the first mirror ditch. But this head change at  $2L$  left of point A will cause the head at  $2L$  to the right of point B to change over time, which will need a mirror ditch at  $4L$  to neutralize this effect, and so on. We will thus end up with an infinite number of mirror ditches to make sure that boundary conditions at both sides of our strip of land are kept that their values.

The lower picture in figure 5.12 intends to make this clear. Each arrow represents a mirror ditch and its direction indicates whether the water level in it goes down or goes up.

Is this solution with this scheme of mirror ditches correct? Well, this is in fact easy to see at a glance. Just look at the lower picture in figure 5.12 and consider the point B, in which the head should remain zero. As it is immediately clear, each ditch with lowered water level to the right of point B is exactly canceled at B by the ditch at the same distance to the left of point B with rising level. Hence the effect in point B of all ditches to the right are exactly canceled by all ditches to the left of point B, so the head at point B remains at zero. On the other hand all ditches to the right of point A are compensated at point A by all ditches to the left of point A, except for the ditch at point A. Hence, the net effect of all ditches at A is the same as that of only the ditch at A itself. That too can be seen at a glance from the lower picture in figure 5.12.

It does not matter whether point A or point B is chosen to be  $x = 0$ . However, because the scheme is anti-symmetrical around  $B$ , point  $B$  is the most convenient location to start the  $x$ -axis. If we take  $x = 0$  at point B, as is shown in figure 5.12, the distance of any of the right-hand ditches to a point with coordinate  $x$  is  $(2i - 1)L + x$  and the distance from any of the left-hand ditches to a point at  $x$  will be  $(2i - 1)L - x$ . Hence the  $x$  in the argument of the  $\text{erfc} \left( x \sqrt{\frac{S}{4kDt}} \right)$  has to be replaced by the distances to the mirror ditches. This yields for the head change within the strip of land:

$$s(x, t) = A \sum_{i=1}^{\infty} \left\{ \text{erfc} \left[ \{(2i-1)L+x\} \sqrt{\frac{S}{4kDt}} \right] - \text{erfc} \left[ \{(2i-1)L-x\} \sqrt{\frac{S}{4kDt}} \right] \right\}$$

$$Q(s, t) = A \sqrt{\frac{kDS}{\pi t}} \sum_{i=1}^{\infty} \left\{ \exp \left[ -((2i-1)L+x)^2 \frac{S}{4kDt} \right] + \exp \left[ ((2i-1)L-x)^2 \frac{S}{4kDt} \right] \right\}$$

Note that the second term in the formula for  $s(x, t)$  has a minus sign because of the water level in the right-hand ditches was lowered. However, the second term in the

formula for  $Q(s, t)$  has a plus, as both the left-and the right-hand ditches cause a positive flow, i.e. in the positive direction of the x-axis.

When you implement this scheme in Python, make sure you start the sum (loop) with  $i = 1$  and not  $i = 0$ .

Figure 5.13 shows the results for several times. Because the point  $x = 0$  was chosen to be at the point B (right of the strip), the x-values with in the strip are now negative. Also note that the steady state solution that is reached after about 3 days, has a head that decreases linearly from 2.5 m at the left to 0 at the right of the strip. The flow, therefore, must be  $Q = A/L \times kD = 2.5/250 \times 600 = 6 \text{ m}^2/\text{d}$ . Which is the case all along the width of the strip.

### 5.5.3 Shifting the zero point of the $x$ -axis.

It is straightforward to choose a different point for  $x = 0$ . For instance, to shift the point  $x = 0$  to the middle of the strip just subtract  $L/2$  from  $x$  to get

$$s(x, t) = A \sum_{i=1}^{\infty} \left\{ \operatorname{erfc} \left[ \left\{ (2i-1)L + x - \frac{L}{2} \right\} \sqrt{\frac{S}{4kDt}} \right] - \operatorname{erfc} \left[ \left\{ (2i-1)L - \left( x - \frac{L}{2} \right) \right\} \sqrt{\frac{S}{4kDt}} \right] \right\}$$

This way, one can shift the point  $x = 0$  to any desired location.

### 5.5.4 Arbitrary non-symmetrical case

Now consider the general case, in which the head at the left and right change by different values. Again, we need mirror ditches. This time not only to fix the left-hand head at the desired level, but also the right-hand head. Of course, you can regard this case from the perspective of the problem that we just solved. It is then the sum of the case in which the left-hand level was raised by  $A$  m and the right-hand level was kept at zero and the same case of which the right-hand size was raised by  $B$  m and the left-hand side was kept at zero.

But let's just solve it, after taking the  $x = 0$  at a convenient location, which would be in the center. Note however, you can put it at another location, but then the formulas change accordingly.

The image at the bottom of figure 5.15 shows the strip and the mirror ditches. By looking at that picture is should immediately be clear that this scheme of mirror ditches is correct. To see this, look at point A. You will then notice that each ditch to the left of A is compensated exactly by one at the right of A. The only effect of all the ditches at point A is the ditch at that point, all others cancel at A. Then look at point B and notice that this is also true for point B. Hence at point A, the only effect that remains is that of the head change A, and at point B, the only effect that remains is that o the head change at point B.

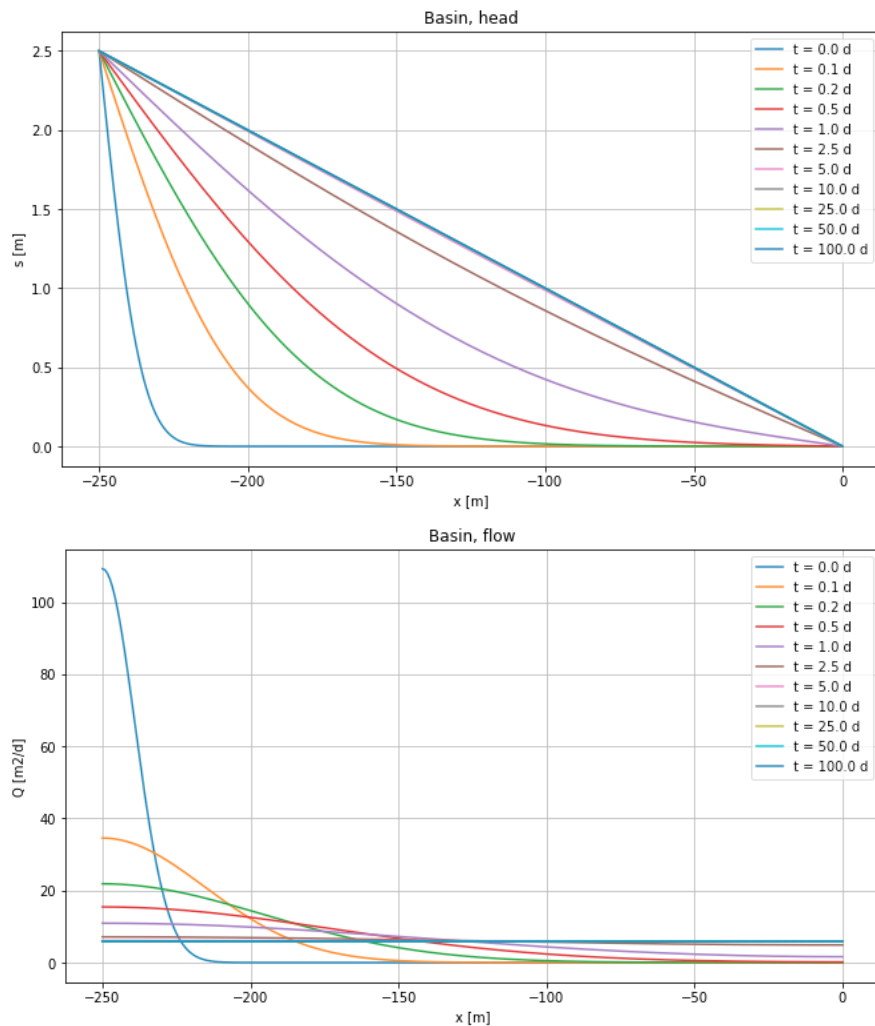


Figure 5.13: Top: head. Bottom: flow. After sudden head rise of  $A = 2.5$  m for various times,  $L = 250$  m,  $kD = 600 \text{ m}^2/\text{d}$ ,  $Sy = 0.1$

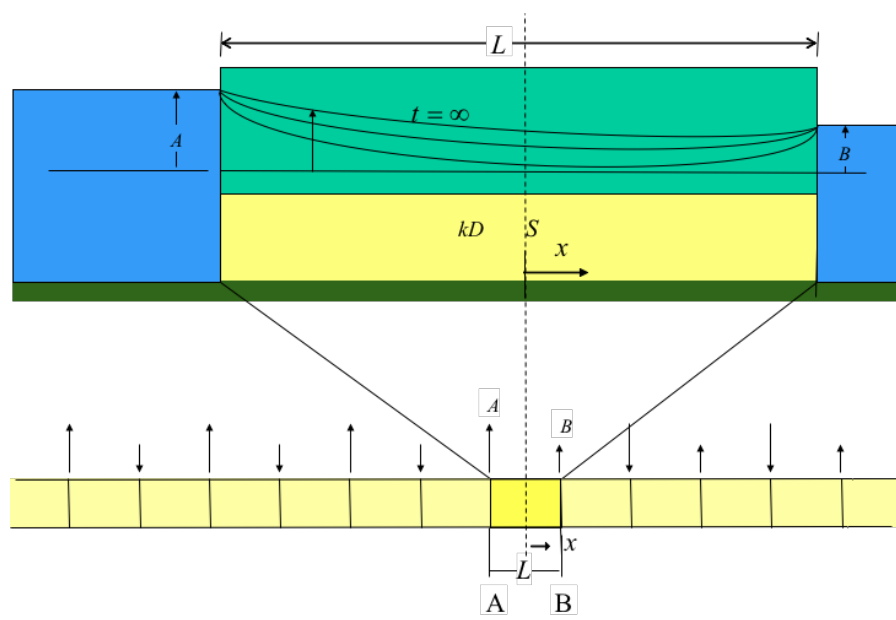


Figure 5.14: As figure 5.12 but the water level is raised independently on the left and right side by  $A$  and  $B$  respectively, and the  $x$ -axis is now centered in the center of the strip. The lower picture shows the superposition scheme; the arrows show where the water level is suddenly raised or lowered.

With this in mind, it's straightforward to write the expression for the head in the strip. To do that, just consider a point  $x$  and write the distance to all the ditches in terms of strip width  $L$  and  $x$ . Doing this, we get

$$s(x, t) = \dots$$

$$\begin{aligned} & A \sum_{i=1}^{\infty} \left\{ \operatorname{erfc} \left[ \left\{ (2i-1)L + \left( x - \frac{L}{2} \right) \right\} \sqrt{\frac{S}{4kDt}} \right] - \operatorname{erfc} \left[ \left\{ (2i-1)L - \left( x - \frac{L}{2} \right) \right\} \sqrt{\frac{S}{4kDt}} \right] \right\} + \dots \\ & \dots + B \sum_{i=1}^{\infty} \left\{ \operatorname{erfc} \left[ \left\{ (2i-1)L - \left( x + \frac{L}{2} \right) \right\} \sqrt{\frac{S}{4kDt}} \right] - \operatorname{erfc} \left[ \left\{ (2i-1)L + \left( x + \frac{L}{2} \right) \right\} \sqrt{\frac{S}{4kDt}} \right] \right\} \end{aligned}$$

Like it was done above, a similar expression can be written down for the flow.

An example result is shown in figure 5.15 for the case where at  $t = 0$  the head at the left boundary was raised by  $A = 2.5$  m and at the right side by  $B = 1.5$  m. Again, a steady state is reached after about 5 days, the flow is then constant, i.e.  $(A - B)/L \times kD = 1/250 \times 600 = 2.5$  m<sup>2</sup>/d. The flows are initially high and opposite on both sides. That is, during a short period, water infiltrates into the strip from both sides.

### 5.5.5 Symmetrical case, $A = B$

The symmetrical case is obtained when the rise of the water level at the left-hand boundary is the same as that at the right-hand boundary, so  $A = B$ . Of course, this case is included in the former one. However, we'll still work it out as we need it in the next section to compare it with a completely different expression for the same case that we'll use to generalize our understanding of the transient characteristics of groundwater basins.

Figure 5.16 shows the situation, same as before but the rise is  $A$  m at both sides. Taking  $x = 0$  at the center of the strip like before, we can draw the mirror scheme. This was done in the lower picture of figure 5.16. Like before, by first focusing on the symmetry around point A and then on the symmetry around point B, you should see at a glance that the scheme is correct. We can write the expression a bit more compact than before like this (See also Carslaw and Jaeger, p97, eq 9)

$$s(x, t) = A \sum_{i=1}^{\infty} \left\{ (-1)^{i-1} \left[ \operatorname{erfc} \left( \left[ \left( i - \frac{1}{2} \right) L + x \right] \sqrt{\frac{S}{4kDt}} \right) + \operatorname{erfc} \left( \left[ \left( i - \frac{1}{2} \right) L - x \right] \sqrt{\frac{S}{4kDt}} \right) \right] \right\} \quad (5.14)$$

This case, in which the water level at both boundaries suddenly rises by the same amount, can also be regarded as a transient drainage after a heavy shower of rain on the

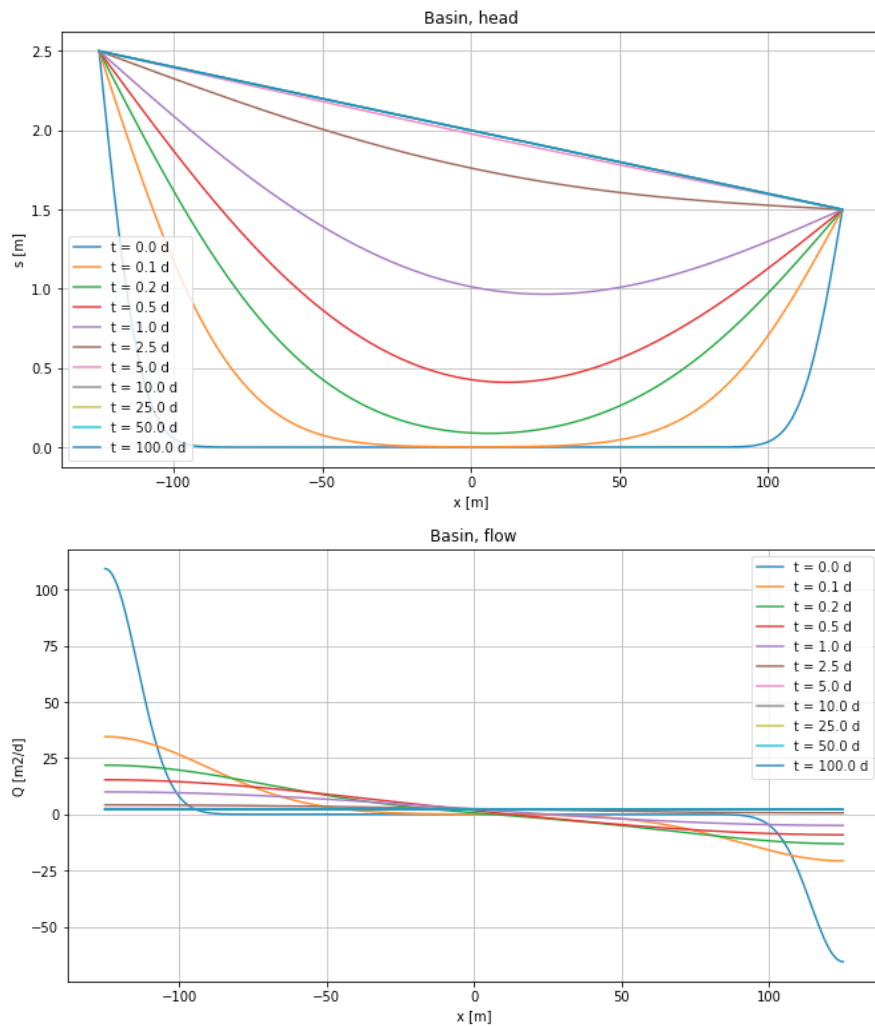


Figure 5.15: Top: head Bottom: flow. After sudden head rise by  $A = 2.5 \text{ m}$  at  $x = -L/2$  and  $B = 1.5 \text{ m}$  at  $x = +L/2$  for various times,  $kD = 600 \text{ m}^2/\text{d}$ ,  $Sy = 0.1$ ,  $L = 250 \text{ m}$ .

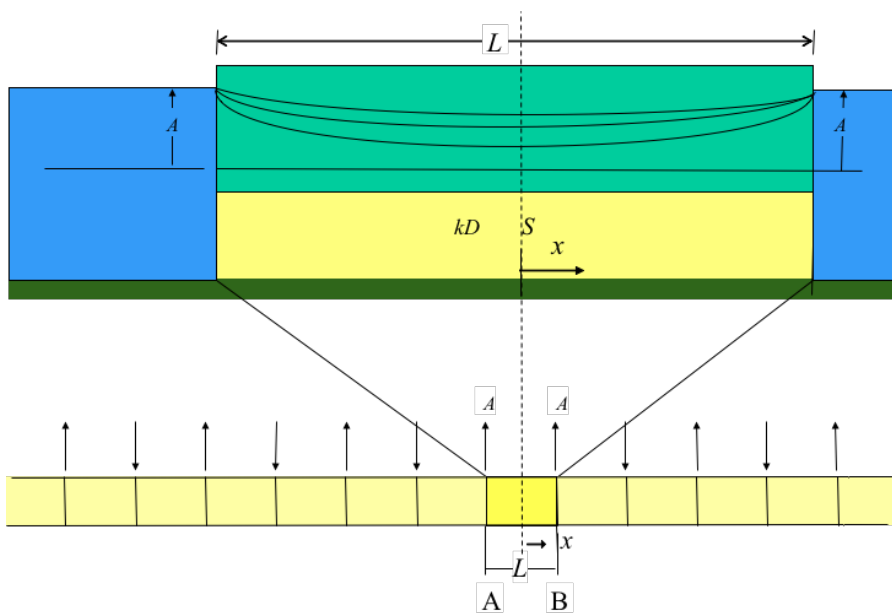


Figure 5.16: Groundwater basin bounded by surface water in direct contact on either side in which the water level is raised by  $A$  on both sides. The lower picture shows the superposition scheme with the errors indicating where the water level is raised or lowered for the superposition.

strip. If we assume that the rain surplus reaches the water table immediately, then the water level in the entire strip would suddenly rise by the amount  $A = \frac{P}{S}$  in which  $P$  is the rain (that part of it that reaches the water table) and  $S$  is the specific yield. Hence after such a shower, the head in the entire strip would be at  $A$  m above the water level in the ditches on either side. After this shower, the strip starts draining immediately. The picture that is thus obtained is the same as that of the ditches rising by  $A$  at  $t = 0$ , be it that the drainage picture is turned upside-down. This situation is illustrated in figure 5.17.

To use this equation to compute the drainage of a groundwater basins one may write  $s(x, t) = A(1 - \sum \dots)$ .

The discharge at any point  $x$  is obtained as usual by using Darcy's law, i.e.  $Q = -kD(\partial s/\partial x)$ :

$$Q(x, t) = -A \sqrt{\frac{kDS_y}{\pi t}} \times \dots$$

$$\dots \times \sum_{i=1}^{\infty} \left\{ (-1)^{i-1} \left[ \exp \left( - \left[ \left( i - \frac{1}{2} \right) L + x \right]^2 \frac{S}{4kDt} \right) - \exp \left( - \left[ \left( i - \frac{1}{2} \right) L - x \right]^2 \frac{S}{4kDt} \right) \right] \right\} \quad (5.15)$$

As can be seen, immediately after the head change, the water table drops very fast near the edges of the strip. Very soon, however, the head takes the shape of a cosine and the strip drains gradually until its final equilibrium is reached.

The cosine shape at later drainage stages follows from another form of analytical solution of the same strip, as will be discussed in the next section.

An example is shown in figure 5.18. In this case the so-called half times are used as times. The halftime is  $n\Delta t$ , with  $\Delta t = 0.28 \times (L/2)^2 S/kD$ , see next section. After each halftime, the difference between the head and the equilibrium final head is halved.

### 5.5.6 Questions

1. Set up a mirror scheme for the case of a strip of land bounded by straight surface water on either side, where the surface water stage of the right-hand side canal suddenly changes by a fixed value.
2. Show, explain on the hand of the obtained mirror scheme that the result is correct, i.e. that the result with all the mirror strips match the boundary conditions exactly.
3. What would be the mirror scheme for the strip if the right-hand boundary was closed?

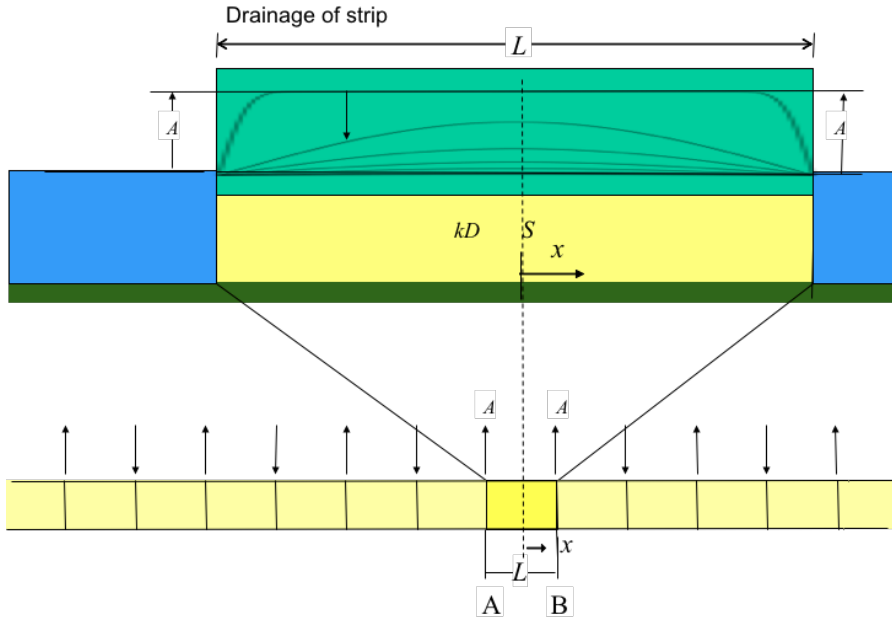


Figure 5.17: Symmetrical strip draining after heavy shower.

## 5.6 Symmetrical drainage from a land strip bounded by straight head boundaries (characteristic time of flow basins)

Here we introduce a solution for the drainage of a land strip that initially has uniform head  $s(0, x) = A$  and is bounded by two straight head boundaries at  $x = \pm b$  with head at  $s(\pm b, t) = 0$ . This solution looks completely different from the one we obtained by infinite mirroring of strips of land as we did in the previous sections, yet it provides the same result for the symmetrical case. The advantage of this form of the solution is that it can be further analyzed to deduce general drainage patterns and their time scale.

### 5.6.1 Analytical solution

In the previous section, we solved the symmetric one-dimensional basin by superposition of an infinite number of solutions for the half strip. While this is perfectly o.k., other solutions exist, which may look different, but are mathematically equivalent and yield the same results. For instance one of [Carslaw and Jaeger (1959)], p97, eq. 8, also published by [Verruijt (1999)], p87, is widely known in the Netherlands as “Kraaijenhoff van der Leur”). It reads

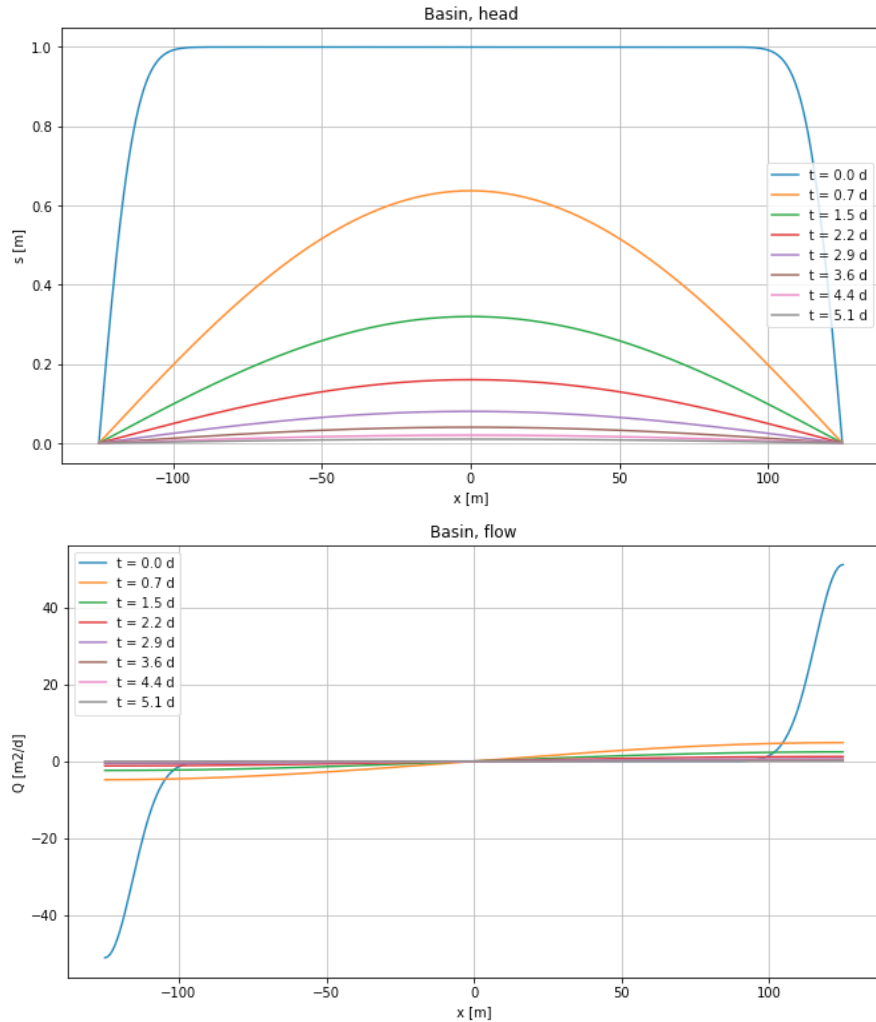


Figure 5.18: Top: head. Bottom: flow. Drainage after a sudden shower of 100 mm, such that with  $S = 0.1$ ,  $A = 1 \text{ m}$  at  $t = 0+$ . Thereafter, the strip drains towards the surface water at both sides, the water level of which is kept constant.  $kD = 600 \text{ m}^2/\text{d}$ ,  $S = 0.1$ ,  $L = 250 \text{ m}$ . Situation for several times.

$$s(x, t) = A \frac{4}{\pi} \sum_{j=1}^{\infty} \left\{ \frac{(-1)^{j-1}}{2j-1} \cos \left[ (2j-1) \left( \frac{\pi}{2} \right) \frac{x}{b} \right] \exp \left[ -(2j-1)^2 \left( \frac{\pi}{2} \right)^2 \frac{kD}{b^2 S} t \right] \right\} \quad (5.16)$$

From this we obtain the flow by setting  $Q = -kD \frac{\partial s}{\partial x}$ , which yields

$$Q(x, t) = +2kD \frac{A}{b} \sum_{j=1}^{\infty} \left\{ (-1)^{j-1} \sin \left[ (2j-1) \left( \frac{\pi}{2} \right) \frac{x}{b} \right] \exp \left[ -(2j-1)^2 \left( \frac{\pi}{2} \right)^2 \frac{kD}{b^2 S} t \right] \right\}$$

As always,  $s(x, t)$  is the head relative its equilibrium value, which is  $s(x, \infty) = 0$ . The  $x$ -axis is taken such that  $x = 0$  in the center and  $x \pm b$  corresponds to the sides with fixed boundary conditions  $s(\pm b, t) = 0$ . The initial head is  $s(x, 0) = A$  inside the section,  $-b < x < b$ . The formula describes the drainage that follows after the initial situation.

This behavior is characteristic for a basin after a sudden shower causing the head in it to suddenly rise everywhere by the same amount, while the level in the ditches at both sides is kept the same. After the shower, the drainage sets in and gradually continues until equilibrium is finally reached (which theoretically takes infinite time).

Equation 5.16 yields the same head as was obtained previously with superposition of an infinite number of erfc-functions, even though the solution presented here looks mathematically completely different. We will use this solution to derive drainage characteristics that can be applied in practice on different scales.

Figure 5.19 gives the results as an example. The lines are the same as in figure 5.18 and the dots are the results of equation 5.16 for the same times. The results are the same. The lower picture in this figure shows the computed flows using both approaches.

Finally, Showing the individual terms of the series in equation 5.16 for head and for flow together with the total solution obtained by the summation.

**Exercise:** Implement equation 5.16 yourself together with the solution using superposition of mirror ditches and show that the outcomes are the same when simulation free drainage of a strip of land. You should obtain figure 5.19.

### 5.6.2 Long-term drainage behavior, characteristic drainage time

Expression 5.16 looks complicated at first, but it can be broken down to yield useful and practical insights pertaining to the dynamic characteristics of draining groundwater basins. For that purpose, we analyze the expression under the summation.

The  $2j-1$  is just the series  $1, 3, 5, 7, \dots$  and  $(-1)^{2j-1} = +1, -1, +1, -1, \dots$ . Next, we have a product of a cosine and an exponent. The cosine will fluctuate between -1 and +1 and it only depends on  $x$ . Then notice the exponent, which only depends on time. For simplicity write it as

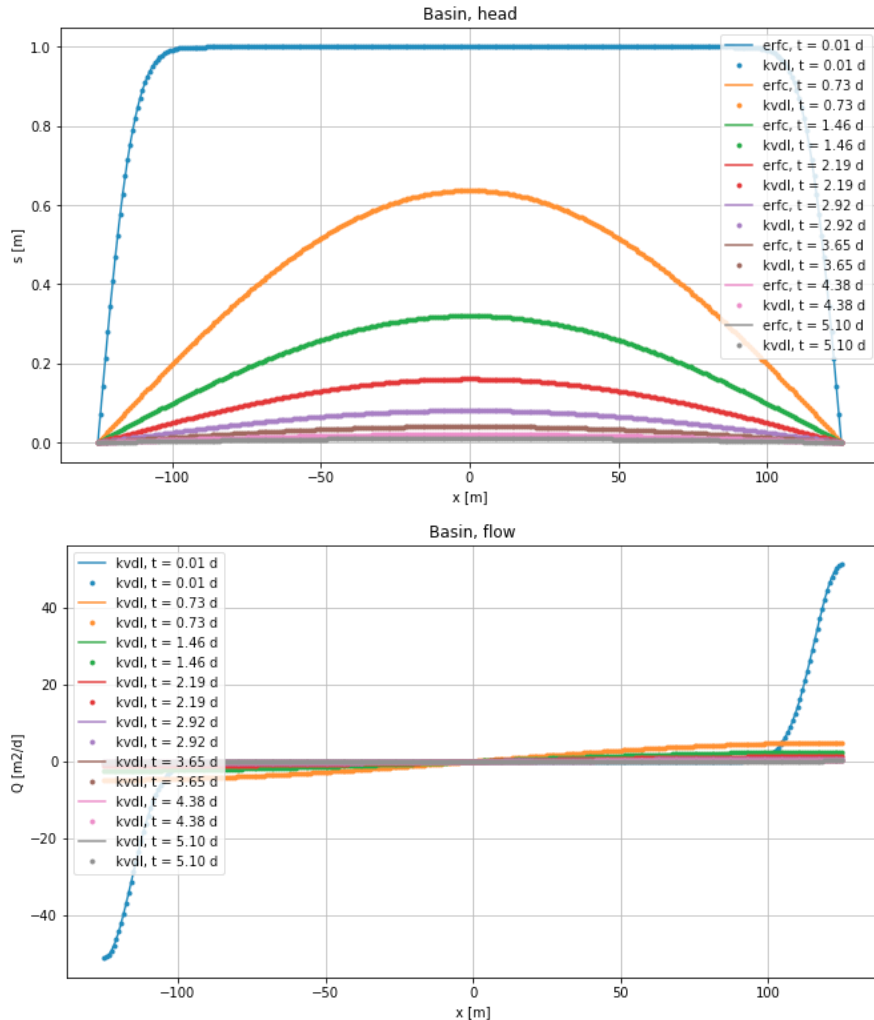


Figure 5.19: Top: head. Bottom: flow. Free drainage of basin from initial head at  $A = 1$  m for various times,  $kD = 600 \text{ m}^2/\text{d}$ ,  $Sy = 0.1$ ,  $L = 250 \text{ m}$ . Drawn lines were computed with the `erfc` functions and are the same as in figure 5.17; the dots were computed with equation 5.16. The lines from both approaches completely overlap.

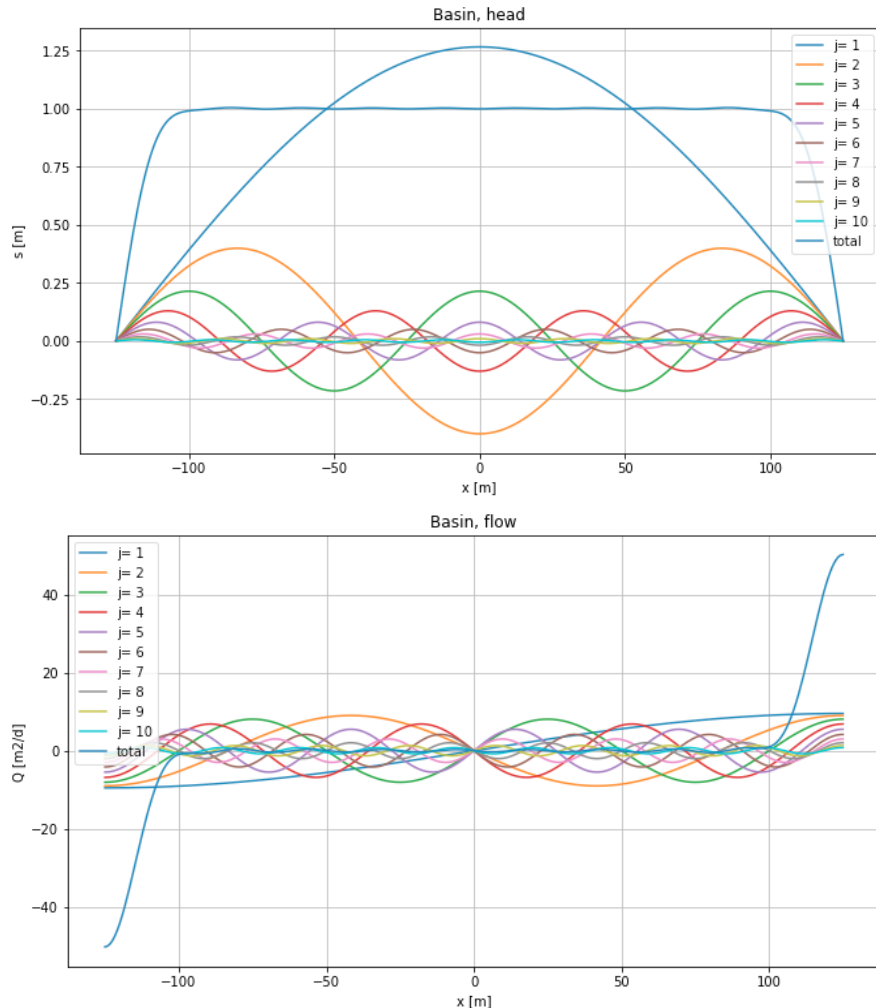


Figure 5.20: Showing the individual terms of the series in equation 5.16 for head and for flow together with the total solution obtained by the summation. This is done for  $t = 0.0073$  d. Other values are the same as in figure 5.19.

$$\exp \left[ -(2j-1)^2 \left( \frac{\pi}{2} \right)^2 \frac{t}{T} \right]$$

where  $T = \frac{b^2 S}{kD}$ .  $T$  may thus be regarded as a characteristic time of the drainage. The exponent terms in the series now become

$$\exp \left( -\left( \frac{\pi}{2} \right)^2 \frac{t}{T} \right), \exp \left( -9 \left( \frac{\pi}{2} \right)^2 \frac{t}{T} \right), \exp \left( -25 \left( \frac{\pi}{2} \right)^2 \frac{t}{T} \right), \dots$$

Because  $\frac{t}{T} > 0$ , the second and higher terms will finally become much smaller than the first and may, therefore, be neglected when  $t > t_n = nT$  where  $n$  needs to be estimated. So let us see when the second term becomes much less than the first one, so that only the first term matters and we can neglect all other terms. Therefore, compare the first term with the second and demand that it's much larger than the second:

$$\exp \left( -\pi^2 \frac{t}{T} \right) \gg \exp \left( -9\pi^2 \frac{t}{T} \right)$$

or

$$\exp \left( -\left( \frac{\pi}{2} \right)^2 \frac{t}{T} \right) = G \exp \left( -9 \left( \frac{\pi}{2} \right)^2 \frac{t}{T} \right)$$

where  $G$  is just a large positive number. We may choose  $G = 100$ , which means, we neglect all higher terms, when the first term is at least 100 times a large as the second.

where one may choose  $\epsilon = 0.01$  for example. Taking the log at both sides yields

$$-\left( \frac{\pi}{2} \right)^2 \frac{t}{T} = \ln G - 9 \left( \frac{\pi}{2} \right)^2 \frac{t}{T}$$

hence,

$$8 \left( \frac{\pi}{2} \right)^2 \frac{t}{T} = \ln G$$

so that

$$\frac{t}{T} = \frac{\ln G}{8 \left( \frac{\pi}{2} \right)^2} = \frac{\ln 100}{8 \left( \frac{\pi}{2} \right)^2} \approx 0.23$$

For the chosen  $G = 100$ , we find  $t = 0.23T$ . Therefore, we conclude that all higher terms are negligible when  $t > 0.23T$ .

This means that when  $t > 0.23T$  the expression given above reduces to only one term

$$s(x, t) = A \frac{4}{\pi} \cos \left( \frac{\pi x}{2b} \right) \exp \left( -\left( \frac{\pi}{2} \right)^2 \frac{t}{T} \right), \text{ with } t > 0.23T, \text{ and } T = \frac{b^2 S}{kD}$$

This is a simple-to-understand expression. It is a cosine with its top equal to  $\frac{4}{\pi}A$  in the center where  $x = 0$  and zero where  $x = \pm b$ . This cosine-shaped groundwater mound gradually declines according to the exponent.

An exponential decline can always be characterized by its halftime, i.e. the time in which the head reduces by half. So if  $t$  increases by one halftime,  $\Delta t_{50\%}$ , the head  $s(x, t)$  is reduced by a factor 0.5.

To obtain this halftime, write down that half the head at time  $t$  is obtained at time  $t + \Delta t_{50\%}$ . So literally translated into mathematics, we have

$$0.5 \exp\left(-\left(\frac{\pi}{2}\right)^2 \frac{t}{T}\right) = \exp\left(-\left(\frac{\pi}{2}\right)^2 \frac{t + \Delta t_{50\%}}{T}\right)$$

Taking the logarithm on both sides yields

$$\ln 0.5 - \left(\frac{\pi}{2}\right)^2 \frac{t}{T} = -\left(\frac{\pi}{2}\right)^2 \frac{t + \Delta t_{50\%}}{T}$$

and so

$$\ln 0.5 = -\left(\frac{\pi}{2}\right)^2 \frac{\Delta t_{50\%}}{T}$$

and, therefore,

$$\frac{\Delta t_{50\%}}{T} = \left(\frac{2}{\pi}\right)^2 \ln 2 \approx 0.28$$

This implies that when time progresses by  $\Delta t_{50\%} = 0.28T$ , the drawdown is halved (under the condition that  $t > 0.23T$ ).

This result allows us to immediately compare the halftimes of the free drainage of groundwater basins of widely different sizes and with widely different aquifer properties. Let the size of the basin be expressed by it's representative half-width  $b$ . Of course, when a groundwater basin does not have has the shape of a long strip bounded by two straight canals, ditches or rivers, one should estimate a reasonable half-width based on the distance from the water divide to its drainage base, be it ditches, canals, streams, lakes, rivers or the coast.

Table 5.1 gives the characteristic time  $T = b^2 S_y / kD$  and the halftime  $\Delta t_{50\%} = 0.28T$  for some groundwater basins.

As can be concluded from the equations and the numerical examples in the table, characteristic times and halftimes of groundwater basins will vary enormously depending

Situation	Country	$kD$ $m^2/d$	$S_y$ [ $]$	$b$ m	$T$ d	$T_{50\%}$ d	$T$ yr	$T_{50\%}$ yr
Nubian Sandstone	Egypt	500	0.001	5.00E+05	500000	140000	384	418
Kalahari	Botswana	500	0.1	3.00E+05	18000000	5040000	13808	15051
Veluwe area	Netherlands	6000	0.27	20000	18000	5040	14	15
Dunes	Netherlands	200	0.22	2000	4400	1232	3	4
Power bulb parcel	Netherlands	200	0.1	50	1.25	0.35	0.001	0.001

Table 5.1: Characteristic times  $T = b^2 S_y / kD$  and halftimes  $\Delta t_{50\%} = 0.28T$  of the drainage of various groundwater systems

on the aquifer properties, but especially depending on their representative width, because the latter works to the power 2. A simple meadow or arable field in the Netherlands bounded between two ditches just 100 m apart may have a halftime in the order of one day. Large systems, notable deserts, like the Kalahari example may have a halftime in the order of 10000 years. This implies that the small meadow in the Netherlands, will hardly remember the rain shower that fell one week ago, while the Kalahari is still draining the water that it collected during previous wet episodes, like the last ice age. Recent research with respect to the world's largest aquifer, the Nubian sandstone, showed that this aquifer, which extends over much of Sudan, Egypt and Libya, may be regarded as a water table aquifer that is slowly draining the water collected during wet episodes when the Sahara was still wet (especially between the onset of the Holocene until about 4600 years ago, [Powell and Fensham (2015), Voss and Soliman (2014) ] and that the current oases represent the last remains of the water table that was much higher thousands of years ago.

### 5.6.3 Questions

1. Show on the hand of equation 5.16 what the half-time of the drainage of this system is. Derive it yourself.
2. How does the characteristic time relate to halftime? Show this mathematically?
3. Implement equation 5.16 and make a graph of some of the first terms of the series and of its sum.
4. Show that equation 5.16 equals equation 5.14 by implementing both, which you may do using a language like Python or a spreadsheet like Excel. Notice that the *first = 1 - second*.
5. Derive the discharge from equation 5.16 and show that it is the same as that in equation 5.15 by implementing both in the same spreadsheet.
6. Show some of the first terms of the series in equation 5.14 in Python or Excel.

# 6 Transient flow to wells

## 6.1 Introduction

This chapter deals with the flow to wells in aquifers. The flow to a well is treated as axially symmetric and horizontal. Vertical resistance to flow within the aquifer itself is neglected in this course. This is the so-called Dupuit-Forchheimer approximation. It is a very useful approximation because it allows computing regional groundwater flow in aquifers accurately in a vertically integrated manner by considering the flow to be horizontal. This way, we don't have to deal with head losses due to vertical flow components. Important vertical components may, however, occur in the vicinity of wells that only partially penetrate the aquifer. Disturbances of the essentially horizontal flow due to partial penetration of well screens is, however, only important in the vicinity of the wells, at distances less than 1.5 times the aquifer thickness, and can be dealt with by a correction on the drawdown as will be outlined in the facultative section 6.4 (section “Partial penetration of well screens”) on page 125.

We will handle more complicated situations, such as well fields and wells near specific boundaries, by superposition of mirror wells. By the way, also partial penetration is effectively handled by superposition.

We start this chapter with an overview of the analytical solutions that we will deal with and their related steady-state versions.

In the past, groundwater-flow solutions were computed by looking up values in tables. Nowadays, because everyone has access to Excel or Python, we will compute the values of the different well functions using those powerful computational means rather than looking them up in tables. However, tables remain extremely important as a means to verify our own numerical implementation of solutions and functions. Further, not all required mathematical functions may be available in our computational program, especially not in Excel. In that case we can implement them ourselves. This can be done in Excel using Visual Basic as well as in other languages, such as Python. In the course and the exercises we will use the more modern Python, because it is so much more powerful than Excel and nowadays it's free. Basic. Generally only a few lines are needed to use or, when necessary, implement the most important transient groundwater flow solutions.

## 6.2 Wells and well functions overview

The next three figures provide an impression of what wells are, without entering in the details of their construction or the installation of pumps, pump cellars, electricity and so on. What matters for us is the position of the screen inside the aquifer.

Figure 6.1: Large-diameter open well in India (copied from Newspaper NRC some years ago).



There exist numerous types of wells: open wells, dug wells, drilled wells, tube wells, horizontal wells and more. In this course, we limit ourselves to that are essentially of small diameter, i.e. of small well radius indicated as  $r_0$ . This limitation suffices for most practical situations. For special cases not covered, one has to refer to the literature where analytical solutions are published or rely on a numerical model. Many solutions can be found in [Carslaw and Jaeger (1959)] and in [Bruggeman (1999)]. With respect to well testing and pumping test analyses, [Kruseman and De Ridder (1970)]. It has been used in all continents for about four decades (the first issue is of 1970). The second version of this book, of 1994e, can be downloaded from the Internet for free ([https://www.hydrology.nl/images/docs/dutch/key/Kruseman\\_and\\_De\\_Ridder\\_2000.pdf](https://www.hydrology.nl/images/docs/dutch/key/Kruseman_and_De_Ridder_2000.pdf)). The book is a very good reference covering the relevant literature in a practical way and also providing tables with the values for many of the analytical groundwater functions. You may need of want these for reference.

The solution for large-diameter wells, is one such special cases, useful for situations like illustrated in figure [Large-diameter open well in India \(copied from Newspaper NRC some years ago\)](#). The implementation of the solution for large-diameter wells with in-bore water storage is also provided in section [6.7, Large-diameter wells \(not for the exam\)](#) on page [152](#) for reference. But it is not part of the course.

Figure [6.2](#) is a sketch of a (tube) well in an unconfined aquifer (synonymous with “water-table aquifer” and with “phreatic aquifer” and is opposite to “confined aquifer”). Figure

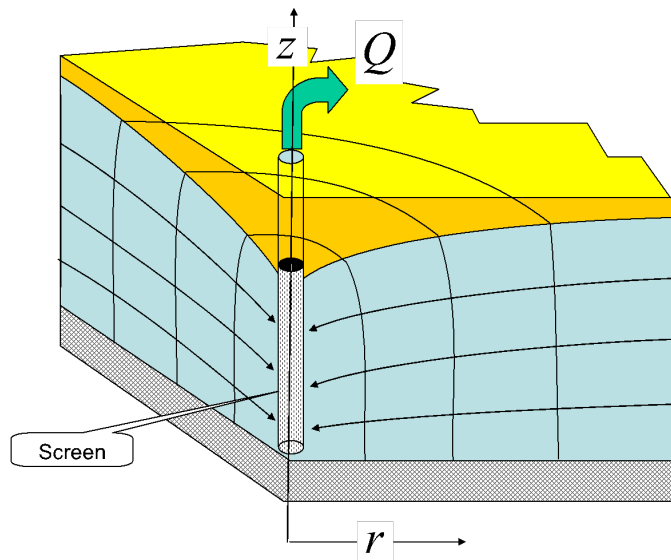


Figure 6.2: A tube well in an unconfined aquifer

6.3 gives a sketch of a tube well in a (semi) confined aquifer. The difference between a confined and a semi-confined aquifer, is that the top and bottom of the confined aquifer are both impervious (there is no vertical leakage), while the semi-confined aquifer has vertical leakage through its ceiling, its floor or both. The screen, i.e. the perforated portion of the well is considered to fully penetrate the (wet) section of the aquifer, see in figure 6.2. The well screen is not completely penetrating the aquifer in figure 6.3. Very often, the penetration of the aquifer by the screen is only minor where aquifers are thick because this saves drilling, material and installation cost. It should be noted however, that due to partial penetration of a well screen, the streamlines in the vicinity of the screen are no longer all horizontal. The concentration of the streamlines towards the top and the bottom of a partially penetrating screen cause extra head loss relative to the situation with a fully penetrating screen. This head loss can be taken into account when necessary as outlined in the facultative section 6.4 on page 125.

The right-hand side of figure 6.3 shows the streamlines in the case of a completely confined aquifer, one without vertical leakage. The left-hand side of figure 6.3 shows the streamlines in a semi-confined aquifer that is recharged by seepage from an overlying layer. Of course, seepage may also occur from underlying layers, but we will not deal with such multilayer groundwater-flow systems in this syllabus. The modern theory for multilayer aquifer systems can be looked up in [?], [Maas (1986)] and in [Bruggeman (1999)].

It is important to realize that flow due to an extraction by a well in a water-table or perfectly confined aquifer of infinite lateral extent will never reach equilibrium, it will always remain transient. The reason is that all the water has to come from storage. Or more precise, the extraction does not cause water external to the aquifer to enter the aquifer. Even rain does not have any effect on the drawdown caused by the extraction.

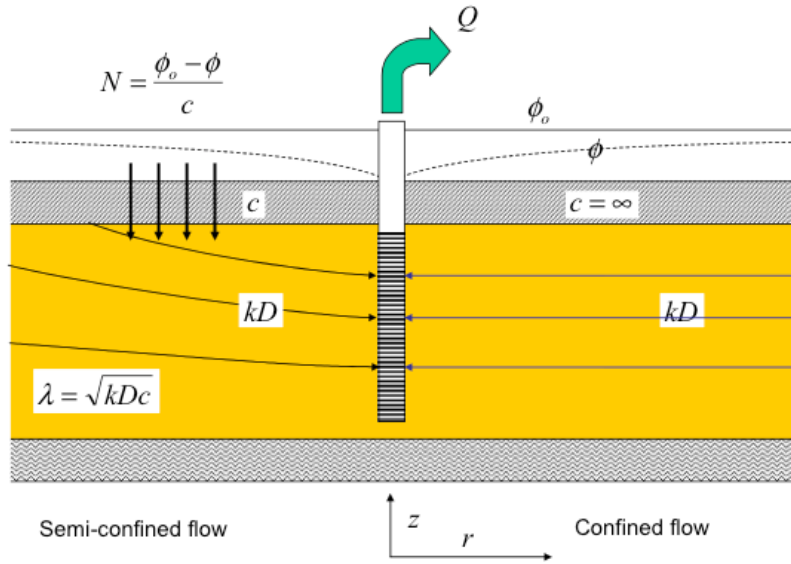


Figure 6.3: Tube well with stream lines in a semi-confined and a confined aquifer

Of course, it changes the head, but not due to the well. This recharge has an effect that can be superimposed independently from the that due to the extraction. Only when a well extraction causes water to flow across aquifer boundaries as an effect of the gradients created by the well extraction, can the flow reach an equilibrium, i.e. steady state after a limited time. Therefore, a continuous extraction from a confined aquifer of infinite extent never reaches steady state, but a continuous extraction from a semi-confined aquifer does reach steady state, as does an extraction by a well in an aquifer that is bound by some fixed-head boundaries. Of course, if the flow through the semi-confined layer drains higher-stock aquifers or layers or an overlying marsh, then this steady-state situation may not be reached or not be maintained for a very long time. In that case we would experience delayed yield, which is outlined in the facultative section 6.6 on 142. In practice, it is always important to realize that extraction from a semi-confined layer may drain overlying layers such that the leakage through the confining cover may stop over time, after which the aquifer will start behaving like a confined or unconfined layer without vertical leakage.

Governing equations are important as they express the physical foundation and the approximations made to solve a problem analytically. They will be presented further down. However, the general relation between solutions for a water-table aquifer and a confined aquifer is presented next.

The transmissivity in a water-table aquifer is given by  $T = kh$  where  $h$  is the distance from the water table to the bottom of the aquifer, which is assumed to be horizontal. The transmissivity of a confined aquifer is  $T = kD$  with  $D$  the thickness of the confined aquifer.  $h$  depends on the water table, which is variable as it changes due to the pumping

and perhaps also due to other factors like varying boundary conditions. Notice that there are no analytical solutions dealing with a time-variable water table; they all approximate the water-table situation by taking  $D \approx h$ , where  $h$  should be a suitable average over the area of interest. As always, the partial differential equation is linearized before solving it. Superposition can be applied on linearized solutions, so that we may add an arbitrary number of different solutions to the same groundwater system and solve it by superposition. It also means that the effect of the wells themselves remains completely separated from effects of other factors or boundary conditions. This is because the partial differential equation that we deal with is linear. This means that precipitation and evaporation play no role when it comes to computing the changes of the groundwater heads and flows caused by wells. This simplification may fail, however, when the groundwater system does not obey to the assumptions underlying our partial differential equation. This is the case, for example, when plant evaporation is reduced in a **nonlinear** fashion by the drawdown of the water table caused by the wells (we stress the word **nonlinear**). One should keep such exceptions in mind when solving practical problems and stay aware of the limitations to the calculation methods and formulas applied. The same is true when applying groundwater models.

Table 6.1 shows the most important groundwater-well solutions. Only the first one deals with a water-table aquifer; all other wells solutions require the transmissivity to be constant. To use these solutions for water-table aquifers, the drawdown must remain small compared to the wet aquifer thickness; it may not change by more than say 20% of the original aquifer thickness. However, one may often overcome such conditions by using a proper average for the aquifer thickness. The water-table solution depends on  $h^2 - H^2$ . Note that this can be converted into a product of the drawdown and the aquifer thickness as follows

$$h^2 - H^2 = (h - H)(h + H) \approx 2sH = 2sD \quad (6.1)$$

Replacing  $h^2 - H^2$  in the first solution by  $2sH$  yields the second. Equation 6.1 also gives a clue to the accuracy of using a confined-aquifer solution for an water-table case, as we will often do in practice. It requires that  $h + H \approx 2D$ . A head change of  $h$  of 20% of  $H$  then causes an error in the computed drawdown of about 10%, which is acceptable in most circumstances.

Clearly, the second Thiem solution is directly related to the transient Theis solution, but they are not equivalent because the Theis solution has no steady state. However, the difference between the transient heads at two different finite distances from the well does become steady state over time, and that steady state is equivalent to the Thiem solution for constant aquifer thickness. The steady-state solution for flow to a well in a leaky aquifer, according to De Glee (1930), is the steady state equivalent of the transient solution of [Hantush (1955)]. Also notice that **all** steady-state solutions have a 2 in the denominator of the factor multiplying the well function or the logarithm, while **all** transient solutions have a 4 at that position. From this it immediately follows that the Hantush solution for  $t \rightarrow \infty$  is

$$\frac{Q}{4\pi kD} W \left( u_{t \rightarrow \infty}, \frac{r}{\lambda} \right) = \frac{Q}{2\pi kD} K_0 \left( \frac{r}{\lambda} \right)$$

so that

$$W \left( u_{t \rightarrow \infty}, \frac{r}{\lambda} \right) = 2K_0 \left( \frac{r}{\lambda} \right)$$

where  $W \left( r, \frac{r}{\lambda} \right)$  is the Hantush well function and  $K_0 \left( \frac{r}{\lambda} \right)$  is the modified Bessel function of the second kind and zero order.

### 6.3 Theis: transient well in an infinite aquifer with constant transmissivity and storativity

In 1935, [Theis (1935)] published a new solution for the dynamic change of head caused by a well that, at  $t = 0$ , begins pumping at a constant rate from an infinite aquifer having uniform transmissivity and storativity.

The solution by Theis has been one of the major breakthroughs in groundwater hydrology. For the first time, it was possible to analyze the dynamics of the heads and flows caused by extracting wells. Before Theis, only steady-state flow solutions for the groundwater flow due to wells existed, which very much limited possible analyses of actual pumping regimes. According to Theis, when a well pumps from an aquifer of infinite extent, all water must come from storage; there are no extra sources<sup>1</sup>. Clearly, the flow to a well extracting well in an infinite aquifer is axially symmetric. Therefore, only the distance to the well,  $r$ , and time,  $t$ , matter as independent variables. To analyze the flow to such a well, we consider continuity of a ring around it with thickness  $dr$  between radii  $r$  and  $r + dr$ . The situation is given in figure 6.4. Notice that this figure shows a cross section through an axially symmetric groundwater system. Also notice that in the figure the thickness of the aquifer is the height of the water table above the base of the aquifer. However, we in the derivation we assume that this thickness is constant

---

<sup>1</sup>Of course, there may be other sources of water, but their rate of in- or outflow of the aquifer is independent of the gradients caused by the well. This is the essence here.

Name	Water table?	Leakage?	Transient?	Solution
Thiem	yes	no	no	$h^2 - H^2 = \frac{Q}{\pi k} \ln \frac{R}{r}$
Thiem	no	no	no	$s = \frac{Q}{2\pi kD} \ln \frac{R}{r}$
De Glee (1930)	no	yes	no	$s = \frac{Q}{2\pi kD} K_0 \left( \frac{r}{\lambda} \right)$
Theis (1935)	no	no	yes	$s = \frac{Q}{4\pi kD} W(u)$
Hantush (1955)	no	yes	yes	$s = \frac{Q}{4\pi kD} W(u, \frac{r}{\lambda})$

Table 6.1: Overview of the most important groundwater-well solutions. In all formulas  $\lambda = \sqrt{kDc}$  and  $u = \frac{r^2 S}{4kDt}$

and equal to  $D$  everywhere in the aquifer. This assumption is acceptable only as long as the drawdown is small with respect to the thickness of the aquifer. We also take the storativity  $S$  to be constant throughout the aquifer. The head in the aquifer is initially  $\phi_0$ . The drawdown,  $s$ , is, therefore,  $\phi_0 - \phi$ , when we consider drawdown positive. In stead of drawdown, we may prefer to use the more general term “head change” and use  $\phi - \phi_0$  instead, i.e. positive when the head rises and negative when it declines; the only difference between “drawdown” and “head change” is the sign. There is no real preference to use either of the two. In pumping tests, drawdown is mostly preferred.

To see what's in Theis' solution, we look first at the partial differential equation that he solved together with his boundary and initial conditions. The first thing always is to derive a governing PDE of the problem at hand. For this, we just consider continuity, which is the water budget of a small concentric ring of width  $dr$  around the well, disregarding any physical laws except the principle of continuity. The water budget of the ring at time  $t$  reads

$$q(2\pi r) - \left(q + \frac{\partial q}{\partial r} dr\right)(2\pi(r+dr)) = S \frac{\partial \phi}{\partial t}(2\pi r) dr$$

which can be simplified to

$$q(2\pi r) - \left(q + \frac{\partial q}{\partial r} dr\right)(2\pi r) - \left(q + \frac{\partial q}{\partial r} dr\right)2\pi dr = S \frac{\partial \phi}{\partial t}(2\pi r) dr$$

or

$$-\frac{\partial q}{\partial r} - \left(q + \frac{\partial q}{\partial r} dr\right) \frac{1}{r} = S \frac{\partial \phi}{\partial t}$$

Letting  $dr \rightarrow 0$ , we obtain our continuity or water balance equation for the ring

$$-\frac{\partial q}{\partial r} - \frac{q}{r} = S \frac{\partial \phi}{\partial t}$$

At this point we switch to a constitutional law, i.e. Darcy's law, by writing

$$q = -kD \frac{\partial \phi}{\partial r}$$

So that, combining Darcy's law with continuity, we get

$$-\frac{\partial}{\partial r} \left(-kD \frac{\partial \phi}{\partial r}\right) - \frac{kD}{r} \frac{\partial \phi}{\partial r} = S \frac{\partial \phi}{\partial t}$$

And because it was assumed that  $kD$  is constant, this equation simplifies to

$$\frac{\partial^2 \phi}{\partial r^2} + \frac{1}{r} \frac{\partial \phi}{\partial r} = \frac{S}{kD} \frac{\partial \phi}{\partial t}$$

which is the PDE that Theis solved for the following initial and boundary conditions.

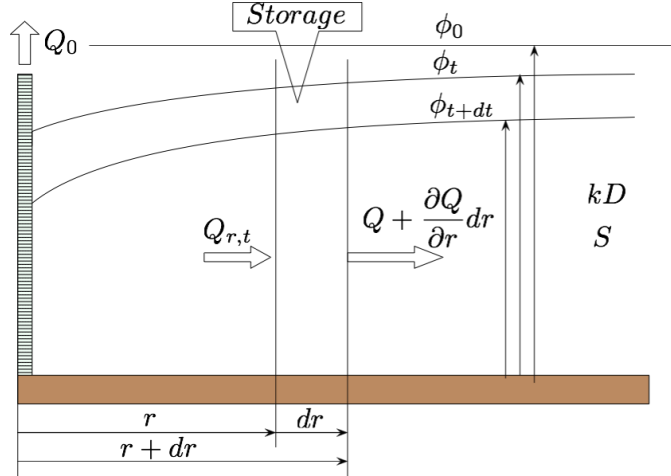


Figure 6.4: Scheme axial symmetric flow to an extraction well according to Theis

$$\begin{aligned}\phi_{r,0} &= \phi_0 \\ \phi_{\infty,t} &= 0 \\ Q_0 &= -2\pi r k D \left( \frac{\partial \phi}{\partial r} \right)_{r \rightarrow 0}\end{aligned}$$

This has as its solution

$$s = \phi - \phi_0 = \frac{Q}{4\pi k D} W(u), \quad u = \frac{r^2 S}{4k D t}$$

in which  $W(-)$  is called Theis' well function among hydrogeologists, see below.

Notice that it is not the head that is important, only the difference from the initial head matters, which is the head change or the drawdown. Also notice that all steady-state well formulas have the factor  $2\pi k D$ , while the transient solutions all have the factor  $4\pi k D$ . Finally notice that the well function  $W(-)$  does not depend on  $r$  or  $t$  separately, but on a single variable, called  $u$ , which combines  $r$  and  $t$  together with  $S$  and  $k D$  in a specific way. All formulas describing transient flow to wells have this variable  $u$ .

The function  $W()$  is known as Theis' well function among hydrologists. However, mathematicians knew that function long before Theis; they have a name for it, the exponential integral

$$\text{expint}(u) = E_1(u) = \int_u^\infty \frac{e^{-y}}{y} dy \quad (6.2)$$

Clearly, the well function has is given in tables in book on pumping test analysis like [Kruseman and De Ridder (1970)] (1994 edition is available for free on the Internet)

and in mathematical table books like [[Abramowitz and Stegun \(1964\)](#)]. Nowadays, this function is readily available in software such as Python and Matlab, but in Excel it has to be implemented, preferably using Visual Basic, to use it with ease in computations.

Next to its integral representation, the exponential integral can be expressed as a power series. The power series representation will reveal indispensable when studying general behavior of the well function. The power series representation is ([[Kruseman and De Ridder \(1994\)](#)])

$$W(u) = -\gamma - \ln u + u - \frac{u^2}{2 \times 2!} + \frac{u^3}{3 \times 3!} - \frac{u^4}{4 \times 4!} + \dots \quad (6.3)$$

with

$$\gamma = 0.577216\dots$$

This  $\gamma$  is the so-called “Euler constant”. It is a fundamental constant like other constants in mathematics such as  $\pi$  and  $e$ ; it is only less known by the wider public.

**Unconfined flow approximation by Theis:** The solution by Theis holds for confined flow or for unconfined aquifers in which the drawdown varies only little compared to the thickness of the aquifer, [[Theis \(1935\)](#)] himself used linearization as described in equation 6.1, writing  $2sD \approx h^2 - D^2$  and  $u = \frac{r^2 S}{4k\bar{h}}$  with  $\bar{h} = 0.5(h + D)$  he obtained as a good approximation to be used for the transient flow to a well in an unconfined aquifer

$$h^2 - D^2 = \frac{Q}{2\pi k} W(u), \quad u = \frac{r^2 S}{4k\bar{h}}$$

### 6.3.1 Implementation of the Theis well function

Below an implementation of the Theis well function is shown for Python and for Excel, using Excel’s Visual Basic. The Python implementation is always much more powerful, because one function call can handle millions of numbers at once, whereas Excel requires copying a formula in every spreadsheet cell in which a number is desired. Python is also more versatile in many other aspects, like reuse of code, and flexibility in combining with other models. Especially superposition is generally much more straightforward in Python and less cumbersome. The probably most important aspect is that Python scripts the problem at hand into individual steps that are executed in the same order every time. Such step sequences are much easier to debug and to document than a spreadsheet. Nevertheless spreadsheets come in handy at times, mostly because most people are already familiar with them, so they take less learning and perhaps less mental effort initially. In this course, we’ll use Python. This does not mean that students may prefer using other tools like R when they are already familiar with it.

#### 6.3.1.1 In Python

For the implementation in Python, we don’t have to look far; the exponential integral is right in the module `scipy.special.exp1`, where it is defined as

$$\exp1(z) = \int_1^\infty \frac{e^{-zt}}{t} dt = \int_z^\infty \frac{e^{-y}}{y} dy$$

The first expression is from *scipy*, the second is obtained by replacing  $dt/t = d(zt)/(zt)$  and adapting the lower boundary of the integral. A check in the table of [Kruseman and De Ridder (1994)] reveals that this is indeed the correct function. Therefore, in Python we have the well function available as `exp1(z)` from the *scipy* module.

The power series implementation is almost straightforward. There are three issues:

1. For  $u > 15 \rightarrow \exp1(u)$  is essentially zero.
2. Instead of computing the individual terms using ever larger powers and factorials, we will express the next term in the previous one. This gives  $\frac{u^{n+1}}{(n+1)(n+1)!} = \frac{u^n}{n \times n!} \times \text{term}$ , where  $\text{term} = u \frac{n}{(n+1)^2}$ .
3. For  $u > 1$ , the terms in the series do not converge. However, they converge in pairs. Therefore, the two last terms are remembered in the loop and their sum is compared with a chosen tolerance, here  $10^{-16}$ . You can use the `verbose` variable to get a print of the loop cycle number where convergence was achieved. The maximum reached is 65.

```

1 def W(u, verbose=False):
2     '''Theis well function as a power series'''
3     gamma = 0.577216
4     u = np.fmin(u, 15)
5     w = - gamma - np.log(u) + u
6     term0 = u
7     for n in range(1, 1000):
8         term1 = - u * n / (n + 1) ** 2 * term0
9         w += term1
10        if np.all(np.abs(term0 + term1) < 1e-16):
11            if verbose:
12                print('Power series converged at n = {}'.format(
13                    n))
14            break
15        else: term0 = term1
16    return w

```

### 6.3.1.2 Implementation in Excel

In Excel, functions that Excel does not provide, can be implemented using Excel cells, better and far more effectively in Visual Basic. Visual Basic is available under the *Developer* tab.

The integral can be numerically computed. Because  $u$  will span many orders of magnitude in practice, it is wise to carry out the integration on a logarithmic axis. As  $dy/y = d\ln y$  we may write the integral as follows

$$W(u) = \int_{\ln u}^{\infty} e^{-y} d(\ln y)$$

Writing  $\ln y = \nu$ , so that  $y = e^\nu$ , changes the integration into

$$\begin{aligned} W(u) &= \int_{\ln u}^{\infty} e^{-e^\nu} d\nu \\ &\approx \int_{\ln u}^{20} e^{-e^\nu} d\nu \\ &\approx d\nu \sum_{\ln u}^{20} e^{-e^\nu} \end{aligned}$$

where we replaced  $\infty$  by a practical upper limit of 20, which corresponds to  $e^{20} \approx 5 \times 10^8$ . In the practical summation, we choose  $d\nu$  as a small fraction of a log cycle, say  $d\nu = 0.01$ .

Figure 6.5 gives an implementation as user-defined function in Visual Basic in Excel.

A power-series implementation in Excel using Visual Basic is shown in figure 6.6. It is similar to the Python implementation shown above.

**Exercise:** Implement the exponential integral or `exp1` from *scipy.special* and the power-series form and show graphically that both implementations yield the same outcomes. This way you prove your implementations are correct.

### 6.3.2 Type-curve for the Theis well function

All books on groundwater pumping tests show the Theis type curve (Figure 6.7). The type curve is the well function plotted on double logarithmic scale in a way that makes it directly comparable with an actual drawdown curve on double log axes; it then looks like the drawdown shown vertically upward as a function of time on the horizontal axis. The type curve is a plot of the well function on the vertical axis versus  $1/u$  on the horizontal axis. Using  $1/u$  on the horizontal axis makes this axis proportional to time, because  $1/u = \frac{4kDt}{r^2S}$ . This type curve can be used to read values off the well function for given values of  $1/u$ . But we can also use it for the analysis of a pumping test in an aquifer that fulfills the assumptions that underlie the Theis solution. These assumptions are:

```

Public Function Expint(u As Double) As Double
'Exponential integral (Theis well function computed by integration)
'TO 151211

Dim dlny, y, w, lnINF As Double

lnINF = 20           'end of integration
dlny = 0.01          'step size for integration, small part of log cycle
lny = Log(u) + 0.5 * dlny   'first location on log axis, use +0.5dlny to move to center of steps

w = 0                'Initialize and loop till lnINF wasreached
While lny < lnINF
    y = Exp(lny)
    w = w + Exp(-y)
    lny = lny + dlny
Wend

'finally multiply by the step size, all at once is more efficient than while looping
Expint = w * dlny

End Function

```

---

Figure 6.5: Theis well function (expint) implemented in Visual Basic for Excel

```

Function Wtheis(u As Double) As Double
'Theis well function implemented as a power series
Dim gamma, deltaStop, term, term1, term2 As Double
Dim N, NMax As Integer

If u >= 10 Then
    Wtheis = 0#
Else
    gamma = 0.577216 'Euler's constant

    deltaStop = 1e-06
    NMax = 100: N = 1
    term = u: term1 = term: term2 = term
    w = -gamma - Log(u) + term

    While (Abs(term1 + term2) > deltaStop) And (N <= NMax + 1)
        term = -term * u * N / ((N + 1) * (N + 1))
        w = w + term: N = N + 1
        term2 = term1: term1 = term
    Wend

    Wtheis = w
End If

```

Figure 6.6: Theis well function as power series implemented as User Defined Function in Visual Basic for Excel

1. The aquifer has uniform transmissivity and uniform storativity (either elastic when confined, or specific yield when phreatic). In case of a phreatic aquifer, the drawdown should be small with respect to the aquifer thickness so that the transmissivity is not changed much.
2. The aquifer extends to infinity. In practice, this means that the aquifer extends far enough such that the pumping test is not affected by boundaries of the groundwater system.
3. The well is pumped at a constant rate from a given point in time, which is set to  $t = 0$  in the formula.
4. The diameter of the well is small.

### 6.3.3 Theis classic pumping-test analysis

In a pumping test, a well pump is switched on and continues to pump at a virtually constant rate. The analysis assumes that the flow rate of the well is constant. The test needs to be done in either a confined or unconfined aquifer without leakage from overlying or underlying layers. To allow applying Theis's equation, the aquifer should be confined or unconfined with a drawdown that should be less than the aquifer thickness to not stretch the assumption of a constant and uniform transmissivity too much. The aquifer needs to extend enough so that flow boundaries do not interfere with the drawdown during the time that the test lasts. Further, the head is measured in one or more piezometers placed at different distances and in different directions from the well. At least three directions are necessary to discover whether or not the aquifer is anisotropic in the horizontal plane. Making sure that observation wells are situated in at least three directions from the well is not often done in practice, which may lead to erroneous interpretations. The heads in the piezometers must be measured from some time before pumping starts. The measurement frequency should allow following the evolution of the drawdown accurately when the points are plotted on a logarithmic time scale. This requires at least 5 to 8 points per log-cycle. If possible, two to three log-cycles of the time axis should be covered by the data; four log cycles would imply the first measurement after one minute, the last one after 10000 minutes. The measurements before the start of pumping is to establish the initial head, which we need to compute the drawdown, which is the measured head minus the initial head. This method of computing the drawdown assumes that the undisturbed head equals the one just before the well starts pumping. However a strong background trend in the head, or more often a wet period during the test or strong changes of the barometer pressure may hinder simple computation of the drawdown. In such cases the effect of the other factors has to be estimated before the drawdown can be computed.

After the test has finished and the data collected, it's time to plot the data. One could of course plot drawdown versus time, but that yields a different curve for each piezometer, which then would have to be interpreted individually. However, the type

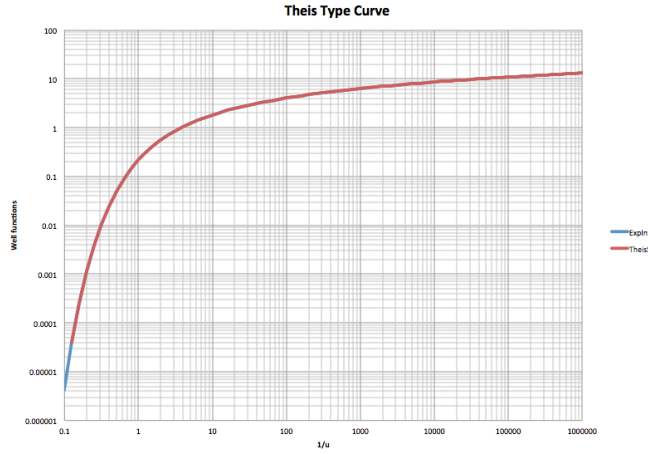


Figure 6.7: Theis type curve (implemented in Excel). The two implementations perfectly overlap each other.

curve is a function of  $1/u = \frac{4kD}{S} \frac{t}{r^2}$ . This implies that if we plot the drawdown versus  $t/r_w^2$  instead of just versus  $t$ , the data of all piezometers should just fall on the same graph. This is shown in figure 6.8 where the drawdown in 4 piezometers during the pumping test are presented versus time (top figure). Both axes are logarithmic. The bottom figure shows the same 4 piezometers, but now they are plotted versus  $t/r_w^2$ , where  $r_w$  is the distance between the piezometer and the well. In the bottom figure, the drawdown of all four piezometers fall on the same curve. The measurement errors only play where the drawdown is small, so the don't matter much for the interpretation.

The classical way to interpret such a pumping test in a confined or unconfined aquifer is by overlapping the drawdown  $s$  versus  $t/r_w^2$  double log graph with the theis type curve of  $W(u)$  versus  $1/u$  also on double log scales (see figure 6.9). With these two graphics on two sheets of transparent paper, they are laid on top of each other, keeping the axis parallel, and shifted so that the measured drawdowns overlaps the Theis type curve as well as possible. With these graphs kept fixed, choose one point (by pressing a pin through both papers) and then read the drawdown and the  $W$ values corresponding to the pin from the two vertical axes, and read the  $1/u$  and the  $t/r_w^2$  values corresponding to the pin from the two horizontal axes. See also description in the caption of figure 6.9.

Because both the horizontal and the vertical axes are logarithmic, a relative shift means a multiplication by a factor given by the shift. Let's call the vertical shift factor  $V$  and the horizontal shift factor  $H$ . Then write what we then have corresponding with the pin:

$$s_p = V \exp1(u_p)$$

$$(t/r^2)_p = H \frac{1}{u_p}$$

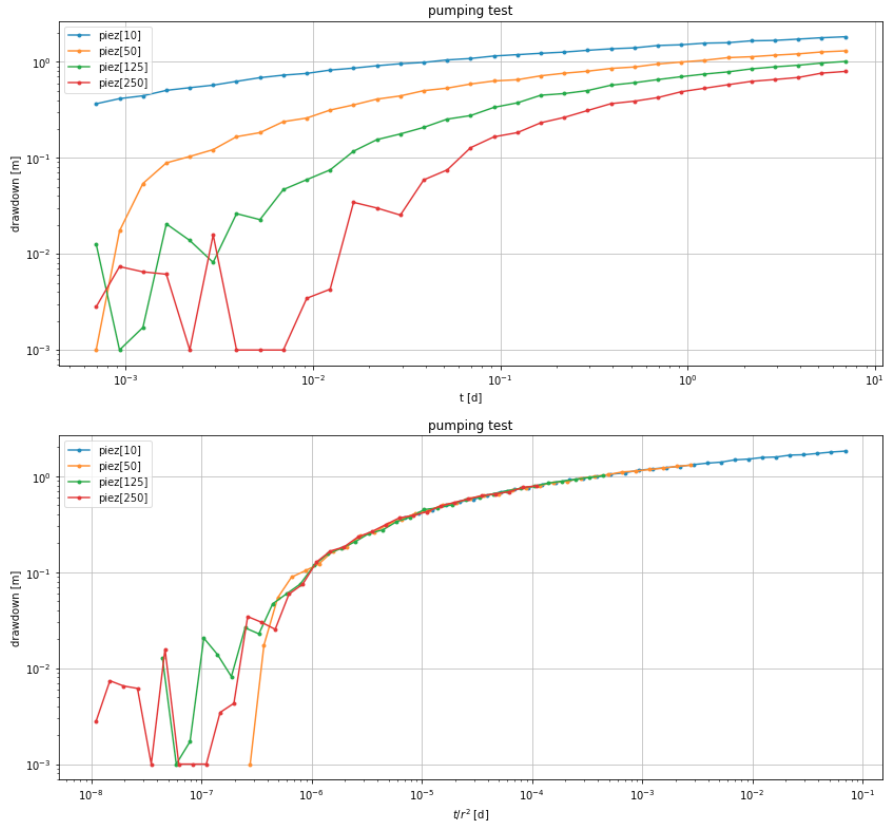


Figure 6.8: Drawdown in 4 piezometers during a pumping test in a confined aquifer. Top: Drawdown versus time. Bottom: Drawdown versus  $t/r_w^2$  where  $r_w$  is the distance of the piezometer to the well in m. Extraction is  $Q = 1200 \text{ m}^2/\text{d}$ . Measurement times are 8 times per log-cycle between 1 and 10000 minutes. The graph is, however shown with time in days. The randomness is due to measurement errors with a standard deviation of 1 cm.

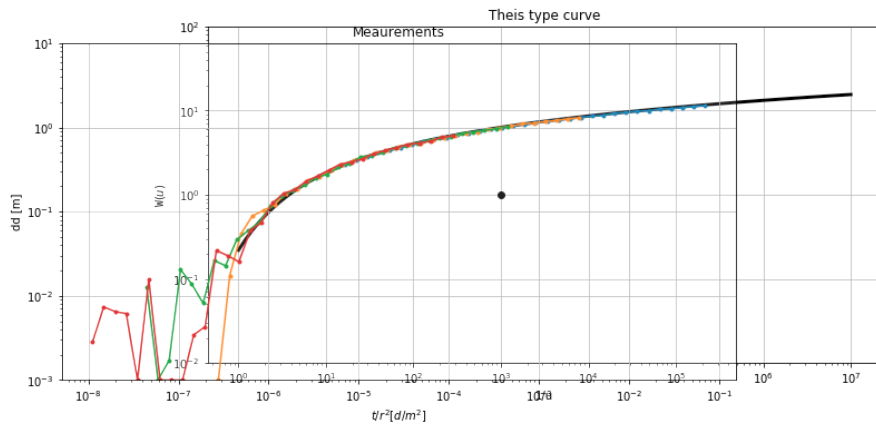


Figure 6.9: Classical Theis pumping test interpretation using the type-curve and the measurements on separate plots with double log axes. The black dot is the chosen pin point. The measurement plot was shifted over the type curve (thick black line) until both matched as well as possible (which is indeed very good in this case). Using the pinpoint read the corresponding value of  $t/r^2$  from the horizontal axis of the measurement plot and the value of  $1/u$  from the horizontal axis of the type-curve plot and read the corresponding drawdown from the vertical axis of the measurement plot and the value of  $W$  from the vertical axis of the type-curve plot. Use these values to compute the transmissivity and the storage coefficient as described in the text.

where  $s_p$ ,  $\exp1(u_1)$ ,  $(t/r^2)_p$  and  $\frac{1}{u_p}$  are the values we just read from the graphs. So we can compute the values of  $V$  and  $H$ . Now write

$$s_p = \frac{Q}{4\pi kD} \exp1(u_p)$$

$$\left(\frac{t}{r^2}\right)_p = H \frac{1}{u_p} \rightarrow u_p = H \left(\frac{r^2}{t}\right)_p = \frac{r^2 S}{4kDt}$$

from which immediately follows that

$$V = \frac{Q}{4\pi kD}$$

$$H = \frac{S}{4kD}$$

Because  $V$  and  $H$  are known, as well as  $Q$ , the first expression gives us the transmissivity  $kD$ . With  $kD$ , the second then gives us  $S$ . So this pumping test yields the value for the aquifer transmissivity and the value for the storage coefficient.

**Exercise:** with the data from this pumping test, retrieve the transmissivity and the storage coefficient. The data for the test in figure 6.8 are in table 6.2, from which they may be copied and pasted.

#### 6.3.4 Standard behavior obtained from simplified Theis well function

The type curve of the Theis solution on linear vertical and logarithmic horizontal scale showing  $1/u$  reveals already much of the drawdown behavior. It shows that for a point at some distance  $r$  it takes some time before the drawdown sets on. Then after some time the drawdown becomes linear on this half-logarithmic graph.

When we draw the data from the previous pumping test with a linear vertical axis that increases downward we obtain the graphs in figure 6.11. Again we see that the separate drawdown curves that we obtain when plotting them versus  $t$ , become a single overlapping curve when we plot them versus  $t/r_w^2$ . Of course, the measurements are similar to the type curve.

We can analyze this behavior and draw some important consequences from a simplification of the Theis type-curve that lends itself for easier analysis.

Given the power series representation in equation 6.3, and noting that for small values of  $u$ , say  $u < 0.1$  only the first two terms matter. Therefore, we can simplify the Theis solution for such cases. We'll show this in a few steps:

Start with the power series representation and ignore all terms with  $u$ . Writing  $W$  instead of  $\exp1$  for convenience, this yields

$$W(u) \approx -577216 - \ln u + \dots$$

Table 6.2: Data of the pumping test shown in figure 6.8

		piez [10] [250]	piez [50]	piez [125]	piez
	t [min]				
1	1.00	0.37	0.00	0.01	0.00
2	1.33	0.41	0.02	0.00	0.01
3	1.78	0.44	0.05	0.00	0.01
4	2.37	0.50	0.09	0.02	0.01
5	3.16	0.54	0.10	0.01	0.00
6	4.22	0.57	0.12	0.01	0.02
7	5.62	0.63	0.17	0.03	0.00
8	7.50	0.68	0.18	0.02	0.00
9	10.00	0.73	0.24	0.05	0.00
10	13.34	0.76	0.26	0.06	0.00
11	17.78	0.82	0.31	0.07	0.00
12	23.71	0.86	0.36	0.12	0.03
13	31.62	0.91	0.41	0.15	0.03
14	42.17	0.95	0.44	0.18	0.03
15	56.23	0.99	0.50	0.21	0.06
16	74.99	1.05	0.53	0.25	0.07
17	100.00	1.08	0.59	0.28	0.13
18	133.35	1.15	0.63	0.34	0.17
19	177.83	1.19	0.65	0.37	0.18
20	237.14	1.23	0.72	0.45	0.23
21	316.23	1.26	0.76	0.47	0.26
22	421.70	1.32	0.80	0.50	0.31
23	562.34	1.37	0.85	0.57	0.37
24	749.89	1.40	0.88	0.61	0.39
25	1000.00		1.48	0.95	0.65
26	1333.52		1.51	0.99	0.70
27	1778.28		1.56	1.04	0.75
28	2371.37		1.58	1.11	0.79
29	3162.28		1.65	1.13	0.84
30	4216.97		1.67	1.17	0.89
31	5623.41		1.72	1.21	0.92
32	7498.94		1.78	1.27	0.97
33	10000.00		1.82	1.30	1.01
34					0.79

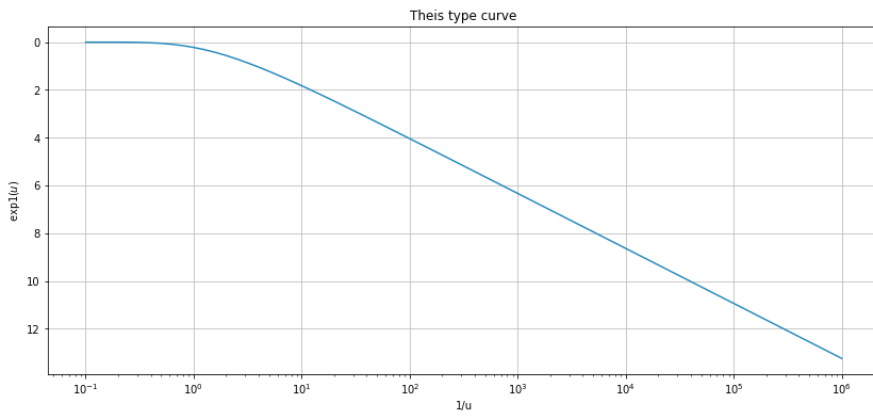


Figure 6.10: Theis type curve on with linear vertical scale that increases downward.

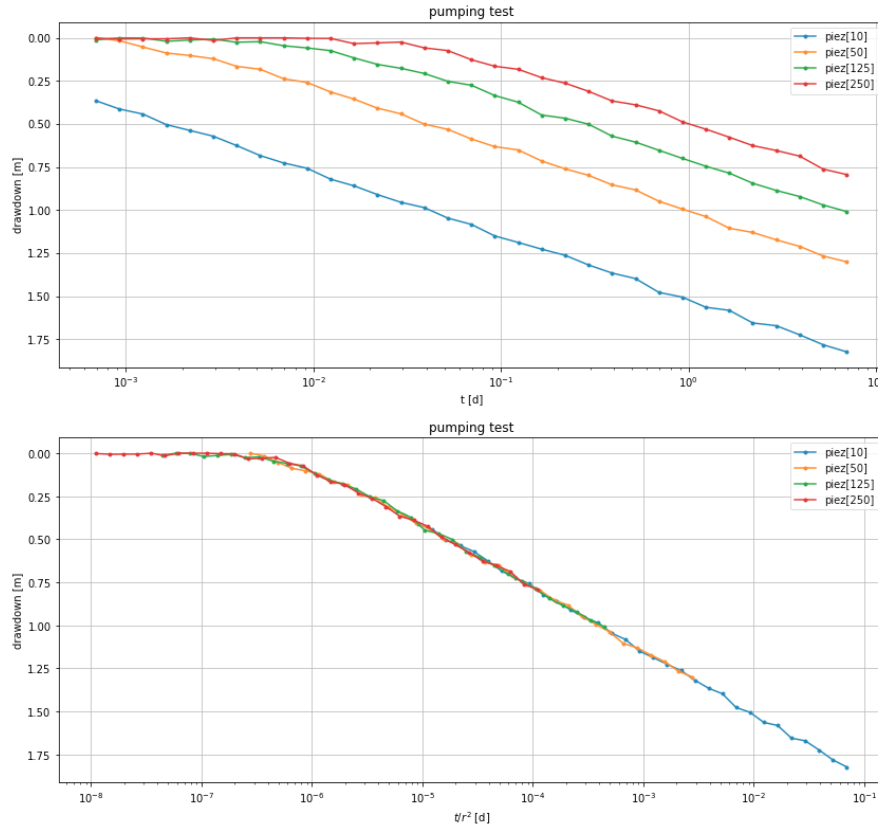


Figure 6.11: Same pumping test as in figure 6.8, but the drawdown downward positive and the vertical axis linear.

which is valid for sufficiently small  $u$  (i.e. for large times and small  $r$ ). Then turn the constant into a logarithm, use  $u = r^2 S / (4kDt)$  and combine the two logs.

$$\begin{aligned} w(u) &\approx -\ln(1.7811) - \ln\left(\frac{r^2 S}{4kDt}\right) \\ &\approx -\ln\left(\frac{r^2 S}{2.25kDt}\right) \end{aligned}$$

Finally, reverse the sign:

$$w(u) \approx \ln\left(\frac{2.25kDt}{r^2 S}\right) \quad (6.4)$$

Equation 6.4 is important; we'll explore its consequences in the next section. Equation 6.4 could also be written as

$$w(u) \approx \ln\left(\frac{0.563}{u}\right)$$

Hence, for small  $u$  the well function can be approximated by the simple logarithmic expression given in equation 6.11.

### 6.3.5 Derived behavior using the logarithmic approximation of $w(u)$

Behavior of  $w(u)$  with respect to time is easily demonstrated by splitting the log in a part with and without time

$$w(u) \approx \ln\left(\frac{2.25kD}{r^2 S}\right) + \ln(t) \quad (6.5)$$

Hence, the well function is a constant plus the log of  $t$ , which corresponds with the top image in figure. We see that, after some time, the drawdown will increase linearly with the logarithm of time.

For each different distance to the well, the constant is different, but the  $\ln t$  term is the same. Hence, the time drawdown curves of points at different distances from the well are all parallel; they are only shifted along the horizontal time axis. This is shown in figure 6.12. This figure reveals that for any piezometer, the drawdown sets in after some time, which is longer, the larger the distance between the well and the piezometer. Then there is a transition period. And finally the drawdown becomes linear on logarithmic time axis. The thick lines are the full Theis drawdown curves and the thin lines are its logarithmic approximation. The first term in equation 6.5 is the value that each straight drawdown line intersects at  $t = 1$ , which is shown in the figure by the black circles in

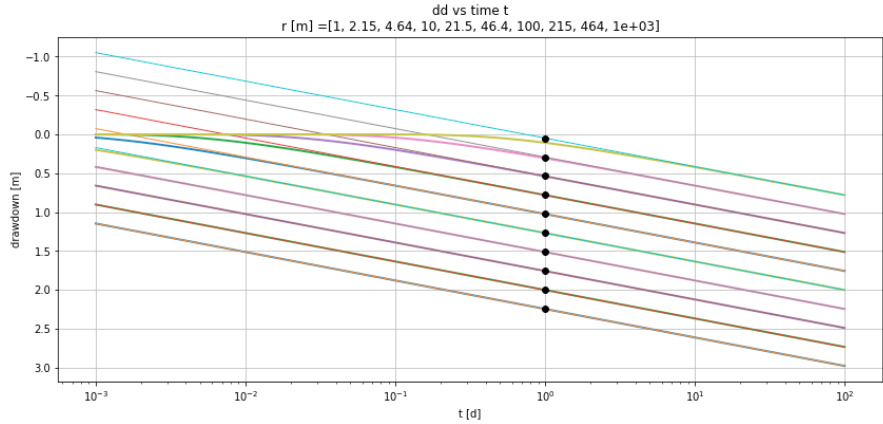


Figure 6.12: Drawdown (notice that positive drawdown is plotted downwards) versus time according to Theis (thick lines) and logarithmic approximation (thin lines) for different distances as given in the head of the picture.  $Q = 1200 \text{ m}^2/\text{d}$ ,  $kD = 600 \text{ m}^2/\text{d}$  and  $S = 0.001$ . The circles are the first log term in equation 6.5.

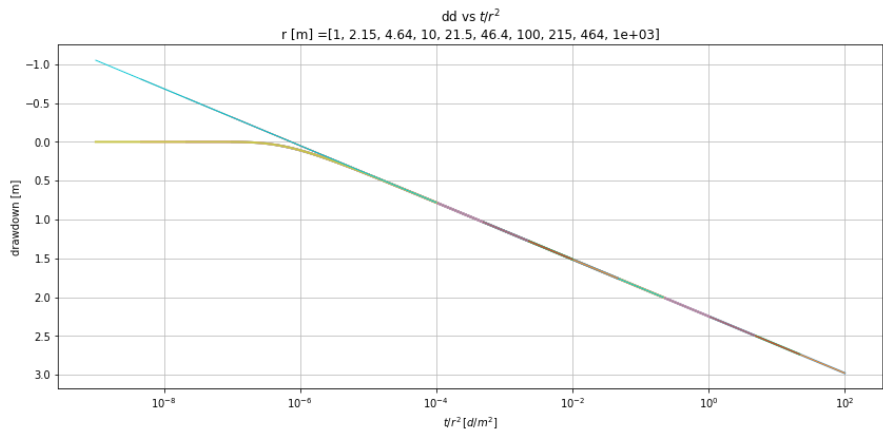


Figure 6.13: Same as figure 6.12, but now plotted versus  $t/r^2$  instead of versus  $t$ . The drawdown curves of different piezometers fall all on the same line.

figure 6.12. Also, notice how the drawdown curves of all the piezometers fall on the same line if plotted versus  $t/r^2$  instead of  $t$ . This is illustrated in figure 6.12.

How the well function increases per log-cycle of time is also of great practical importance. For easier reference switch to  $\log_{10}$  instead of  $\ln()$ . That is

$$s(r, 10t) - s(r, t) \approx \frac{Q}{4\pi kD} 2.3 \log_{10} \left( \frac{2.25kD}{r^2 S} (10t) \right) - \frac{Q}{4\pi kD} 2.3 \log_{10} \left( \frac{2.25kD}{r^2 S} t \right)$$

$$\Delta s_{10} \approx \frac{2.3Q}{4\pi kD} \log_{10}(10)$$

$$\Delta s_{10} \approx \frac{2.3Q}{4\pi kD}$$

From this it follows that drawdown in any piezometer at two times such that times 2 is 10 times time 1, this is  $\Delta s_{10}$  is independent of the distance from the well and time itself, as long as values correspond to the straight part of the Theis curve on half-log paper. With the now given value of  $\Delta s_{10}$  and the known well rate  $Q$  we obtain the value for the transmissivity

$$kD \approx \frac{2.3Q}{4\pi \Delta s_{10}}$$

Now using the same approximation

$$s \approx \frac{2.3Q}{4\pi kD} \log_{10} \left( \frac{2.25kDt}{r^2 S} \right)$$

we see that  $s = 0$  when the argument of the logarithm is 1. So look up the value of  $t/r^2$  where  $s = 0$  and set

$$\frac{2.25kD}{S} \frac{t}{r^2} = 1 \rightarrow S = 2.25kD \frac{t}{r^2}$$

with now  $kD$  and  $t/r^2$  given, the storage coefficient is obtained. This too completes the pumping test interpretation.

This simple analysis is always applicable when  $u < 0.1$ , hence for large  $t$  and small  $r$ . This, therefore, becomes particularly interesting for the analysis of pumping tests where the only measurements available are those of the drawdown in the well itself, i.e. for very small  $r$ ! Such a test is called a well test. The radius  $r$  in a well is so small, that the logarithmic approximation of the drawdown sets in very early. This implies that even a relatively short well test is enough to determine the transmissivity of the aquifer. This is an advantage also in semi-confined aquifers, in which the drawdown becomes steady after some time, beyond which the Theis solution fails. However, shortly after the pump starts, the drawdown does behave according to Theis. So this method is widely applicable to obtain the transmissivity, independently even of well clogging, partial penetration of the well screen and vertical anisotropy. However, to also obtain the storage coefficient  $S$  we need at least 1 observation well, because the drawdown in the well itself is affected by well bore clogging, partial penetration and vertical anisotropy. Therefore we cannot

set measured water level in the extraction well equal to the drawdown we would obtain just outside the screen of an unclogged fully penetrating well, which is what we would mathematically do. An observation well is affected by clogging. It may be affected by partial penetration of the well screen, then its distance to the well is less than about  $1.5D$ . However, a (partly) clogged piezometer may yield delayed and therefore wrong results when it can't follow fast enough the rapid decline of its water level shortly after the start of a nearby pump. The factor 1.5 is a practical value, which may be larger if the aquifer is strongly vertically anisotropic. However, these sideline nuances do not affect the determination of the transmissivity.

**Exercise:** Apply the described analysis using figure 6.11.

### 6.3.6 Drawdown at a fixed time at different $r$

The counterpart of the drawdown versus time graph for a given location is the drawdown versus distance graph at a given time. In general, this drawdown is much more difficult to observe because it requires having multiple piezometers at different distances, which are, obviously, almost never available in practice. Another difficulty counteracting the interpretation of such a pumping test with multiple piezometers with the simplified well function is, that piezometers at larger distances will not yet behave according the the logarithmic approximation because their value of  $u$  is still too large. Finally, their drawdown may be impacted by leakage from overlying or underlying layers, which requires Hantush's well solution.

Nevertheless, some insight in the drawdown behavior can still be obtained from the approximation. Making  $r$  explicit yields

$$W(u) \approx \ln\left(\frac{2.25kDt}{S}\right) - 2\ln r \quad (6.6)$$

The first logarithm is a constant at any fixed point in time for every piezometer, irrespective of its distance to the well. The impact of the distance to the well is completely confined to the second term. We see that the drawdown is proportional to  $\ln r$  and hence gives a straight line on the drawdown versus log distance graph. The drawdowns versus  $r$  at different times are all parallel like it was the case with the drawdowns versus time that we discussed before. Only the drawdown versus distance curves are twice as steep on the half-log chart than those versus time.

Figure 6.14 shows the drawdowns as a function of  $r$  at different times as indicated in its header. The first logarithm in equation 6.6 represents the intersections of the logarithmic approximation with the vertical line where  $r = 1$  m; these intersections are indicated in the figure by black circles. Again, the drawdown was plotted with the positive axis downward so it complies more intuitively with the concept of a the groundwater head being lowered by pumping. Here too, all lines fall on the same graph when plotted versus  $u$  instead of versus  $r$  or, equivalently when plotted versus  $r^2/t$  instead of just  $r$ , which is shown in figure 6.15.

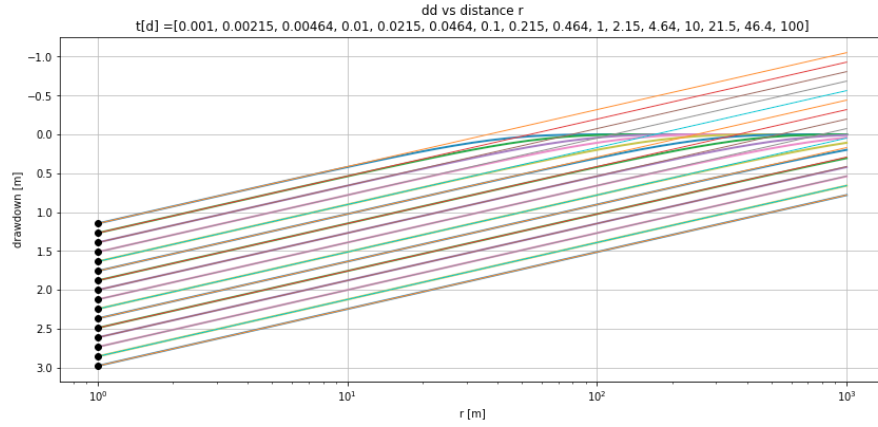


Figure 6.14: Drawdown (notice that positive drawdown is plotted downwards) versus distance  $r$  according to Theis (thick lines) and logarithmic approximation (thin lines) for different distances as given in the head of the picture.  $Q = 1200 \text{ m}^2/\text{d}$ ,  $kD = 600 \text{ m}^2/\text{d}$  and  $S = 0.001$ . The circles are the first log term in equation 6.6.

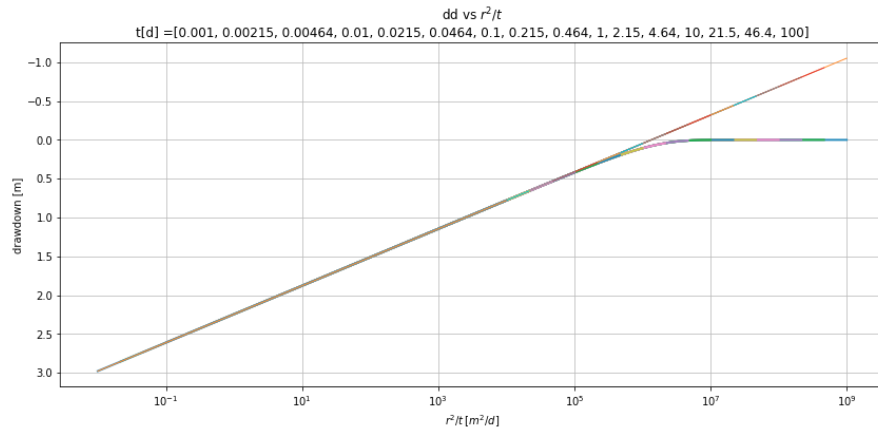


Figure 6.15: Same as figure 6.14, but now plotted versus  $u$  instead of versus  $r$ . A similar results is obtained if plotted versus  $r^2/t$  instead of  $r$ . The drawdown curves of different piezometers fall all on the same line.

### 6.3.7 Radius of influence

The well function clearly shows that it takes some time for the drawdown to reach a piezometer at distance. Therefore, we may talk about a “radius of influence” which is dynamic and indicates to how far from the well the drawdown is perceived. It is an important insight. Clearly, we can define the radius of influence in different ways. For instance, we could say the radius of influence is the distance where the drawdown is 1 cm, 10 cm or whatever is appropriate to us. However we could, and we do that here, opt for a more general definition. If we look at the logarithmic approximation of the Theis well function, we notice that the drawdown is always a straight line in the graph that shows drawdown versus the log of time. It is natural to now define the radius of influence to be the distance at which the straight drawdown line intersects drawdown  $s = 0$ .

The analysis is then straightforward. Starting with the approximation

$$W(u) \approx \ln\left(\frac{2.25kDt}{r^2S}\right) = 0$$

we that

$$\frac{2.25kDt}{r^2S} = 1$$

and so

$$r = \sqrt{\frac{2.25kDt}{S}}$$

This radius is, therefore, proportional with  $\sqrt{t}$ . It is, obviously, also larger when the transmissivity is larger, so that influence can spread faster, and it is smaller when the storage coefficient is larger, which reduces the spreading of influence of the well. This simple expression is very practical to estimate how far the influence of a well under the conditions envisioned by Theis reaches as a function of time.

Of course, one may adopt the relation such that it gives a certain drawdown  $s_{min}$

$$s_{min} \approx \frac{Q}{4\pi kD} \ln \frac{2.25kDt}{r^2S}$$

which can be manipulated to

$$r \approx \sqrt{\frac{2.25kDt}{S} \exp\left(\frac{4\pi kD}{Q}s_{min}\right)}$$

But this does not give a good answer, because the approximation of the well function is not valid for small drawdowns. What we, therefore, should do instead, is use the actual well function

$$s_{min} = \frac{Q}{4\pi kD} W(u)$$

and then determine the value of  $W(u)$  that gives the desired answer

$$W(u)_{min} = s_{min} \frac{4\pi k D}{Q}$$

Then determine the value  $u_{min}$  that belongs to the value of  $W(u)_{min}$ , so that

$$u_{min} = \frac{r^2 S}{4kDt}$$

and, finally,

$$r = \sqrt{\frac{4u_{min}kDt}{S}}$$

If we compare this with our first approach, we have here  $4u_{min}$  instead of 2.25. Both approaches are valid, but the latter is exact in terms of the drawdown if we use a specific minimum value as a threshold to determine the radius of influence. However, the definition of zero drawdown according the approximate logarithmic expression given above, is much more practical and easier to comprehend, derive and remember.

### 6.3.8 Relation with the solution for the steady-state situation

We obtain a steady-state situation after some time when we use a negative mirror well at some distance  $R$  from our well.

Let's use the simplified Theis solution to compute the result.

$$s = s_1 + s_2 = \frac{Q}{4\pi k D} \ln\left(\frac{2.25kDt}{r_1^2 S}\right) - \frac{Q}{4\pi k D} \ln\left(\frac{2.25kDt}{r_2^2 S}\right)$$

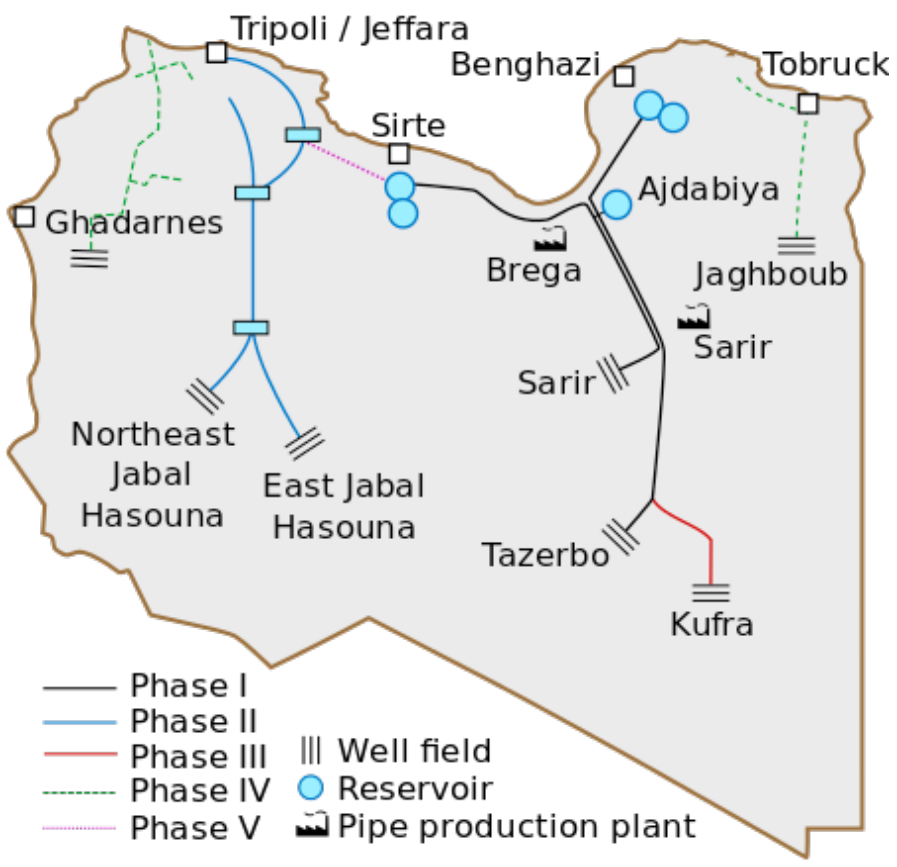
For the drawdown in the well, we have  $r_1 = r_w$ , the well's radius, and  $r_2 = R$ , hence

$$\begin{aligned} s &= \frac{Q}{4\pi k D} \ln\left(\frac{R^2}{r_w^2}\right) \\ &= \frac{Q}{2\pi k D} \ln\left(\frac{R}{r_w}\right) \end{aligned}$$

So if there is a fixed head boundary somewhere, which in this case we created by putting a mirror well with opposite sign at distance  $R$  (so that the line perpendicular through the midpoint of the connection line between the two wells keeps drawdown zero), the drawdown will reach a steady-state after some time. Remember that the logarithmic approximation is only valid after sufficient time has elapsed since the start of pumping. Also notice that the square under the logarithm leads to  $2\pi k D$  (steady) instead of  $4\pi k D$  (transient) in the numerator of the factor in front of the logarithm, which is always the case in steady-state solutions for wells. The steady state is certainly attained when  $u$  is sufficiently low in the power-series expression of the exponential integral (the well function). This is the case when  $|u| \ll |\ln(u)|$ . For  $u = 0.05$  we have  $|u/\ln(u)| \approx 0.01$ , which may be regarded sufficient small to take  $u < 0.05$  as a criterion for having reached steady state in this case. From this  $u$  the time after which steady state can be practically guaranteed can be computed using  $u = r^2 S / (4kDt)$ .

### 6.3.9 Exercises

1. The book [Kruseman and De Ridder (1994)] describes a pumping test “Oude Koredijk” and provides the data. Interpret that test.
2. An unconfined aquifer has a transmissivity of  $kD = 500 \text{ m}^2/\text{d}$  and a specific yield of  $S_y = 0.15$  and is situated above an impervious base. Groundwater is extracted during 2 weeks. During the first 10 days, the extraction rate is  $Q = 1000 \text{ m}^3/\text{d}$ ; during the last 4 days, the abstraction is  $Q = 3000 \text{ m}^3/\text{d}$ . What is the drawdown  $s$  at the end of this 2-week period at a distance  $r = 80 \text{ m}$  from the well?
3. A square building pit with sides of  $L = 50 \text{ m}$  needs its construction floor at 7 m below ground surface to be put dry. The water table is initially at 4 m below ground surface. The aquifer is unconfined with its bottom at 50 m below ground surface. The hydraulic conductivity is estimated at  $k = 20 \text{ m/d}$  and the specific yield is  $S_y = 0.25$ . The construction need to start in 4 weeks, so the floor of the building pit must be dry by then. It takes one week to install a well at each corner of the building pit. What capacity  $Q$  must each these wells have to realize a groundwater level that is 50 cm below the building-pit floor in 4 weeks?
4. The Nubian sandstone aquifer is the world’s largest known aquifer system (See Wikipedia and figure 6.16). It measures 2 million  $\text{km}^2$ , covering large parts of NW Sudan, NE Chad, SE Libya and most of Egypt. It contains an estimated amount of 150000  $\text{km}^3$  of fossil groundwater. It may be considered confined with a transmissivity of 600  $\text{m}^2/\text{d}$ . Libya under Gaddafi created the so-called Great Man-Made River Project. It began extracting 2.4  $\text{km}^3/\text{year}$  (6.6 million  $\text{m}^3/\text{d}$  or 275000  $\text{m}^3/\text{h}$  or 76  $\text{m}^3/\text{s}$ ) in the mid 1990. The wells of Kufra can be easily found on Google Earth; they are 400 km away from the Egyptian border. Assume that the wells in Kufra extract 15  $\text{m}^3/\text{s}$  from the Nubian aquifer. If continued, how will the drawdown in the Nubian aquifer develop at the border between Egypt and Libya?
6. Groundwater is extracted from an unconfined aquifer to irrigate crops by means of a pivot, i.e. a well connected to an irrigation frame that slowly turn around the well. This pivot irrigates a disc of a surface area of 50 ha. 50% of the irrigated waters is consumed by the crop and hence evaporated by it; the remaining 50% is water that returns to the aquifer. A crop consumes a water volume equivalent to a layer of 75 cm over the area served. Two crops can be harvested each year. What is the required pumping capacity of the well and how will the groundwater head below the pivot develop? To answer this question, compute the drawdown over time at the following distances from the well a) 0.2 m (=inside the well, required to see if the well could fall dry in the near future), b) at the edge of the irrigated 50ha circular area served by the well, c) at 2 and 5 times this radius to estimate its impact on neighboring wells.



5. a)

Figure 6.16: Picture of the GMMR project in Libya

7. An area in Morocco is irrigated by means of drainage tunnels (qanats, or khettaras, see Wikipedia, see figure 6.17). The water to the aquifer is rainwater that was captured in the nearby hills and mountains. The general groundwater flow away from the foot of the mountains causes a gradient of the natural groundwater, which is exploited by the drainage tunnels. These tunnels run from their downstream outlet in the villages with a small upward gradient towards the foot of the mountains, where they intersect the water table, so that groundwater will drain and flow towards the village through these tunnels. Assume that the average drawdown caused by these tunnels is 2 m. A developer intends develop a farm to grow crops in a new area nearby and wants to install wells for irrigation. The area to be irrigated is 50 ha and the required net consumption is 0.75 m/year, hence a required year-average extraction of  $0.75 \times 50000/365 = 1030\text{m}^3/\text{d}$ . What will be the impact of the extraction wells on the existing khettaras? Take into consideration that the aquifer at the foot of the mountains is closed and that its open to infinity away from these mountains. Assume the specific yield is 20% and the transmissivity is  $500 \text{ m}^2/\text{d}$ . Realize that there are no fixed-head boundaries, i.e. the groundwater will always be in dynamic equilibrium. So the effect of the new development will also be transient. Compute the drawdown that it causes over time in the drainage area of the qanats. Realize that the mountain face works as a groundwater barrier.
- 8.
9. Some thoughts about the problem stated above. It may not seem immediately obvious to provide an answer with the simple tools of this course. But we can give it a try. We can compute the transient drawdown by the new well compute its effect near the foot of the mountains. With this, we can compute the drawdown everywhere, and therefore, also at every point of the qanats where they tap the groundwater, which is in the qanat drainage area. We may assume that the yield of the qanats is proportional to the drawdown they cause, which was 2 m. When we subtract the drawdown of the new well at the khettaras from that of the khettaras themselves, we have at least an estimate of the impact. A difficulty arises only from the integration of the drawdown impact along each khettara. However, we can just take the drawdown at the center of their tapping length as an approximation.
1. In the Mid-West of the United States, rights for water extraction from a creek have been fixed since the nineteenth century. A new development wants to circumvent those rights by using groundwater. Due to the distance from the creek, i.e. 800 m, no impact on the creek's discharge is expected. But will this be true? The aquifer is unconfined with a specific yield of 0.24, a depth of 60 m and a conductivity of about  $25 \text{ m/d}$ . Compute whether there is an impact of the extraction by the new farmer who intends to extract a year-round average of  $1000 \text{ m}^3/\text{d}$ . If so, how will this impact grow over time? When will it reach its maximum? What will be the maximum impact of this extraction?

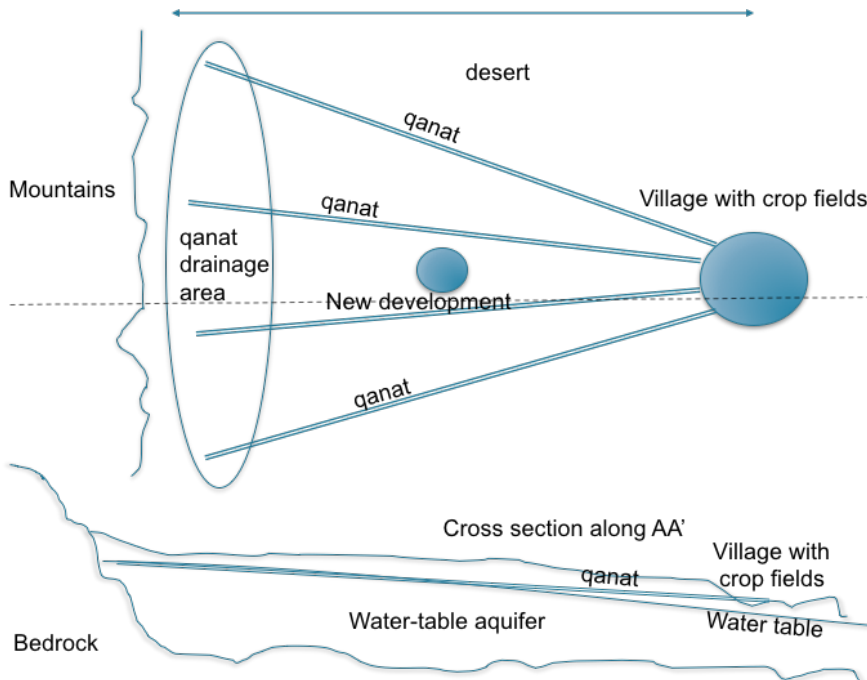


Figure 6.17: Qanats new mountain area with village and projected new development in desert

### 6.3.10 Flow at distance $r$ from the well

How much water is released from storage between two distances  $r_1$  and  $r_2$ , or how much is the flow toward the well at distance  $r$ . For such type of questions we need the flow in the aquifer at distance  $r$ . We can determine this flow from the drawdown, by taking the derivative with respect to  $r$ .

$$s = \frac{Q_0}{4\pi k D} W(u)$$

$$\begin{aligned} Q_r &= -2\pi r k D \frac{\partial s}{\partial r} \\ Q_r &= -\frac{2\pi r k D Q_0}{4\pi k D} \frac{dW(u)}{du} \frac{\partial u}{\partial r} \end{aligned}$$

with  $u = r^2 S / (4kDt)$  it follows that

$$\frac{\partial u}{\partial r} = \frac{2rS}{4kDt} = \frac{2}{r} \frac{r^2 S}{4kDt} = \frac{2u}{r}$$

hence

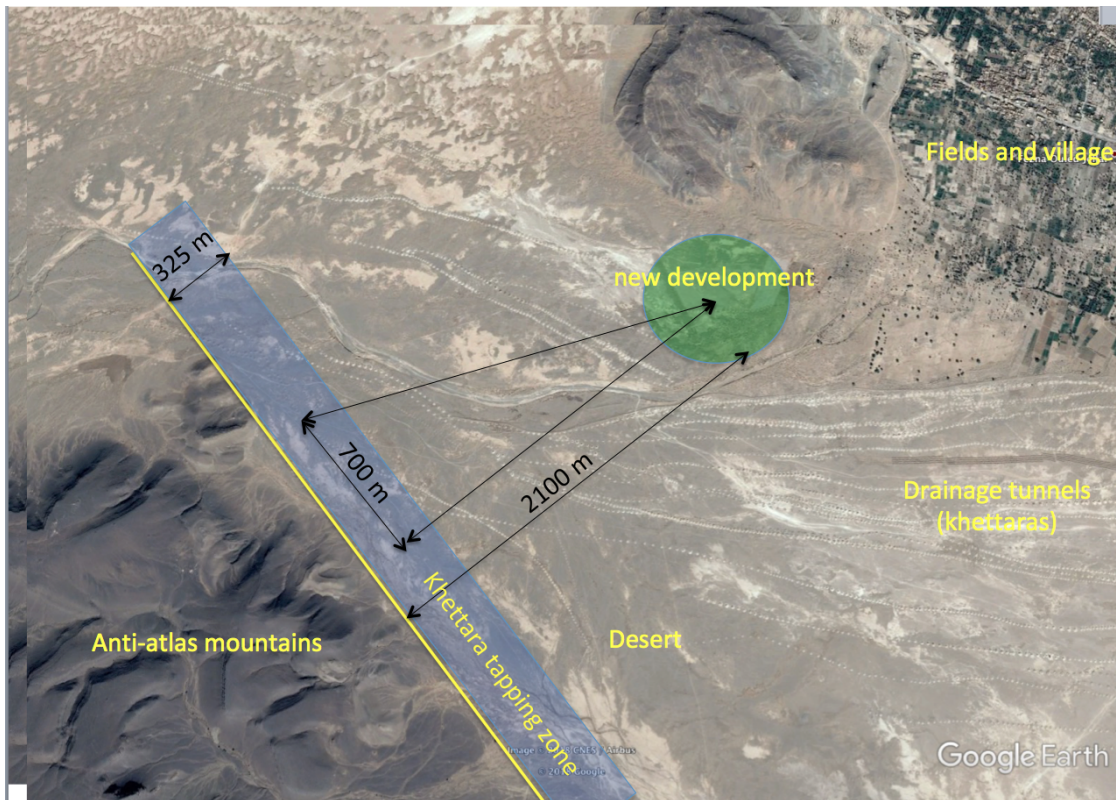


Figure 6.18: Khetтара (qanats / drainage tunnels) to the west of Erfoud in Morocco draining groundwater from the foot of the Anti-Atlas mountains at the left to the fields and villages at the right (coordinates lat 31.506, lon -4.484). The width of the figure is 5600 m.

$$\begin{aligned}
\frac{Q_r}{Q_0} &= -u \frac{dW(u)}{du} = -u \frac{d \int_u^\infty \frac{e^{-y}}{y} dy}{du} \\
&= +u \frac{e^{-u}}{u} \\
\frac{Q_r}{Q_0} &= e^{-u}
\end{aligned} \tag{6.7}$$

or

$$\frac{Q_r}{Q_0} = \exp\left(-\frac{r^2 S}{4kD t}\right)$$

This is a very simple relationship between the flow  $Q_r$  at distance  $r$  and the constant extraction  $Q_0$  from the well. Because  $u$  is proportional to  $r^2$ , this ratio diminishes exponentially with the distance from the well, meaning the water comes from storage for say 99% within a given radius from the well, this radius extending dynamically. Because  $u$  is proportional to  $1/t$ , it means that the ratio goes to 1 within increasing time over any distance  $r$ . This implies that the flow becomes essentially steady, i.e. reaches 99% of the total extraction rate within a given radius after a certain time. A constant flow equal to  $Q_0$  within a certain distance implies that the gradients will also become constant within the same distance. This means that the difference between the drawdowns in observation wells will become also constant and equal to the difference between the head in the steady state case. This implies that we can then interpret the pumping test like we do with a steady-state one, based on the head differences between observation wells. Of course this requires enough observation wells. And, of course, one cannot obtain a storage coefficient from a steady-state analyses.

By way of example, the drawdown and the accompanying ratio  $Q_r/Q_0$  in equation 6.7 is shown graphically in figure 6.19 firstly as a function of  $t$  for different values of  $r$ . Of course, all curves collapse to the same graph if plotted versus  $u$  or  $1/u$  (which is not shown). The current figures emphasize the delay with distance; but with the time axis logarithmic, all graphs look the same, except for the delay. Also, notice that once the drawdown becomes a straight line versus log time, the gradients with respect to distance will be constant. This implies that by then, the ratio  $Q_r/Q_0$  should have asymptotically approached the value of 1. This is easily verified by laying a ruler long the declining branches of the drawdown curves and see from where these curves have become straight, and compare this with the extent by which the graph of  $Q_r/Q_0$  has approached the value of 1.

The total volume flown across a radius  $r$  between  $t = 0$  and  $t = t$  may be computed as

$$V_r = \int_0^t Q_r dt = Q_0 \int_0^t e^{-u} dt = \int_0^t \exp\left(-\frac{T}{\tau}\right) d\tau, \quad T = \frac{r^2 S}{4kD}$$

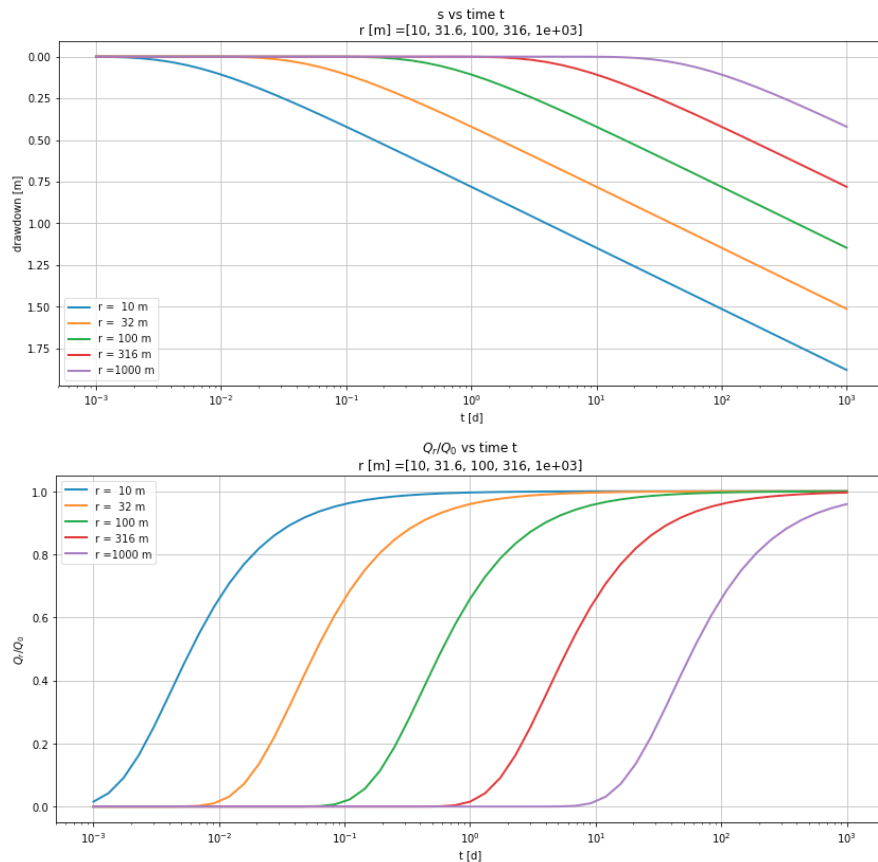


Figure 6.19: Top: drawdown. Bottom  $Q_r/Q_0$  as a function of  $r$  for different times and as a function of time for different  $r$ . As before,  $Q = 1400 \text{ m}^2/\text{d}$ ,  $kD = 600 \text{ m}^2/\text{d}$  and  $S = 0.1$ .

Although this integral does not look difficult, its outcome is still nasty. It can be obtained using the integral calculator on the Wolfram site <https://www.wolframalpha.com/calculators/integral-calculator/>. Although the mathematical solution exists, it is far from trivial. Anyway, because  $Q_r \rightarrow Q_0$  with increasing  $t$ , the integral has an asymptotic result

$$\lim_{t \rightarrow \infty} V_r = Q_0 t$$

For small  $t$  one can always carry out the integration numerically.

### 6.3.11 Superposition in time

A well may be switched on and off at will. The effect of this switching can be taken into account by superposition. For instance, a well that has been pumping for a time  $\Delta t_i$  since  $t = 0$ , after which it is switched off, can be viewed as two wells that pump continuously. The first starts at  $t_0 = 0$  with extraction  $Q_0$  and the second at  $t = t_0 + \Delta t_i$  with extraction  $-Q_0$ . This way, the net extraction will be zero for  $t > t_0 + \Delta t$ . This superposition can be applied with a large number of changes of the flow rate at arbitrary times. The problem may only be that after many such changes one needs to carry on a large number of “wells” at the location of the real well to compute the current state. This is merely a computational burden, one that can be effectively dealt with through application of convolution, explained elsewhere in this syllabus.

Hence, we have for a well that switches on at  $t = t_0$  and then switches off at  $t = t_0 + \Delta t$

$$s_t = \frac{Q_0}{4\pi k D} W(u_{t-t_0}) - \frac{Q_0}{4\pi k D} W(u_{t-(t_0+\Delta t)})$$

where the second term is omitted al long as  $t < t_0 + \Delta t$ .

To deal with a well with varying extraction, we subdivide time in episodes during which the extraction from the well may be considered sufficiently constant. In this superposition we start a new well at the same position each time the flow rate changes. We let this new well extract the difference between the new rate and that of the previous well.

For example, let the flow rate change at rate-change times  $t_0, t_1, t_2, t_3, \dots$  after which the flow rate is  $Q_0, Q_1, Q_2, Q_3, \dots$ , respectively. We can simulate the heads by starting a new well at each of these rate-change times with extraction

$$Q_0, Q_1 - Q_0, Q_2 - Q_1, Q_3 - Q_2, \dots$$

because after  $t_0$  the total extraction is  $Q_0$ , after  $t_1$  ti is  $Q_0 + Q_1 - Q_0 = Q_1$ , after  $t_2$  it is  $Q_1 + Q_2 - Q_1 = Q_2$  etc. Applying superposition then yields

$$s_t = \frac{Q_0}{4\pi k D} W(u_{t-t_0})_{t>t_0} + \frac{Q_1 - Q_0}{4\pi k D} W(u_{t-t_1})_{t \geq t_1} + \frac{Q_2 - Q_1}{4\pi k D} W(u_{t-t_2})_{t \geq t_2} + \frac{Q_3 - Q_2}{4\pi k D} W(u_{t-t_3})_{t \geq t_3} + \dots$$

To check, take any time, say  $t_i$  so that all wells  $0 \rightarrow i$  are active and add all the flows for these well to get  $Q_i$  which is the true total extraction at that time.

With this in mind, superposition for an arbitrarily varying well becomes straightforward. Just assemble the list  $t_i$  and  $Q_i$  for  $i = 0 \rightarrow n$ . The flow of the wells to be

switched on at times  $t_i$  is then simple the difference of consecutive flows. Let's call these flow changes  $\Delta Q$ , then  $\Delta Q_i = Q_i - Q_{i-1}$  for  $i > 0$  and  $\Delta Q_0 = Q_0$

**Example:**

Consider an aquifer of infinite lateral extend with  $kD = 600 \text{ m}^2/\text{d}$  and  $S_y = 0.1$ . If well extracts at the following flows during according to the middle picture in figure 6.20. The drawdown at 5 different distances (see title of top picture) are computed by superposition and are shown the top picture. The distance  $r = 0.01$  represents the well face. The lower picture of figure 6.20 illustrates the superposition better for the piezometer at 50 m distance. It shows not only the result of the superposition, but also the contribution of each individual change of the well rate.

Of course, it is rather straightforward to carry out superposition with many well simultaneously, where each of them has a flow rate that varies independently of the other wells, and compute the resulting varying head or drawdown at an arbitrary location. And if we do this for many location simultaneously, we can show the the head contours in an entire region fluctuating under the influence of many wells of which each extracts at it's own will.

### 6.3.12 Superposition in space

The contributions of an arbitrary number of pumping wells can be added together, because the underlying partial differential equation is linear. Therefore, superposition works in space as well as in time. One can have an arbitrary number of wells pumping arbitrary amounts of water, and compute the drawdown at any number of arbitrary points simultaneously by superposition of the ensemble of wells, while per well the superposition in time is done as explained in the previous section. Because superposition is valid, the drawdown can be superimposed on the actual groundwater head.

**Example:** Consider an area with are four wells. Each well each is constructed and starts exactly one year after the previous well. The four wells are placed on a square area with sides of 1 km. The order in which they are constructed is NW, NE, SE SW. The extraction is  $600 \text{ m}^3/\text{d}$  at from each well. The transmissivity is  $kD = 600 \text{ m}^2/\text{d}$  and the specific yield is  $S_y = 0.24$ . Visualize the drawdown in the center of the area between these wells as a function of time for a period of 10 years. Show spatial snapshots of the drawdown at times  $t = [0.5, 1.5, 2.5, 3.5, 4.5]$  years after the start of the first extraction well.

Figure 6.21 shows the result of superposition in time for the point in the center of the square with the four wells at the corners. This is the same as in the previous example. Both the total result and the effect of each individual well are shown. It is practical in this case, to work in years and convert the transmissivity and the extraction to years instead of days.

For the spatial snapshot we compute the drawdowns in a dense-enough spacial grid to allow contouring of the drawdown at a specific point in time. The grid used is 10 m spacing between -1000 and +1000 m for both the  $x$  and the  $y$  axis. With these coordinates, the distance is computed to each of the wells. The distance from the grid

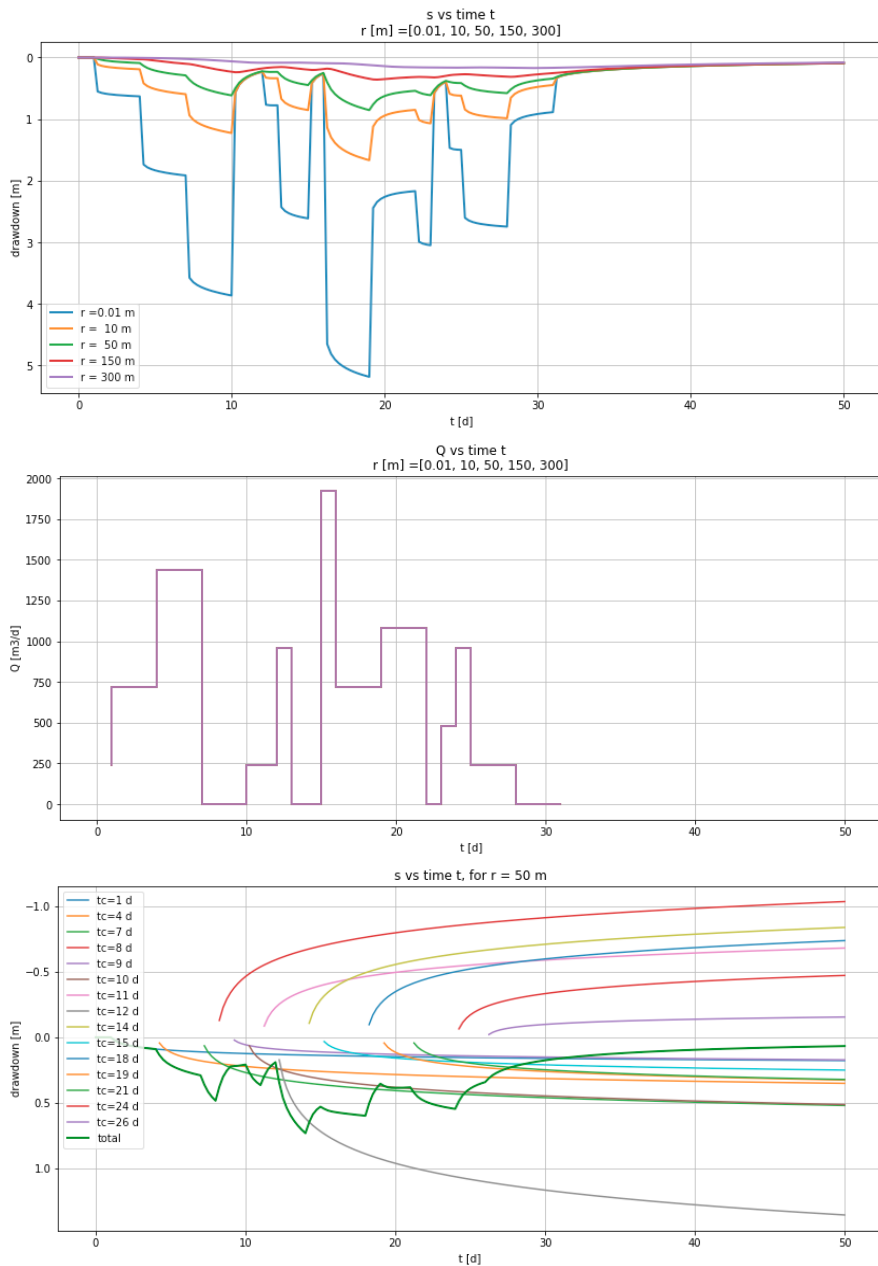


Figure 6.20: Superposition in time (for data given in the text example).  $kD = 600 \text{ m}^2/\text{d}$ ,  $S = 0.1$ .

points to one well is already 160000 points (this requires Python, Excel can't hardy handle this). To prevent division by zero make sure the the minimum distance is  $r_w$ , the well radius. Zero distance occurs of a grid point happens to coincided with the position of a well.

Finally, for each of the four required snapshot times, add the contribution of each of the four wells and for each well use the time since the extraction from that well started. The last step is to contour the results as presented in figure 6.21. The figure uses the same contour lines in all four snapshots, but the values are not indicated in the figure. This, could, however, been done by using full colors and placing a color bar next to each figure. Each snapshot is taken 0.5 years after the previous well started.

**Exercise:** In Egypt, an investments to grow fruits have been made in the desert along the motorway between Cairo and Alexandria. Imagine the enterprise's premises to be 2 km wide having 500 ha of cropped area, that is 2 km along the road by 250 m perpendicular to the road. The crop requires 1 m of water per year irrigation. Four wells are used arranged parallel to the road. They all have their screen from -50 to -100 m. What will be the drawdown in the middle two wells after 1 month, 1 year, 10 years and 50 years. Also compute what will be the drawdown at the neighbor farms 2, 4, 6, 8 and 10 km away. Finally, what would be the drawdown in the center wells if these neighbors up to 10 km away on both sides would pump at the same rate? The transmissivity of the aquifer is  $kD = 2000 \text{ m}^2/\text{d}$ , the specific yield is  $S_y = 0.24$ , the depth of the aquifer is 240 m and the distance below ground surface was 40 m initially. (See also the paragraph on partial penetration).

### 6.3.13 Questions

1. What groundwater situations are solved by Theis? What are the conditions for the underlying groundwater system, and the initial and boundary conditions so that Theis applies?
2. Why do we prefer drawing the Theis well function (type curve) on a double log graph using  $1/u$  instead of  $u$  on the horizontal axis?
3. Explain how we can interpret a pumping test in a confined aquifer based on the Theis type curve on a double log graph?
4. What is the preferred variable to use on the horizontal axis when plotting the drawdown data coming from different observation wells, and why?
5. What is the physical meaning of the partial differential equation on which the Theis solution is based?
6. Is there a final steady state situation that matches the Theis solution?

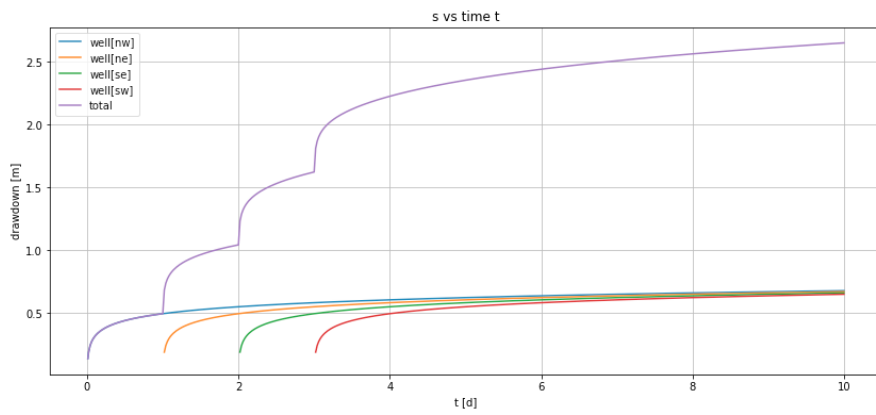


Figure 6.21: Computed drawdown for the example in the center between the four wells (thick black line) and at well #1 (thick dashed purple line)

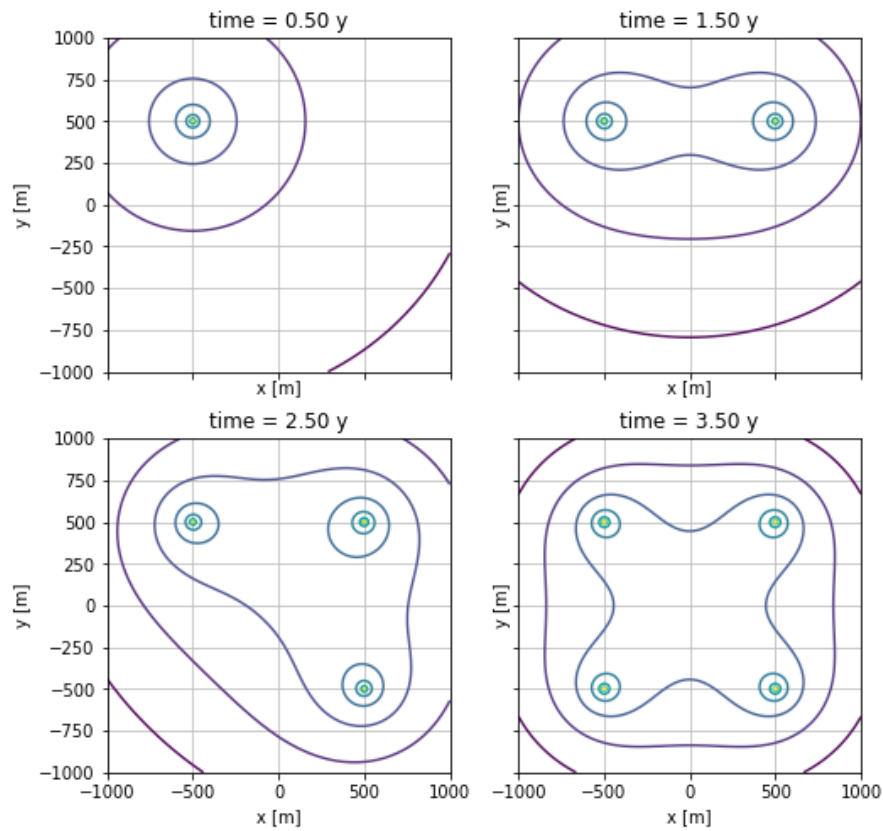


Figure 6.22: Snapshot of drawdown after 50 years of pumping; the colors match the drawdown shown in figure 6.21.

7. How is the outcome  $h^2 - H^2 = \frac{Q}{2\pi k} W(u)$  related to that of a confined situation,  $h - H = \frac{Q}{4\pi kH} W(u)$ ?
8. How can you determine  $u$  as a ratio of time  $t$  and a characteristic time  $T$ ?
9. Show how you can simplify the Theis well function for small values of  $u$ .
10. What is the general shape of the Theis drawdown curve on linear vertical and logarithmic horizontal scale?
11. What part of this general shape is covered by the simplification of the Theis drawdown?
12. Explain the shape of the drawdown versus distance using the simplified Theis well function  $s = Q / (4\pi kD) \ln(2.25kDt / (r^2 S))$ .
13. Express this simplified function in terms of the ratio of distance and a characteristic distance for a chosen fixed time.
14. Explain the radius of influence mathematically using the simplified Theis well function.
15. What is the drawdown per  $\log_{10}$ -cycle of time? Show this using the simplified formula?
16. What is the mathematical standard function that is equivalent to the Theis well function?
17. Given the Theis well function as a power series (equation 6.3), show the relation between two consecutive terms.
18. How would you use the Theis well function to compute the drawdown of a well in an aquifer of infinite extent to compute the transient drawdown due to a well at a given distance from a river that fully penetrates the aquifer without entry resistance?
19. Write down mathematically the superposition in time of a well that changes the extraction in steps from time to time.
20. How would you compute the drawdown due to a well in an aquifer bounded by two parallel fully penetrating canals in direct contact with the aquifer? The canals are a distance  $L$  apart and the well is at a distance  $l$  from one of them.
21. Does the situation posed in the previous question result in a steady-state situation on the long run? Explain your answer.
22. Assume that Libya's large pumping station in Kufra (E 24.149163°, N 23.392326°), with wells in the Nubian sandstone at 162 km from the Egypt's border extracted 1 million  $m^3/d$  starting in 2000. How long would it take for the drawdown to

influence the head at the border of Egypt? Assume  $kD = 600 \text{ m}^2/\text{d}$ ,  $S = 0.005$ . What would be the drawdown at Kufra after 10 and 50 years. What would be the drawdown at the Egyptian border after 10 and 50 years. For the Kufra well field use an effective well radius of 10 km. (have a look at the site on the given coordinates in Google Earth).

23. If the conductivity of the Nubian sandstone measured in the lab at  $20^\circ\text{C}$  would be  $k = 10 \text{ m/d}$ . What would the conductivity be in the Nubian sandstone at 600 m depth where the water temperature is  $50^\circ\text{C}$ ? And so what conductivity should you use in your computations?
24. The water table in a building pit of  $50 \times 50 \text{ m}$  has to be lowered by 5 m. For this, wells are placed at the corners of the pit building pit. The transmissivity  $kD = 1000 \text{ m}^2/\text{d}$  and the specific yield is  $S_y = 0.2$ . Compute the necessary extraction if the water level in the center has to reach this objective (5 m drawdown) within two weeks of pumping. After reaching the necessary drawdown, the drawdown has to be maintained for 6 months. Compute the necessary extraction such that the objective is fulfilled. How much may the extraction be reduced after two weeks, to maintain the desired drawdown, such that the objective is met after 6 months? Hint. If you have code this situation in Python and you use one rate per month, you can just tweak the extraction values until the drawdown matches the requirements.
25. A well is drilled in an unconfined aquifer to secure water for a refugee camp in Jordan. The transmissivity is small, only  $250 \text{ m}^2/\text{d}$ , and the storage coefficient also is modest with  $S_y = 0.005$ . The water table is at 50 m below ground surface. What is the necessary depth of the screen so that the well will still yield the required demand of  $\text{m}^3/\text{d}$  after 10 years?

## 6.4 Partial penetration of well screens

More often than not, well screens only partially penetrate the exploited aquifer because aquifers may be much thicker than the screen length that is needed to produce the required amount of water. Limiting well depth saves money for the owner, although at the cost of some extra pumping energy, because of the extra head loss due to the fact that the streamlines of the water flowing towards the well have to concentrate near the screen, which causes it to accelerate, and higher velocities entail greater losses of energy.

### 6.4.1 Huisman's method

The flow due to only the fact that the screen is partially penetrating can be superimposed on the ideal situation in which the streamlines are all horizontal and parallel with respect to top and bottom of the aquifer when towards a fully penetrating screen, for which the standard groundwater-well formulas were all derived. There are at least two ways to deal

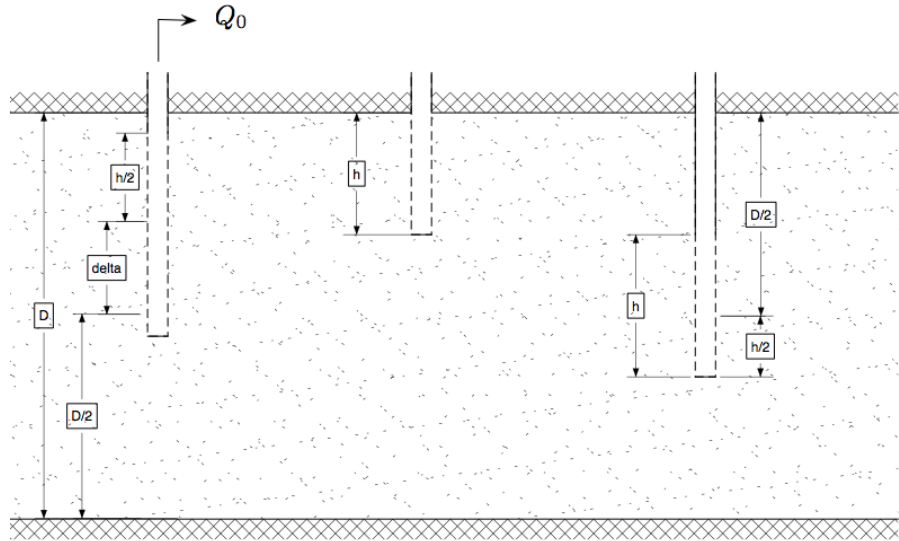


Figure 6.23: Partially penetrating wells

with it; both lead to an extra drawdown that must be added to the drawdown obtained with the standard formula.

The first method is to compute the effect of partial penetration based on the exact solution for the effect, which was derived for a confined aquifer by Hantush (see Kruseman and the Ridder, 1994). The other is a method developed by Huisman (1972), which summarizes the first method by a simple relation for the extra head loss in the well itself. He writes (p130): “With a random position of the well screen as shown in figure 6.24 (left), the additional drawdown at the well face is given by

$$\Delta s_0 = \frac{Q_0}{2\pi kD} \frac{1-p}{p} \ln \frac{\alpha h}{r_0}$$

with  $\alpha$  a function of the amount of penetration  $p = h/D$  and the amount of eccentricity  $e = \delta/D$ . The value of  $\alpha$  as a function of these parameters is given in table 6.3.

The screen in the center of figure 6.24 shows the position that is most usual. This simplifies the formula, at least for penetrations larger than 20%, yielding:

$$\Delta s_0 = \frac{Q_0}{2\pi kD} \frac{1-p}{p} \ln \frac{(1-p)h}{r_0}$$

The partial penetration for the right-most screen in figure 6.24 leads to a simplified formula:

$$\Delta s_0 = \frac{Q_0}{2\pi kD} \frac{1-p}{p} \ln \frac{(1-p)h}{2r_0}$$

Table 6.3: Huisman's (1972) partially penetration table showing the values of  $\alpha$  in the formula as a function of the relative screen length  $p = h/D$  and the eccentricity  $e = \delta/D$  with  $D$  the thickness of the aquifer,  $h$  the screen length and  $\delta$  the distance of the center of the screen to the center of the aquifer (see figure 6.24).

$p \setminus e \rightarrow$	0	0.05	0.1	0.15	0.2	0.25	0.3	0.35	0.4	0.45
alpha	0.54	0.54	0.55	0.55	0.56	0.57	0.59	0.61	0.67	1.09
0.1	0.54	0.54	0.55	0.55	0.56	0.57	0.59	0.61	0.67	1.09
0.2	0.44	0.44	0.45	0.46	0.47	0.49	0.52	0.59	0.89	
0.3	0.37	0.37	0.38	0.39	0.41	0.43	0.50	0.74		
0.4	0.31	0.31	0.32	0.34	0.36	0.42	0.62			
0.5	0.25	0.26	0.27	0.29	0.34	0.51				
0.6	0.21	0.21	0.23	0.27	0.41					
0.7	0.16	0.17	0.20	0.32						
0.8	0.11	0.13	0.22							
0.9	0.06	0.12								

For wells in a phreatic aquifer, where the thickness of the aquifer depends on the drawdown, the factor

$$\Delta s_0 2H = \frac{Q_0}{\pi k} \frac{1-p}{p} \ln \frac{\alpha h}{r_0}$$

has to be added to the value of  $H^2 - h^2$ , where  $H$  is the initial thickness of the water-table aquifer and  $h$  is the final thickness of that aquifer at the well. In this case, the amount of penetration  $p$  and the eccentricity  $e$  should be based on the depth of the water table  $h_0$  that is valid for the fully penetrating well.

#### 6.4.2 Hantush's solution for partial penetrating screens

Huisman's (1972) method is a summary for the effect of partial penetration in the well only. To also obtain the impact of partial penetration for points outside the well, we need a more general analytical solution. The extra drawdown due to partial penetration can be computed from the analytical solution for the extra drawdown due to partial penetration given by Hantush. It reads ([Kruselman and De Ridder (1994)])

$$\Delta s = \frac{Q_0}{2\pi k D} \frac{2D}{\pi d} \sum_{n=1}^{\infty} \left\{ \frac{1}{n} \left[ \sin\left(\frac{n\pi z_1}{D}\right) - \sin\left(\frac{n\pi z_2}{D}\right) \right] \cos\left(\frac{n\pi z}{D}\right) K_0\left(\frac{n\pi r}{D}\right) \right\} \quad (6.8)$$

The variables are shown in figure 6.24. Notice that the distance can be either measured from the top or from the bottom of the aquifer.

This equation allows to compute the extra drawdown due to partial penetration at any point in the aquifer as specified by the coordinates  $r$  and  $z$ . Hence, to estimate this extra drawdown for the well itself, one should choose some points at distance  $r_0$ , the well radius, and average over them, because, contrary to a real well screen that has a constant head inside, the derivation of the influence of partial penetration was under the assumption of a constant discharge per unit screen length. The latter causes some

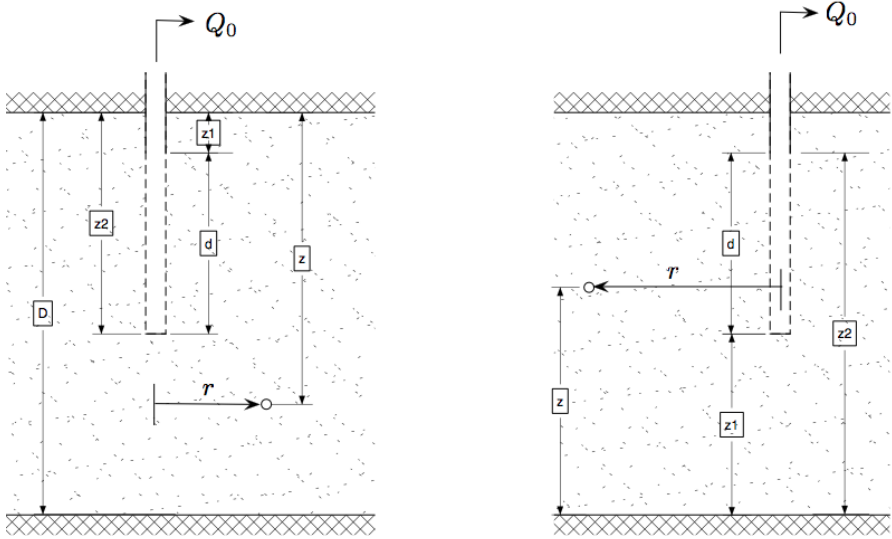


Figure 6.24: Partial penetrating screens with variables as used in equation 6.8

variation of head along the screen, while a uniform head causes some variation of the inflow along the screen. But the errors are not great.

The extra drawdown due to partial penetration given the expression 6.8 a steady-state solution, which cannot account for dynamics. However, the effect of water released from storage close to the well due to the partial penetration alone is essentially elastic. The fully penetration solution takes care of the slow storage release in case of a water table aquifer with a large storage coefficient, i.e. a specific yield  $S_t$ . Therefore the effect of partial penetration along becomes steady-state already after a very short time. One could estimate this time as the time it takes for gradients become stable within the reach in the aquifer where of the partial-penetration effect matters. To determine that time, we can use the derived relation for the flow  $Q_r$  in equation 6.7. Considering that any concentration of stream lines is over beyond about  $r > 1.5D$ , we may state that the condition for this distance is (for instance)

$$Q_R > 0.9Q_0$$

and so, with equation 6.7 we get

$$\begin{aligned} 0.9 &= e^{-u} \\ \ln 0.9 &= -u \\ -0.10536 &= -u \end{aligned}$$

so that

$$u = \frac{r^2 S}{4kDt} \approx 0.1$$

$$t > 10 \frac{r^2 S}{4kD}$$

To illustrate this, let  $r = 2D$ , a conservative estimate, so that  $t > 10SD/k$ . Take  $D = 50$  m and  $k = 25$  m/d then  $t > 20S$ , so that for  $S = 0.001$  we find that  $t > 0.02$  d (half an hour).

Although the range of  $r$  where effects of partial penetration can play is generally said to be  $r \leq 1.5D$ , we may need a larger distance when the aquifer is vertically anisotropic as given by different values of the horizontal and vertical conductivity,  $k_r$  and  $k_z$  respectively. In those cases

$$r \leq 1.5D \sqrt{\frac{k_r}{k_z}}$$

**Exercise:** Implement the partially penetration formula in Python and show its effect on the head lines near the well. You should get the same results as the example in the section below.

#### 6.4.3 Example

After having implemented equation 6.8 in Python, we can compute the effect of partial penetration for any point in the aquifer and add it to the drawdown for the fully penetrating well. This was done. Figure 6.25 shows the head contours due to a partially penetrating screen between  $30 \leq z \leq 40$  m placed in an aquifer where  $0 \leq z \leq 50$  m. The actual situation, shown in the bottom picture, is the superposition of the heads due to a fully penetrating well, shown in the top picture, and the effect of partial penetration, shown in the middle picture. The streamlines (not plotted) are perpendicular to the head contours and show the contraction of the flow near the screen, especially near the ends of the screen. The bottom picture in Figure 6.25 was obtained by adding equation 6.8 to a simple Dupuit solution  $s = Q/(2\pi kD) \ln(R/r)$ , where  $R = 100$  was chosen. The contribution of the head due to partial penetration has a positive zone in front of the screen, where the drawdown is increased and negative zones above and below the screen, where the drawdown is reduced by partial penetration, but where the flow is much smaller than directly opposite the screen. As can be seen from the pictures, the effect of the partial penetration does not reach farther than about one aquifer thickness from the well (in this vertically isotropic aquifer). So the 1.5D mentioned above for the practical reach of the impact of partial penetration is good for most practical situations, unless the aquifer is very anisotropic in the vertical sense.

In conclusion, for such a detailed picture and computation of the head around a well screen we don't need a large 3D numerical model at all. And, if you have such a model, you can use the analytical approach to verify that you haven't made mistakes in this big model.

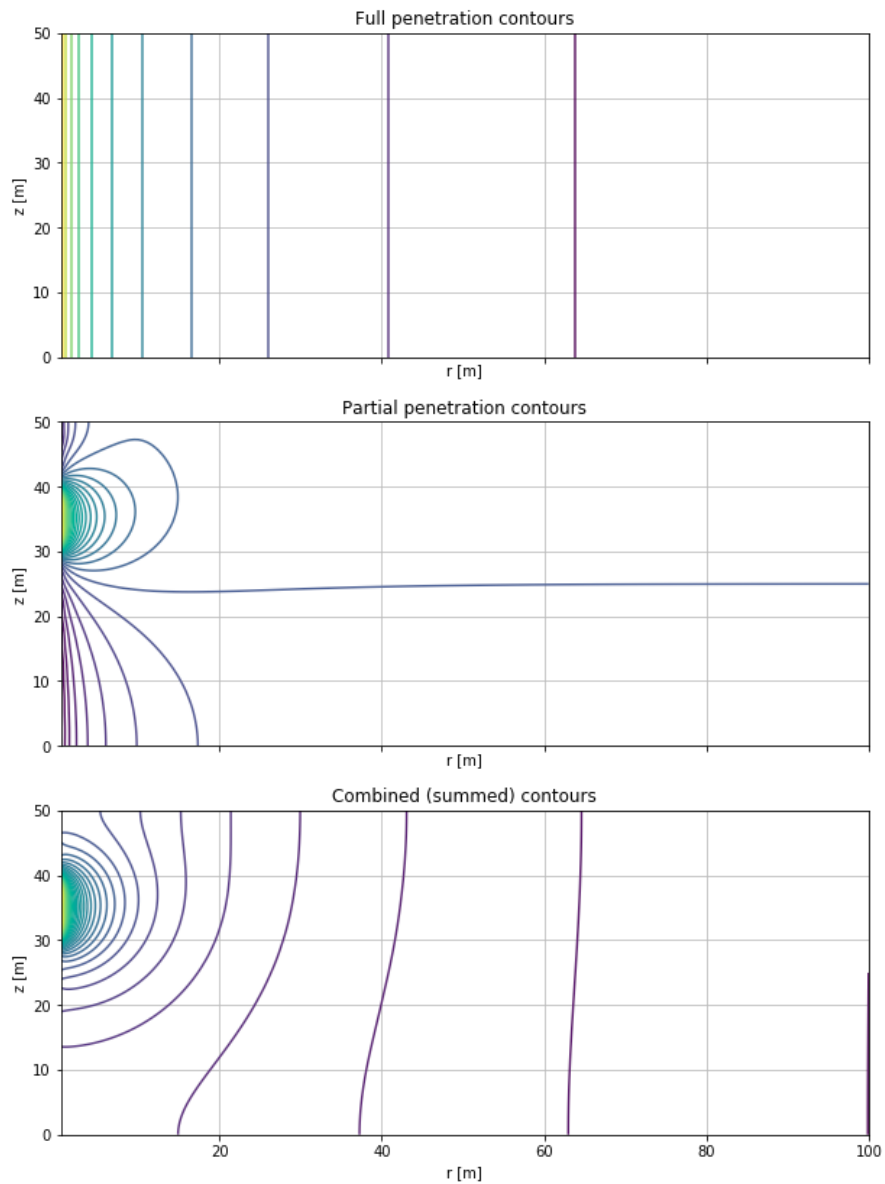


Figure 6.25: Effect of partial penetration: Top: Head contours due to extraction by a fully penetrating well. Middle: The head change due to partial penetration, equation 6.8. Bottom: Partial penetration impact superimposed on the heads of the fully penetrating well. (Bottom = Top + Middle). The flow is axially symmetric.  $kD = 600 \text{ m}^2/\text{d}$ ,  $Q = 1200 \text{ m}^2/\text{d}$ .  $s(r = 100) = 0$ . Drawn are 15 contours between  $s = -1$  and  $s = 6 \text{ m}$ . The same contours were drawn in all three pictures.

#### 6.4.3.1 Python implementation of partial penetration

The Python implementation is given in the listing below. The listing also has the code that generated the pictures in figure 6.24

```
1 def dspp(r=None, z=None, zt=None, zts=None, zbs=None, zb=None, n
=20):
2     '''Return drawdown effect of partial penetration of well
3         screen without the factor Q/(2 pi kD).
4         parameters
5             r, z : vectors (np.ndarray)
6                 vertical and horizontal coordinates
7             zt, zts, zbs, zb: four floats
8                 top aquifer, top screen, bottom screen, bottom aquifer
9                 respectively
10            The values must decrease to be consistent
11            n: int
12                maximum in sum
13            ,,
14            if np.any(np.diff(np.array([zt, zts, zbs, zb])) > 0):
15                raise ValueError('zt, zts, zbs and zb must be
16                    descreasing in value.')
17            if np.any(r<=0):
18                raise ValueError('r must be all positive')
19            if np.any(np.logical_or(z > zt, z < zb)):
20                raise ValueError('z must be $le$ zt and $ge$ zb')
21
22            D, d = zt - zb, zts - zbs
23            R, Z = np.meshgrid(r, z)
24
25            ds = np.zeros_like(R)
26            for i in range(1, n + 1):
27                p = i * np.pi/D
28                ds += (1/i) * (np.sin(p * zts) - np.sin(p * zbs)) * np.
29                    cos(p * Z) * K0(p * R)
30
31
32            # Example worked out
33            rw = .5 # well radius
34            R0 = 100. # Fixed head boundary
35
```

```

36 zt , zts , zbs , zb = 50, 40, 30, 0
37 r = np.logspace(np.log10(rw), np.log10(R0), 100)
38 z = np.linspace(zb, zt, 101)
39 R, Z = np.meshgrid(r, z)
40
41 Q = 1200 # m3/d
42 kD = 600 # m2/d
43 S = 0.0
44
45 s = Q / (2 * np.pi * kD) * np.log(R0 / R)
46 ds = Q / (2 * np.pi * kD) * dspp(r, z, zt, zts, zbs, zb, n=20)
47
48 fig, ax = plt.subplots(3, 1, sharex=True, sharey=True)
49 fig.set_size_inches(10, 14)
50 ax = ax.ravel()
51 titles = [ 'Full penetration contours', 'Partial penetration
      contours', 'Combined (summed) contours' ]
52 for a, title in zip(ax, titles):
53     a.set_title(title)
54     a.set_xlabel('r [m]')
55     a.set_ylabel('z [m]')
56     a.grid()
57
58 levels = np.linspace(np.floor(np.min(s + ds)), np.ceil(np.max(s
      + ds)), 50)
59 ax[0].contour(r, z, s, levels=levels)
60 ax[1].contour(r, z, ds, levels=levels)
61 ax[2].contour(r, z, s + ds, levels=levels)

```

#### 6.4.4 Questions

1. What is partial (screen) penetration?
2. When is partial penetration important? To how far away from the well?
3. A screen penetrates the first third of the aquifer depth. Explain how the drawdown is affected by the partial penetration relative to the drawdown due to a fully penetrating well? Indicate where the drawdown is more and where it is less than the drawdown due to a fully penetrating screen.
4. Why is the effect of partial penetration steady already after a short time after the extraction from the well started?
5. How could you handle partial penetration in a real case when you have to determine the drawdown from a screen that only penetrates part of the aquifer thickness.

## 6.5 Hantush: transient flow due to a well in a semi-confined (leaky) aquifer

Mahdi S. Hantush (1955) published a solution for the drawdown caused by a fully penetrating well pumping in a semi-confined aquifer, the situation of which is depicted in figure .... The situation differs from the one by Theis, in that now the aquifer is overlain by a by a semi-pervious layer, called an aquitard, on top of which a fixed head (water level) is maintained. So there is vertical leakage through the aquitard, which linearly depends on the head difference across it. Hantush (1955) formulated the problem as follows:

*"The non-steady drawdown distributed near a well discharging from an infinite leaky aquifer is presented. Variation of drawdown with time and distance caused by a well of constant discharge in confined sand of uniform thickness and uniform permeability is obtained. The discharge is supplied by the reduction of storage through expansion of the water and concomitant compression of the sand, and also by leakage through the confining bed. The leakage is assumed to be at a rate proportional to the drawdown at any point. Storage of water in the confining bed is neglected."*

We will implement the Hantush well function by numerical integration and by series expansion and then apply it. Both implementations are highly accurate across the entire range of values in tables given in the original paper and in various groundwater-hydrology books such as for instance the most well-known book on pumping-test analysis (Kruseman & De Ridder, 1994, free on the internet).

### 6.5.1 Hantush's partial differential equation and solution

The derivation is the same as for the Theis equation, which one addition, the vertical leakage through the overlying aquitard.

From continuity we obtain for a ring between  $r$  and  $r + dr$  from the well center over a given time step  $\partial t = t \rightarrow t + dt$  we have:

$$q_r(2\pi r) - q_{r+dr}(2\pi(r+dr)) + n_r 2\pi r dr = S(2\pi r dr) \frac{\partial \phi}{\partial t}$$

where not  $n_r$  is the leakage from (or to) the overlying layer with fixed head. Working out this continuity equation in the same way as we did before for the Theis solution, yields

$$-\frac{\partial q}{\partial r} - \frac{q_r}{r} + n_r = S \frac{\partial \phi}{\partial t}$$

The leakage can be set to

$$n_r = \frac{\phi_0 - \phi}{c}$$

with  $c$  the resistance of the top layer against vertical flow and  $\phi_0$  the maintained head in the top layer. With Darcy's law filled in we then obtain

$$\frac{\partial^2 \phi}{\partial r^2} + \frac{1}{r} \frac{\partial \phi}{\partial r} + \frac{\phi_0 - \phi}{kDc} = \frac{S}{kD} \frac{\partial \phi}{\partial t}$$

Whenever we deal with semi-confined flow systems we write

$$\lambda^2 = kDc$$

or

$$\lambda = \sqrt{kDc}$$

where we call  $\lambda$  [L] the spreading length or the characteristic length of this semi-confined aquifer system. Hence the PDE in terms of head is

$$\frac{\partial^2 \phi}{\partial r^2} + \frac{1}{r} \frac{\partial \phi}{\partial r} + \frac{\phi_0 - \phi}{\lambda^2} = \frac{S}{kD} \frac{\partial \phi}{\partial t}$$

Because the derivative of  $\phi - \phi_0$  is the same as that of  $\phi$ , because  $\phi_0$  is a constant, we may write as well

$$\frac{\partial^2 (\phi - \phi_0)}{\partial r^2} + \frac{1}{r} \frac{\partial (\phi - \phi_0)}{\partial r} - \frac{\phi - \phi_0}{\lambda^2} = \frac{S}{kD} \frac{\partial (\phi - \phi_0)}{\partial t}$$

Note that the sign of the third term has changed.

So that we see that the PDE does not depend on both  $\phi$  and  $\phi_0$  but only on  $\phi - \phi_0$ , the difference from the initial head. Generally we call  $s = \phi - \phi_0$  the drawdown. In fact, it is the head change relative to the initial head. (Notice the lowercase  $s$  for the head change, contrary to the storativity  $S$ , which we always write in uppercase).

So, the final PDE for semi-confined flow is

$$\frac{\partial^2 s}{\partial r^2} + \frac{1}{r} \frac{\partial s}{\partial r} - \frac{s}{\lambda^2} = \frac{S}{kD} \frac{\partial s}{\partial t}$$

which was solved by Hantush for specific initial and boundary conditions.

- Initial  $s$  zero everywhere.

$$s(r, 0) = 0$$

- Head change at infinity is always zero

$$s(\infty, t) = 0$$

- Head in upper aquifer always the same.

$$s_0 = 0$$

- Flow at the well face is constant for  $t > 0$  and zero for  $t \leq 0$ .

$$Q_{r \rightarrow 0, t0} = 2\pi r k D \frac{\partial s}{\partial r} \Big|_{r \rightarrow 0} = Q_0$$

Notice also, that, because the partial differential equation is linear, superposition may be applied to its solutions. That means that the value of the initial head  $\phi_0$  is immaterial; it may even vary in an arbitrary way in space; the differential equation only describes the change of the head due to the well alone without being affected by what happens elsewhere.

The solution obtained by Hantush is

$$s = \phi - \phi_0 = \frac{Q_0}{4\pi k D} W_h \left( u, \frac{r}{\lambda} \right)$$

where  $W_h()$  is Hantush's well function. It is mathematically written as

$$W_h \left( u, \frac{r}{\lambda} \right) = \int_u^{\infty} \frac{\exp \left( -y - \frac{(\frac{r}{2\lambda})^2}{y} \right)}{y} dy$$

You may prove that the solution is correct by filling it into the partial differential equation and verifying that both sides of the PDE are then equivalent.

[Bruggeman (1999)] gives also a power series expression to compute Hantush's well function

$$W_h(u, \rho) = \sum_{n=0}^{\infty} \frac{(-1)^n}{n!} \left( \frac{\rho}{2} \right)^{2n} u^{-n} E_{n+1} \left( \frac{\rho^2}{4u} \right)$$

$$E_{n+1} = \frac{1}{n} \{ e^{-u} - u E_n(u) \}, (n = 1, 2, 3\dots)$$

but we won't bother with that one as it may be quite nasty to always guarantee convergence. The integral expression is straightforward and easy to implement and works well.

### 6.5.2 Implementing Hantush's well function

One way is to directly integrate the argument over the range  $u < y < \infty$ , where  $\infty$  needs to be replaced by a sufficiently high value, i.e.  $\infty \approx 10^{20}$ . Furthermore, because of the enormous range that needs to be covered by the integral, take a series of values for  $y$  on logarithmic scale:

```
1 y = np.logspace(np.log10(np.min(u)), np.log10(inf), n)
```

Which assumes that  $u$  will be a given array. This means that the range between the lowest value in  $u$  and  $\infty$  also contains all other values of  $u$  that needs to be integrated from. To make sure that we have the exact values of all  $u$  in the array of  $y$  we can add them and sort the array as is done in the listing. To be even more accurate, also add

the array  $u - \epsilon$  where  $\epsilon$  is a very small number like  $10^{-100}$ . This will make sure that the integration of all higher  $u$  values will be as accurate as possible. Once we have this in place, we compute the argument of the well function for all these values of  $y$ . Then we compute the the value of  $dy$  to multiply. We do that in two steps to make sure that also the first and the last value will be accurate. The rest is just to sum the  $arg \times dy$  from each starting  $u$  value up to infinity. This approach allows to efficiently deal with entire arrays of  $u$  to return an entire array of values of the well function. Of course, there are many ways to implement this function in Python or in Excel. A possible Excel listing is also given, but when implemented it will be one value per spreadsheet shell, whereas th Python approach allows thousands of values to be computed and visualized at once.

```

1 # Hantush's well function for scalar input
2
3 def wh(u, rho, n=1000):
4     '''Return wh(u, rho) simple for u and rho scalars'''
5     inf = 20
6     y = np.logspace(np.log10(u), 20, n)
7     a = np.exp(-y - (rho/2)**2 / y) / y
8     dy = np.diff(y)
9     dy2 = np.zeros_like(y)
10    dy2[:-1] += 0.5 * dy
11    dy2[1:] += 0.5 * dy
12    return np.sum(dy2 * a)
13
14 # Hantush's well function for vector input of u
15 def Wh(u, rho, n=5000):
16     '''Return Wh(u, rho) for rho scalar'''
17     if not np.isscalar(rho):
18         raise ValueError('rho must be scalar')
19     if not isinstance(u, np.ndarray):
20         u = np.array(u)
21     eps, inf = 1.0e-100, 20.0
22     y = np.hstack((u, u-eps, np.logspace(np.log10(np.min(u)),
23                                         inf, n)))
24     y.sort() # sort y in place
25     a = np.exp(-y - (rho/2)**2 / y) / y # argument
26     dy = np.diff(y)
27     dy2 = np.zeros_like(y)
28     dy2[:-1] += 0.5 * dy
29     dy2[1:] += 0.5 * dy
30     w = np.zeros_like(u)
31     for i, uu in enumerate(u): # Just sum from each u to inf
32         w[i] = np.sum(a[y >= uu] * dy2[y >= uu])
33     return w

```

An Excel implementation is given in figure 6.26.

**Exercise:** It is left to the student to implement it and see if both implementations yield the same result. The implementation can be verified using table 4.2 p298-299 in [Kruseman and De Ridder (1994)], which can be downloaded from the Internet.

### 6.5.3 Hantush type curves and comparison with Theis

Having implemented the Hantush well function in Excel or Python, we can compute the so-called Hantush type curves that are presented in nearly every book on pumping tests. The idea is to show the function in on double logarithmic axis so that it is directly comparable with a drawdown time curve. Thus we make graphs showing the Hantush function  $W_h$  on the vertical axis (because proportional to the drawdown) and the  $1/u$  on the horizontal axis (because proportional to time). We do so for distinct values of  $r/\lambda$  and we also add the Theis function as it is equivalent to the Hantush function if leakage were absent, that is when  $c \rightarrow \infty$ .

We see from the type curves that the Hantush solution is equivalent to the Theis function for sufficiently small values of time (i.e. of  $1/u$ ), and that they all reach a constant value after a certain time that depends on the value of  $r\lambda$ . The larger the vertical resistance, the smaller the value of  $r/\lambda$ , the longer it takes before steady state equilibrium is reached.

It is also interesting to see the type curves on linear vertical and logarithmic horizontal scale (figure 6.28). This yields the character of the absolute drawdown as a function of logarithmic time.

These curves have an S-shape because it takes some time before the drawdown sets in and after some more time equilibrium (steady state flow) is reached. The only exception is the Theis curve, which never reaches an equilibrium, whose drawdown continues to grow forever, be it at an ever slower rate. All Hantush curves represent a situation where the aquifer is recharged from above in proportion to the drawdown. These Hantush cases will reach an equilibrium drawdown because of this recharge by induced leakage.

Because the well-known steady-state solution of a well extracting in a semi-confined aquifer is

$$s = \frac{Q}{2\pi kD} K_0 \left( \frac{r}{\lambda} \right)$$

it follows that  $K_0 \left( \frac{r}{\lambda} \right) = \frac{1}{2} W_h(u_{t=\infty}, \frac{r}{\lambda}) = \frac{1}{2} W_h(0, \frac{r}{\lambda})$ . Because  $u = \frac{r^2 S}{4kDt}$ , so  $t \rightarrow \infty$ , it follows that for the steady state situation  $u \rightarrow 0$ , hence  $W_h(0, \frac{r}{\lambda})$ .

The curves in figure 6.28 have an inflection point at which the drawdown is exactly halfway zero and its final equilibrium. The drawdown at this point thus equals  $s = \frac{Q}{4\pi kD} K_0 \left( \frac{r}{\lambda} \right)$  (notice the 4 in the denominator).

It can be proven (see for instance Bruggeman (1999, p877) that the inflection point is obtained for  $u = \frac{r}{2\lambda}$ . With this knowledge, we can compute a characteristic time for

```

Public Function Whan(u As Double, rho As Double) As Double
' Hantush's well function (by integration, similar to Expint)
Dim dlny, y, w, lnINF, rho2 As Double

lnINF = 20           'end of integration
dlny = 0.01          'step size for integration, small part of log cycle
lny = Log(u) + 0.5 * dlny   'first location on log axis, use +0.5dlny to move to center of steps
rho2 = rho * rho / 4
w = 0               'Initialize and loop till lnINF wasreached
While lny < lnINF
    y = Exp(lny)
    w = w + Exp(-y - rho2 / y)
    lny = lny + dlny
Wend

'finally multiply by the step size, all at once is more efficient than while looping
Whan = w * dlny

End Function

```

Figure 6.26: Hantush' well function in Visual Basic for Excel

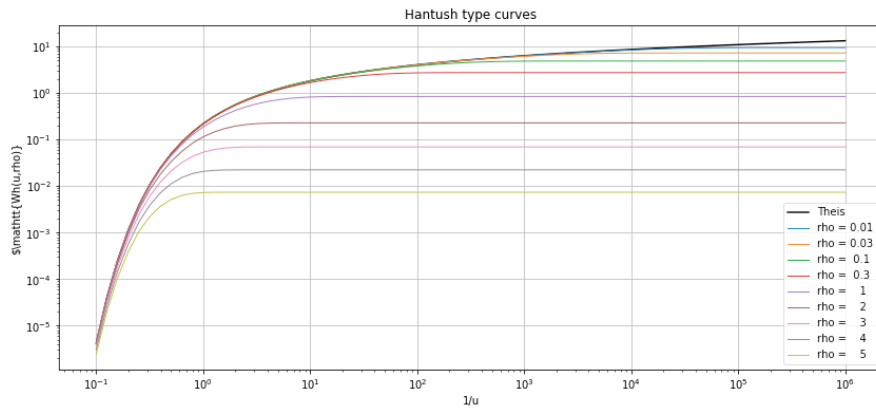


Figure 6.27: Theis and Hantush type curves plotted in Excel. The Hantush type curves are for different values of  $\rho = r/\lambda$  as indicated by the numbers in the legend to the right.

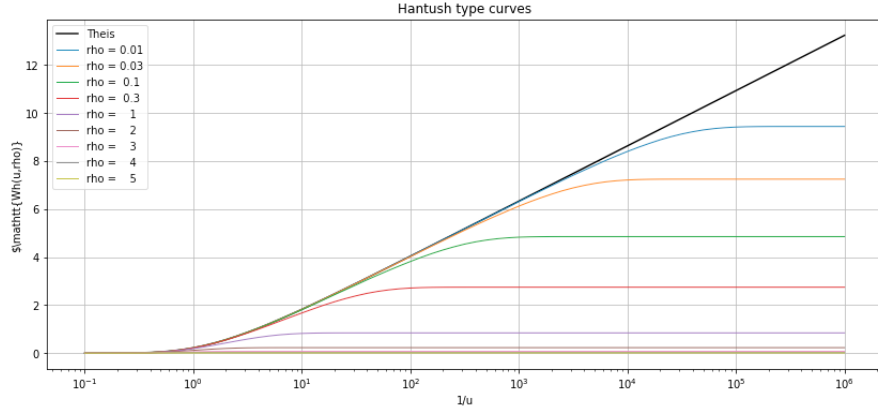


Figure 6.28: Theis and Hantush curves on a linear vertical scale while the horizontal scale is still logarithmic.

the drawdown development of the well in a semi-confined aquifer, i.e. the time  $t_{50\%}$ , at which the drawdown is half the equilibrium value, noting that  $\lambda = \sqrt{kDc}$

$$\begin{aligned}
 u &= \frac{r^2 S}{4kDt_{50\%}} = \frac{r}{2\lambda} \\
 \frac{r^2 Sc}{2\lambda^2 t_{50\%}} &= \frac{r}{2\lambda} \\
 t_{50\%} &= Sc \frac{r}{2\lambda}
 \end{aligned} \tag{6.9}$$

This time bears two characteristics. First is the distance from the well relative to the characteristic length of the groundwater system, i.e.  $r/(2\lambda)$ . The 2 is not strange as we encounter it in both  $u$  and in the mathematical Theis and Hanush well functions. The other characteristic is  $Sc$ , a combination that is associated with the time an aquifer is filled by leakage. To show this, consider an aquifer without horizontal flow with a top layer with constant head  $\phi_0 = 1$  m. Let the initial head in the aquifer be  $\phi = 0$  at  $t = 0$ . The leakage from the overlying layer will then set in and slowly raises the head of the aquifer through the overlying aquitard. Using drawdown or head difference instead of heads, where  $s = \phi - \phi_0$ , without horizontal flow, the partial differential equation reduces to

$$-\frac{s}{c} = S \frac{ds}{dt}$$

which may be readily solved by integration

$$\begin{aligned}
 \frac{ds}{s} &= -\frac{dt}{cS} \\
 \ln s + C &= \frac{t}{cS}
 \end{aligned}$$

with as initial condition the drawdown  $s_0$  at  $t = 0$ , which yields the integration constant

$$t = 0, \quad s = s_0 \rightarrow C = -\ln s_0$$

so that

$$\frac{s}{s_0} = \exp\left(-\frac{t}{Sc}\right)$$

With  $T = Sc$ , this can be written as

$$\frac{s}{s_0} = \exp\left(-\frac{t}{T}\right)$$

Where we see that  $T$  functions as the characteristic time of that system: the drawdown  $s$  will be reduced by a factor  $1/e = 0.36788$  every time  $T$  further in the future. You may be more familiar with the word “halftime”, where each halftime further in the future implies that in this case  $s$  is reduced by a factor 2. This halftime can easily be derived by looking for the time  $t_{50\%}$  where  $s/s_0 = 0.5$

$$\begin{aligned} 0.5 &= \exp\left(-\frac{t_{50\%}}{T}\right) \\ \ln 0.5 &= -\frac{t_{50\%}}{T} \\ t_{50\%} &= T \ln 2 \\ &\approx 0.7T \end{aligned}$$

This is always the case; the halftime of a system is just about 70% of its characteristic time.

We, therefore, notice that the quantity  $T = Sc$  is the characteristic fill-up time of the leaky aquifer, which we also encountered in equation 6.9, which gave the time that the drawdown due to a well extracting from the semi-confined aquifer reaches half its final value.

**Exercise:** Show the flex-points in the Hantush type curves.

**Exercise:** Show that the Hantush function becomes the Theis function when  $c \rightarrow \infty$ .

#### 6.5.4 Questions

1. What are the properties of the groundwater system leading to a Hantush-type of drawdown in a pumping test? Or: what groundwater system envisioned Hantush when he developed his well formula?
2. How does the final drawdown expressed in terms of the Hantush-well solution relate to the steady state solution for a well in a semi confined aquifer? Write down your answer mathematically.

3. At what time does the Hantush drawdown reach half its final steady-state value? Give your answer in mathematical terms.
4. What is the characteristic time of the adaptation of the head in a semi confined aquifer to a sudden change of the barometer pressure?
5. Explain why the Hantush type-curves with the lowest  $r/\lambda$  ratio resemble the Theis-type curve most?
6. Explain why the Theis type curve is an extreme case of the Hantush type curve?
7. What is the characteristic length  $\lambda$  of a semi-confined aquifer (or, alternatively, the spreading length)? Give your answer mathematically.
8. How does the Hantush-type curve change when the spreading length is increased?
9. Explain this change in terms of the transmissivity of the aquifer and the resistance of the overlying aquitard.
10. What is the general shape of the Hanush-well function graphed using a linear vertical and logarithmic horizontal axis?
11. Consider an semi-confined aquifer with a constant transmissivity  $kD = 900 \text{ m}^2/\text{d}$  and  $S = 0.001$  with the vertical resistance of the overlying layer equal to  $c = 400 \text{ d}$ . For an observation point at  $r = 600 \text{ m}$  distance, determine when the drawdown has become steady state (to at least to 95%). Use the Hantush-type curves to determine your answer.
12. For the same situation, when is the drawdown at this point equal to half the final drawdown?
13. For the same situation, when becomes the drawdown essentially larger than zero, say at least 5% of the final drawdown. Tip: use the Hantush type curves to determine your answer.
14. What is the relation between the the answer to the previous question and the radius of influence of the Theis well?
15. The head in a building pit of  $50 \times 50 \text{ m}$  extent, dug into a semi-confined aquifer with transmissivity  $kD = 1000 \text{ m}^2/\text{d}$ , resistance  $c = 360 \text{ d}$  and storage coefficient  $S = 0.002$  has to be lowered by 3.5 m. The wells are placed in the corners of the building pit. How long does one need to pump to reach the steady-state drawdown and what is the final drawdown in the center of the building pit?
16. What will be the head in the building pit one day after pumping started?
17. What will be the head in the building pit one day after pumping ended?

### 6.5.5 Pumping test Dalem (Kruseman & De Ridder, 1994)

[Kruseman and De Ridder (1994)] describe a pumping test in a leaky aquifer near the village Dalem in The Netherlands, that was carried out in 1961. The pumping rate was  $Q = 761 \text{ m}^3/\text{d}$ . The cross section based on the drillings is given in figure 6.29. They also provide the data for that site and work out the test applying several methods. The student is asked to work out this pumping test as an exercise/part. Because the test concerns a semi-confined aquifer, the aim must be to determine not only the transmissivity  $kD$  and the storage coefficient  $S$ , but also the resistance  $c$ , of the overlying semi-pervious layer.

The task is to work out the pumping test in the classical way by using the type curves. Clearly, by having implemented the well functions, one should be able to do the whole interpretation in Excel, including the graphics.

**Hint:** Plot your data on the same double log graph as the Hantush-type curves and move your data such that they overlay a particular type curve as well as possible. You move your data upward or downward by multiplying your drawdowns by a factor, and you move your data to the left or right by multiplying your time by a factor. The interpretation follows from the two factors after the measurements fit the graphs.

The exercise is part of the assignment for this course.

Figure 6.30 shows the data for all students and piezometers. The data for each students and 3 piezometers can be found in the accompanying Excel workbook Student-DataDalemPumpTest.xls.

## 6.6 Delayed yield (delayed water-table response)

### 6.6.1 Introduction

Pumping-tests drawdowns do not always resemble the Theis or Hantush type curves; sometimes the drawdown shows a double dip, which is known as delayed yield. Because delayed yield is quite ubiquitous, it has been studied extensively by scholars in the past, most noticeably by Boulton (1954), Pricket (1971) and Neuman (1972). While Boulton introduced an extra delay parameter to explain the phenomenon. Pricket (1971) demonstrated for a large number of pumping tests in his home state in the USA that the Boulton solution well matched the curves obtained from real-world tests. However, there was no direct physical mechanism behind Boulton's delay parameter. It remains, therefore, unclear what its precise origin was. It was often assumed that it had to be the unsaturated zone, which is not accounted for in the known groundwater flow solutions. And, indeed, early groundwater-flow models, that accounted for saturated and unsaturated flow simultaneously were able to match the curves that had been measured by Pricket (Cooley, 1970). However, it was Neuman (1972), who solved the problem by showing that the delayed yield could be completely described by the combination of

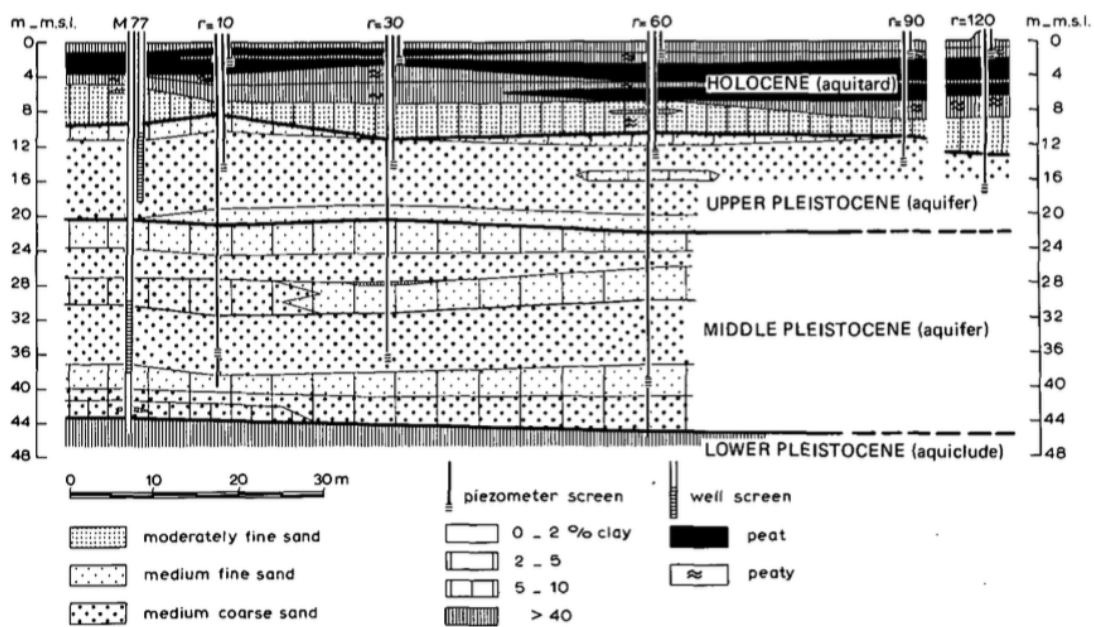


Figure 4.2 Lithostratigraphical cross-section of the pumping-test site 'Dalem', The Netherlands (after De Ridder 1961)

Figure 6.29: Dalem pumping-test site (Kruseman & De Ridder, 1994)

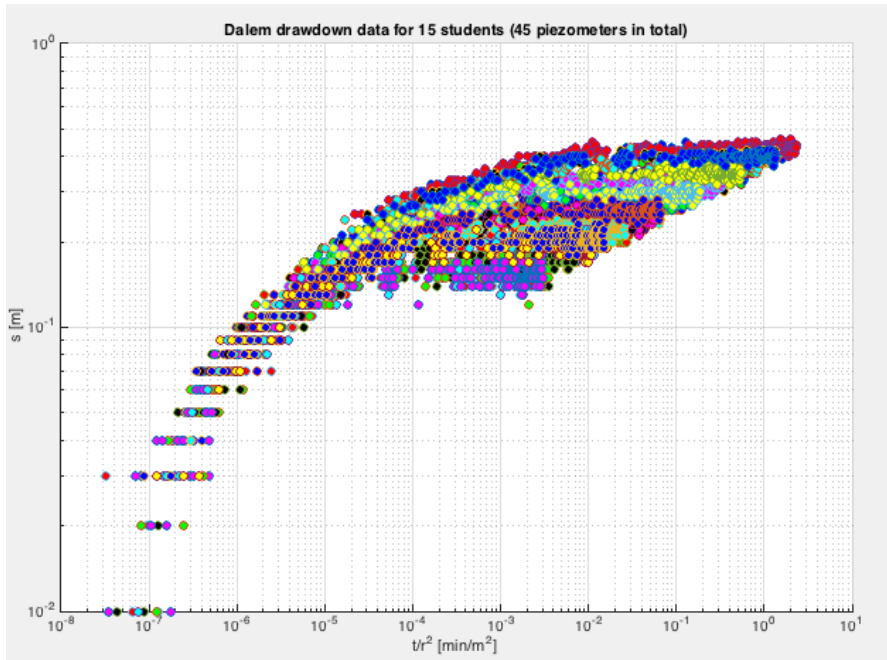


Figure 6.30: Piezometer data for students for Dalem pumping test (see accompanying Excel workbook *StudentDataDalemPumpTest.xls*)

elastic storage, which operates throughout the aquifer, and storage from the decline of the water table, which is generally accounted for by specific yield. Neuman (1972) derived an analytical solution for the flow to a well in a water-table aquifer, while taking into account vertical flow components. He showed that the released water initially stems from elastic storage, due to the expansion of the water and the compaction of the soil skeleton, which is a fast process due to the low value of this storage. He further showed that very soon after the start of the pump, the water table starts declining, which releases much more water by emptying pores near the water table, which, therefore is a slow process. It means that after some time, the release of pore water at the water table becomes the dominant process. The result in drawdown line is a graph that resembles two Theis curves, an early Theis curve in accordance with the elastic storage, and a late Theis curve, in accordance with specific-yield storage.

### 6.6.2 Water-table aquifer

We may show the phenomena on the hand of some numerical simulations as shown in figure 6.31. The first picture shows the drawdown versus time for a number of points at different distances from the well and for different depths as expressed in % of the aquifer thickness. The colors correspond to three depths. The blue curves are near the top of the aquifer, the magenta curves in the center of the aquifer, and the green curves near the bottom. As the figure indicates, the drawdownon differs with depth, but only

for piezometers that are not far from the well; at later times this difference disappears. The second picture in the same figure shows the depth-averaged drawdown for a number of distances from the well. The later curves correspond to larger differences. One sees that the curves initially correspond to the Theis drawdown computed for the elastic storage coefficient, while later on they match the drawdown that corresponds to the Theis solution for the specific yield. The shorter the distance to the well, the more pronounced the transition between the two Theis curves is. Obviously, the curves that correspond to the larger distances are later. The effect of depth has been eliminated from the second chart by taking the average head over the full depth of the aquifer at each distance. The third picture in figure 6.31 demonstrates the difference of the drawdown at different depths at the same location, which was chosen at  $r = 28.4$  m from the well. From these graphs, it becomes especially manifest that the closer to the water table, the later the drawdown graph.

These graphs in figure 6.31 were computed using a numerical axially-symmetric model with elastic storage everywhere, but only specific yield at the water table. There is no unsaturated zone in the model. This is in accordance with Neuman (1972) who explained that the phenomenon of delayed yield can be fully explained by the simultaneous action of the elastic storage in the whole aquifer and the specific yield at the water table.

### 6.6.3 Generalization to semi-confined aquifers

We may now generalize delayed yield, by extending it to any groundwater system in which a water table will decline in a reaction to pumping. This especially holds true for semi-confined aquifers. The Hanush assumptions underlying his solution include a fixed head in the overlying layer. When in reality this head cannot be maintained, it will cause a delayed-yield effect. This may be the case in many practical situations without it being determined in a pumping test, because the pumping has stopped long before the delayed yield would become visual in the drawdown curves. The reason is the delay that is caused by the resistance against vertical flow from the overlying layer. That this is the case, is explained by the characteristic time for filling the semi-confined aquifer given an initial head difference with the overlying layer. This characteristic time,  $T$ , equals  $T = Sc$  where  $S$  is the elastic storage coefficient of the aquifer and  $c$  the resistance of the overlying layer against vertical flow. With typical values of say  $S = 0.001$  and  $c = 500$  d, we have  $T = 0.5$  d. This means that a sudden lowering of the head in the semi-confined aquifer would be fully compensated by increased leakage in about  $5T \approx 2.5$  d. This characteristic time affects only the level of the transition zone between the two Theis curves. We can show this by computing the drawdown in a semi-confined aquifer. For this we use an aquifer system consisting of a resistance cover layer that is  $D_{cover} = 12$  m thick on top of a  $D_{aquif} = 35$  m thick aquifer. The well is fully penetrating. Four models are compared that differ only in the vertical resistance of the cover layer, with values is  $c = [10, 100, 1000, 10000]$  days respectively. Specific yield is  $S_y = 0.2$ , the elastic storage coefficient of the aquifer is  $S = 0.002$ , i.e.  $S_s = S/D_{aquif}$ ; the hydraulic conductivity of the aquifer is  $k_h = 10\text{m/d}$ , hence the transmissivity  $kD = 350\text{ m}^2/\text{d}$ . The results are

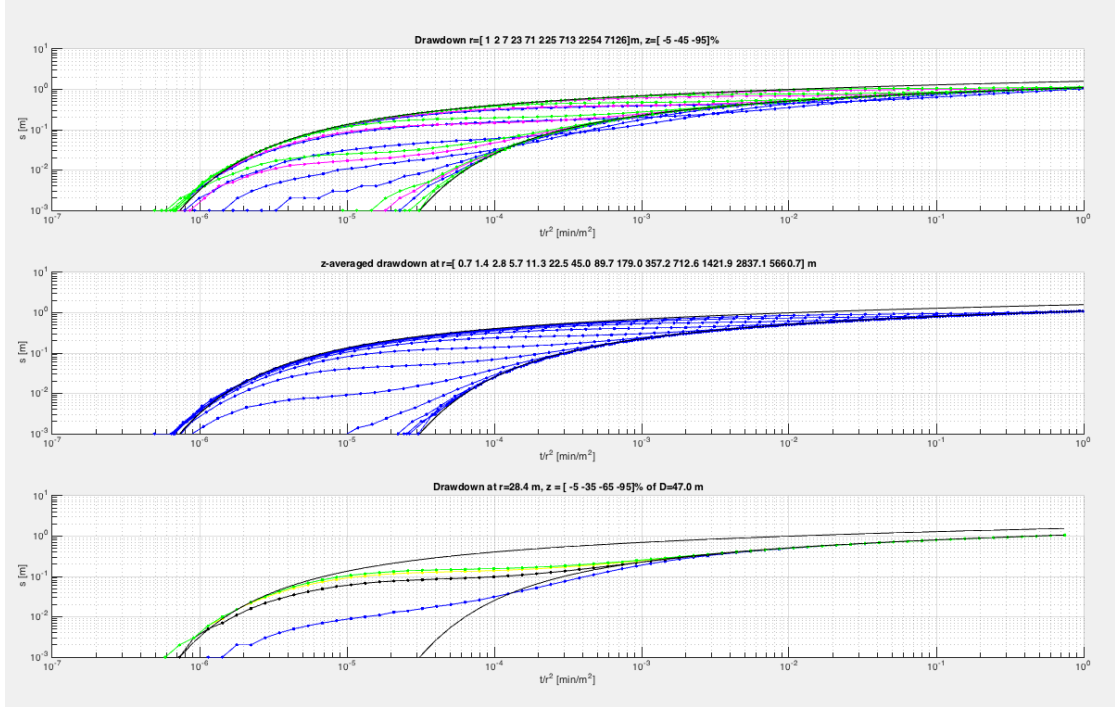


Figure 6.31: Delayed yield in a water table aquifer with a fully penetrating screen. The black lines in all three curves correspond with the Theis drawdown. The middle picture shows the elevation-averaged drawdown at different distances from the well. All lines are blue, but the closer to the water table, the later the drawdown is. The third pictures shows the drawdown at 28.4 m from the well at different depths. The colors indicate the depths, blue is shallow, then black then yellow and finally green for the deepest piezometer. The first figure shows the drawdown at a number of distances and at three different depths. Blue is shallow depth, magenta is the center of the aquifer and green near the bottom of the aquifer.

presented figure 6.32.

This figure shows the drawdown averaged over the thickness of the aquifer for different distances from the well. We expect the first branch of the graphs to resemble Hantush's semi-confined drawdown, for which the value of  $r/\lambda$  determines the elevation of their horizontal equilibrium branch. The spreading lengths of the four models are  $\lambda = [59, 187, , 591, 1870]$  m respectively. The lower the value of  $r/\lambda$ , the more the Hantush curve deviates from the Theis curve. This effect is clearly visible when the first picture is compared with the fourth. When the vertical resistance is high, the transfer to the late Theis curve is much delayed. One sees this in the fourth picture, where the graphs don't even reach the second Theis branch at the end of the simulation time, which was as large as 600 days! When the resistance is low, as in the first figure, the graphs do show a clear transfer from the elastic Theis curve to the water-table Theis curve (first picture). The picture also shows that the drawdown for points near the well resemble the elastic Theis curve, while the points at large distances do not reveal any elastic behavior; they immediately follow the specific-yield Theis curve. The reason is that the first branch should follow Hantush which has an equilibrium  $Q/(2\pi kD) K_0(r/\lambda)$ , which approaches zero for large  $r$ . Hence, points at larger  $r$ , say at  $r > 3\lambda$  will never see the elastic drawdown due to the leakage. The second branch, however, is a pure Theis curve, which has no equilibrium, because it has no recharge (all its water comes from water-table storage). Therefore, points far away from the well will eventually all feel the phreatic drawdown as predicted by Theis (if there are no head boundaries might prevent this).

To determine the resistance of the overlying layer, one should use the piezometers that reach a Hantush-equilibrium and use the Hantush solution to interpret them. This also yields the elastic storage coefficient. If the test is sufficiently long, so that one or more piezometers reach the phreatich Theis branch, then also the specific yield of the overlying layer can be determined by applying the Theis solution to the second branch. As was said earlier, the resistance of the overlying layer does not determine the position of the two bounding Theis curves; it only determines the height of the horizontal branch of the curves where they transfer from the elastic to the specify yield Theis curve.

the more

Figure 6.33 shows the drawdown at one distance, i.e.  $r = 28.4$  m, in the top of the overlying layer and in all 35 model layers of the aquifer. First of all, one sees that the head difference between the top and the bottom of the aquifer can be neglected; only the model with the low resistance shows a small difference. This is because in that case the the vertical velocities in the aquifer are large enough to cause a small head loss between the top and the bottom of the aquifer (notice that  $k_z = k_r = 10$  m/d was used). Again, one observes that the horizontal branch climbs with reduced  $r/\lambda$  between the four models. The blue line is the drawdown in the top of the overlying layer, i.e. that of the water table itself. This blue line thus reveals the emptying of the top layer due to the downward leakage invoked by the drawdown in the pumped aquifer below.

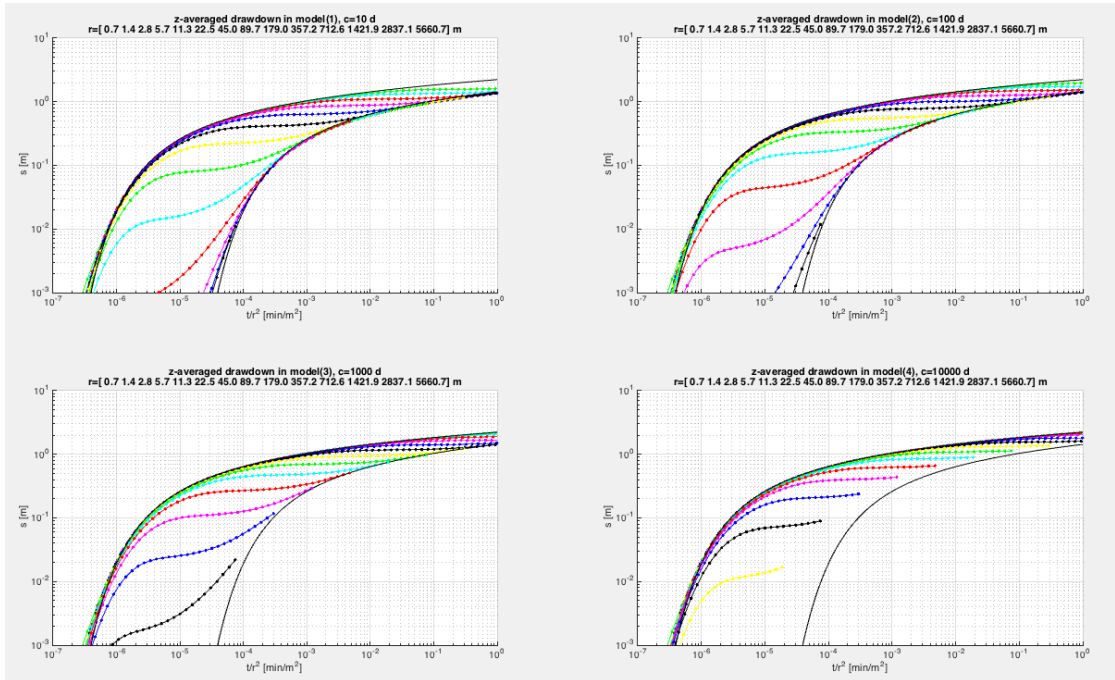


Figure 6.32: z-averaged drawdown in the aquifer at different distances. Four models differing only in the vertical resistance of the top layer. The Theis elastic storage Theis curve and the specific yield Theis curve are also shown (black lines)

#### 6.6.4 The two Theis bounding curves

It was explained before that position of the two bounding Theis curves only depend on their respective storage coefficients and not on the resistance of the covering layer. Notice that we have for the two Theis curves

$$\frac{1}{u_1} = \frac{4kD}{S} \frac{t}{r^2}, \quad \frac{1}{u_2} = \frac{4kD}{S_y} \frac{t}{r^2}$$

Hence, the horizontal axes of both Theis curves only differ in their storage coefficient. And so

$$\frac{u_2}{u_1} = \frac{S_y}{S}$$

Hence the horizontal axis of the specific-yield Theis curve is the one of the elastic-storage Theis curve multiplied by  $S_y/S$ . On the logarithmic scale this is a horizontal shift. Because we have chosen values  $S_y/S=100$ , the second Theis curve is shifted over exactly two log-cycles to the right of the first, elastic-storage Theis curve, which can be verified immediately in the graphs.

This also implies the following for the determination of the specific yield from a pumping test that shows a clear delayed-yield behavior. Simply determine the horizontal shift of the second with respect to the first Theis curve, which is factor  $\tau$ , and then apply  $S_y = \tau S$ .

Figure 6.34 shows the drawdown of the water table (blue lines), at the top of the aquifer (cyan) and at the bottom of the aquifer (magenta) for different distances from the well as noted in the title of the pictures. The figure is essentially equal to the previous picture but the graphs are now drawn for several distances. Once again, the time-drawdown curves for points inside the aquifer stay between the two bounding Theis curves. The curve for the water table lags behind and only joins the specific-yield Theis curve late. This join point falls later the higher the vertical resistance of the overlying layer and the distance from the well. The lower the resistance of the overlying layer, the more will this semi-confined aquifer system resemble the purely phreatic aquifer system that we discussed in the beginning of this chapter.

#### 6.6.5 Influence of partial penetration of the well screen

It should be clear that partial penetration causes the drawdown near the well screen to become larger than the Theis drawdown predicts. Hence, one should first correct piezometers closer than about 1D from the well for partial penetration (see section on partial penetration) before analyzing any pumping test. This is illustrated in figure 6.35. It shows the drawdown in the top (cyan) and bottom (magenta) of the aquifer for a nearby point ( $r = 9$  m, thick lines) and a distant point ( $r = 90$  m, thin lines). The figures show that at a point at a large distance from the well is not influenced by partial penetration, as the drawdown in the top and bottom of the aquifer are practically the

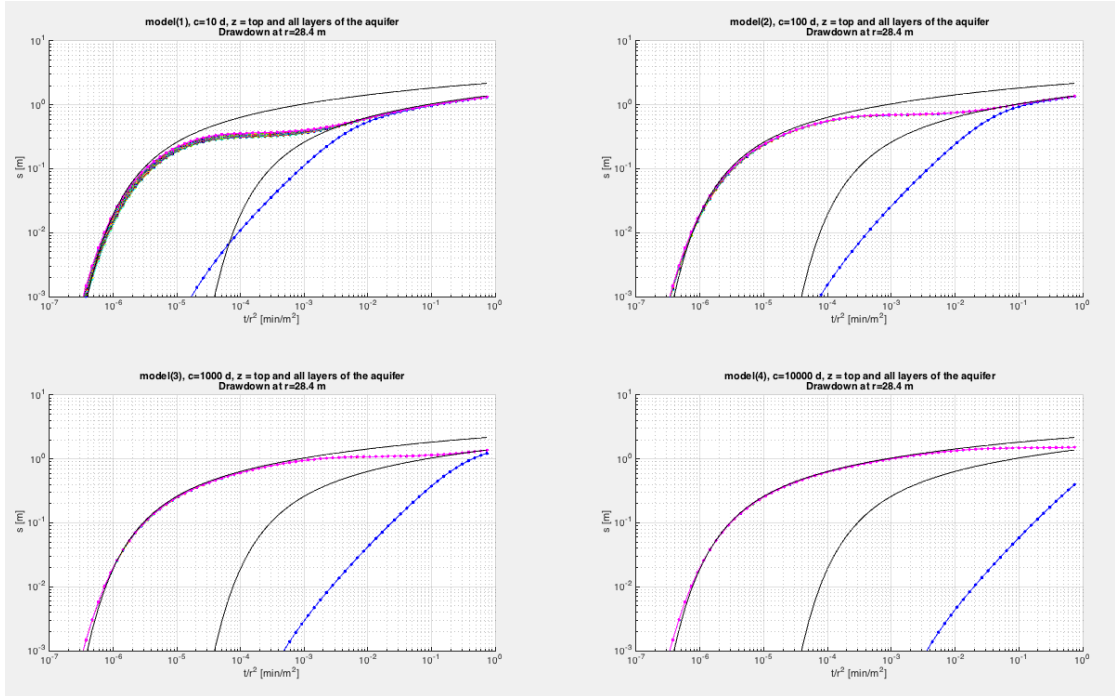


Figure 6.33: The drawdown at  $r = 28.4$  m from the well in the top of the overlying layer and in all 35 model layers of the aquifer for models differing only in the resistance of the overlying layer. The blue line is the drawdown of the water table, all 35 other lines are at different elevation in the aquifer at the same distance from the well, they essentially fall on top of each other.

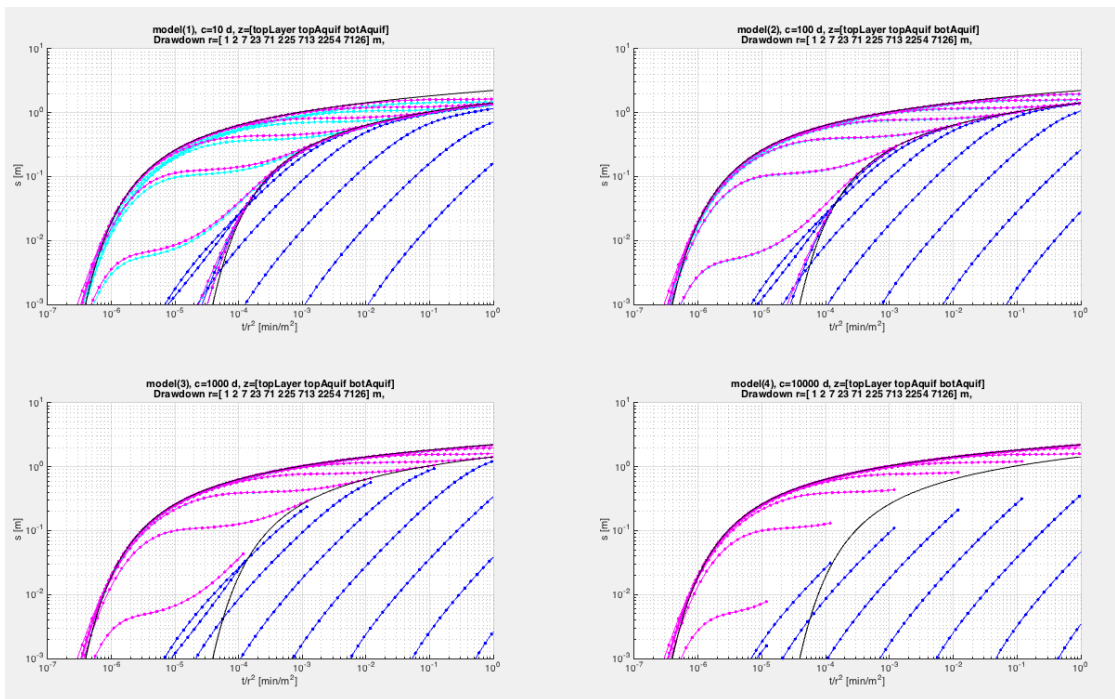


Figure 6.34: Drawdown in overlying layer (water table, blue), top of the aquifer (cyan) and bottom of the aquifer (magenta) for different distances to the well.

same and the curves stay between the Theis envelopes, which are the same as in the cases with fully penetrating screens. However, a point close to the well, i.e. less than about 1 to 1.5 aquifer thicknesses away, may experience a serious deviation caused by partial penetration. The point opposite the well screen at the top of the aquifer (thick cyan line) has a drawdown that is larger than that for a fully penetrating screen; the point at the same distance but at the bottom of the aquifer (far below the screen, thick magenta line) has a much lower drawdown than would be the case with a fully penetrating screen. Moreover, these differences do not disappear with time. On the other hand, if we correct for partial penetration by subtracting the effect from all measurements, we regain the fully penetrating drawdowns, which are then directly amenable to interpretation using the standard solutions of Theis and Hantush.

### 6.6.6 Questions

1. Explain the cause of delayed yield.
2. Is delayed yield limited to water table aquifers?
3. What are the bounding curves of the delayed yield curves.
4. How do the two bounding curves of the delayed yield relate? (What is the relation between the two?)
5. What determines the elevation of the transition curve (the more or less horizontal branch of the delayed yield curve between the two bounding curves)?

## 6.7 Large-diameter wells (not for the exam)

The solution of Theis for transient flow in an unbounded confined or unconfined aquifer is based on the assumption that the storage inside the well casing can be neglected. While this is generally a valid assumption for tube wells, and, therefore, for wells in semi-confined and confined aquifers, it may not hold in unconfined aquifers when large-diameter dug wells are used, such as the one shown in Figure 44, which is a picture of a large open well in India. Especially when the transmissivity of the aquifer is low, the storage in a large diameter well represents a large portion of the water extracted, at least on the short run, and will thus have a substantial influence on the drawdown. This influence must be taken into account when interpreting drawdown tests on such wells. It should be clear that the formula for a large-diameter well will also hold true when pumping water from a pond.

Papadopoulos and Cooper (1967) (see [Kruseman and De Ridder (1994)], p175) derived an analytical solution for the drawdown in a fully penetrating large-diameter well, taking into account the storage in the casing of the well. The partial differential equation upon which it is based is the same as the one used by Theis. However, the boundary condition at the well face differs; the extraction must now match both the inflow from the aquifer and the drawdown inside the well casing. It thus becomes

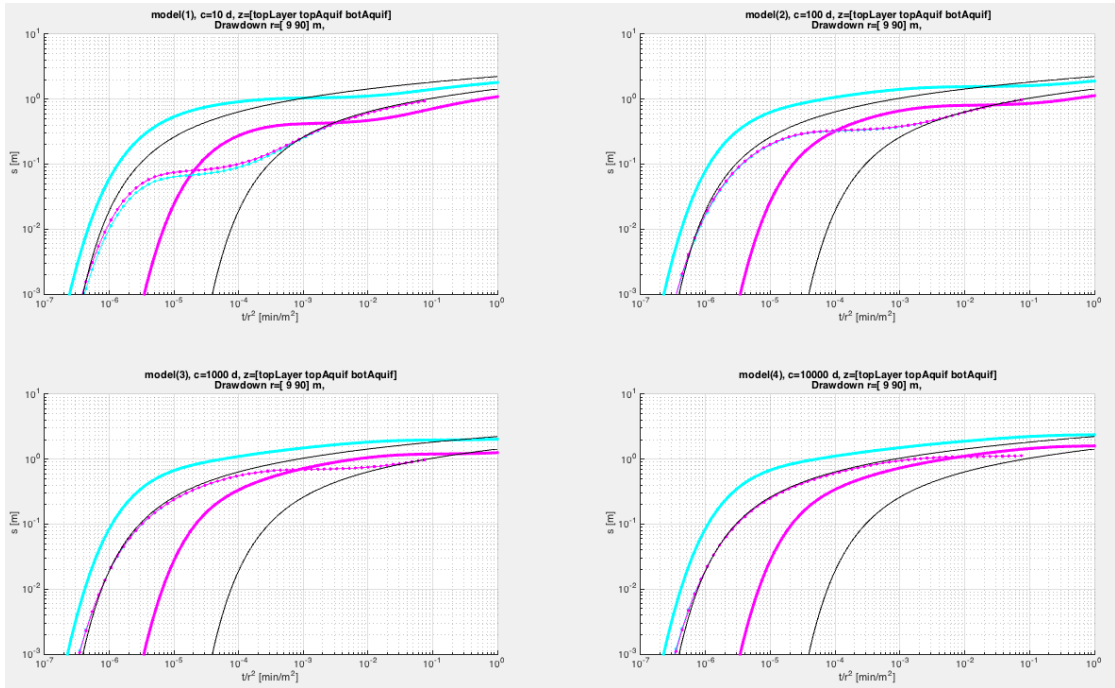


Figure 6.35: Effect of partial penetration. The screen of only 7 only perforating the top of the 35 m thick aquifer. Drawdown in top and bottom of the aquifer at 9 and 90 m from the well.

$$Q = \pi r^2 \frac{\partial h}{\partial t} - 2\pi r k h \frac{\partial h}{\partial t}, \quad \text{for } r = r_w$$

where  $Q$  is the constant extraction from the well for  $t > 0$ . Notice the difference between the well radius  $r_w$  and the radius of the well casing  $r_c$ .

The solution was derived by means of the Laplace Transform, while linearizing by taking  $kh \approx k\bar{h}$ . It reads

$$s = \frac{Q}{4\pi k D} F \left( u_w, \alpha, \frac{r}{r_w} \right)$$

with

$$F = \frac{8\alpha}{\pi} \int_0^\infty \left( 1 - e^{-\frac{\beta^2}{4u_w}} \right) \frac{J_0\left(\frac{r}{r_w}\beta\right) Y - Y_0\left(\frac{r}{r_w}\beta\right) J}{\beta^2 \{Y^2 + J^2\}} d\beta$$

and in which

$$\begin{aligned} J &= \beta J_0(\beta) - 2\alpha J_1(\beta) \\ Y &= \beta Y_0(\beta) - 2\alpha Y_1(\beta) \end{aligned}$$

$J(-)$  and  $Y(-)$  are Bessel functions and  $\alpha = r_w^2 S / r_c^2$  with  $S$  the storage coefficient (specific yield) and  $u_w = \frac{r_w^2 S}{4kht}$ .

These expressions may be implemented in Python (see listing below). Type curves for different values of  $\alpha$  but constant ratio  $r_w/r_c = 1$  are given in figure ..

### 6.1

```

1 def ldwell(rw=None, rc=None, kD=None, S=None, t=None, r=None):
2     '''Return the drawdown for a large-diameter well
3     parameters
4     -----
5     rw, rc: floats
6         well radius in aquifer, and wider upper part with
7             storage above the screen
8     kD, S: float
9         transmissivity and storage coefficient
t : ndarray

```

Figure 6.36: A large-diameter well having a well casing radius  $r_c$  different from the well-bore radius  $r_w$

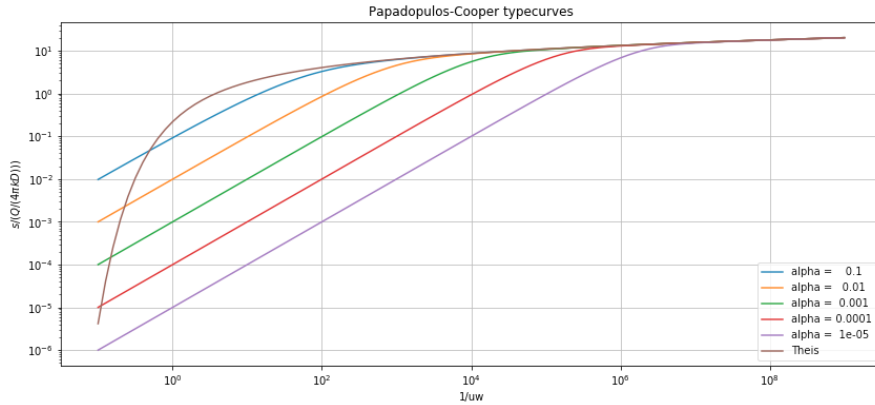


Figure 6.37: Large-diameter well typecurves of Papadopoulos-Cooper function  $F(u_w, \alpha, \frac{r}{r_w})$  for different values of  $\alpha$  versus  $1/u_w$ , for  $r = r_w$  and  $r_c = r_w$  and different values of  $\alpha = \left(\frac{r_w}{r_s}\right)^2 S$ .

```

10           time at which drawdown is desired
11   r: scalar
12       distance to well
13   , ,
14   uw = rw ** 2 * S / (4 * kD * t)
15   alpha = S * (rw / rc) ** 2
16   rrw = r / rw
17   return ppc067(uw, alpha, rrw)
18
19
20 def ppc067(uw=None, alpha=None, rrw=None):
21     '''Return function values for solution of Papadopoulos and
22     Cooper for large diameter well
23     parameters
24     _____
25     uw : float or array
26     uw = rw ** S / (4 kD t)
27     alpha: float
28     alpha = S (rw / rc) ** 2
29     rrw = r / rw
30     , ,
31     if not np.isscalar(rrw):
32         raise ValueError('rrw must be a float (scalar).')
33     if not np.isscalar(alpha):
34         raise ValueError('alpha must be a float (scalar).')
35     if np.isscalar(uw):

```

```

35     uw = np.array([uw])
36
37     uw = uw[np.newaxis, :]
38
39     beta = np.logspace(-6, 20, 2000)[:, np.newaxis]
40     J = beta * J0(beta) - 2 * alpha * J1(beta)
41     Y = beta * Y0(beta) - 2 * alpha * Y1(beta)
42     F = 8 * alpha / np.pi * (J0(beta * r / rw) * Y - Y0(beta * r
43                               / rw) * J) / (beta ** 2 * (Y ** 2 + J ** 2))
44
45     arg = (1 - np.exp(-beta ** 2 / (4 * uw))) * F
46     db = np.zeros_like(beta)
47     db[:-1, 0] += np.diff(beta[:, 0]) / 2.
48     db[1:, 0] += np.diff(beta[:, 0]) / 2.
49
return np.sum(arg * db, axis=0)

```

Figure 6.38 gives an example of the drawdown in a large diameter well and compares it with the Theis drawdown.

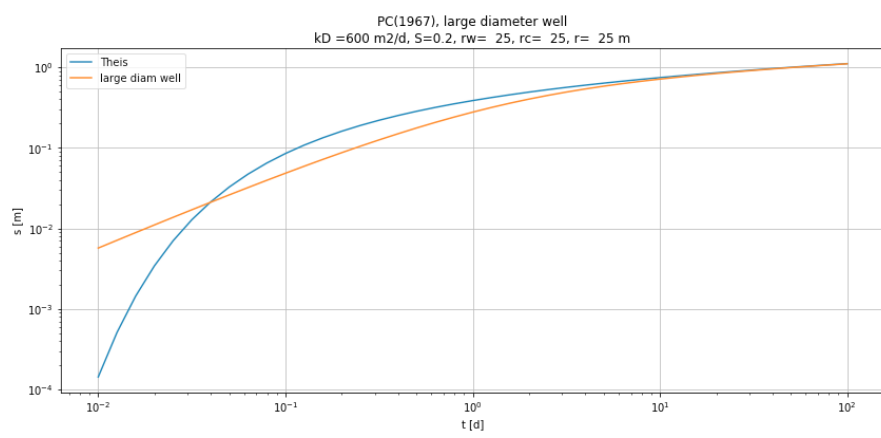


Figure 6.38: Example of drawdown in large-diameter well.  $Q = 1200 \text{ m}^3/\text{d}$ . Other parameter are in the figure title.

# 7 Convolution

## 7.1 What convolution is and how it works

Convolution is applied in many branches of science. Because it is so widely and flexibly applicable, it is important to have a thorough understanding of it.

Convolution is a general principle that can be seen as smart superposition, which allows for efficient simulation of linear systems with arbitrary time (or space) varying inputs. In dealing with groundwater it allows interpreting pumping tests with arbitrarily varying extractions. It further allows simulation of the groundwater head due to arbitrarily varying river stages as well has groundwater head fluctuations as a function of varying recharge. It is also heavily used in time-series analysis. In mathematical course books, convolution is mostly explained in connection with the Laplace transform, which has some advantages in dealing with it mathematically. However, it is not necessary to understand or apply it. So we do not need this here. In the end convolution boils down to a moving weighted average of the past input data, in which the weight are the response to a unit pulse.

The essential condition for convolution to work is that the response of the system in question due to some physical pulse is unique and proportional to the magnitude of that pulse. A short rain shower is an example of such a pulse due to which the groundwater level will respond by first rising and subsequently declining until the effect of the shower has completely disappeared. The reaction of the system in question to a pulse of unit magnitude is called the impulse response  $\text{IR}(\tau)$ . The impulse response depends only on  $\tau$ , i.e. the time  $t_0$  since the pulse took place, hence  $\tau = t - t_0$  (see figure 7.1). Notice that the dimension of the pulse (in this case 1 mm of rain for instance) may be completely different from the dimension of the reaction of the system (change of head or change of flow for instance).

We can subdivide any arbitrary time-input into a series of subsequent pulses, for instance, daily rain figures can be seen as such a continuous input as well as a series of rain pulses. But also a time-varying pumping rate or river stage, can be regarded as a series of hourly or daily pulses. If one imagines an infinite series of unit pulses glued together, say after  $t = t_0$ , then for  $t > t_0$  we have a continuous unit input (a unit input that is an input with the value equal to 1, like 1 mm/d continuous rain). The response of the system to such a continuous unit input after  $t = t_0$  is called the step response,  $\text{SR}(\tau)$ . In our example this could mean that the well starts pumping at a rate  $Q = 1$  at  $t = t_0$  and it keeps pumping with this rate forever.

Notice that most analytic solutions of groundwater flow are, in fact, step responses. For instance, the solution for the change of groundwater head or discharge due to a sudden change of the water level of the river, i.e. the expression  $s(x, t) = A \text{erfc}(u)$ ,  $u =$

$\sqrt{x^2S/(4kDt)}$  is such an example. The same is true for the Theis and the Hantush solutions, they too assume a sudden change from zero to a fixed extraction at  $t = 0$ , which remains forever constant thereafter.

Because the step response can be regarded as the response due to an infinite number of unit pulses for  $t > t_0$ , it immediately follows that

$$\begin{aligned}\text{SR}(\tau) &= \int_{t=0}^{\tau} \text{IR}(\nu) d\nu \\ \text{IR} &= \frac{\partial \text{SR}(\tau)}{\partial \tau}\end{aligned}$$

In practice, we deal with pulses that have a given duration, such as the rainfall during one day. Of course, the rain will vary during the day, but in the end we may not possess data on a shorter time scale than one day, and, therefore, the daily rainfall may be the best and most detailed data that we than obtain in a given case. We will then probably treat these figures as the average rainfall for each day as the best approximation of the time-varying precipitation. Of course, if one has hourly data, one may use these data as average values for each hour as the best approximation.

So in general, we will have a series of figures for daily (or hourly, weekly or monthly) precipitation, evapotranspiration, river stage, extraction rate etc.

We then need the so-called block response  $\text{BR}(\tau, \Delta\tau)$ . The bock response is the result of a sudden change of an input variable, for instance rain, with a unit magnitude, that is constant during a given time  $\Delta\tau$  and zero thereafter. It's the result of a unit pulse of fixed duration. The easiest way to compute the block response is by superposition

$$\text{BR}(\tau, \Delta\tau) = \text{SR}(\tau) - \text{SR}(\tau - \Delta\tau)$$

Which is what we have been doing by our superposition. For instance, with a well in an groundwater system of infinite extent, that fulfills the presumptions underlying the Theis solution, we may write

$$\text{BR}(\tau, \Delta\tau) = 0, \quad \tau \leq 0 \quad (7.1)$$

$$\text{BR}(\tau, \Delta\tau) = \frac{1}{4\pi kD} W\left(\frac{r^2 S}{4kD\tau}\right), \quad 0 < \tau \leq \Delta\tau \quad (7.2)$$

$$\text{BR}(\tau, \Delta\tau) = \frac{1}{4\pi kD} \left[ W\left(\frac{r^2 S}{4kD\tau}\right) - W\left(\frac{r^2 S}{4kD(\tau - \Delta\tau)}\right) \right], \quad \tau > \Delta\tau \quad (7.3)$$

Based on the previous superposition we can readily compute the required response of the system using the standard groundwater solutions.

Figure 7.2 shows how standard superposition would work once we have the block response as explained above. For every subsequent actual input pulse of, let's say a day,

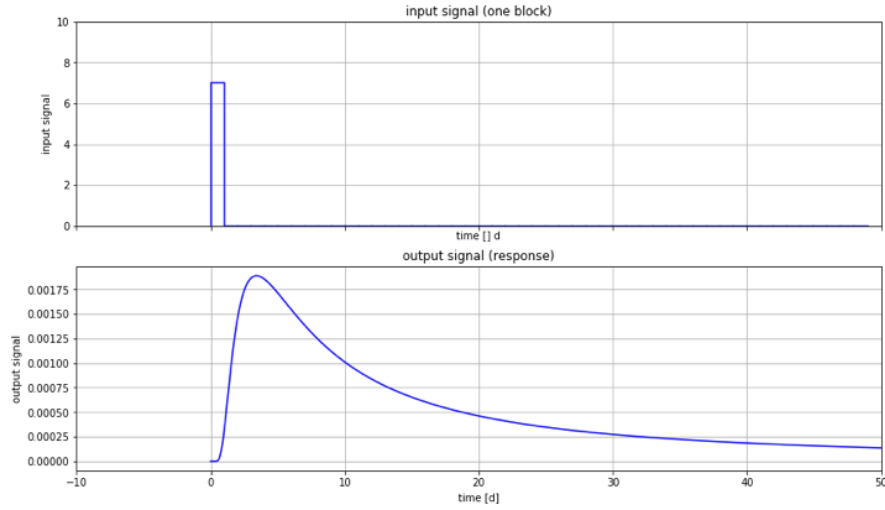


Figure 7.1: The response of a system to a pulse. Top: the pulse. Bottom: the response of the system to that pulse. Note that the dimensions of pulse and system response are generally different. For example, the discharge as a reaction to a water level change. The response of the system to a pulse holds all the information of the dynamics of the system in question.

we would have multiply the block response and with the actual magnitude of the input to obtain its true response, shown as the set of black curves in figure 7.2. Each such system reaction, i.e. each curve, would have to be shifted down the time axis time in accordance with the moment that the pulse occurred, and finally all these reaction curves have to be superimposed to obtain the combined reaction of the system at the desired time. This procedure is what we actually do with superposition and is illustrated in figure 7.2.

Convolution as a smart way of doing this superposition; it takes a different perspective, one that is illustrated in figure 7.3: the essence is that it turns the system response around. Let's see how that works.

Consider a fixed point in time  $t$ , which is a time  $\tau$  after the pulse. The top image shows this pulse, its reaction, the  $\text{IR}(\tau)$  or the  $\text{BR}(\tau, \Delta\tau)$ . It also shows the considered time  $t$ , which is indicated by the vertical line connecting the two graphs. The impact of the pulse at time  $t - \tau$  on the system at time  $t$  is the pulse or block response for  $\tau$  multiplied by the actual height of the pulse,  $p$ . Hence the result  $s$  of the pulse is

$$s = p(t - \tau) \text{ IR}(\tau) \quad (7.4)$$

as indicated in the top figure. Read this formula as the “result of the pulse at  $t$  equals the impulse response  $\text{IR}(\tau)$  multiplied by the magnitude of the pulse at time  $t - \tau$ , i.e. at  $\tau$  days ago.”

But this is identical with what we get in the bottom figure, where the impulse response is taken relative to  $t$  itself and is reversed in time. Taking this perspective, we would

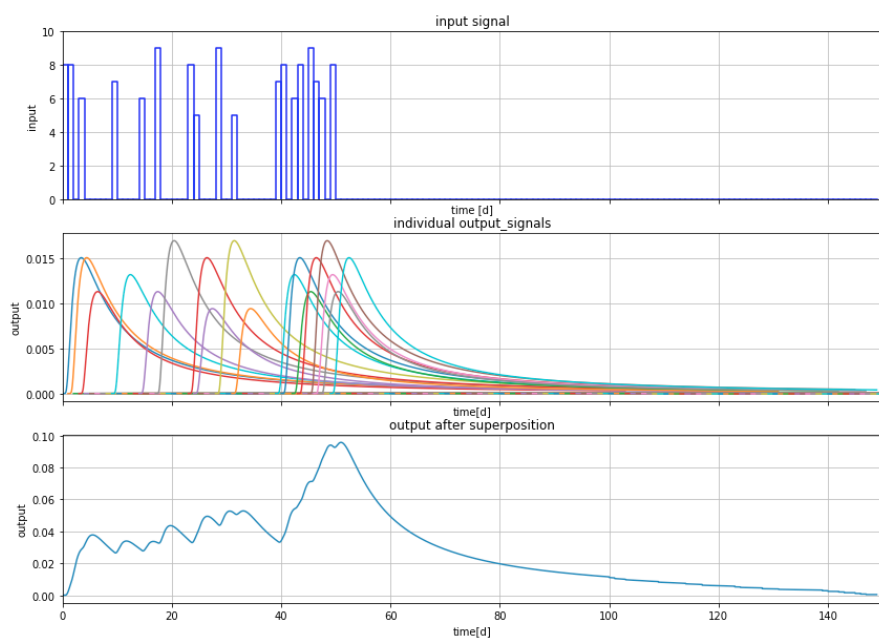


Figure 7.2: The effect of a series of pulses. Each pulse has its own system response. Top: input signal. Middle: the individual responses, each proportional to the size of its pulse. Bottom: After superposition, i.e. summing all the individual pulses. This is the final output of the system due to the input time series. This is regular superposition in time.

say: “the effect of a pulse at time  $t - \tau$  (or “a time  $\tau$  ago”) equals the reversed impulse response at  $\tau$ , i.e.  $\text{IR}(\tau)$  times the height of the pulse at  $t - \tau$ .” This is exactly the same as equation 7.4. This perspective is illustrated in the bottom picture of figure 7.3.

But this is true the effect at time  $t$  now of any pulse in the past. There is no need to shift the reversed curve at all. So with this perspective, the only thing we have to do to compute the result at time  $t$  due to all inputs of the past, i.e. for time  $-\infty < \text{time} < t$ , is to multiply each pulse happening a time  $\tau$  ago, that is at time  $t - \tau$  by the value of the impulse response at  $\tau$ . This is illustrated in figure 7.4, and the result if given in figure 7.5. If we compare this procedure with the basic superposition shown in figure 7.2, we see that, to compute the state of the system at any given point of time due to what happened in the past, requires only one reversed impulse response, which has to be multiplied with the corresponding the past input (such as rain, river stage or flow rate).

Mathematically this can be generalized as follows

$$h = \int_{\tau=0}^{\infty} \text{IR}(\tau) p(t - \tau) d\tau \quad (7.5)$$

where the input  $p$  is continuous. In the case we split up the past in discrete steps of length  $\Delta\tau$  for which we the average intensity (daily values, say), we use the block response for the corresponding step length  $\Delta\tau$ . Then we have

$$h = \sum_{i=1}^{\infty} \text{BR}(\tau, \Delta\tau) p_{t-\tau_i-\Delta\tau \rightarrow t-\tau_i} \quad (7.6)$$

where  $p_{t-\tau_i-\Delta\tau \rightarrow t-\tau_i}$  means the intensity of the input between  $t - \tau_i - \Delta\tau$  and  $t - \tau_i$  with  $\text{BR}(\tau, \Delta\tau)$  as defined in equation 7.3. This procedure is called convolution. It is continuous when we work with the impulse response or discrete in case we work with the block response, what we’ll always do in practice.

Final note: Mathematicians mostly take the integral in equation 7.5 over  $-\infty < \tau < \infty$ , which is equivalent to  $\infty < \tau < 0$ , because the  $\text{IR}(\tau)$  is zero for  $t < 0$  for physical reasons: a response can only exist after it has happened.

## 7.2 Examples

### 7.2.1 Arbitrarily fluctuating river stage

We can readily carry out a convolution in a spreadsheet or in Python. Python is more straightforward and flexible, therefore we’ll use Python. To do convolution, we need input data, like a time series of the river water level and the impulse response (instantaneous pulse of zero-length but with given magnitude equal to 1) or block response block response (a pulse of of intensity 1 during a fixed time  $\Delta\tau$ , i.e. the river level rises suddenly by 1 m and falls again by 1 m after time  $\Delta\tau$ , which will be the length of our time step).

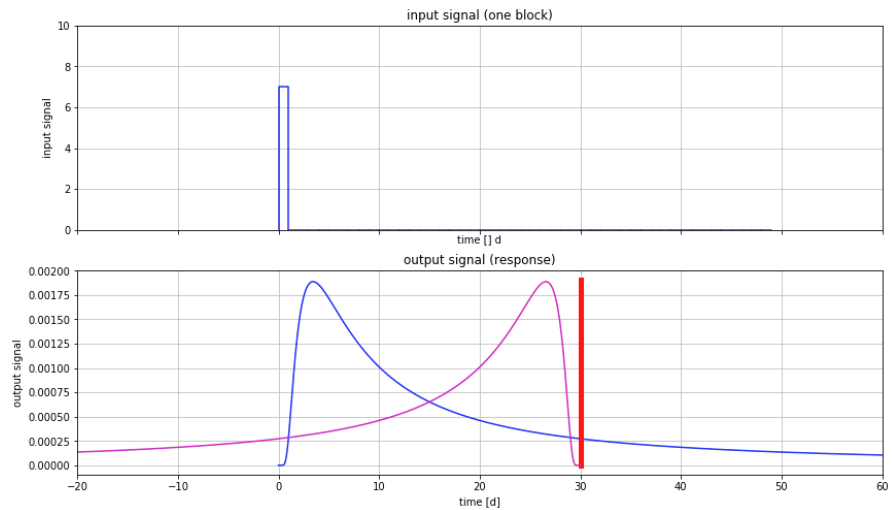


Figure 7.3: The red bar shows the response of the system 30 days after its pulse. It equals the size of the pulse times the block response. Because the value of the pulse in the top figure is 7, the length of the red bar in the bottom figure, which is the system response, therefore equals 7 times the length of height of the blue block-response. The magenta line is the block-response but inverted in time, so that it looks backward. The distance between the pulse at  $t = 0$  and the focus time  $t = 30$  is the same for both the original and the reverse block response. Thus, to get the system's response at  $t = 30$  d, just multiply the value of the block-response at the time of the pulse with that pulse.

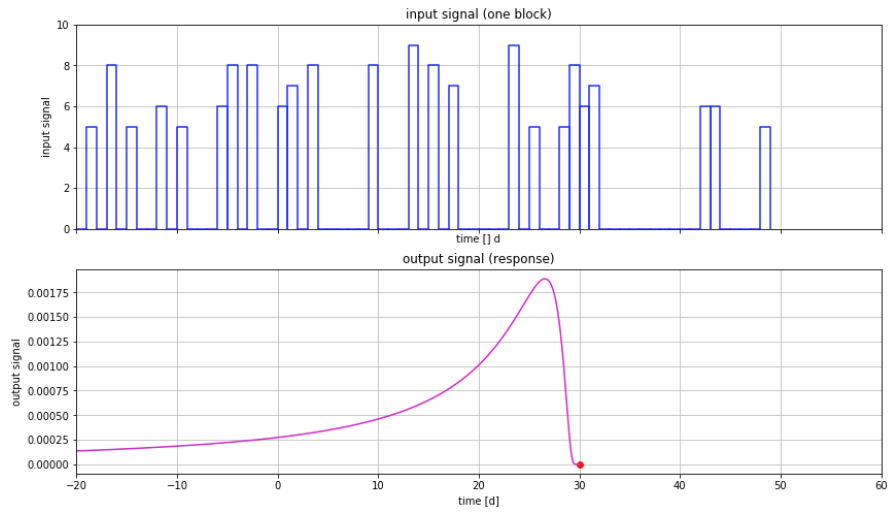


Figure 7.4: Convolution is the multiplication of the value of the block response  $BR(\tau)$ , backwards in time from the focus time (here the red dot) multiplied with each corresponding pulse in the past and summing the results to get the system's response at the focus time, and then shift the focus time, until the whole time axis has been processed. In fact, the system's response along the time axis is just a moving average of the past input where the weights is the shape of the block-response backward in time.

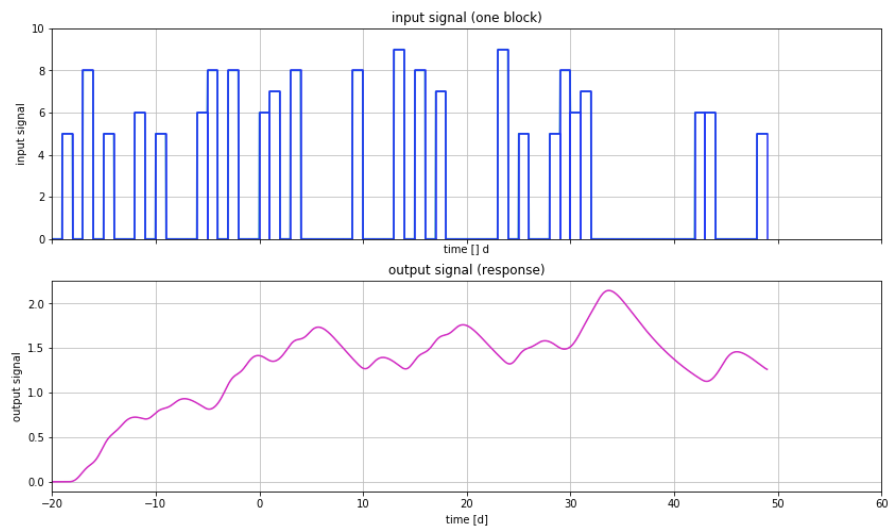


Figure 7.5: Result of the convolution.

Working with the block response is easiest to comprehend, so we'll use that. When we have both the input and the block response, we have to carry out the convolution. The convolution for one time  $t$  is the past input up to time  $t$ , weighted by the block response reversed in time, that is we multiply the input at  $t - \tau$  with the block-response value for  $\tau$ . Both the past input and the block response are entire arrays. So, the input array up to time  $t$  is multiplied by the block-response array reversed in time to get the effect of all past input at time  $t$ . This is for one point in time,  $t$ . To get the result of the convolution for all times, we have to repeat this procedure for all times. What you notice, is, that convolution is in essence a moving weighted average of the input. The input is weighted by the reversed block response and for each time.

In mathematics, convolution is a standard procedure. Many engineering problems are solved through it. Single processing engineers use it all the time to analyze signals. Also in hydrology, convolution is used to analyze time hydrological time series. Therefore, in practice we can make use of standard procedures and functions to carry out the work. In Python, the convolution can be carried out by the **scipy.signal.lfilter** function, or by the **scipy.signal.convolve** function.

The first example is to compute the groundwater head resulting from an arbitrary fluctuation of the surface-water level over time of due to an arbitrary varying extraction from a well. The block response is

$$\text{BR}(\tau, \Delta\tau) = \text{erfc}\left(\sqrt{\frac{x^2 S}{4kD\tau}}\right) - \text{erfc}\left(\sqrt{\frac{x^2 S}{4kD(\tau - \Delta\tau)}}\right) \quad (7.7)$$

Let's use the following figure:  $kD = 600 \text{ m}^2/\text{d}$ ,  $S = 0.1$  and we use river level data of the river Meuse at Eijsden on the border between Belgium and The Netherlands. The data can be downloaded from the Internet for a 28 most recent period (Search for "Rijkswaterstaat peil" and find your way). Measurements are taken every 10 minutes. Hence, we use  $\Delta\tau$  is 10 min as well. The data for 28 days thus hold 4030 measurements of the river Meuse stage. Reading the .csv file into Python is straightforward using Pandas ([McKinney (2017)]). Pandas is the worldwide most-used Python package to handle data tables, a must-know when working with lots of data and tables.

The next listing load the **Pandas** module and **dateutil.parser.parse** function to parse dates and times. Then it reads the **.csv** data file for Eijsden specifying the separation between items and which columns to read. Then the data and time columns (both contain just strings) are parsed such that we at a list of datetime objects that is converted into a new index. Finally, we drop the date and time columns we no longer need. The resulting DataFrame than has only one column 'Meting' with the measurements, in cm, which we convert to m.

```

1 # Get the Meuse water level data for station 'Eijsden'
2 from dateutil.parser import parse
3 import pandas as pd
4
5 eijs = pd.read_csv('NVT_WATHTE_EIJS.csv', sep=';', usecols=[0,
       1, 4])

```

```

6
7 # Parse the data and time column to get a datetime index
8 eijs.index = [parse(d + ' + t, dayfirst=True) for d, t in zip(
9     eijs['Datum'].values, eijs['Tijd'].values)]
10 eijs = eijs.drop(columns=['Datum', 'Tijd'])
11 eijs['Metting'] /= 100. # cm to m

```

The next 2 lines compute **dtau** and **tau**. These lines do that directly from the index, which contains only timestamps (**datetime** objects). The first line subtracts the second **datetime** from the first **datetime** to get the difference as a **timedelta** object. This is tau already, however to convert it into days as a floating point number, it has to be divided by the **datetime** object for one day. This generates the value 0.00694. Which is 10 minutes as a day, i.e.  $10/(24 * 60)$ . This seems overdone, but the point is, that this method will work for any dataset irrespective of the interval length it happens to use.

Subtracting the first **datetime** from the entire index yields a list of **timedelta** objects. Dividing this by the **timedelta** of one day, yields **tau** in days as a floating point array, with one value every 10 minutes, expressed in days.

```

1 dtau = (eijs.index[1] - eijs.index[0]) / np.timedelta64(1, 'D')
2 tau = np.asarray(eijs.index - eijs.index[0]) / np.timedelta64(1,
    'D')

```

This means that we have now our data in place, as a procedure which automates reading the data and converting them where we need. The job that rests is computing plotting the results for a set of  $x$ -values, with  $x$  the distance of an observation well from the river.

```

1 ax2.plot(eijs.index, eijs['Metting'], label='Eijsden')
2 for x in [25, 50, 100, 200]:
3     br = BRriver(tau, dtau, x, kD, S)
4     h = eijs['Metting'].mean() +
5         lfilter(br, 1., eijs['Metting'] - eijs['Metting'].mean())
6     ax2.plot(eijs.index, h, label='x={:4g} m'.format(x))
7     ax3.plot(tau, br, label='x={:4g} m'.format(x))
8 ax2.legend()
9 ax3.legend()

```

The function **BRriver** computes the block response using the following function

```

1 def BRriver(tau, dtau, x, kD, S):
2     '''Return block response for river level change
3     parameters
4     -----
5     tau: ndarray
6         time after block response
7     dtau: float

```

```

8      , , , width of block that generates the response
9
10     BR = erfc((x ** 2 * S) / (4 * kD * tau))
11     BR[1:] == BR[:-1]
12     return BR

```

The result is computed using the function `scipy.signal.lfilter` in this line (shown in the code before)

```

1 h = eijs[ 'Meting' ].mean() +
2         lfilter(br, 1., eijs[ 'Meting' ] - eijs[ 'Meting' ].mean())

```

Because we have no infinite past, we start with the mean value of the data that we have a an estimate of the most likely value to start with. Then we apply the linear filter `lfilter` (from the `scipy.signal` module) on the measurements minus the average. We could do without using the average value, but than it takes a run-in period to get rid of the start-value, which is zero by default. The length of the run-in period is equal to the length of the block response. In the current situation, this response is reasonable short, but in other situations that might not be the case, for instance with Theis wells that will never reach equilibrium. We'll handle a Theis case hereafter.

The results of this exercise are show in figure 7.6

### 7.2.2 Impulse response, block response, and step response comparison

Let us now illustrate the difference between impulse response and block response, also for the river stage.

The block response of the river stage is given in equation 7.7, while the step response is the known solution itself:

$$SR(\tau) = \operatorname{erfc} \left( \sqrt{\frac{x^2 S}{4kD\tau}} \right)$$

The impulse response is obtained by differentiation of the step response with respect to time.



Figure 7.6: Convolution of river stage. Bottom: the block responses for different distances from the river. Top: The river stage at Eijsden and the resulting fluctuations of the groundwater at different distances from the river.  $kD = 600 \text{ m}^2/\text{s}$  and  $S = 0.2$ . The data and simulations are at 10 min interval. Data from Rijkswaterstaat site, The Netherlands.

$$\text{IR}(\tau) = \frac{\partial}{\partial \tau} \left\{ \text{erfc} \left( \sqrt{\frac{x^2 S}{4kD\tau}} \right) \right\} \quad (7.8)$$

$$= \frac{\partial}{\partial \tau} \left( \int_u^\infty \frac{2}{\sqrt{\pi}} e^{-\nu^2} d\nu \right), \quad u = \sqrt{\frac{x^2 S}{4kD\tau}} \quad (7.9)$$

$$= -\frac{2}{\sqrt{\pi}} e^{-u^2} \frac{\partial u}{\partial \tau} \quad (7.10)$$

$$= -\frac{2}{\sqrt{\pi}} e^{-u^2} \left( -\frac{1}{2\tau\sqrt{\tau}} \sqrt{\frac{x^2 S}{4kD}} \right) \quad (7.11)$$

$$= \frac{\sqrt{\frac{x^2 S}{4kD\tau}}}{\tau\sqrt{\pi}} e^{-u^2} \quad (7.12)$$

$$= \frac{u}{\tau\sqrt{\pi}} e^{-u^2}$$

Note that time is embedded in  $u$ . For small step widths  $\Delta\tau$ , the values of the block response almost equal those of the impulse response when multiplied by  $\Delta\tau$ ,

$$\text{BR}(\tau, \Delta\tau) \approx \text{IR}(\tau) \Delta\tau$$

This should be obvious because the content of the block response is its intensity, which is equal to 1 spread over the duration of the block, which is  $\Delta\tau$ , while the impulse response is a pulse of zero duration but of total contents equal to 1. Hence, the numerical value of the block response is  $\Delta\tau$ , which is also the value of the impulse response multiplied by  $\Delta\tau$ . This is also obvious mathematically,

$$\text{BR}(\tau, \Delta\tau) = \text{erfc}(.., \tau) - \text{erfc}(..., \tau - \Delta\tau) \approx \frac{\partial \text{erfc}(..., \tau)}{\partial \tau} \times \Delta\tau$$

For values of  $\tau \gg \Delta\tau$  the difference disappears. This is illustrated in figure 7.7. The two responses are virtually identical except for smaller  $\tau$  and especially for  $\tau < \Delta\tau$ , but this does not affect practical use of either. In practice, I prefer to always use the block response as it is exact and always obtainable from the given step response by a simple subtraction.

### 7.2.3 Arbitrarily fluctuating extraction of multiple Theis wells

Convolution is also suitable to compute the results of a varying extraction of wells. The same procedure as before can be applied using the Theis (or Hantush) well function.

The block response of the well is

$$\text{BR}(\tau, \Delta\tau) = \frac{1}{4\pi kD} \left[ W \left( \frac{r^2 S}{4kD\tau} \right) - W \left( \frac{r^2 S}{4kD(\tau - \Delta\tau)} \right) \right]$$

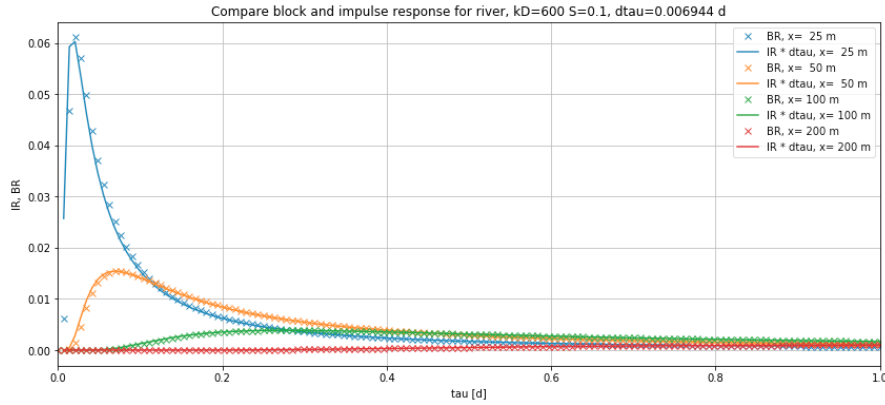


Figure 7.7: Block response,  $\text{BR}(\tau, \Delta\tau)$ , Impulse Response  $\text{IR}(\tau) \times \Delta\tau$  for the situation in figure 7.6. One sees that  $\text{IR}(\tau) \times \Delta\tau$  rapidly approaches  $\text{BR}(\tau, \Delta\tau)$  for increasing values of  $\tau$

with  $W(-)$  the Theis well function (or `scipy.special.exp1(-)`), and the notion that the second term only comes in when  $\tau > \Delta\tau$ .

```

1 def BRtheis(tau, dtau, r, kD, S):
2     u = r ** 2 * S / (4 * kD * tau)
3     BR = exp1(u)
4     BR[1:] -= BR[:-1]
5     return BR

```

For this example the signal can just as well be generated. For this first get a time array. In this case we take days starting in the past, 350 days ago or 350 days before a given date. Then generate an array of random values between 0 and 1. The length of the array is the same as that of the array of times. Subtract 0.5 to get values between -0.5 and 0.5. Filter using a moving average of length 25, to smooth the data somewhat. Finally multiply by  $Q_0$  to get a time-varying extraction that covers the entire simulation period.

```

1 Q0 = 1200 # m^3/d
2 t = np.arange(-350, 0, 1.) # past time in days
3 Qt = Q0 * (1 + lfilter(np.ones(25)/25., 1., np.random.rand(len(t)) - 0.5))

```

The generate extraction is shown in figure 7.8, top image.

Next the block responses for the well, one for each distance  $r$ , have to be computed. The function is given above. The  $\tau$  and  $d\tau$  are readily compute from the time series

```

1 dtau = np.diff(t)[0]
2 tau = np.arange(0, n * dtau, dtau)

```

The results for the block-responses are show in the second image of figure 7.8.

Then the drawdown for the well can be computed for each of the desired distances  $r$ . This is done using the block response and the **lfilter** function. It can be computed and immediately plotted

```
1     ax2.plot(t, lfilter(br, 1., Qt), label='r = {:4g} m'.format(
    ri))
```

The results are shown in the third image of figure 7.8. To illustrate its correctness, also the theis drawdown was plotted for the average extraction, i.e.  $Q_0$ .

A similar plot can be made by plotting the drawdown on logarithmic time axis. However, for that we need to prevent negative times on the time axis, and so we must use the time  $t - t_0$ , with  $t_0$  the time that the well started, which is assumed at the first value of the time series.

```
1     ax3.plot(t - t[0], lfilter(br, 1., Qt), label='r = {:4g} m'.
    format(ri))
```

The results are shown in the bottom image of figure 7.8. Here too, the results of the Theis drawdown or the average extraction are shown on this figure.

#### 7.2.4 Convolution using recharge as input time series to simulate varying groundwater levels

The solution for drainage after a sudden uniform recharge on a strip of land between two canals with maintained water level was given in chapter 5.6 equation 5.16 on page 80. That solution can be seen as an impulse response by itself. When regarding the sudden rise  $A$  as due to a (recharge) shower  $p$ , then  $A = \frac{p}{S}$  and we can write that formula, taking  $p = 1$  as

$$\text{IR}(\tau) = \frac{1}{S} \frac{4}{\pi} \sum_{j=1}^{\infty} \left\{ \frac{(-1)^{j-1}}{2j-1} \cos \left[ (2j-1) \left( \frac{\pi}{2} \right) \frac{x}{b} \right] \exp \left[ -(2j-1)^2 \left( \frac{\pi}{2} \right)^2 \frac{kD}{b^2 S} t \right] \right\}$$

The block response can then be approached by

$$\text{BR}(\tau, d\tau) \approx \Delta\tau \text{IR}(\tau)$$

This block response can be coded as follows

```
1 def IRbasin(tau, x=None, b=None, kD=None, S=None):
2     T = b ** 2 * S / kD
3     s = np.zeros_like(tau)
4     for j in range(1, 20):
5         j2p = (2 * j - 1) * (np.pi / 2)
6         s += (-1) ** (j - 1) / (2 * j - 1) * np.cos(j2p * x / b)
7         * np.exp(-j2p ** 2 * tau / T)
7     return s * 4 / (np.pi * S)
```

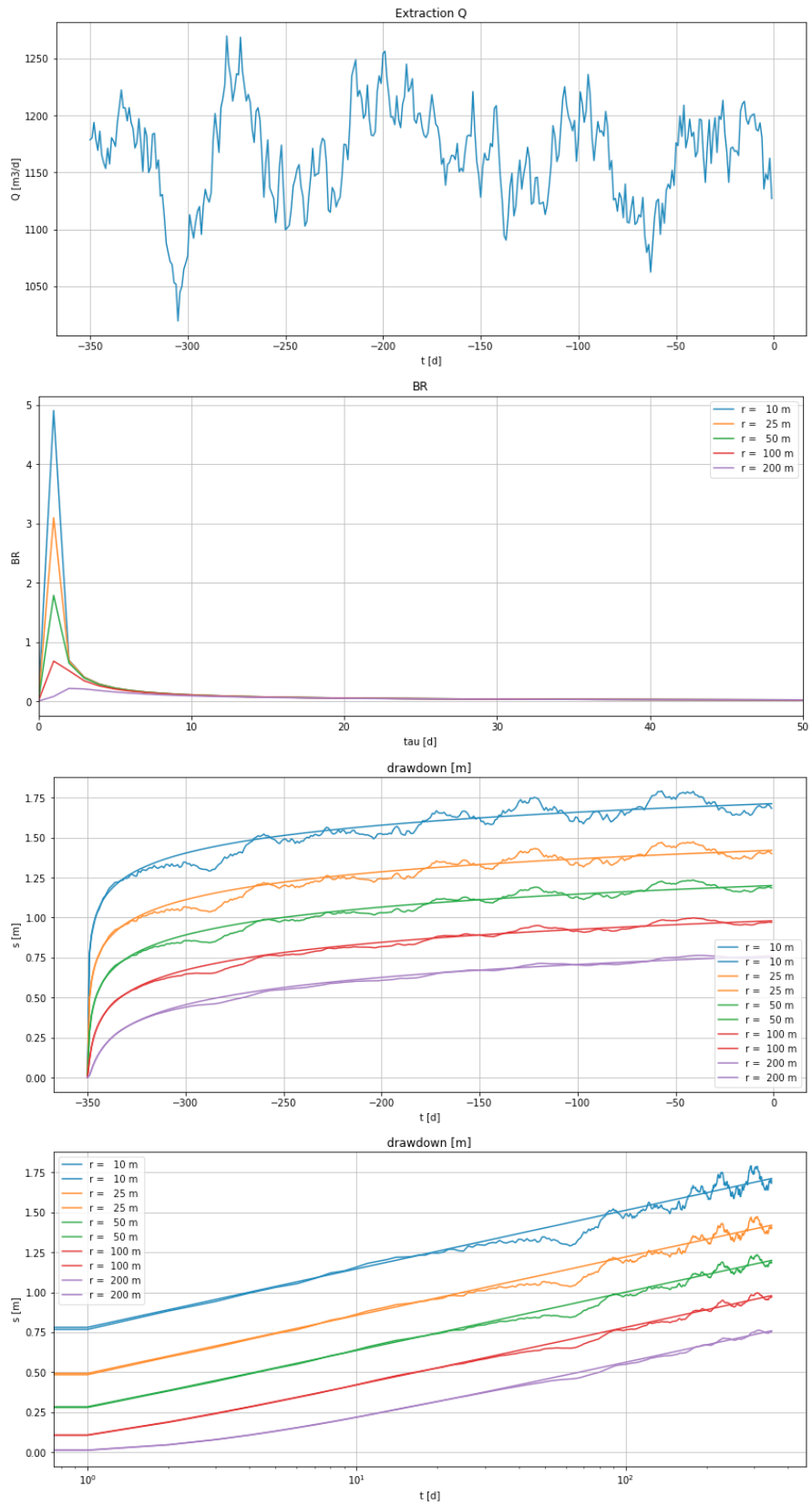


Figure 7.8: Results of the explained example. Five wells, their discharge (left picture) their drawdown (right picture) and the total drawdown (black line in right-hand picture).

To give an example the following aquifer and width values are used

```

1 kD = 600 # m2/d
2 S = 0.2
3 b = 200 # m we'll also use values 750 and 2000 m
4 x = b * np.array([0, 0.5, 0.8, 0.9, 0.95, 0.98, 0.99])
5 T = b ** 2 * S / kD # [d] characteristic time

```

The recharge data are read from the file '**PT-00-08.txt**' using Pandas. We use the index to get the step size  $d\tau$  as the time difference between the first to **datestamps** of the index of the data PE. To take tau sufficiently long we'll use 7 times the characteristic time. The value of this time, T, is shown in the title of the pictures in figure 7.9.

```

1 PE = pd.read_csv('PE-00-08.txt', index_col=0, parse_dates=True,
                   dayfirst=True)
2 PE /= 1000. # convert all to mm/d
3
4 dtau = (PE.index[1] - PE.index[0]) / np.timedelta64(1, 'D')
5 tau = np.arange(0, 7 * T, dtau)

```

The convolution to compute the head is done using **lfilter(-)** as before, where the recharge is the difference of the column 'P' and column 'E' in the Pandas DataFrame PE.

```
1 lfilter(BR, 1, PE['P'] - PE['E'])
```

Implemented in a loop, so that is the head can be computed for number of  $x$ -values. Note that  $x$  is the distance to the center of the basins. The  $x$ -values use are computes as a fraction of the half-width  $b$ .

```
1 x = b * np.array([0, 0.5, 0.8, 0.9, 0.95, 0.98, 0.99])
```

Then the loop that computes the head and plots the head for each  $x$  on a single figure.

```

1 title= '2b = {:4g} m, kD = {:4g} m2/d, S = {:4g}, T = {:.0f} d'
      .format(2 * b, kD, S, T)
2 ax0 = newfig(title='Simulation groundwater in basin\n' + title,
              xlabel='time', ylabel='head')
3 ax1 = newfig(title='Recharge', xlabel='time', ylabel='mm')
4
5 for xi in x:
6     BR = dtau * IRbasin(tau, x=xi, b=b, kD=kD, S=S)
7     ax0.plot(PE.index, lfilter(BR, 1, PE['P'] - PE['E']), label=
               'x = {}'.format(xi))
8     ax1.plot(PE.index, PE['P'] - PE['E'])
9 ax0.legend()

```

Figure 7.9 gives the results for 3 widths of basin (the width is  $2b$ ). It is very clear that the wider the basin, the larger the memory of the system, which is characterized by the characteristic time. This time increase from  $T = 13$  d for  $2b = 400$  m in the

top image to  $T = 1300$  d for  $2b = 4000$  m in the third picture. The factor 100 is due to the fact that the characteristic time is proportional to the square of the basin width. The block responses for the three basins that differ only in width are given in figure 7.10. The larger the memory of the groundwater system, the longer the past period over which the recharge is integrated and has an effect on the head. Because the average recharge in this example (Dutch data) is positive, a large system must show heads that are always above its boundaries (zero). This is indeed the case in the third picture, and more so for points farther away from the boundaries, i.e. more to the center line of the basin. The shorter the system memory, the more often a dry period can cause the heads to fall below the water levels of bounding canals or rivers. Also, the shorter the memory the lower will the average head be relative to the bounding surface water level. This simulation is realistic, except for the fact that it was assumed that the water from a recharge pulse reaches the groundwater immediately. While this may be a good approximation for shallow groundwater, it is not realistic where the water table is 10 m or more below ground surface. In such situations, it may take several months before a recharge pulse causes the flow from the unsaturated zone into the saturated zone to increase. A thick unsaturated zone causes the recharge arrival in the saturated zone to be delayed and somewhat smoothed. If this delay and smoothing can be estimated from an unsaturated zone analyses of measurements, it may be included by filtering the recharge time series before using it as input for the head simulation. Filtering is just a moving averaging procedure, hence a convolution, which can be carried out with the same function `lfilter(-)`, all we need is a block response that relates the recharge to the flux at the bottom of the unsaturated zone.

### 7.3 Questions

1. Explain what convolution is and how it compares with superposition.
2. Explain impulse response, block response and step response.
3. Why did we reverse the direction of the time series in the implementation of convolution in the spreadsheet.
4. What is the consequence of the lack of past data on the results of convolution, especially on those of the oldest times, for which there are no past data available?
5. In terms of system responses, what, in fact, are the solutions of groundwater flow like those for a sudden change of river stage and the Theis and Hantush well functions?
6. Explain in your own words the meaning of equation 7.5?
7. How does the impulse response relate to the step response mathematically?
8. How can you compute the block response  $\text{BR}(\tau, \Delta\tau)$  of a system?

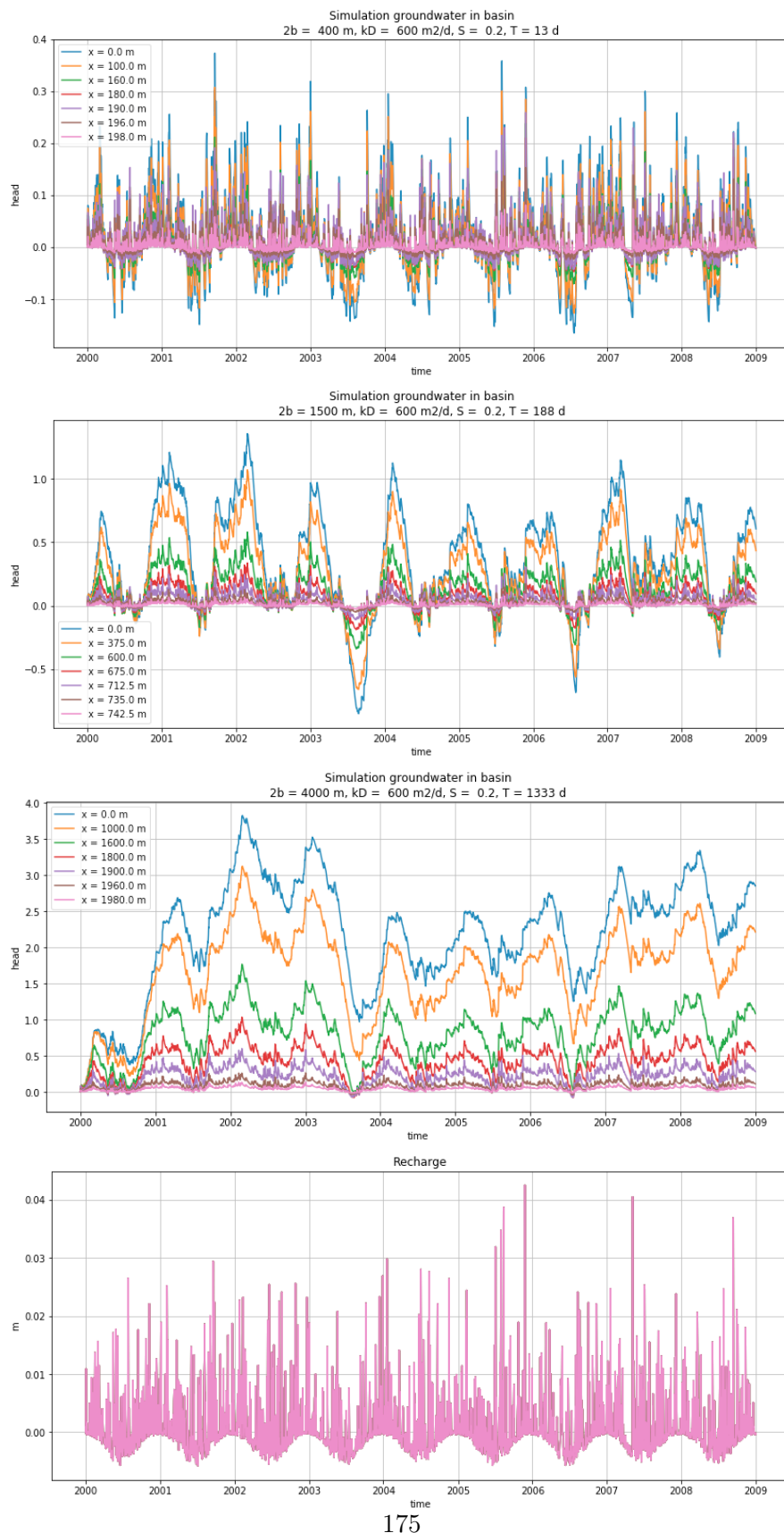


Figure 7.9: Simulation by convolution of head in river basin driven by varying recharge.

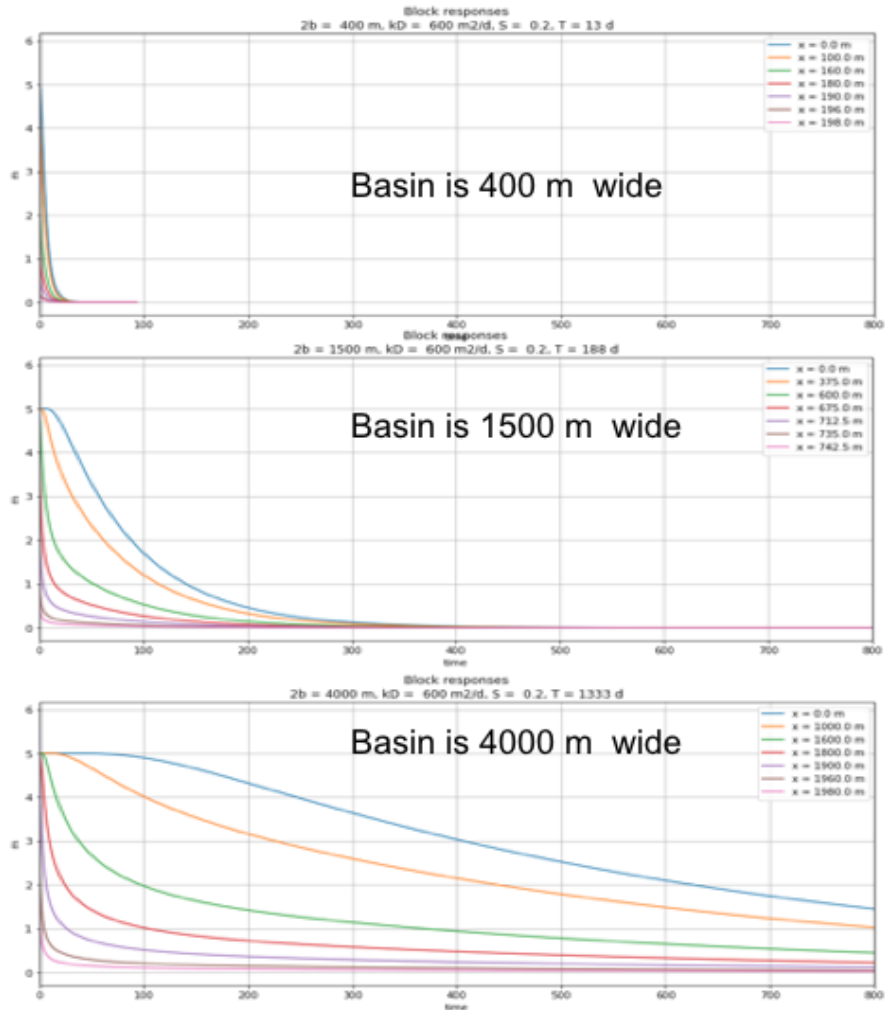


Figure 7.10: Block responses ( $d\tau = 1$  d) of the head after a 1d long recharge pulse for the 3 basins in figure 7.9 that only differ in width. The different curves for each basins represent distance from the center of the basin. The positions relative to the width of each basin are the same in the three figures, namely 0%, 50%, 80%, 90%, 95%, 98% and 0.99% of the half width of the basin measured from the center.

# 8 Laplace solutions (illustration, not for exam)

## 8.1 Sudden head rise at the boundary of a one-dimensional semi-infinite aquifer

The Laplace transform is used to solve the one-dimensional partial differential equation, known as the diffusion equation. The Laplace transform removes time from the partial differential equation after which we only have to solve a steady state situation, whose solution we already know. Once we have this solution in Laplace space we convert it back to time by looking up the result in a Laplace transform table ([[Abramowitz and Stegun \(1964\)](#)]).

We consider a one-dimensional aquifer with constant transmissivity  $kD$  with initial head zero at a boundary a river at  $x = 0$  whose water level is suddenly increased at  $t = 0$ .

The differential equation is

$$\frac{kD}{S} \frac{\partial^2 \phi}{\partial x^2} = \frac{\partial \phi}{\partial t}$$

with as boundary conditions:

$$\begin{aligned}\phi(0, r) &= 0 \\ \phi(t, 0) &= h\end{aligned}$$

Taking the Laplace transform of the differential equation and its boundary conditions yields:

$$\begin{aligned}\frac{kD}{S} \frac{\partial^2 \bar{\phi}}{\partial x^2} - s\bar{\phi} &= 0 \\ \bar{\phi}(s, 0) &= \frac{h}{s}\end{aligned}$$

The solution in Laplace space is easily found as it is the same as the stationary solution for a 1-D leaky aquifer with fixed head at  $x = 0$ :

$$\bar{\phi} = \frac{h}{s} e^{-x/\lambda}$$

The steady state solution was for the differential equation

$$\begin{aligned}\frac{\partial^2 \phi}{\partial x^2} - \frac{\phi}{\lambda^2} &= 0 \\ \phi(0) &= h\end{aligned}$$

$$\phi = h e^{-\frac{x}{\lambda}}$$

From which it follows that

$$\lambda = \sqrt{\frac{kD}{sS}}$$

So that

$$\bar{\phi} = \frac{h}{s} e^{-x\sqrt{\frac{s}{kD}}\sqrt{s}}$$

The inverse transform is given by Abramowitz and Stegun (1964, p1026, item 29.3.83):

$$F(s) = \frac{1}{s} e^{-\kappa\sqrt{s}} \rightarrow f(t) = \operatorname{erfc}\left(\frac{\kappa}{2\sqrt{t}}\right)$$

Hence, with  $\kappa$  replaced by  $\frac{x^2 S}{kD}$  we find

$$\phi = h \operatorname{erfc}\left(\sqrt{\frac{x^2 S}{4kDt}}\right)$$

Which is the sought solution.

## 8.2 Laplace solution for the Theis well function

The Laplace transform is one method, perhaps the most practical and universal to solve partial differential equation that depend on time. The Laplace transform removes the time derivative from the partial differential equation ([Bruggeman (1999)]), after which is can be solved as a steady-state problem. Once we have the steady-state solution in Laplace space, we have to transfer it back to time, which is done with conversion tables ([Abramowitz and Stegun (1964)]). [Bruggeman (1999)] gives a full derivation for the leaky aquifer case of Hantush. Here we apply the Laplace transform on the transient well extraction studied by Theis. You may also want to look at a paper on this, [Loáiciga (200)], showing various approaches.

The partial differential equation for transient flow in an aquifer with constant transmissivity is

$$\frac{\partial^2 \phi}{\partial r^2} + \frac{1}{r} \frac{\partial \phi}{\partial r} = \frac{S}{kD} \frac{\partial \phi}{\partial t} \quad (8.1)$$

$$\frac{Q_0}{2\pi kD} = \lim_{r \rightarrow 0} r \frac{\partial \phi}{\partial r} \quad (8.2)$$

$$\phi(0, r) = 0 \quad (8.3)$$

$$\phi(t, \infty) = 0 \quad (8.4)$$

Denoting the Laplace transform of  $\bar{\phi} = L\{\phi\}$  and the inverse transformation by  $\phi = L^{-1}\{\bar{\phi}\}$ , the Laplace transform of 8.1 through 8.4, becomes, with  $p$  as the Laplace constant:

$$\frac{\partial^2 \bar{\phi}}{\partial r^2} + \frac{1}{r} \frac{\partial \bar{\phi}}{\partial r} - \frac{S}{kD} p \bar{\phi} = 0 \quad (8.5)$$

Its general solution we already know from steady state groundwater flow:

$$\bar{\phi} = AK_0\left(r\sqrt{\frac{Sp}{kD}}\right) + BI_0\left(r\sqrt{\frac{Sp}{kD}}\right) \quad (8.6)$$

It is clear that  $B$  must be zero to meet the condition for  $r \rightarrow \infty$ , because  $I_0(\infty) = \infty$ .

The flow at  $Q_r$  distance  $r$  becomes in Laplace, where  $Q_r/(2\pi kD)$  is a time-invariant, becomes

$$\frac{Q_r}{p} = 2\pi kDr \frac{\partial \bar{\phi}}{\partial r} \quad (8.7)$$

$$Q_r = 2\pi kDprA\sqrt{\frac{Sp}{kD}}K_1\left(r\sqrt{\frac{Sp}{kD}}\right) \quad (8.8)$$

so that, after substituting  $B = 0$  and  $A$  from the previous expression (8.8) into equation 8.6 yields

$$\bar{\phi} = \frac{Q_r}{2\pi kDp} \frac{K_0\left(r\sqrt{\frac{Sp}{kD}}\right)}{r\sqrt{\frac{Sp}{kD}}K_1\left(r\sqrt{\frac{Sp}{kD}}\right)} \quad (8.9)$$

Because  $raK_1(ra) = 1$  for  $r > 0$  and  $a$  a positive constant, we have, writing  $Q_r \rightarrow Q_0$

$$\bar{\phi} = \frac{Q_0}{2\pi kDp} K_0\left(r\sqrt{\frac{pS}{kD}}\right) \quad (8.10)$$

$$\bar{\phi} = \frac{Q_0}{2\pi kD} \int_0^\tau f(p) d\tau \quad (8.11)$$

because

$$L^{-1} \left\{ \frac{1}{p} f(p) \right\} = \int_0^t F(\tau) d\tau \quad (8.12)$$

with, in our case,

$$f(p) = K_0 \left( r \sqrt{\frac{pS}{kD}} \right) \quad (8.13)$$

and from the tables of the Laplace transforms (Abramowitz and Stegun, 1964, p1028)

$$L^{-1} \{ K_0(\kappa\sqrt{p}) \} = \frac{1}{2t} \exp \left( -\frac{k^2}{4t} \right) \quad (8.14)$$

we find

$$\phi = \frac{Q_0}{4\pi kD} \int_0^t \frac{1}{\tau} \exp \left( -\frac{r^2 S}{4kD\tau} \right) d\tau \quad (8.15)$$

$$= \frac{Q_0}{4\pi kD} \int_{\tau=0}^{\tau=t} \frac{r^2 S}{4kD\tau} \exp \left( -\frac{r^2 S}{4kD\tau} \right) d \left( \frac{4kD\tau}{r^2 S} \right) \quad (8.16)$$

Replace

$$\frac{1}{y} = \frac{4kD\tau}{r^2 s}$$

$$\begin{aligned}
\phi &= \frac{Q_0}{4\pi kD} \int_{\tau=0}^{\tau=t} y e^{-y} d\left(\frac{1}{y}\right) \\
&= \frac{Q_0}{4\pi kD} \int_{\tau=0}^{\tau=t} -y e^{-y} \frac{1}{y^2} dy \\
&= \frac{Q_0}{4\pi kD} \int_{\tau=t}^{\tau=0} \frac{e^{-y}}{y} dy \\
&= \frac{Q_0}{4\pi kD} \int_{y=\frac{r^2 S}{4kDt}}^{y=\infty} \frac{e^{-y}}{y} dy \\
&= \frac{Q_0}{4\pi kD} \int_{y=u}^{y=\infty} \frac{e^{-y}}{y} dy \\
&= \frac{Q_0}{4\pi kD} E_1(u) \tag{8.17}
\end{aligned}$$

$$\phi = \frac{Q_0}{4\pi kD} W(u), \quad u = \frac{r^2 S}{4kDt} \tag{8.18}$$

Where  $E_1(-)$  is the exponential integral, a standard function in Matlab and tabled in many groundwater hydrology books as the Theis well function  $W(u)$ . It can be developed in a series expansion as well (Abramowitz and Stegun (1964, p228-229)):

$$\begin{aligned}
E_1(z) &= \int_u^{\infty} \frac{e^{-y}}{y} dy \\
&= -\gamma - \ln u - \sum_{n=1}^{\infty} \frac{(-1)^n u^n}{n n!} \\
&= -\gamma - \ln u + u - \frac{u^2}{2 \times 2!} + \frac{u^3}{3 \times 3!} - \frac{u^4}{4 \times 4!} + \dots
\end{aligned}$$

$$\gamma = 0.5772156649$$

# Bibliography

- [Abramowitz and Stegun (1964)] Abramowitz M. and I.A. Stegun (Eds) (1964) Handbook of mathematical functions with formulas, graphs and mathematical tables. Dover Publications Inc. New York. ISBN 0-486-61272-4
- [Bloemen et al. (1989)] Bloemen, P.J.T.M., Lekkerkerker, C. and Molen, W.H.v.d., 1989. Aardgetijden in grondwater: een voorbeeld uit Burkina Faso (earth tides in groundwater, an example from Burkina Faso). H2O, 22(17): 536-538.
- [Boulton (1963, 1964)] Boulton, N.S. (1963, 1964) Analysis of data from non-equilibrium pumping tests allowing for delayed yield from storage. Proc. Inst. Civ. Eng. 26 (November 1963): 469-482. Discussion, 28 (August 1964): 603-610
- [Bredehoeft (1967)] Bredehoeft, J.D., 1967. Response of Well-Aquifer systems to Earth Tides. Journal of Geophysical Research, 72(12): 3075-3087.
- [Bruggeman (1999)] Bruggeman, G.A. (1999) Analytical solutions of geohydrological problems. Elsevier, Amsterdam etc. 959p ISBN 0-444-81829-4. 999pp.
- [Carslaw and Jaeger (1959)] Carslaw HS and Jaeger JC (1959) Conduction of heat in soils. Oxford Science Publications. Clarendon Press, Oxford, ISBN 0-19-853368-3. 510pp.
- [DuFour (2000)] Dufour, F.C. (2000) Groundwater in the Netherlands, Facts and Figures. Netherlands' Institute of Applied Geoscience, TNO, National Groundwater Survey, Delft Utrecht, The Netherlands. ISBN 90-6743-654-2, 96pp
- [Van der Gun (1980)] Gun, J.A.M., 1980. Schatting van de elastische beringscoëfficiënt van zandige watervoerende pakketten (Estimation of the elastic storage coefficient of sandy aquifers, in Dutch); Dienst Grondwaterverkenning

- TNO, Jaarverslag 1979. Dienst Grondwaterverkenning TNO, Delft, pp. 51-61.
- [Hantush (1955)] Hantush, M.S. (1955) Non-steady radial flow in an infinite leaky aquifer. *Transm. Amer. Geophys. Union*, 36: 95-101
- [Hemker and Maas (1984)] Hemker, C.J. and Maas, C. (1987) Unsteady flow to wells in layered and fissured aquifer systems. *Journal of Hydrology*, 90: 231-249.
- [Shieh et al. (1987)] Hsieh, P.A., Bredehoeft, J.D. and Farr, J.M., 1987. Determination of aquifer transmissivity from earth tide analysis. *Water Resources Research*, 23(10): 1824-1832.
- [Kamp and Gale (1983)] Kamp, G.v.d. and Gale, J.E., 1983. Theory of Earth Tide and Barometric Effects in Porous Formations With Compressible Grains. *Water Resources Research*, 19(2): 538-544.
- [Kruseman and De Ridder (1970)] Kruseman, G.P. and De Ridder, N.A., 1970. Analysis of pumping test data. *Bulletin 11*. ILRI, Wageningen, 200 pp.
- [Kruseman and De Ridder (1994)] Kruseman, G.P. and De Ridder, N.A., (1994). Analysis of pumping test data. Second Edition. ILRI publication 47, ILRI, Wageningen, 377pp. Downloadable from: [https://www.hydrology.nl/images/docs/dutch/key/Kruseman\\_and\\_De\\_Ridder\\_1994.pdf](https://www.hydrology.nl/images/docs/dutch/key/Kruseman_and_De_Ridder_1994.pdf)
- [Loáiciga (200)] Loáiciga, H. (2009) Derivation approaches for the Theis (1935) equation. *Groundwater*.
- [Lee (1999)] Lee, T-C (1999) Applied mathematics in hydrogeology. Lewis Publ. Boca Raton etc. 382pp. ISBN 1-56670-375-1.
- [Maas (1986)] Maas, C. (1986) The use of matrix differential calculus in problems of multiple aquifer flow. *Journal of Hydrology*, 88: 43-67
- [McKinney (2017)] McKinney, W. (2017) Python for Data Analysis. 2nd edition. O'Reilly. Beijing etc. 978-1-491-95766-0. 525pp
- [Olsthoorn (2008)] Olsthoorn, T.N. (2008) Transient Groundwater Flow, Analytical Solutions. Syllabus LN0080/0811. UNESCO-IHE, Delft, Netherlands, 100pp.

- [Powell and Fensham (2015)] Powel O, Fenshem R. (2015) The history and fate of the Nubian sandstone aquifer springs in the oasis depressions of the western desert, Egypt. *Hydrogeology Journal*. DOI 10.1007/s10040-015-1335-1.
- [Rasmussen and Crawford (1997)] Rasmussen, T.C. and Crawford, L.A., 1997. Identifying and removing barometric pressure effects in confined and unconfined aquifers. *Ground Water*, 35(3): 502-511.
- [Theis (1935)] Theis CV (1935) The relation between the lowering of the piezometric surface and rate and duration of discharge of a well using groundwater storage. *Transactions of the American Geophysical Union*. Vol. 16, 519-524.
- [Todd (1959)] Todd, D.K., 1959. *Groundwater Hydrology*. John Wiley & Sons Inc., 336 pp.
- [Todd and Mays (2005)] Todd, D.K. and Mays, L.W., 2005. *Groundwater Hydrology*. John Wiley & Sons Inc.
- [Verruijt (1999)] Verruijt, A. (1999) *Grondmechanica (Soil Mechanics)*. Delft University Press, Delft, 295pp.
- [Voss and Soliman (2014)] Voss C, Soliman S (2014) The transboundary non-renewable Nubian Aquifer System of Chad, Egypt, Libya and Sudan: classical ground- water questions and parsimonious hydrogeologic analysis and modeling. *Hydrogeol J* 22:441–468
- [De Vries (1984)] Vries, J.J. de (1984) Holocene depletion and active recharge of the Kalahari Groundwater - A review and an indicative model. *Journal of Hydrology*.
- [De Vries (2000)] Vries, J.J. de (2000) Groundwater level fluctuations - the pulse of the aquifer. In: *Elevation and protection of groundwater resources*, Conference Wageningen, Netherlands National Committee for IAH, Wageningen, pp 27-43.
- [Wösten et al. (1994)] Wösten, J.H.M., Veerman, G.H. and Stolte, J. (1994) Water retention and hydraulic conductivity functions of top- and subsoils in the Netherlands. *The Staring Series*. Wageningen University, Wageningen.